



SED

Student Experiment Documentation



Document ID: BX19_GRANASAT_SED v5-0_15Jan15

Mission: BEXUS 19

Team Name: GranaSAT

Experiment Title: Attitude determination system for a pico satellite based in a star tracker, a horizon sensor and Earth's magnetic field measurements

| Team | Name | University |
|----------------------|-------------------------------|-----------------------|
| Student Team Leader: | Emilio José Martínez Pérez | University of Granada |
| Team Members: | Teresa Lucía Aparicio Jiménez | University of Granada |
| | Víctor Burgos González | University of Granada |
| | Eva Gamundi Alcaide | University of Granada |
| | Emilio García Blanco | University of Granada |
| | Laura García Gámez | University of Granada |
| | Alejandro García Montoro | University of Granada |
| | Manuel Milla Peinado | University of Granada |
| | Carlos Manuel Morales Pérez | University of Granada |
| | Pedro Manuel Vallejo Muñoz | University of Granada |



Student Experiment Documentation

| | | | |
|----------|------------------------|---------------------|------------------------|
| Version: | Issue Date: | Document Type: | Valid from: |
| 5 | 15 January 2015 | Final report | 15 January 2015 |

Issued by: **The whole team**

Approved by: **Andrés Roldán Aranda**



CHANGE RECORD

| Version | Date | Changed chapters | Remarks |
|---------|------------|---|---|
| 1.0 | 2014-02-16 | New Version | PDR |
| 1.1 | 2014-02-19 | 4.5, 4.6, 5.3.2, 5.3.3, 5.3.4, 5.3.5, 8.1 Appendix C | PDR |
| 1.2 | 2014-03-24 | All chapters | PDR recommendations |
| 2.0 | 2014-04-11 | 1.5, 2, 3, 4.1, 4.2, 4.3, 4.4, 4.5, 4.7, 4.8, 5, 6, 7.4, 8, Appendix B, Appendix C. | CDR |
| 2.1 | 2014-05-28 | 1.5, 2, 3, 4, 5, 6.1, 6.2, 6.3, 6.4, 8, Appendix A, Appendix B, Appendix C | CDR recommendations |
| 3.0 | 2014-07-25 | 2.3, 2.4 3.3.1 3.5 4.1, 4.2.1, 4.3, 4.4.1, 4.4.3 4.4.4 4.4.5 4.5.1 4.5.3 4.5.4 4.5.7 4.6 | IPR Content updated Tasks redistributed Content updated Images updated Redesign Images updated Description improved Images updated Images updated and reordered New section Content improved |



| | | | |
|-----|------------|----------------------|--|
| 3.1 | 2014-08-17 | 4.6.1 | Simulations improved |
| | | 4.6.2 | New section |
| | | 4.7 | Tables updated |
| | | 4.7.1 | Tables and graphs updated |
| | | 4.8.5, 4.8.6 | New sections |
| | | 5.1 | Table updated |
| | | 5.2 | Status updated |
| | | 5.3.5, 5.3.6, 5.3.7, | New sections |
| | | 5.3.8, 5.3.9 | |
| | | 6.1.1 | Images updated |
| | | 6.1.3 | Table updated |
| | | 6.1.4 | Tables updated and description improved |
| | | 6.2 | Content updated and description improved |
| | | 6.3 | Content updated and description improved |
| | | 6.5 | Table updated |
| | | 7.1.1, 7.1.2, 7.1.3 | New sections |
| | | 8.1 | New content added |
| | | 8.2 | Content updated |
| | | APPENDIX B | Images updated and new content added |
| | | C.1, C.5 | Content updated |
| | | C.6 | Table updated |
| | | C.7.7, C.7.8, C.7.9, | New sections |
| | | C.7.10 | |
| | | | IPR Recommendations |



| | | |
|--|----------|--|
| | 1.4 | Discussion about using visible spectrum and not IR in the horizon sensor |
| | 2.2 | Error fixed in P.3 text. Minor changes in P.4 and P.5 text |
| | 2.3, 2.4 | Former O.3 moved to D.20. |
| | 3.3.2 | Updated budget |
| | 3.5 | Error fixed in TC.1 |
| | 4.4 | Dimensions table |
| | 4.4.5.3 | New subsection analysing PCB holes stress |
| | 4.4.5.4 | New subsection analysing mechanical fixations |
| | 4.4.5.6 | New subsection containing a shock simulation |
| | 4.4.7 | New section discussing removal of the second filter |
| | 4.5.1 | Cable colour code added. Minor changes |
| | 4.5.3 | Inner box PCB cable routing |
| | 4.6 | Error fixed in table and column added |
| | 4.6.1.3 | Key added in graph |
| | 4.7.2 | New section discussing SoC |
| | 4.8.2 | Subsections to organise the text |
| | 4.8.2.4 | New subsection discussing timeout to AUTO mode loop |
| | 4.8.2.5 | New subsection discussing thermal control algorithm |

| | | | |
|-----|------------|------------|--|
| 4.0 | 2014-09-07 | 5.1 | Updates according to requirements and test plan changes |
| | | 5.2 | Scheduling updated and summary table added |
| | | 6.1, 6.2 | Flight requirements added. Minor changes |
| | | 7.1 | Analysis plan updated |
| | | APPENDIX D | New section, containing checklists and recovery procedures |
| | | EAR | |
| | | 2.3 | Requirement for the link: D.20 |
| | | 2.6 | Requirement for the boom: O.6 |
| | | 3.5 | Risk register updated |
| | | 4.1 | As-built dimensions |
| | | 4.1.4 | LEDs control subsystem updated |
| | | 4.1.6 | Ethernet CODE A insert |
| | | 4.2.1.2 | Mechanical elements updated |
| | | 4.3 | Experiment components updated |
| | | 4.4.4 | Box closing analysis |
| | | 4.4.5.1 | Modal characterisation added |
| | | 4.4.5.4 | Mechanical fixation updated |
| | | 4.4.5.6 | New subsection analysing gondola attachment |
| | | 4.4.6 | Discussion of camera filters reordered |
| | | 4.4.8 | Subsection removed |
| | | 4.6 | Minor changes |
| | | 4.8.4 | Changes in the horizon sensor algorithm |



| | | | |
|-----|------------|---------------------|---|
| | | 5.1, 5.2 | Content updated after the tests |
| | | 5.3.1, 5.3.10 | New sections containing star tracker and full functional test results |
| | | 6.1.1 | As-built dimensions and masses |
| | | 6.1.4 | Material needed at ESRANGE updated |
| | | 6.2, 6.4 | Content updated |
| | | 7.1.1, 7.1.2, 7.1.3 | Analysis plan updated |
| | | 7.4 | Lessons learned during the test phase added |
| | | C.2, C.3, C.4 | As-built characteristics of outer box, profile and inner box |
| | | C.7 | Content reordered |
| | | C.7.1 | New section covering the star tracker test details |
| | | C.7.3 | Content updated |
| | | C.7.4 | Test procedure added |
| | | C.7.5 | Minor changes in test procedure |
| | | C.7.6 | Test procedure added |
| | | C.7.8 | New section covering the magnetometer calibration details |
| | | C.7.12 | Minor changes in test procedure |
| | | C.7.16 | Test results added |
| | | D.2 | Minor changes in Data Recovery Procedure |
| 4.1 | 2014-09-25 | | EAR Recommendations |
| | | 4 | Images of the flight model added |



| | | | | |
|-----|------------|------------------------------|---|--|
| 5.0 | 2015-01-15 | 4, 6 | Experiment mass consistent throughout all the document | |
| | | 4.1.4 | Images updated | |
| | | 4.3 | Experiment components updated | |
| | | 4.4.2 | Minor changes | |
| | | 4.4.6 | New subsection covering a static load test | |
| | | 4.5 | Thermal sensor updated | |
| | | 4.6.1.4 | New subsection covering the new heat sink | |
| | | 4.7 | Table updated | |
| | | 4.8.2.5 | Timestamp section added | |
| | | 5.3.4, 5.3.5, 5.3.12, 5.3.13 | New subsections covering the results of temperature sensor, thermal, vacuum and vibration tests | |
| | | 6 | Information updated | |
| | | 6.3 | Timeline updated | |
| | | C.7.3 | Test results added | |
| | | C.7.5, C.7.9, C.7.13 | New subsections covering the details of thermal, vacuum and vibration tests | |
| | | D.3 | Assembly procedure added | |
| | | D.4 | Recovery sheet added | |
| | | All chapters | Final Report | |
| | | ABSTRACT | Past tense, typos, minor changes, format changes | |
| | | 1.5 | Results added | |
| | | | Information updated | |



| | | |
|--|--------------|--|
| | 3.1, 3.2 | WBS and Gantt chart updated |
| | 3.3.1, 3.3.2 | Manpower information and budget updated |
| | 3.3.3 | Collaborator added |
| | 4 | Minor changes in images. Minor errors in tables fixed. |
| | 4.2.1 | Minor errors in bolts and nuts tables fixed |
| | 4.5.4 | Flight model PCB photo added |
| | 4.6.1.4 | After flight conclusion added |
| | 4.8.2 | Software repository links added |
| | 4.8.3, 4.8.4 | Algorithms information updated |
| | 5.1 | Verification matrix finished |
| | 6.1.4.2 | Remove Before Flight section updated |
| | 6.1.4.3 | Aurora section updated with actual flight conditions |
| | 7.1.3 | Magnetometer Data Analysis Plan updated |
| | 7.2 | Information about the launch campaign added |
| | 7.3 | Final experiment results added |
| | 7.4 | Lessons learned updated |
| | APPENDIX B | News, articles, conferences and congresses added |
| | APPENDIX C | As-built schematics and CAD model added |



Abstract: This Student Experiment Documentation contains information on the BEXUS 19 experiment GranaSAT whose objective is to design and build a low-cost attitude determination system.

Keywords: BEXUS, SED - Student Experiment Documentation, star tracker, attitude determination, horizon sensor, magnetometer.



CONTENTS

| | |
|---|-----------|
| CHANGE RECORD | 3 |
| CONTENTS | 11 |
| PREFACE | 18 |
| ABSTRACT | 19 |
| 1 INTRODUCTION..... | 20 |
| 1.1 Scientific/Technical Background..... | 20 |
| 1.2 Mission Statement..... | 20 |
| 1.3 Experiment Objectives | 21 |
| 1.3.1 Primary Objectives | 21 |
| 1.3.2 Secondary Objectives..... | 21 |
| 1.4 Experiment Concept..... | 21 |
| 1.5 Team Details..... | 22 |
| 1.5.1 Contact Point..... | 22 |
| 1.5.2 Team Members | 23 |
| 2 EXPERIMENT REQUIREMENTS AND CONSTRAINTS..... | 27 |
| 2.1 Functional Requirements | 27 |
| 2.2 Performance Requirements | 27 |
| 2.3 Design Requirements..... | 27 |
| 2.4 Operational Requirements | 28 |
| 2.5 Software Requirements..... | 28 |
| 2.6 Constraints..... | 29 |
| 3 PROJECT PLANNING | 30 |
| 3.1 Work Breakdown Structure (WBS) | 30 |
| 3.2 Schedule..... | 33 |
| 3.3 Resources..... | 33 |

| | | |
|----------|--|-----------|
| 3.3.1 | Manpower | 33 |
| 3.3.2 | Budget..... | 40 |
| 3.3.3 | External Support..... | 48 |
| 3.4 | Outreach Approach..... | 48 |
| 3.5 | Risk Register..... | 49 |
| 4 | EXPERIMENT DESCRIPTION..... | 55 |
| 4.1 | Experiment Setup | 56 |
| 4.1.1 | Central Control Subsystem..... | 59 |
| 4.1.2 | Camera Attitude Determination Subsystem (CADS)..... | 60 |
| 4.1.3 | Magnetometer Attitude Determination Subsystem (MADS) | 60 |
| 4.1.4 | LEDs Control Subsystem (LCS) | 60 |
| 4.1.5 | Thermal Subsystem (TS)..... | 61 |
| 4.1.6 | Ground Communication Subsystem (GCS) | 61 |
| 4.1.7 | Ground Segment Subsystem (GSS)..... | 62 |
| 4.2 | Experiment Interfaces | 62 |
| 4.2.1 | Mechanical | 62 |
| 4.2.2 | Electrical..... | 72 |
| 4.3 | Experiment Components..... | 72 |
| 4.4 | Mechanical Design..... | 74 |
| 4.4.1 | Inner Box..... | 74 |
| 4.4.2 | Outer Box | 76 |
| 4.4.3 | Outer Box Assembly with the Profile..... | 81 |
| 4.4.4 | Box Closure..... | 83 |
| 4.4.5 | Mechanical Simulations..... | 85 |
| 4.4.6 | Static Load Test | 106 |
| 4.4.7 | Camera Lens Characterisation | 109 |
| 4.4.8 | Changes in the Camera Filters | 116 |
| 4.5 | Electronics Design | 117 |



| | | |
|-------|--|-----|
| 4.5.1 | General Electronic Design | 117 |
| 4.5.2 | Grounding Diagram | 123 |
| 4.5.3 | Inner Box PCB Design..... | 123 |
| 4.5.4 | Outer Box PCB Design..... | 130 |
| 4.5.5 | Magnetometer & Accelerometer Sensor LSM303DLHC | 133 |
| 4.5.6 | Temperature Sensor DS1621 | 135 |
| 4.5.7 | Temperature Sensor TC74 | 137 |
| 4.6 | Thermal Design..... | 139 |
| 4.6.1 | Thermal Simulations..... | 141 |
| 4.6.2 | Heat Transfer Substantiation | 149 |
| 4.7 | Power System | 150 |
| 4.7.1 | Power Consumption Timeline | 152 |
| 4.7.2 | Battery State of Charge (SoC) | 153 |
| 4.8 | Software Design..... | 156 |
| 4.8.1 | Data Budget and CPU Timing Estimation | 157 |
| 4.8.2 | Software Details | 158 |
| 4.8.3 | Actual State of the Star Tracker Software | 162 |
| 4.8.4 | Actual State of the Horizon Sensor Software | 173 |
| 4.8.5 | Magnetometer Attitude Determination Module | 176 |
| 4.8.6 | Attitude Determination Using an Accelerometer | 181 |
| 4.9 | Ground Support Equipment..... | 183 |
| 5 | EXPERIMENT VERIFICATION AND TESTING | 185 |
| 5.1 | Verification Matrix | 185 |
| 5.2 | Test Plan..... | 190 |
| 5.3 | Test Results | 198 |
| 5.3.1 | Star Tracker Test..... | 198 |
| 5.3.2 | Horizon Sensor Test..... | 198 |
| 5.3.3 | Magnetic Field Test | 199 |

| | | |
|--------|---|-----|
| 5.3.4 | Power Electronics Test..... | 199 |
| 5.3.5 | Thermal Test | 201 |
| 5.3.6 | Power Consumption Test | 202 |
| 5.3.7 | Raspberry Pi Test..... | 203 |
| 5.3.8 | Magnetometer Calibration Test | 204 |
| 5.3.9 | Temperature Sensor Test..... | 205 |
| 5.3.10 | Computational Capability Test..... | 206 |
| 5.3.11 | Connection Bandwidth Test..... | 206 |
| 5.3.12 | Vacuum Test | 207 |
| 5.3.13 | Vibration test | 207 |
| 5.3.14 | Fusible Test..... | 209 |
| 5.3.15 | I ² C Bus Extender Test | 211 |
| 5.3.16 | Full Functional Test | 214 |
| 6 | LAUNCH CAMPAIGN PREPARATION | 215 |
| 6.1 | Input for the Campaign / Flight Requirement Plans | 215 |
| 6.1.1 | Dimensions and Mass | 215 |
| 6.1.2 | Safety Risks | 216 |
| 6.1.3 | Electrical Interfaces | 216 |
| 6.1.4 | Launch Site Requirements | 216 |
| 6.2 | Preparation and Test Activities at Esrange..... | 219 |
| 6.3 | Timeline for Countdown and Flight..... | 224 |
| 6.4 | Post-Flight Activities..... | 225 |
| 6.4.1 | Recovery Instructions | 225 |
| 6.4.2 | Presentation during Post-Flight Meeting | 226 |
| 6.4.3 | Input to Campaign Report | 227 |
| 6.4.4 | Final Experiment Report..... | 227 |
| 6.5 | System Success | 227 |
| 7 | DATA ANALYSIS AND RESULTS | 229 |



| | | |
|-------|--|-----|
| 7.1 | Data Analysis Plan | 229 |
| 7.1.1 | Horizon Sensor Analysis | 229 |
| 7.1.2 | Star Tracker Data Analysis | 230 |
| 7.1.3 | Magnetometer and Accelerometer Data Analysis | 231 |
| 7.2 | Launch Campaign..... | 234 |
| 7.2.1 | Flight Preparations | 234 |
| 7.2.2 | Flight Performance | 238 |
| 7.2.3 | Recovery | 240 |
| 7.2.4 | Post-flight activities..... | 241 |
| 7.3 | Results..... | 242 |
| 7.3.1 | Star Tracker Results..... | 243 |
| 7.3.2 | Horizon Sensor Results..... | 251 |
| 7.3.3 | Magnetometer and Accelerometer Results | 259 |
| 7.4 | Lessons Learned | 272 |
| 8 | ABBREVIATIONS AND REFERENCES..... | 277 |
| 8.1 | Abbreviations | 277 |
| 8.2 | References | 280 |
| | APPENDIX A – EXPERIMENT REVIEWS | 285 |
| | APPENDIX B – OUTREACH AND MEDIA COVERAGE | 313 |
| | B.1 Logo | 324 |
| | APPENDIX C – ADDITIONAL TECHNICAL INFORMATION..... | 325 |
| | C.1 Plans | 325 |
| | C.2 Outer Box Characteristics | 326 |
| | C.3 Profile | 326 |
| | C.4 Inner Box Characteristics | 327 |
| | C.5 Electronics Schematics..... | 328 |
| | C.6 Electronics Components | 329 |



| | |
|---|-----|
| C.7 Test Details..... | 333 |
| C.7.1 Star Tracker Test..... | 333 |
| C.7.2 Horizon Sensor Test..... | 344 |
| C.7.3 Magnetic Field Test | 347 |
| C.7.4 Power Electronics Test..... | 355 |
| C.7.5 Thermal Test | 356 |
| C.7.6 Power Consumption Test..... | 363 |
| C.7.7 Raspberry Pi Test..... | 365 |
| C.7.8 Magnetometer calibration Test | 366 |
| C.7.9 Temperature Sensor Test..... | 370 |
| C.7.10 Computational Capability Test | 373 |
| C.7.11 Connection Bandwidth Test | 375 |
| C.7.12 Vacuum Test | 380 |
| C.7.13 Vibration Test | 383 |
| C.7.14 Fusible Test..... | 391 |
| C.7.15 I ² C Bus Extender Test | 392 |
| C.7.16 Full Functional Test | 393 |
| C.8 Simulation Details | 399 |
| C.8.1 Thermal Simulation | 399 |
| APPENDIX D – LAUNCH CAMPAIGN ADDITIONAL INFORMATION | 404 |
| D.1 Launch Campaign Checklists | 404 |
| D.2 Data Recovery Procedure..... | 407 |
| D.3 Assembly Procedure..... | 408 |
| D.3.1 General Procedure | 408 |
| D.3.2 Inner Box Assembly Procedure..... | 408 |
| D.3.3 Outer Box Assembly Procedure..... | 419 |
| D.3.4 Boom Assembly Procedure | 429 |
| D.4 Recovery Sheet | 432 |





PREFACE

This experiment arose from the PFC -the equivalent in Europe to a Master Thesis- of a former student that participated in GranaSAT project, Alejandro González Garrido. In Spain, the PFC is an essential part of a Master's programme and is completed in the final year. Students can choose from a wide variety of applied fields and at the University of Granada (UGR), the most innovative PFCs are space-related.

The REXUS/BEXUS campaign represents a great opportunity for students in technical fields and those in Translation and Interpreting, Maths or Physics to work together and to test the capabilities they have learnt during their university degrees. Moreover, the purpose of this team project is not only to develop the experiment but, also, to motivate other students at our university to take part in this kind of activity and to increase the interest of the whole university community in science and technology.

We really appreciate the generous help of Professor Andrés Roldán Aranda. Without his infinite patience it would be almost impossible to conduct this experiment.

As students of the University of Granada, we would like to thank the Board of the Higher Technical School of Information Technology and Telecommunications Engineering and the Electronics, the Faculty of Sciences and IT Department for their support and all the equipment and facilities provided.



ABSTRACT

GranaSAT designed and built a low-cost attitude determination system, a fundamental system for any spacecraft, based in a star sensor, horizon sensor and the magnetic field and acceleration measurements. The same Charge Coupled Device was used for both the star sensor and the horizon sensor. For the star sensor the Lost in Space functionality was designed, the identification algorithm used is a variation of the Matching Group algorithm proposed by Van Benzooijen; for the horizon sensor a simple detection algorithm is proposed, with the circle fitting method based in Umbach and Jones work and for the magnetometer and accelerometer sensors the attitude was estimated by two vector matching procedure based in Wahba solution.

The star sensor was capable to obtain an attitude matrix for the 97.80 % of the images collected. The relative error in the angles measured was kept below 1% through a camera calibration and the error obtained in the attitude matrix obtained was found less than 250 arcsecs. The horizon sensor was able to process all the images in night conditions, but it did not fulfil the 5° accuracy requirement. Finally, for the magnetometer and accelerometer sensors, an in-flight calibration was used to keep an uncertainty of the attitude angles under 4° with a maximum standard deviation in the magnetometer measurements of 140 nT.

After the results obtained, the most accurate and preferable method is the star sensor, despite its complexity. If low accurate attitude estimation or less complex solutions are required, the horizon sensor or magnetometer and accelerometer sensor solutions are valid for a spacecraft attitude determination system.

1 INTRODUCTION

1.1 Scientific/Technical Background

Satellites need to be sure of what their attitude is with respect to a reference frame in order to orientate themselves or their antennas towards the Earth. At present, there are many systems to obtain the attitude of a spacecraft on the basis of the measurements obtained by devices like sun sensors, gyroscopes, radiofrequency beacons, horizon sensors and star trackers.

We based the experiment in the work of Christopher McBride [1], for the star sensor and that of Mohamed Nazree et al., [2] for the horizon sensor.

The data shown in Table 1-1 [3] indicates the most accurate system is the star tracker. In this project we are going to use three different sensors to obtain the attitude of the experiment: the star tracker, a horizon sensor and a magnetometer.

Table 1-1 Comparison between attitude sensors

| Type | Initial attitude acquisition | Degrees of freedom in attitude | Accuracy |
|------------------------|------------------------------|--------------------------------|--------------|
| Magnetometer | Yes | 3 | 1 arcminute |
| Radio frequency beacon | Yes | 2 | 1 arcminute |
| Horizon sensor | Yes | 2 | 5 arcminutes |
| Sun sensor | Yes | 3 | 1 arcminute |
| Solar panel | Yes | 2 | 1° |
| Star tracker | No | 3 | 1 arcsecond |

1.2 Mission Statement

The GranaSAT experiment aims to study the orientation determination in satellites.

A device called star tracker is normally used to obtain the information about the orientation of a satellite in 3-dimensional coordinates. However, if the camera fails to detect the stellar field, the measurements provided by a magnetometer sensor, an accelerometer sensor and a horizon sensor are used to calculate the attitude.

The experiment is designed to be placed in a university GranaSAT pico satellite. Hence, performing the experiment in conditions environmentally similar to those in outer space may be very instructive for us.

1.3 Experiment Objectives

1.3.1 Primary Objectives

- The main objective of this experiment is to build and test in real conditions an attitude determination system during the BEXUS 19 campaign.
- To test the accuracy of the attitude determination system using a star sensor.
- To test the accuracy of the attitude determination system using a horizon sensor.
- To test the accuracy of the attitude determination system using a magnetometer.
- To check whether or not the attitude determination system is adequate for the GranaSAT pico satellite.

1.3.2 Secondary Objectives

- To gain know-how about space missions and their future application in other UGR space projects.
- To learn how to document a space related project.
- To improve cooperative work skills.

1.4 Experiment Concept

The experiment has tested the accuracy of an orientation determination system and its behaviour in outer space conditions. It consists of three main units: a CCD camera whose pictures have been used for the star tracker and the horizon sensor, a chip that includes a magnetometer and an accelerometer, and the CPU unit.

The CCD camera is focused so that the images it provides include the horizon and the sky. It took photos periodically during the flight. The software decided which algorithm had to be used on the basis of a luminosity threshold experimentally fixed.

The second main unit integrates two sensors: a 3D magnetometer and a 3D accelerometer. It made periodical measurements of the magnetic field and the proper acceleration during the flight. These measurements have been post-processed to obtain the attitude estimation of the spacecraft.

During the flight, all pictures were processed by a credit-card sized computer (Raspberry Pi), which acts as the CPU of the experiment. The measurements of the magnetometer and accelerometer were post-processed after flight.

Even though all data collected were stored in a SD card, the E-Link was used to send the results obtained and some of the pictures taken.

Since the infrared is preferred for every horizon sensor, it is mandatory to explain why the algorithm works in the visible spectrum. This decision was made after the two following constraints:

- The experiment uses the same camera with both attitude measurement algorithms.
- The most accurate of the attitude measurement algorithms, the star tracker, should work in the visible spectrum.

These two issues forced the decision of using a visible spectrum sensor to take the images that should process both the star tracker and the horizon sensor. Although the horizon had to deal with the atmosphere and albedo issues, the star tracker was able to make its processing more easily.

1.5 Team Details

1.5.1 Contact Point

To address any questions about our work you can:

- send an e-mail to grupo.granasat@gmail.com
- reach the Team Leader by phone at +34 627 529 364
- or contact the academic head of the GranaSAT Project, Professor Andrés Roldán Aranda. His contact details are:

Andrés Roldán Aranda



Electronics and IT Department
University of Granada
Faculty of Sciences
Office 11, 2nd floor, Physics
E-18071 Granada - Spain
Phone number: +34-958244010
Fax number: +34-958243230
E-mail: amroldan@ugr.es

1.5.2 Team Members

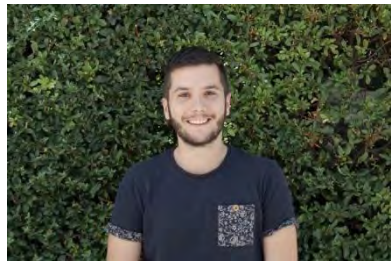


Emilio José Martínez Pérez was born in Jaén, Spain, in 1988. At the moment he is enrolled in the last year of the Telecommunications Engineering Integrated Master's degree at the University of Granada. He is responsible for the planning and scheduling of the experiment, the design and building of whole PCBs and the attitude determination sub-system based in magnetometer and accelerometer. He is the Team Leader of the experiment.



Teresa Lucía Aparicio Jiménez was born in Cádiz, Spain, in 1992. She holds a Bachelor's degree in Telecommunications Technology from the University of Granada and is

responsible for the mechanical design of the experiment.



Víctor Burgos González was born in 1993 in Córdoba, Spain. He is a final-year student of the Telecommunications Technology Bachelor's degree at the University of Granada. He is responsible for the electronic design of the experiment and is in charge of the website.



Eva Gamundi Alcaide was born in Seville, Spain in 1990. She holds a Translation and Interpreting Integrated Master's degree at the University of Granada. She is responsible for the planning and scheduling of the experiment, the translation and the proofreading of most documentation, and is also part of the outreach department.



Emilio García Blanco was born in 1991 in Granada, Spain. He holds a Civil Engineering Integrated Master's degree from the University of Granada. He executed the mechanical and thermal test and simulations.



Laura García Gámez was born in 1991 in Jaén, Spain. She is a last year student of the Telecommunications Engineering Integrated Master's degree at the University of Granada. She is responsible for the thermal subsystem and the budget management.



Alejandro García Montoro was born in 1992 in Granada, Spain. He is currently studying the Computer Science and Mathematics Bachelor's degree at the University of Granada. He designed the horizon sensor and the OBDH software of the experiment, except for the ground segment.



Manuel Milla Peinado was born in 1989 in Jaén, Spain. He holds a Telecommunications Engineering Integrated Master's degree from the University of Granada. He developed the star sensor and implemented the insulation design.



Carlos Manuel Morales Pérez was born in 1989 in Granada, Spain. He holds a Physics Integrated Master's degree from the University of Granada. He is the scientific advisor of the team and is in charge of the tests and the

magnetometer and accelerometer measurements.



Pedro Manuel Vallejo Muñoz was born in Jaén, Spain, in 1993. He is enrolled in the last year of the Telecommunications Technology Bachelor's degree at the University of Granada. He is responsible for the electronic design of the experiment and is a member of the outreach department.



2 EXPERIMENT REQUIREMENTS AND CONSTRAINTS

2.1 Functional Requirements

- F.1: The experiment shall obtain its orientation using the star sensor.
- F.2: The experiment shall obtain its orientation using the horizon sensor.
- F.3: The experiment shall obtain its orientation using magnetic field measurements.

2.2 Performance Requirements

- P.1: The output frequency of the star sensor shall be at least 0.5 Hz.
- P.2: The output frequency of the horizon sensor shall be at least 0.5 Hz.
- P.3: The maximum output frequency of the magnetic field measured shall be no greater than 5 Hz and the minimum shall be at least 0.1 Hz.
- P.4: The star sensor shall be capable of at least 1 arcmin accuracy.
- P.5: The horizon sensor shall be capable of at least 5° accuracy.
- P.6: The range of the magnetic field measured shall be of ± 1.5 to ± 8 gauss.
- P.7: The float altitude of the experiment shall be no lower than 11 Km because of the polar stratospheric clouds.

2.3 Design Requirements

- D.1: The thermal subsystem shall guarantee a temperature between -5 °C and 45 °C for the camera.
- D.2: The mechanical design shall provide protection for the possibility of 10 g vertical and 5 g horizontal shock with the ground.
- D.3: The experiment shall not disturb or harm the gondola.
- D.4: The experiment shall not disturb or harm other experiments.
- D.5: The experiment shall not be disturbed or harmed by other experiments.
- D.6: The experiment needs a box outside of the gondola that shall keep the magnetometer away from magnetic disturbances in order to avoid interferences.
- D.7: The insulation of the boxes shall work in low pressure environment, down to 10 mbar.
- D.8: The insulation of the boxes shall work in low temperature conditions, down to -80° C.
- D.9: The outer box shall keep clear of humidity to avoid condensation in the lens.

- D.10: The link shall use a maximum of 500 Kbps of download rate.
- D.11: The power system shall provide the necessary power to the instruments inside the boxes.
- D.12: The thermal subsystem shall guarantee a temperature between 0°C to 50 °C for the CPU.
- D.13: The experiment shall operate in the temperature profile of the BEXUS balloon.
- D.14: The experiment shall operate in the vibration profile of the BEXUS balloon (especially for shocks).
- D.15: The horizon sensor and the star sensor shall use the same camera.
- D.16: Energy consumption shall be lower than 28 W.
- D.17: The experiment shall resist the vibrations during its transportation.
- D.18: The experiment shall be easily assembled during the pre-launch preparation.
- D.19: The power system shall provide 5 V output voltage.
- D.20: The link between the outer box and the inner box shall have low susceptibility to noise as the experiment has low voltage in some lines (I^2C).

2.4 Operational Requirements

- O.1: The orientation shall be obtained autonomously by the CPU.
- O.2: The whole experiment shall work autonomously after it has been turned on.
- O.3: The flight duration shall not last less than 1 hour at the float altitude.
- O.4: The flight shall take place from 8:00 pm to 5:00 am.
- O.5: The measurements obtained (magnetic field, acceleration, and orientation obtained with the star sensor or the horizon sensor) shall be send to the ground segment to verify the good operation of the system.
- O.6: The vertical gondola strut on which the boom is mounted shall be properly refurbished.

2.5 Software Requirements

- S.1: The system shall take and store images with a frequency of 0.5 Hz.
- S.2: The system shall take and store magnetic measurements with a frequency of 1 Hz.
- S.3: The system shall take and store acceleration measurements with a frequency of 1 Hz.



- S.4: The system shall take and store temperature measurements with a frequency of 0.5 Hz.
- S.5: The system shall process the images with a frequency of 0.5 Hz.
- S.6: The system shall send all the data measured through E-Link with a frequency of 0.1 Hz.

2.6 Constraints

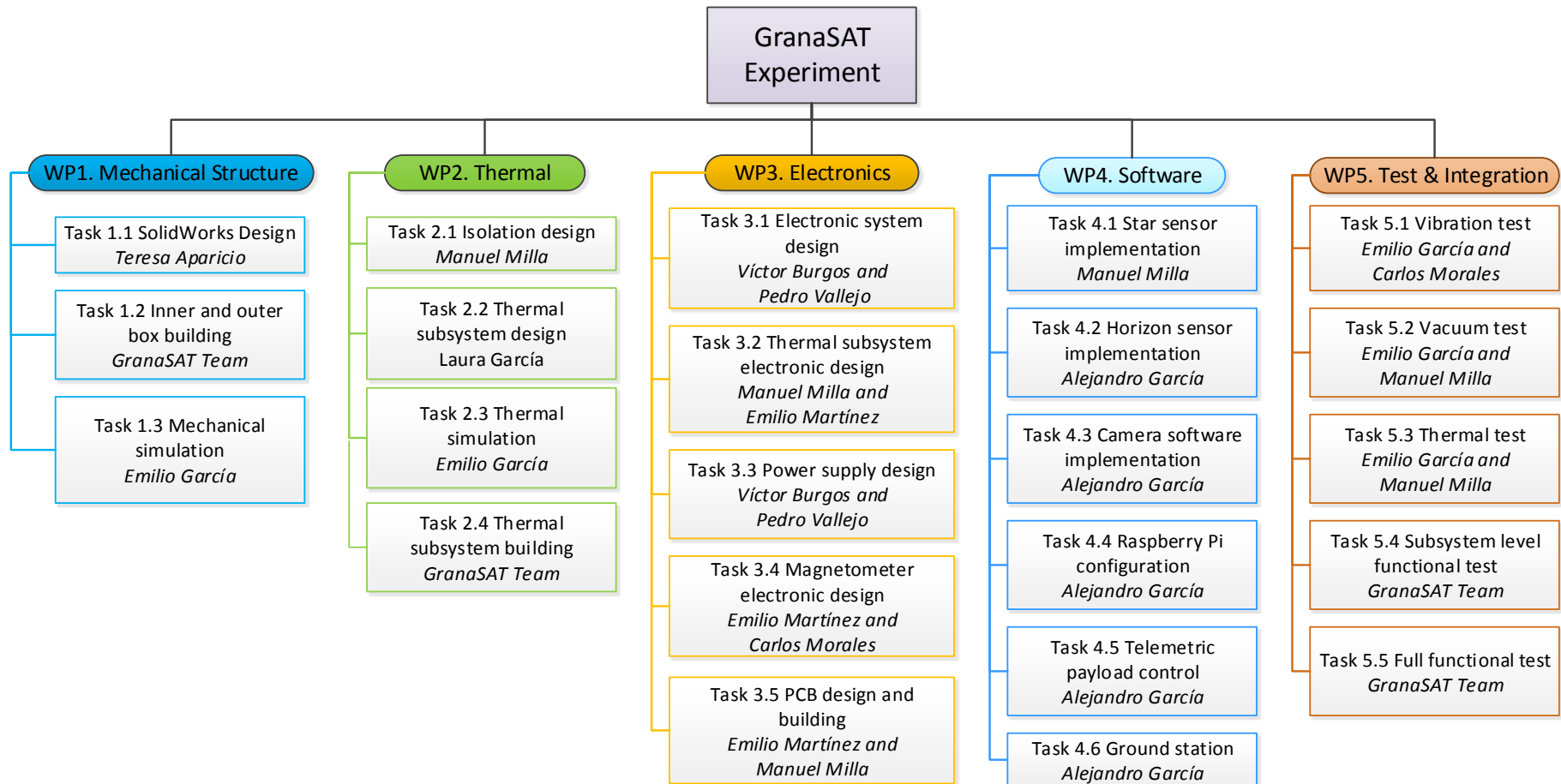
- C.1: The temperature of the experiment is much lower than the commercial and industrial temperature in which its components usually work.
- C.2: The experiment must comply with the BEXUS schedule and guidelines.
- C.3: The minimum budget we have to obtain is more than € 10,000.

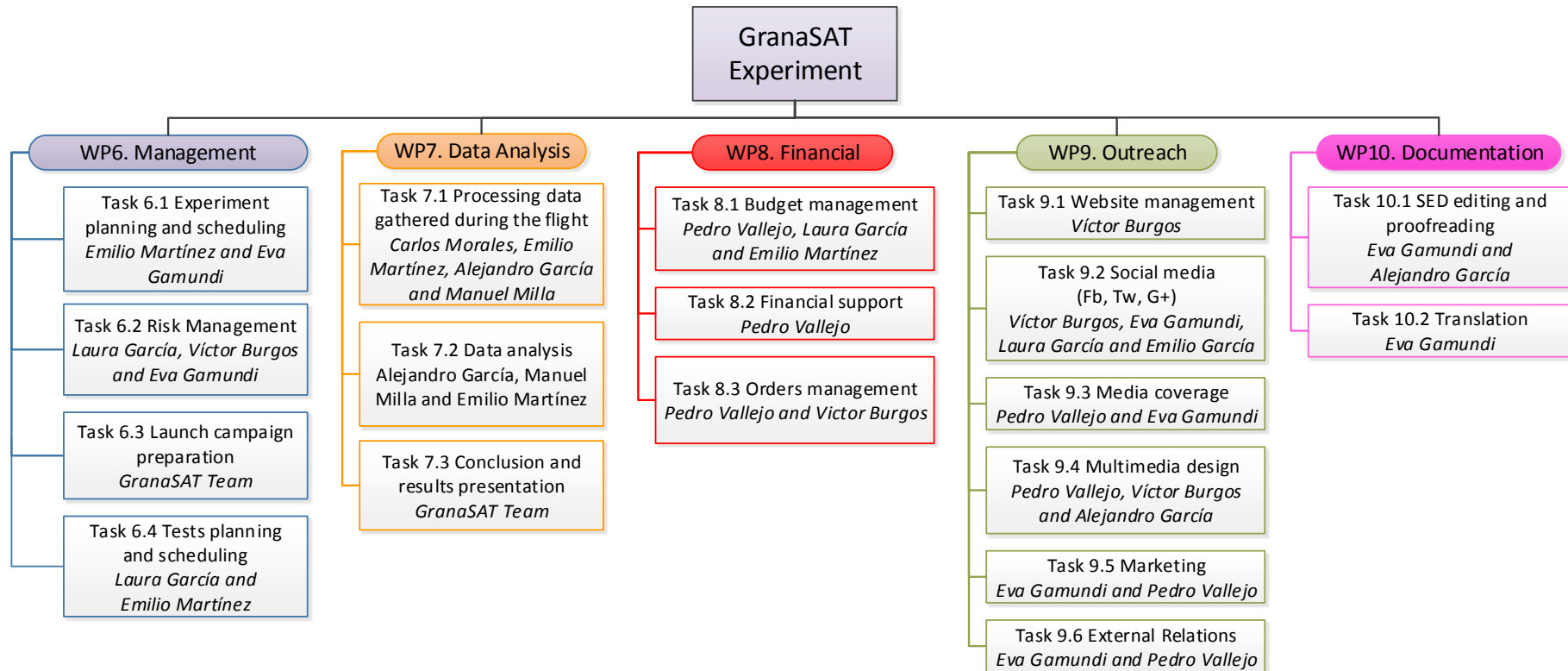


3 PROJECT PLANNING

3.1 Work Breakdown Structure (WBS)

We have designed the WBS based on the ECSS standards [4].







3.2 Schedule

This is the top level Gantt chart for the project.

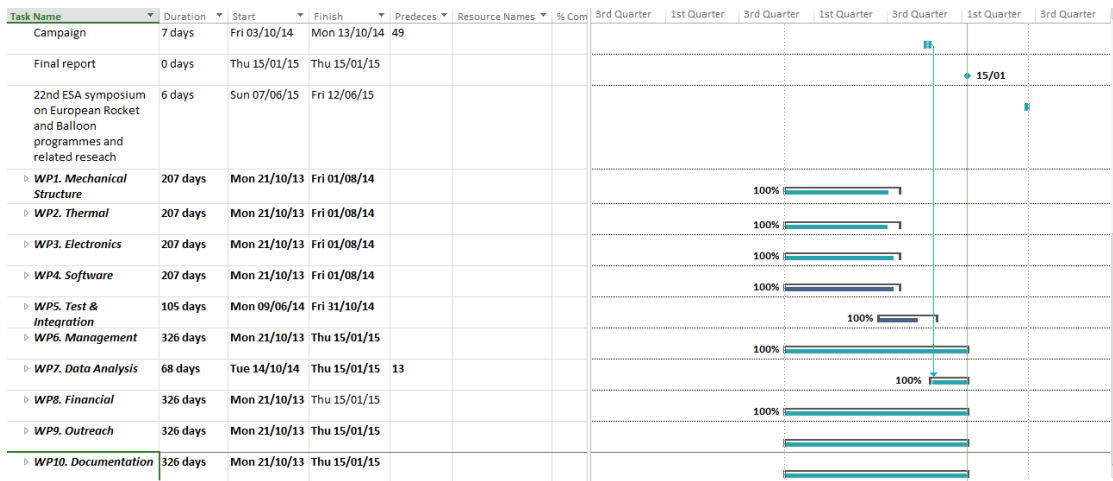


Figure 3-1 Top level Gantt chart

Since the schedule is very large and non-legible in A4 format, we are sending more detailed information in two files with the extension .mpp and .pdf. The files are:

BX19_GRANASAT_SCHEDULE_v5_15Jan15.mpp

BX19_GRANASAT_SCHEDULE_v5_15Jan15.pdf

3.3 Resources

3.3.1 Manpower

Emilio José Martínez Pérez

He is responsible for the following tasks:

- Task 3.4 Magnetometer electronic design
- Task 3.5 PCB design and building
- Task 6.1 Experiment planning and scheduling
- Task 6.4 Test planning and scheduling
- Task 7.1 Processing data gathered during the flight
- Task 7.2 Data analysis
- Task 8.1 Budget management

Emilio would be replaced by Laura García and Eva Gamundi should he be unable to continue with his work.

Table 3-1 Emilio José Martínez Pérez availability

| | |
|-----------------------------|--------------------------------------|
| 12.04.2014 to 13.06.2014 | 20 hours per week (semester time) |
| 14.06.2014 to 10.07.2014 | 40 hours per week (exam period) |
| 11.07.2014 to flight | 40 hours per week |

Teresa L. Aparicio Jiménez

She is responsible for the following tasks:

- Task 1.1 SolidWorks design

Teresa would be replaced by Emilio García should she be unable to continue with her work.

Table 3-2 Teresa L. Aparicio Jiménez availability

| | |
|-----------------------------|--------------------------------------|
| 12.04.2014 to 13.06.2014 | 20 hours per week (semester time) |
| 14.06.2014 to 10.07.2014 | 5 hours per week (exam period) |
| 11.07.2014 to flight | 0 hours per week |

Víctor Burgos González

He is responsible for the following tasks:

- Task 3.1 Electronic system design
- Task 3.3 Power supply design
- Task 6.2 Risk Management
- Task 8.3 Orders management
- Task 9.1 Website management
- Task 9.2 Social media (Fb, Tw, G+)
- Task 9.4 Multimedia design

Víctor would be replaced by Pedro Vallejo should he be unable to continue with his work.

Table 3-3 Víctor Burgos González availability

| | |
|-----------------------------|--------------------------------------|
| 12.04.2014 to 13.06.2014 | 20 hours per week (semester time) |
| 14.06.2014 to 10.07.2014 | 5 hours per week (exam period) |
| 11.07.2014 to flight | 10 hours per week |

Eva Gamundi Alcaide

She is responsible for the following tasks:

- Task 6.1 Experiment planning and scheduling
- Task 6.2 Risk Management
- Task 9.2 Social media (Fb, Tw, G+)
- Task 9.3 Media coverage
- Task 9.5 Marketing
- Task 9.6 External relations
- Task 10.1 SED proofreading
- Task 10.2 Translation

Eva would be replaced by Pedro Vallejo, Teresa Aparicio, Laura García and Emilio Martínez should she be unable to continue with her work.

Table 3-4 Eva Gamundi Alcaide availability

| | |
|-----------------------------|--------------------------------------|
| 12.04.2014 to 13.06.2014 | 30 hours per week (semester time) |
| 14.06.2014 to 10.07.2014 | 40 hours per week (exam period) |
| 11.07.2014 to flight | 30 hours per week |

Emilio García Blanco

He is responsible for the following tasks:

- Task 1.3 Mechanical simulation
- Task 2.3 Thermal simulation
- Task 5.1 Vibration test
- Task 5.2 Vacuum test
- Task 5.3 Thermal test

Emilio would be replaced by Carlos Manuel Morales and Teresa Aparicio should he be unable to continue with his work.

Table 3-5 Emilio García Blanco availability

| | |
|-----------------------------|--------------------------------------|
| 12.04.2014 to 13.06.2014 | 10 hours per week (semester time) |
| 14.06.2014 to 10.07.2014 | 5 hours per week (exam period) |
| 11.07.2014 to flight | 40 hours per week |

Laura García Gámez

She is responsible for the following tasks:

- Task 3.2 Thermal subsystem electronic design
- Task 6.2 Risk management
- Task 6.4 Tests planning and scheduling
- Task 8.1 Budget management
- Task 9.2 Social media (Fb, Tw, G+)

Laura would be replaced by Emilio Martínez and Eva Gamundi should she be unable to continue with her work.

Table 3-6 Laura García Gámez availability

| | |
|-----------------------------|--------------------------------------|
| 12.04.2014 to 13.06.2014 | 25 hours per week (semester time) |
|-----------------------------|--------------------------------------|



Student Experiment Documentation

| | |
|-----------------------------|--------------------------------|
| 14.06.2014 to 10.07.2014 | 5 hours per week (exam period) |
| 11.07.2014 to flight | 10 hours per week |

Alejandro García Montoro

He is responsible for the following tasks:

- Task 4.2 Horizon sensor
- Task 4.3 Camera software
- Task 4.4 Raspberry Pi configuration
- Task 4.5 Telemetric payload control
- Task 4.6 Ground station
- Task 9.4 Multimedia design

Alejandro would be replaced by Manuel Milla should he be unable to continue with his work.

Table 3-7 Alejandro García Montoro availability

| | |
|-----------------------------|--------------------------------------|
| 12.04.2014 to 13.06.2014 | 30 hours per week (semester time) |
| 14.06.2014 to 10.07.2014 | 40 hours per week (exam period) |
| 11.07.2014 to flight | 40 hours per week |

Manuel Milla Peinado

He is responsible for the following tasks:

- Task 2.1 Insulation design
- Task 3.2 Thermal subsystem electronic design
- Task 3.5 PCB design and building
- Task 4.1 Star sensor implementation

Manuel would be replaced by Alejandro García, Pedro Vallejo, Emilio García and Carlos Moreno should he be unable to continue with his work.

Table 3-8 Manuel Milla Peinado availability

| | |
|-------------------------|----------------------|
| 12.04.2014 to flight | 40 hours per week |
|-------------------------|----------------------|

Carlos Manuel Morales Pérez

He is responsible for the following tasks:

- Task 3.4 Magnetometer electronic design
- Task 5.1 Vibration test
- Task 7.1 Processing data gathered during the flight

Carlos would be replaced by Teresa L. Aparicio and Emilio García should he be unable to continue with his work

Table 3-9 Carlos Manuel Morales Pérez availability

| | |
|-----------------------------|--------------------------------------|
| 12.04.2014 to 13.06.2014 | 20 hours per week (semester time) |
| 14.06.2014 to 10.07.2014 | 15 hours per week (exam period) |
| 11.07.2014 to flight | 40 hours per week |

Pedro Manuel Vallejo Muñoz

He is responsible for the following tasks:

- Task 3.1 Electronic system design
- Task 3.3 Power supply design
- Task 8.1 Budget management
- Task 8.2 Financial support
- Task 8.3 Orders management
- Task 9.3 Media coverage
- Task 9.4 Multimedia design
- Task 9.5 Marketing



- Task 9.6 External relations

Pedro would be replaced by Victor Burgos and Eva Gamundi should he be unable to continue with his work.

Table 3-10 Pedro Manuel Vallejo Muñoz availability

| | |
|-----------------------------|--------------------------------------|
| 12.04.2014 to 13.06.2014 | 20 hours per week (semester time) |
| 14.06.2014 to 10.07.2014 | 5 hours per week (exam period) |
| 11.07.2014 to flight | 15 hours per week |

GranaSAT team:

Some tasks will require the all or most of the team members of the GranaSAT project:

- Task 1.2 Inner and outer box building
- Task 2.4 Thermal subsystem building
- Task 5.4 Subsystem level functional test
- Task 5.5 Total experiment functional test
- Task 6.3 Launch campaign preparation
- Task 7.3 Conclusion and presentation results

The total manpower available per week is 240 hours during semester time (12.04.2014 to 13.06.2014), 120 hours during the exam period (14.06.2014 to 10.07.2014) and 320 hours during the summer (11.07.2014 to flight).

3.3.2 Budget

Table 3-11 Income and project cost

| | | |
|----------------------------------|--|------------------|
| ACTUAL INCOME (€) | Vice-Rector's Office for Students (VROS) ¹ | 2,976.00 |
| | Higher Technical School of Information Technology and Telecommunications Engineering | 250.00 |
| | University of Granada | 1,008.77 |
| | ESA | 7,756.73 |
| | Euroinnova (Sponsor) | 800.00 |
| | Inesem (Sponsor) | 600.00 |
| | Total income | 13,421.00 |
| TOTAL ACTUAL PROJECT COST | € 13,334.71 | |

Key for the statuses of the items:

TBD (To Be Determined) means we have not yet decided which element we are going to purchase.

Ordered means we have already ordered the element and we are waiting for its delivery.

Available means we have purchased the element and it has been delivered.

✓ means our sponsors have already reimbursed the expenses.

¹ The VROS will cover exclusively the travel and accommodation expenses.

**Table 3-12 Mechanical department budget**

| Mechanical department | Units | Cost ($\text{€}/\text{unit}$) | Total (€) | Funding | Status |
|-------------------------------------|-------|---|-------------------------------|---------|-----------|
| 45x45 Profile | 1 | 166.97 | 166.97 | Sponsor | Available |
| Nuts, bolts and washers | - | - | 52,1 | | Available |
| Insulating connectors | 20 | 0.09 | 1.80 | | Available |
| Thermal insulation for wires | 1 | 4.00 | 4.00 | | Available |
| Aluminium plate 3mm (200x150 mm) | 1 | 120.00 | 120.00 | | Available |
| Shipping profile | 1 | 58.77 | 58.77 | | Available |
| Lens cleaner | 1 | 12 | 12 | | Available |
| Subtotals | | | 415.64 | | ✓ |

Table 3-13 Electronic department budget

| Electronic department | Units | Cost ($\text{€}/\text{unit}$) | Total (€) | Funding | Current status |
|-----------------------|-------|---|----------------------------------|---------|----------------|
| Capacitor (in) | 1 | 0.52 | 0.52 | Sponsor | Available |
| Fast Diode | 1 | 0.05 | 0.05 | | Available |
| Capacitor (out) | 1 | 0.34 | 0.34 | | Available |
| Inductor | 1 | 0.91 | 0.91 | | Available |
| Regulator | 1 | 3.76 | 3.76 | | Available |
| Diode LED | 10 | 0.15 | 1.50 | | Available |
| LED SMD | 20 | 0.01 | 0.20 | | Available |
| Fuse | 1 | 0.20 | 0.20 | | Available |
| Fuse holder | 1 | 1.44 | 1.44 | | Available |
| Mushroom push button | 1 | 25.49 | 25.49 | | Available |



| | | | | |
|-------------------------------------|----|-------|---------------|-----------|
| Amphenol PT02E8-4P | 1 | 8.65 | 8.65 | Available |
| Amphenol MS3102A-14S-2P | 1 | 30.24 | 30.24 | Available |
| PX0842 USB Connector | 1 | 9.18 | 9.18 | Available |
| Amphenol RJF21B | 1 | 32.17 | 32.17 | Available |
| Cable Gland | 1 | 6.00 | 6.00 | Available |
| Accelerometer & magnetometer sensor | 5 | 3.67 | 18.35 | Available |
| Power MOSFET | 5 | 0.90 | 4.50 | Available |
| Resistor | 2 | 0.46 | 0.92 | Available |
| LED holder | 6 | 0.27 | 1.62 | Available |
| MOSFET Potentiometer | 5 | 1.07 | 5.36 | Available |
| NMOS SMD | 50 | 0.04 | 2.05 | Available |
| Regulator | 5 | 2.72 | 13.60 | Avaible |
| Rectifier Diode | 5 | 0.60 | 2.99 | Available |
| C 100uF/50V | 5 | 0.83 | 4.14 | Available |
| C 1000uF/6.3V | 5 | 0.47 | 2.33 | Available |
| L 100uH | 2 | 2.00 | 4.00 | Available |
| Power Connector Male | 1 | 23.99 | 23.99 | Available |
| Power Connector Female | 1 | 34.75 | 34.75 | Available |
| Amphenol USB wire | 1 | 19.26 | 19.26 | Available |
| Limiter Current | 3 | 1.09 | 3.27 | Available |
| FR4 sheet | 6 | 35.00 | 210.00 | Available |
| Subtotals | | | 471.78 | ✓ |

**Table 3-14 Thermal department budget**

| Thermal department | Units | Cost (€/unit) | Total (€) | Funding | Status |
|----------------------------|-------|------------------|---------------|---------|-----------|
| Temperature sensor DS1621 | 3 | 5.00 | 15.00 | Sponsor | Available |
| Temperature sensor TC74 | 8 | 1.18 | 9.44 | | Available |
| Temperature sensor DS18B20 | 4 | 3.75 | 15.00 | | Available |
| Insulator | 4 | 2.00 | 8.00 | | Available |
| T-VAC | 1 | 100.00 | 100.00 | UGR | Available |
| Subtotals | | | 147.44 | | ✓ |

Table 3-15 Software department budget

| Software department | Units | Cost (€/unit) | Total (€) | Funding | Status |
|----------------------------|-------|------------------|---------------|---------|-----------|
| Camera + lens | 1 | 850.00 | 850.00 | UGR | Available |
| Micro SD memory 32 Gb | 1 | 22.00 | 22.00 | | Available |
| Raspberry Pi | 4 | 31.90 | 127.60 | | Available |
| Subtotals | | | 999.60 | | ✓ |

Table 3-16 Marketing department budget

| Marketing department | Units | Cost (€/unit) | Total (€) | Funding | Status |
|-----------------------------|-------|------------------|---------------|---------|-----------|
| Folders | 14 | 1.00 | 14.00 | Sponsor | Available |
| Business cards | 60 | 0.10 | 6.00 | | Available |
| Poster | 2 | 43.56 | 87.12 | | Available |
| Flyers | 10 | 1.00 | 10.00 | | Available |
| Subtotals | | | 117.12 | | ✓ |

**Table 3-17 Office supplies budget**

| Office supplies department | Units | Cost (€/unit) | Total (€) | Funding | Status |
|-----------------------------------|-------|---------------|---------------|--|-----------|
| Bookbinding | 10 | 3.00 | 30.00 | Higher Technical School of Information Technology and Telecommunications Engineering | Available |
| Documentation (pages) B/N | 3,000 | 0.03 | 90.00 | | Available |
| Documentation (pages) color | 400 | 0.40 | 160.00 | | Available |
| Subtotals | | | 280.00 | | ✓ |

Table 3-18 Selection Workshop budget

| Selection Workshop (Noordwijk) | Units | Cost (€/unit) | Total (€) | Funding | Status |
|--|----------|---------------|-----------------|---------|-----------|
| Bus (Granada - Málaga) | 4 | 16.03 | 64.12 | ESA | Available |
| Plane (Málaga - Rotterdam) | 4 | 85.63 | 342.52 | | Available |
| Bus (Rotterdam airport - Rotterdam Centraal) | 4 | 3.00 | 12.00 | | Available |
| Train (Rotterdam Centraal - Leiden Centraal) | 4 | 7.30 | 29.20 | | Available |
| Bus (Leiden Centraal - Noordwijk) | 4 | 4.00 | 16.00 | | Available |
| Stay in Noordwijk | 4x4 | 30.00 | 480.00 | | Available |
| Bus (Noordwijk - Leiden Centraal) | 4 | 4.00 | 16.00 | | Available |
| Train (Rotterdam Centraal - Leiden Centraal) | 4 | 6.80 | 27.20 | | Available |
| Bus (Rotterdam Centraal - Rotterdam airport) | 4 | 3.00 | 12.00 | | Available |
| Plane (Rotterdam - Málaga) | 4 | 85.62 | 342.48 | | Available |
| Bus (Málaga - Granada) | 4 | 11.19 | 44.76 | | Available |
| Subtotals | 4 | | 1,386.28 | | ✓ |

Table 3-19 Student Training Week budget

| Student Training Week (Kiruna) | Units | Cost (€/unit) | Total (€) | Funding | Status |
|---------------------------------------|-------|---------------|-----------|---------|-----------|
| Bus (Granada - Madrid) | 2 | 21.12 | 42.24 | VROS | Available |



| Student Training Week (Kiruna) | Units | Cost (€/unit) | Total (€) | Funding | Status |
|---|----------|------------------|-----------------|---------|-----------|
| Train (Bus station - Madrid Airport) | 2 | 2.15 | 4.30 | | Available |
| Plane (Madrid - Stockholm) | 2 | 169.78 | 339.56 | | Available |
| Plane (Stockholm - Kiruna) | 2 | 181.84 | 363.68 | | Available |
| Stay in Kiruna | 2 x 6 | 65.00 | 780.00 | | Available |
| Plane (Kiruna - Stockholm) | 2 | 104.64 | 209.28 | | Available |
| Plane (Stockholm - Madrid) | 2 | 93.68 | 187.36 | | Available |
| Train (Madrid Airport - Bus station) | 2 | 2.15 | 4.30 | | Available |
| Bus (Madrid - Granada) | 2 | 22.12 | 44.24 | | Available |
| Subtotals not sponsored | | | 1,974.96 | | |
| Sponsored by programme | 4 | 600.00 | 2,400.00 | ESA | Available |
| Subtotals | 6 | | 4,374.96 | | ✓ |

Table 3-20 Critical Design Review budget

| CDR (Noordwijk) | Units | Cost (€/unit) | Total (€) | Funding | Status |
|-----------------------------------|----------|------------------|-----------------|------------------------|-----------|
| Travel (not sponsored) | 1 | 327.74 | 327.74 | VROS and sponsor | Available |
| Stay in Noordwijk (not sponsored) | 1 x 2 | 30.00 | 60.00 | | Available |
| Subtotals (not sponsored) | | | 447.74 | | |
| Travel (electronics responsible) | 1 | 418.59 | 418.59 | ESA | Available |
| Travel (rest of the team) | 3 | 327.74 | 983.22 | | Available |
| Subtotals (sponsored) | 4 | | 1,401.81 | | |
| Subtotals | 5 | | 1,849.55 | | ✓ |

Table 3-21 Launch Campaign budget

| Launch Campaign (Kiruna) | Units | Cost (€/unit) | Total (€) | Funding | Status |
|---------------------------------|-------|------------------|-----------|---------|-----------|
| Sponsored by programme | 4 | 490.11 | 1,960.44 | ESA | Available |
| Delivery of components | 1 | 58.77 | 58.77 | Sponsor | Available |



| Launch Campaign (Kiruna) | Units | Cost (€/unit) | Total (€) | Funding | Status |
|--------------------------|-------|------------------|-----------------|---------|--------|
| Subtotals | | | 2,019.21 | | ✓ |

Table 3-22 ESA Symposium budget

| ESA Symposium on European Rocket and Balloon Programmes and Related Research (Tromsø) | Units | Cost (€/unit) | Total (€) | Funding | Status |
|---|-------|------------------|---------------|---------|-----------|
| Sponsored by programme (estimation) | 1 | 381.10 | 381.10 | ESA | TBD |
| Registration | 1 | 226.60 | 226.60 | | |
| Poster | 1 | 45 | 45 | | Available |
| Subtotals | | | 653.70 | | |

Table 3-24 Vacuum test travel budget

| T-VAC (Barcelona) | Units | Cost (€/unit) | Total (€) | Funding | Status |
|-------------------|-------|------------------|---------------|---------|-----------|
| Stay in Barcelona | 2 | 82.86 | 165.72 | VROS | Available |
| Travel | 2 | 241.53 | 483.06 | | |
| Subtotals | | | 648.78 | | ✓ |

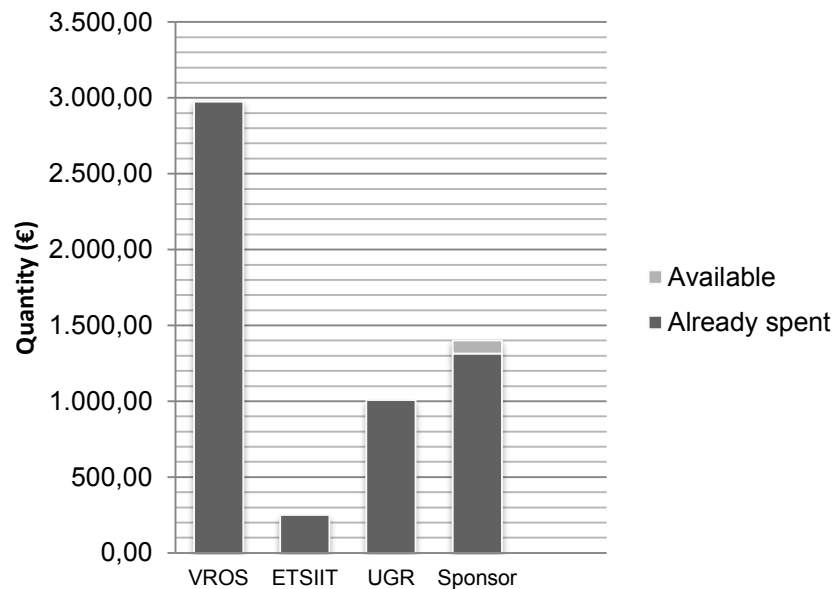


Figure 3-2 Overview of credit available

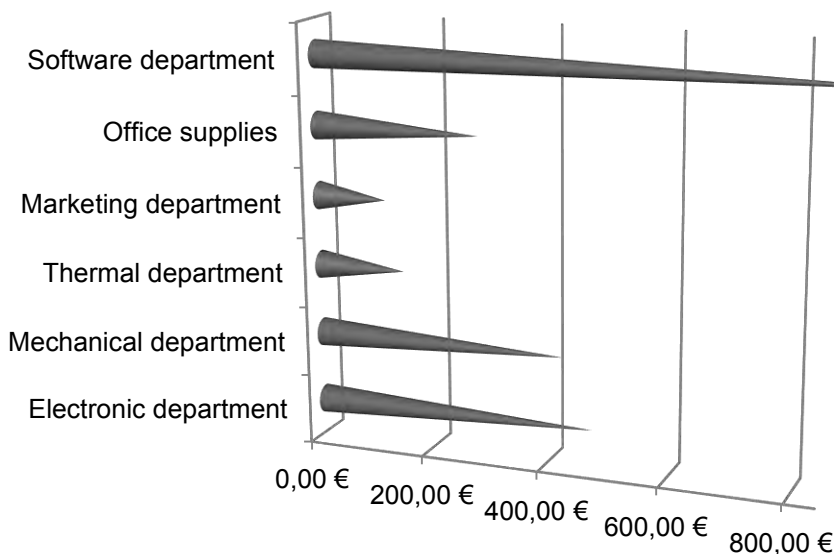


Figure 3-3 Graph comparing expenses by department (Trips are not considered because of the large difference in cost)

3.3.3 External Support

Professor Andrés Roldán Aranda, the academic head of GranaSAT, has been our main supporter from the very beginning. Thanks to him, the Electronics and IT Department of the University of Granada has provided us with materials and has allowed us to use its laboratories in the Faculty of Sciences. In addition, we have received support from other teachers who have helped with technical problems.

Mario Román García, currently studying the Computer Science and Mathematics Bachelor's degree at the University of Granada, has been crucial for the software development. He has designed and implemented the Ground Station software, including the client side of the communication with the gondola and the graphical user interface. He has also collaborated in the design and coding of the communication protocol. Without his work -which can be seen in his GitHub repository [5], the software would not have been ready for the flight.

The Higher Technical School of Information Technology and Telecommunications Engineering is paying for our copies and printouts and has allowed us to use its classrooms for meetings.

The Students Association of the University of Granada has also been willing to help. Since their headquarters is in the only UGR building that remains open at night and during weekends, they have offered us to use this space for late-night and weekend meetings. In their building, we can use the wide desks, chairs, projectors and whiteboards and we can scan, print and make copies of any document we need.

The Vice-Rector's Office for Students has awarded us with a € 2,976 grant to cover travel expenses.

The chief managers of Cocorocó, a coworking space at the very heart of Granada, have decided to support the project by allowing us to use their installations at any time. Furthermore, they are going to advise and guide us with the advertising and marketing.

In addition, INESEM and Euroinnova, two companies based in Cowoking, another coworking space in Granada, are donating € 1,400 to the project.

3.4 Outreach Approach

The main ongoing activities in this field are the following:



- Website: <http://granasat.ugr.es>. The team's website is used to keep a detailed backup of the work done by all departments, with technical articles and scientific information that can be consulted by anyone. The website is available to possible partners as a public place to advertise themselves. We have contacted the Faculty of Translation and Interpreting and a tutor and a group of students under his supervision have translated most of the articles into English.
- Social media accounts:
 - Twitter: <https://twitter.com/granasat>
 - Facebook: <https://www.facebook.com/granasat>
 - Google+: <https://plus.google.com/u/0/109416968570285086576/>
- University mailing lists
- Articles on institutional websites
- Institutional contact
- Press contact
- Congresses
- TV and videos
- Conferences
- Press conference

More detailed information about the Outreach Approach and our logo can be consulted in APPENDIX B – Outreach and Media Coverage.

3.5 Risk Register

Risk ID

TC – technical/implementation
 MS – mission (operational performance)
 SF – safety
 VE – vehicle
 PE – personnel
 EN – environmental
 TR – transportation

Probability (P)

- A. Minimum – Almost impossible to occur
- B. Low – Small chance to occur
- C. Medium – Reasonable chance to occur

- D. High – Quite likely to occur
 E. Maximum – Certain to occur, maybe more than once

Severity (S)

1. Negligible – Minimal or no impact
2. Significant – Leads to reduced experiment performance
3. Major – Leads to failure of subsystem or loss of flight data
4. Critical – Leads to experiment failure or creates minor health hazards
5. Catastrophic – Leads to termination of the project, damage to the vehicle or injury to personnel

Table 3-23 Risk register

| E | Low | Medium | High | Very high | Very high |
|---|----------|----------|----------|-----------|-----------|
| D | Low | Low | Medium | High | Very high |
| C | Very low | Low | Low | Medium | High |
| B | Very low | Very low | Low | Low | Medium |
| A | Very low | Very low | Very low | Very low | Low |
| | 1 | 2 | 3 | 4 | 5 |

Table 3-24 Risk register

| ID | Risk (& consequence if not obvious) | P | S | P x S | Action |
|------|--|---|---|----------|---|
| TC.1 | Camera does not work | A | 4 | Very low | No action taken |
| TC.2 | Picture taken was not good to the proper function of the star sensor | D | 2 | Low | Use magnetic measurements; have it calibrated on the flight to improve the accuracy in the measurements |
| TC.3 | Software Linux fails during flight | B | 4 | Low | Test the experiment for several days |
| TC.4 | Critical component is destroyed during testing | B | 2 | Very low | Buy spare components |
| TC.5 | Drain the gondola power | B | 2 | Very low | Keep to calculated power budget margins for the mission |



Student Experiment Documentation

| ID | Risk (& consequence if not obvious) | P | S | P x S | Action |
|-------|---|---|---|----------|---|
| TC.6 | Long delivery time for components | B | 1 | Very low | Order components long beforehand; consider more than one provider |
| TC.7 | Critical component does not arrive on time | B | 2 | Very low | Order components long beforehand; consider more than one provider |
| TC.8 | Total power failure, leads to the loss of all samples because of low temperatures | A | 4 | Very low | Power converters must work flawlessly also in vacuum conditions; ensure this by performing endurance tests; converters will have short circuit and overheating protection |
| TC.9 | Detachment of the outer box | B | 4 | Low | Do static load test, perform a good clamp design and use a safety cable |
| TC.10 | General or subsystem failure during Launch Campaign | B | 4 | Low | Have redundancy elements prepared |
| MS.1 | Short time power loss will shut down the whole experiment temporarily | A | 3 | Very low | System should be capable of rebooting and continuing at last saved time; to do so we will use a watchdog |
| MS.2 | Experiment lands in water, can cause electronic disruptions and short circuits, might affect the whole experiment or only parts | A | 2 | Very low | Use an SD card and turn off the system before landing to ensure safe data storage |



| ID | Risk (& consequence if not obvious) | P | S | P x S | Action |
|------|--|---|---|----------|---|
| MS.3 | Failure of thermal design interrupts the electronics design because of the temperature range | B | 3 | Low | Use a good insulation, do reliable simulations and intensively test the thermal subsystem |
| MS.4 | Shock loads at launch and landing can damage some subsystems of the experiment | D | 1 | Low | Perform multiple, well-calibrated tests |
| MS.5 | Electrostatic behaviour of the materials can damage the electronics | B | 3 | Low | Make sure electronics do not touch polystyrene |
| MS.6 | Telematic shut down of experiment fails | B | 4 | Low | Place a general power button for manual shut down |
| MS.7 | Mechanical SD card fastener damages the card during the flight | B | 4 | Low | Use a MMC card adapter for micro SD card |
| VE.1 | Reduction in gondola batteries capacity due to intensive testing | A | 4 | Very low | Design the power system to adapt it to these needs |
| VE.2 | Ethernet link fails and the communication is lost during the flight | A | 4 | Very low | Store data in SD card |
| VE.3 | Shut down the experiment (pressing to the power-off button) accidentally during flight | A | 5 | Low | Slide the experiment on the "L beams" in the direction of their E-link and power connector (further into the gondola) to avoid accidental pressing to the power-off button. |



| ID | Risk (& consequence if not obvious) | P | S | P x S | Action |
|------|---|---|---|----------|--|
| EN.1 | Not dark enough to see stars | A | 3 | Very Low | We have our horizon sensor working to get the attitude determination |
| EN.2 | Aurora interfere with the star tracker | A | 2 | Very low | Design a robust algorithm; test the algorithm with images with the aurora |
| PE.1 | A team member is temporarily unavailable | C | 2 | Low | Ensure the rest of the team can take over the tasks of that person for him/her |
| PE.2 | A team member abandons the project | C | 2 | Low | Find another person interested in the project to replace him/her |
| PE.3 | Cannot obtain enough funding for the experiment | B | 2 | Very Low | Use personal funding; apply for scholarships in our country and our university; look for further sponsoring |
| PE.4 | Some components cannot be purchased | A | 1 | Very Low | Use similar components |
| PE.5 | Bad working atmosphere | B | 3 | Low | Talk with the interested parts and try to resolve the problem between them |
| PE.6 | Schedule delays during testing or implementation phase | B | 3 | Low | Design a good and realistic test and implementation plan beforehand; recruit students to collaborate with us |
| PE.7 | There are not enough team members that can attend the launch campaign | A | 3 | Very low | Design a realistic launch campaign and schedule long beforehand |



| ID | Risk (& consequence if not obvious) | P | S | P x S | Action |
|------|---|---|---|----------|---|
| PE.8 | Assembly of the experiment during the launch campaign is not completed because of schedule delays | B | 3 | Low | Design a realistic launch campaign and schedule long beforehand |
| PE.9 | Electrostatic behaviour of some materials can cause an electrostatic discharge on a person | B | 2 | Very low | Include a well-designed grounding diagram |
| TR.1 | Experiment shipment to Kiruna is delayed | C | 3 | Low | Ship the experiment in advance |
| TR.2 | Vibration during transportation damages the electronics | B | 4 | Low | Intensive testing before launch |



4 EXPERIMENT DESCRIPTION

The following sections describe the whole experiment design in detail. However, first of all, we need to outline the purpose and behaviour of the main sensors.

Star tracker:

A star tracker is a device that uses an image from the sky in which you can detect the stars. Once the device has taken the picture and detected the stars, you can find a pattern by comparing the image with a star catalogue. When the system recognises which stars appear in the photo, its orientation can be calculated because the stars are a reference frame that is fixed near the Earth.

Further information about star sensor can be found in the standard “Star sensors terminology and performance specification” [6].

Horizon sensor:

A horizon sensor determines the nadir vector, which is defined as the vector connecting the centre of the spacecraft to the centre of the Earth, using images taken from a CCD sensor. Thus, the orientation is fully determined about the roll and pitch axes.

The horizon sensor used in this experiment is a fixed-head type sensor and it works in the visible light spectrum in order to combine both image algorithms (star tracker and horizon sensor) in only one CCD sensor.

Magnetometer:

The main purpose of this sensor is the study and observation of Earth’s Magnetic Field in order to estimate the attitude of the spacecraft. Furthermore, we wanted to evaluate the size and direction of Geomagnetic Field to compare it with the standard I.G.R.F. (International Geomagnetic Reference Field) model and to verify the quality of the model.

Accelerometer:

The variation of the position provided by the accelerometer has been used to correct the location of the magnetic axes that provide the reference needed for the magnetometer.

4.1 Experiment Setup

This section is an overview of the experiment's conceptual structure. It describes the design subsystems and details the architecture used. The top-level block diagram of the experiment is shown in Figure 4-1.

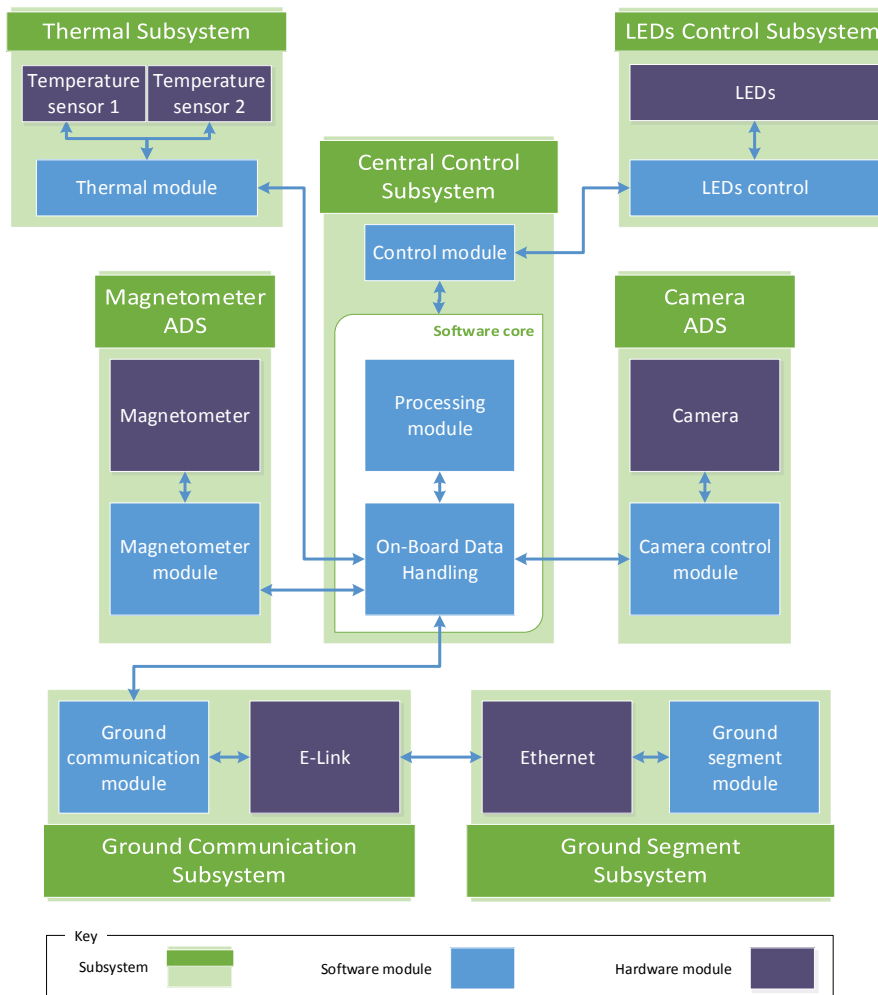


Figure 4-1 Experiment subsystems architecture

Table 4-1 Subsystem functions and components

| SUBSYSTEM | MAIN FUNCTIONS | COMPONENTS |
|---------------------------------|--|---|
| Central Control Subsystem (CCS) | <ul style="list-style-type: none"> • Software module scheduling | <ul style="list-style-type: none"> • On-Board computer (H/W) |



| SUBSYSTEM | MAIN FUNCTIONS | COMPONENTS |
|--|--|---|
| | <ul style="list-style-type: none"> • On-board data handling • Software error control • Power management | <ul style="list-style-type: none"> • On-Board Data Handling (S/W) • Processing module (S/W) • Control module (S/W) • Power supply PCB (H/W) |
| Camera Attitude Determination Subsystem (CADS) | <ul style="list-style-type: none"> • Camera control • Image processing • Attitude determination | <ul style="list-style-type: none"> • Camera module (S/W) • Camera (H/W) |
| Magnetometer Attitude Determination Subsystem (MADS) | <ul style="list-style-type: none"> • Magnetometer control | <ul style="list-style-type: none"> • Magnetometer module (S/W) • Magnetometer (H/W) |
| LEDs Control Subsystem (LCS) | <ul style="list-style-type: none"> • Box LEDs control | <ul style="list-style-type: none"> • LEDs control module (S/W) • LEDs (H/W) |
| Thermal Subsystems (TS) | <ul style="list-style-type: none"> • Temperature sensor | <ul style="list-style-type: none"> • Thermal module (S/W) • Temperature sensors (H/W) |
| Ground Communication Subsystem (GCS) | <ul style="list-style-type: none"> • Communication control • Data sent scheduling | <ul style="list-style-type: none"> • Communication module (S/W) • Ethernet connection (H/W) |
| Ground Segment Subsystem (GSS) | <ul style="list-style-type: none"> • Data receiving • GUI control • Uplink command controls | <ul style="list-style-type: none"> • Ground software (S/W) • Laptop computer (H/W) • Ethernet connection (H/W) |

The experiment setup, depicted in Figure 4-2, shows the connection details, the relationship between the components and the interfaces between them. For further information about the electronic design, the power supply lines and the voltage feeding every component, see Appendix C.1 Plans.

Figure 4-2 also shows the physical distribution of the components, which consists of two boxes: an inner box and an outer box. The former was placed inside the gondola, and the latter was mounted on a profile on the top of the vehicle with a critical constraint: it should be separated from the gondola at a sufficient distance to keep it away from magnetic disturbances. The configuration is showed in Figure 4-3 and is fully described in Mechanical Design section.

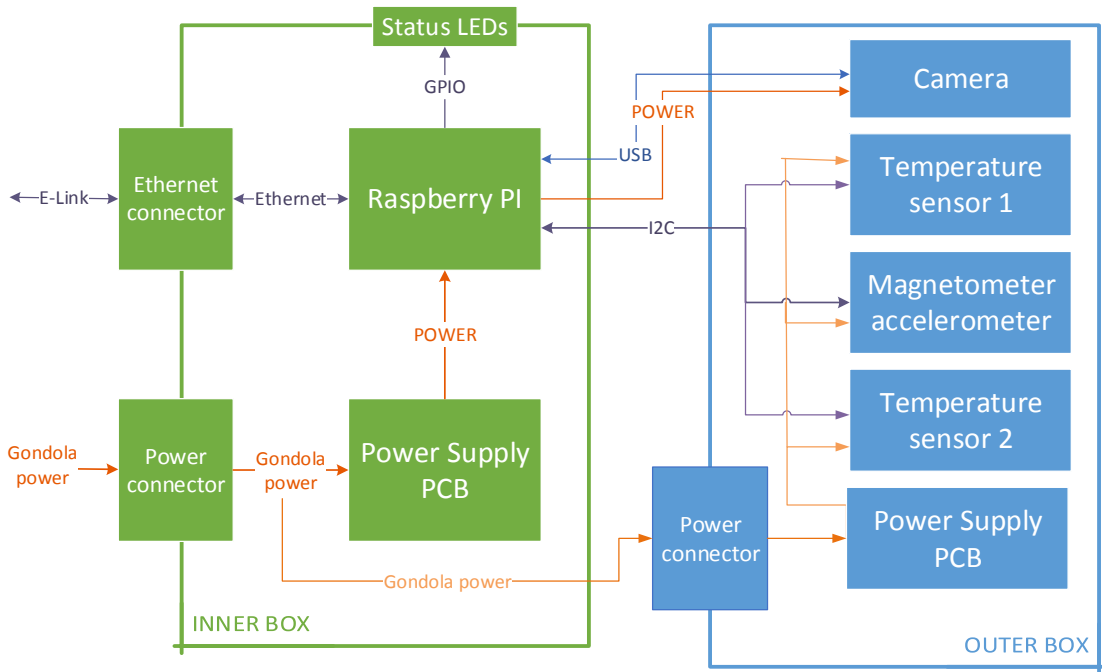


Figure 4-2 Interfaces between the different blocks

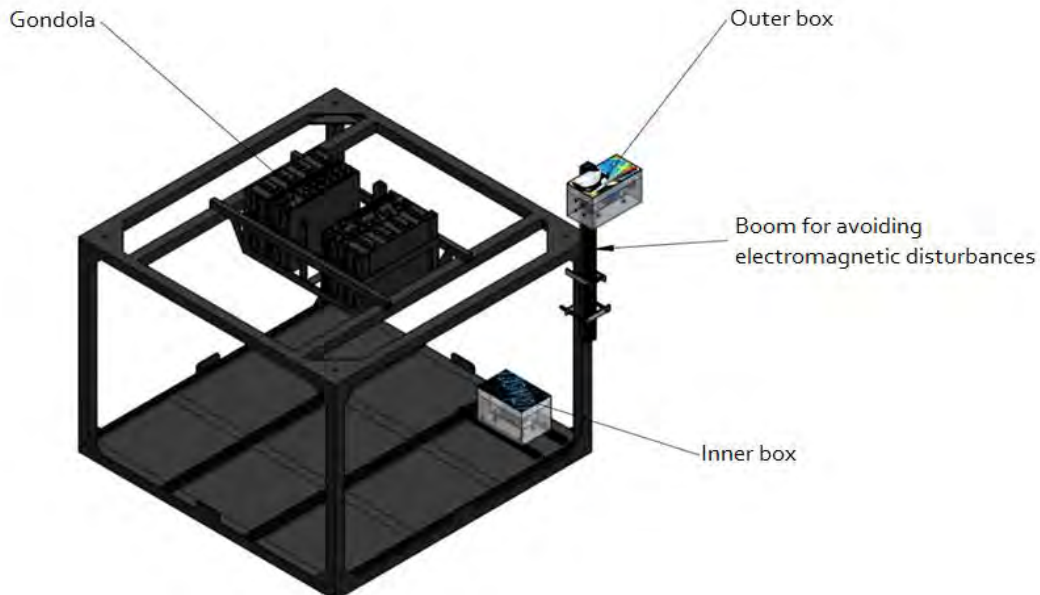


Figure 4-3 Physical distribution in the gondola

4.1.1 Central Control Subsystem

The structure of the CSS is the following:

The PCB was placed on top of the Raspberry Pi. The PCB has a stackable GPIO connector in order to make the Raspberry pins available to other uses. Both components were inside the inner box.

The connection with the gondola batteries was through the military MS3112E8-4P connector (see Figure 4-112) placed in one of the side panels of the box, as seen in Table 4-2, which describes the interfaces between the Central Control Subsystem and other devices of the experiment.

Table 4-2 Central control subsystem interfaces with the rest of the experiment

| Device | Interface |
|----------------------------|-----------------------|
| Camera | USB |
| Magnetometer/accelerometer | |
| Temperature sensor (1) | I ² C |
| Temperature sensor (2) | |
| E-Link system | MS3112E8-4P connector |



| Device | Interface |
|----------------------|-----------------|
| Gondola power system | Amphenol RJF21B |

4.1.2 Camera Attitude Determination Subsystem (CADS)

The CADS consists of a DMK 41BU02.H monochrome camera [7] (with a Sony ICX205AL CCD sensor) with a H1214-M lens mounted on it. It was placed in the outer box so that it framed the major part of the sky and, at the same time, the horizon of the Earth.

4.1.3 Magnetometer Attitude Determination Subsystem (MADS)

The MADS, placed in the outer box, consists of the following two sensors, both encapsulated in a LSM303DLHC module:

- A magnetometer sensor
- An accelerometer sensor

This module, together with the temperature sensor, was placed in a second PCB, placed in the outer box (see diagram in Appendix C.5 Electronics Schematics).

4.1.4 LEDs Control Subsystem (LCS)

Table 4-3 LEDs information code

| Status LEDs | Function | Blinking frequency (Hz) |
|-------------|----------------------------|-------------------------|
| Red | Camera | 1 |
| Green | Power ON | 1 |
| White | Magnetometer/Accelerometer | 1 |
| Blue | Ethernet | 1 |
| Orange | Image processing | 1 |

Description of functions:

- Camera: camera is working properly.
- Power ON: main experiment program is working properly
- Magnetometer/Accelerometer: sensor is working properly
- Ethernet: connection with the ground station is established
- Image processing: the attitude determination algorithms are working

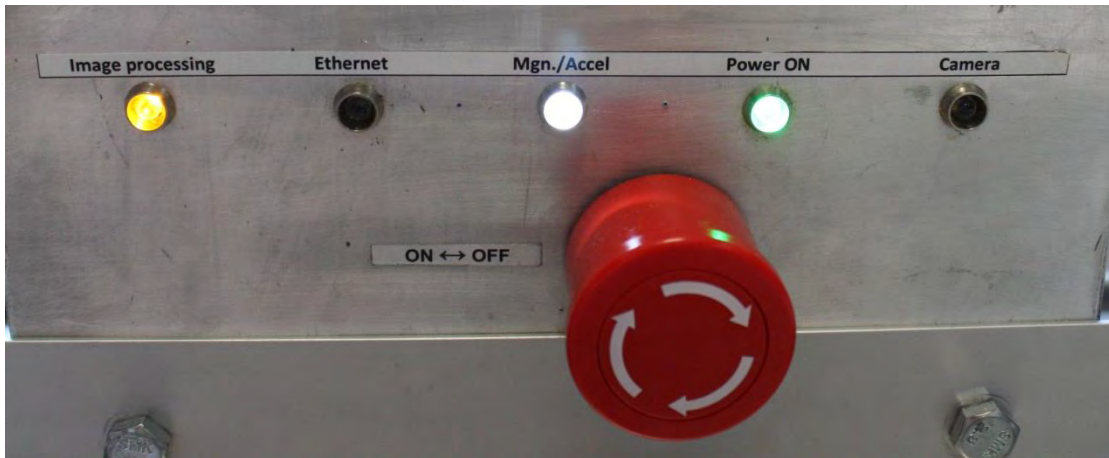


Figure 4-4 LEDs panel

4.1.5 Thermal Subsystem (TS)

The TS consists of two temperature sensors and its electronic power control, as shown in Figure 4-1.

All this elements were placed in the outer box. One of the sensors was close to the camera, in order to measure its temperature for potential overheating problems. The second sensor was used to measure the whole box temperature.

4.1.6 Ground Communication Subsystem (GCS)

The GCS consists of a communication module, which can be considered a submodule of the On-Board Data Handling, and the Ethernet connection with the E-Link system. The Amphenol RJF21B connector used for this purpose was mounted on the side panel of the inner box.



Figure 4-5 RJF21B CODE A insert

After the IPR, the Ethernet connector CODE A insert was properly assembled, as recommended in the BEXUS manual.

4.1.7 Ground Segment Subsystem (GSS)

The GSS consisted of a laptop computer in which the ground segment software run. As in the GCS, there was an Ethernet connection with the E-Link system.

4.2 Experiment Interfaces

4.2.1 Mechanical

The design consists of two different boxes connected through a 45 x 45 x 1,125 mm profile. The final design is shown in Figure 4-6.



Figure 4-6 Flight model of the experiment

They were connected to the gondola as follows:

4.2.1.1 Inner Box

The box was held to the gondola rails with transverse rails as described in Figure 4-7. We used M6 mounting bolts that passed through the gondola rails and held the rails that fixed the box. All the mounting bolts used washers, nuts and glue to ensure an adequate fixation.

The rails that connected with the gondola fixed the inner box with M6 bolts nuts and washers. Thread fixe glue was used to fix them.

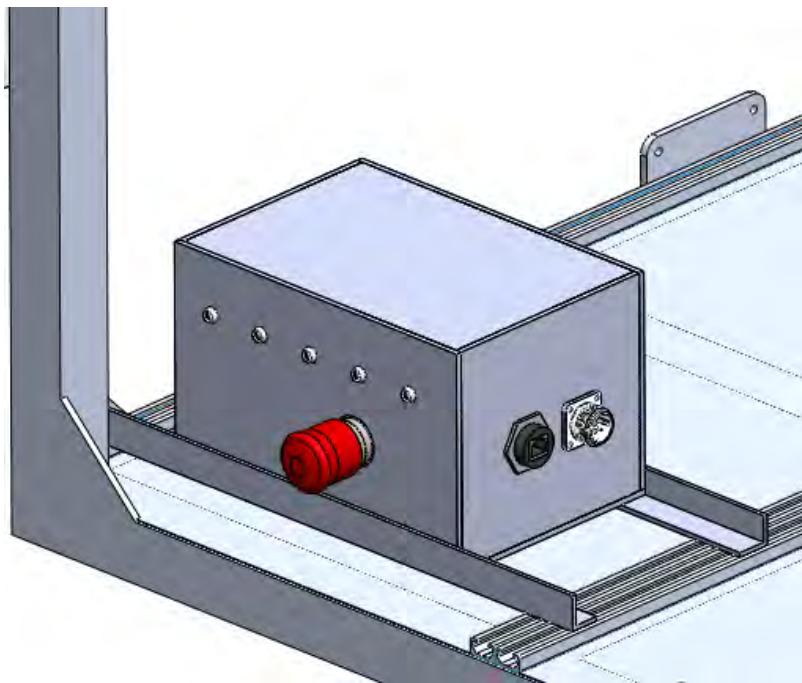


Figure 4-7 Mounting interface of the inner box

As the content inside the gondola is light by comparison to the aluminium box, we chose to put the box on the central part of the rails.

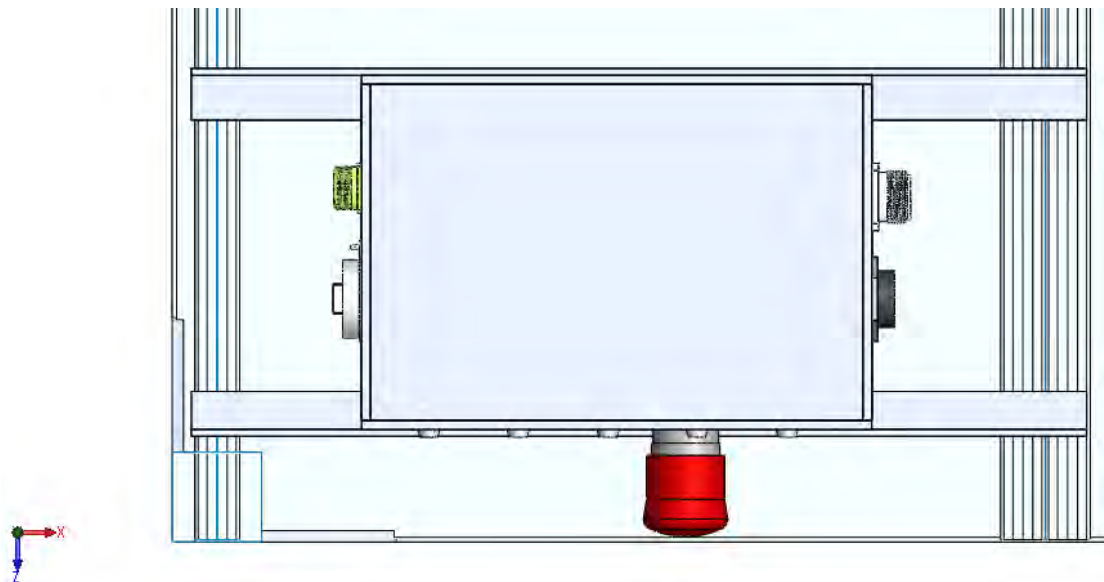


Figure 4-8 Top view of the inner box fixation

The flight model of the inner box is shown in Figure 4-9

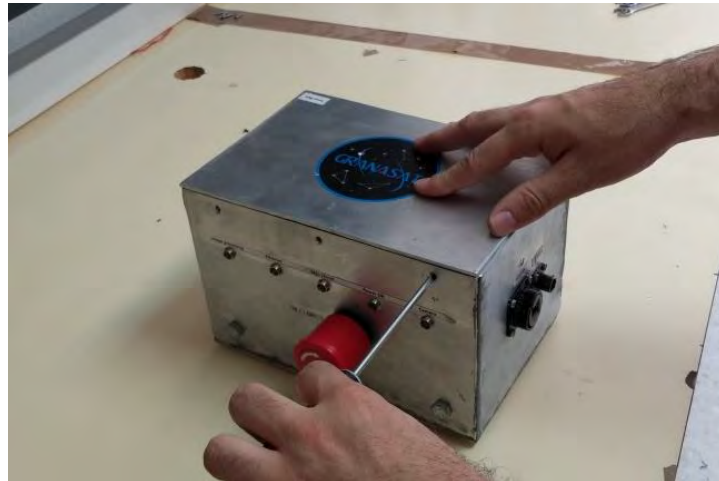


Figure 4-9 Flight model of the inner box

4.2.1.2 Profile

As described before, a profile had to be used to support the outer box. This allowed the outer box to avoid the electromagnetic disturbances produced inside the gondola, giving the magnetometer a chance to measure real values of the electromagnetic field of the Earth. Here, we decided to use the same approach as other BEXUS projects. In space applications the magnetometer is generally placed in an extended boom, as far from the spacecraft as possible. Magnetometers are sensitive to the magnetic fields created by electric currents and ferrous metal components, so the further away it is from the gondola, the better our measurements would be.

The profile chosen is the one with the biggest innertia moment and the most homogeneus mass distribution.

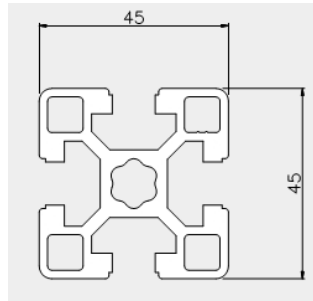


Figure 4-10 Profile

Table 4-4 Profile details

| | | |
|-----------------------------------|---------------|---------------|
| Area (mm ²) | 776 | |
| Weight (kg/m) | 2.1 | |
| Inertia moment (cm ⁴) | I · x = 15.22 | I · y = 15.22 |

With a length of 1,225 mm, the profile had to be positioned on one of the four edges of the gondola, and it used the following fixation:

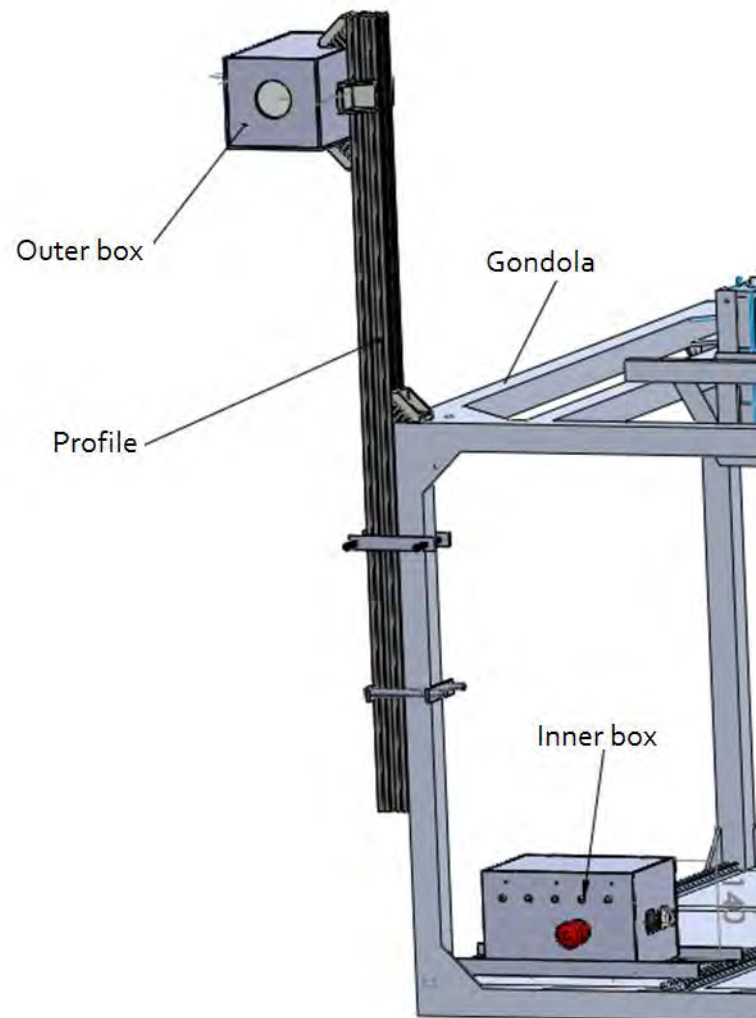


Figure 4-11 Interfaces profile-gondola

A junction element was attached to the profile to fix the 400 mm distance between the roof of the gondola and the outer box. The profile has open-end covers.

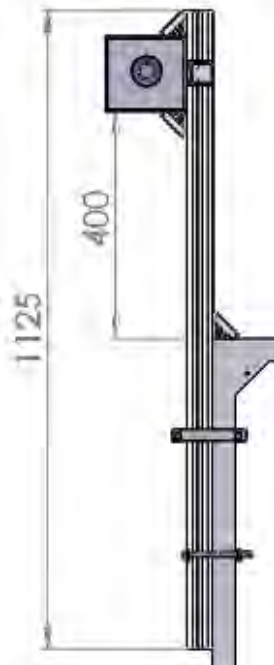


Figure 4-12 Details of the outer box height

The final assembly of the outer box with the boom is shown in Figure 4-13.



Figure 4-13 Flight model of the outer box

In order to avoid damages in the gondola during the campaign, a rubber piece between the boom and the gondola was used. The final procedure is shown in Figure 4-14



Figure 4-14 Rubber piece between boom and gondola

The attachments elements were as follows:

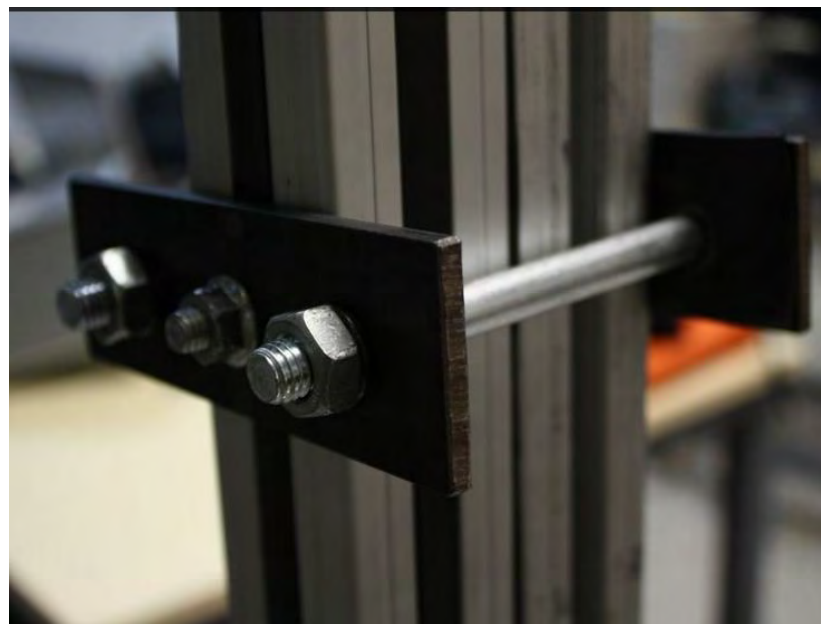


Figure 4-15 Detail of the attachment



These gripping elements were built with aluminium and M10 screws. Depending on the side, the screws had different lengths.

Table 4-5 Bolts in the mechanical interfaces

| Bolts | Length (mm) | Amount |
|-------|-------------|--------|
| M10 | 110 | 4 |
| M8 | 20 | 8 |
| M6 | 60 | 7 |
| M6 | 20 | 9 |
| M4 | 10 | 24 |
| M3 | 40 | 2 |
| M2 | 4 | 4 |

Table 4-6 Nuts in the mechanical interfaces

| Nuts | Amount |
|------|--------|
| M10 | 4 |
| M8 | 8 |
| M6 | 7 |
| M6 | 9 |
| M4 | 24 |
| M3 | 2 |
| M2 | 0 |

Table 4-7 Washers in the mechanical interfaces

| Washer | Amount |
|--------------|--------|
| M10 | 4 |
| M8 | 8 |
| M6 | 13 |
| M6 (plastic) | 6 |
| M4 | 24 |
| M3 | 2 |
| M2 | 0 |

For safety reasons, a safety cable of 4 mm was used to fix the profile and the outer box to the gondola. This cable is made of steel.

4.2.1.3 Requirements for the Mechanical Interfaces

The box inside the gondola had to be as close as possible to the profile to have short I²C wires. It was as defined in Figure 4-12. Thus, communication was robust, and data did not have to be retransmitted through I²C.

4.2.2 Electrical

Table 4-8 Interface with the E-Link system

| | |
|-----------------------|------------|
| Data rate of downlink | 500 Kbit/s |
| Data rate of uplink | 0.1 Kbit/s |
| Protocol | TCP/IP |
| Connector type | Ethernet |

4.3 Experiment Components

A further detailed experiment components table can be seen in C.6 Electronics Components.

Table 4-9 Experiment summary

| | | |
|---|--------------|--|
| Experiment mass (in kg): | Outer box | 2.195 |
| | Inner box | 2.630 |
| | Profile | 1.643 |
| | Attachments | 1.546 |
| | Total | 8.014 |
| Experiment dimensions (in m): | Outer box | 0.142 x 0.128 x 0.248 |
| | Inner box | 0.157 x 0.144 x 0.228 |
| | Profile | 0.045 x 1.125 x 0.045 |
| Experiment footprint area (in m ²): | Outer box | $35.216 \cdot 10^{-3}$ |
| | Inner box | $35.796 \cdot 10^{-3}$ |
| | Profile | $2.025 \cdot 10^{-3}$ |
| | Total | $73.037 \cdot 10^{-3}$ |
| Experiment volume (in m ³): | Outer box | $4.508 \cdot 10^{-3}$ |
| | Inner box | $5.155 \cdot 10^{-3}$ |

| | | |
|---|--------------|---|
| | Profile | $2.531 \cdot 10^{-4}$ |
| | Total | $9.916 \cdot 10^{-3}$ |
| Experiment expected COG (centre of gravity) position (in m): | Outer box | X = -0.005 Y = 0.018 Z = 0.013 |
| | Inner box | X = -0.480 Y = -0.430 Z = 1.620 |
| | Profile | X = 0 Y = 0 Z = 0 |

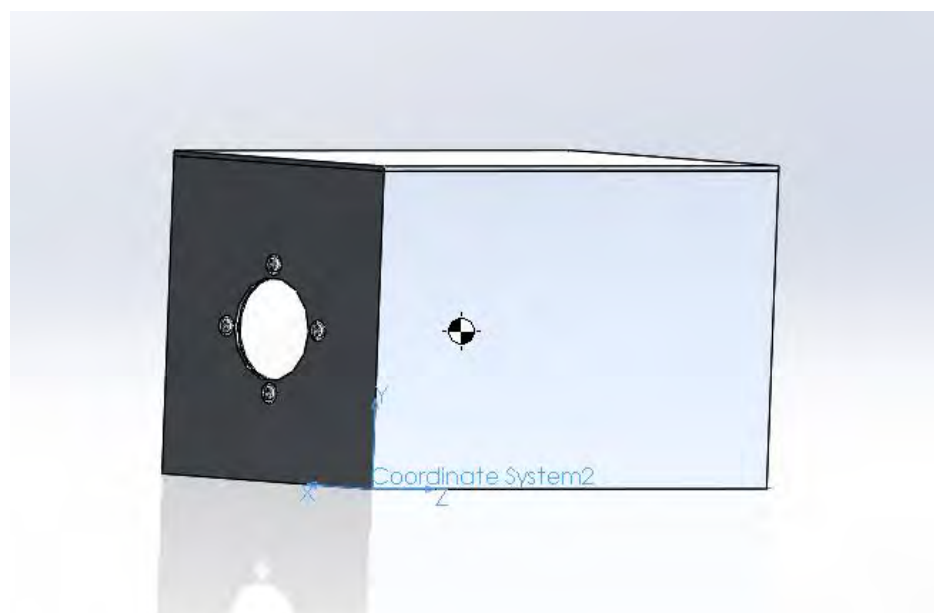


Figure 4-16 Outer box

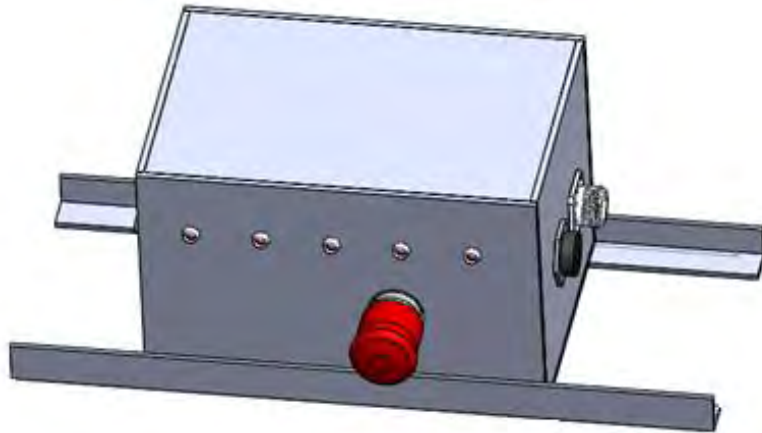


Figure 4-17 Inner box

4.4 Mechanical Design

Table 4-10 Experiment dimensions (in m)

| | |
|-----------|-----------------------|
| Inner box | 0.157 x 0.144 x 0.228 |
| Outer box | 0.142 x 0.128 x 0.248 |
| Profile | 0.045 x 1.125 x 0.045 |

4.4.1 Inner Box

The box was built using aluminium, and will have 40 mm extruded polystyrene (XPS) insulation. It housed the Raspberry Pi and the power electronics:

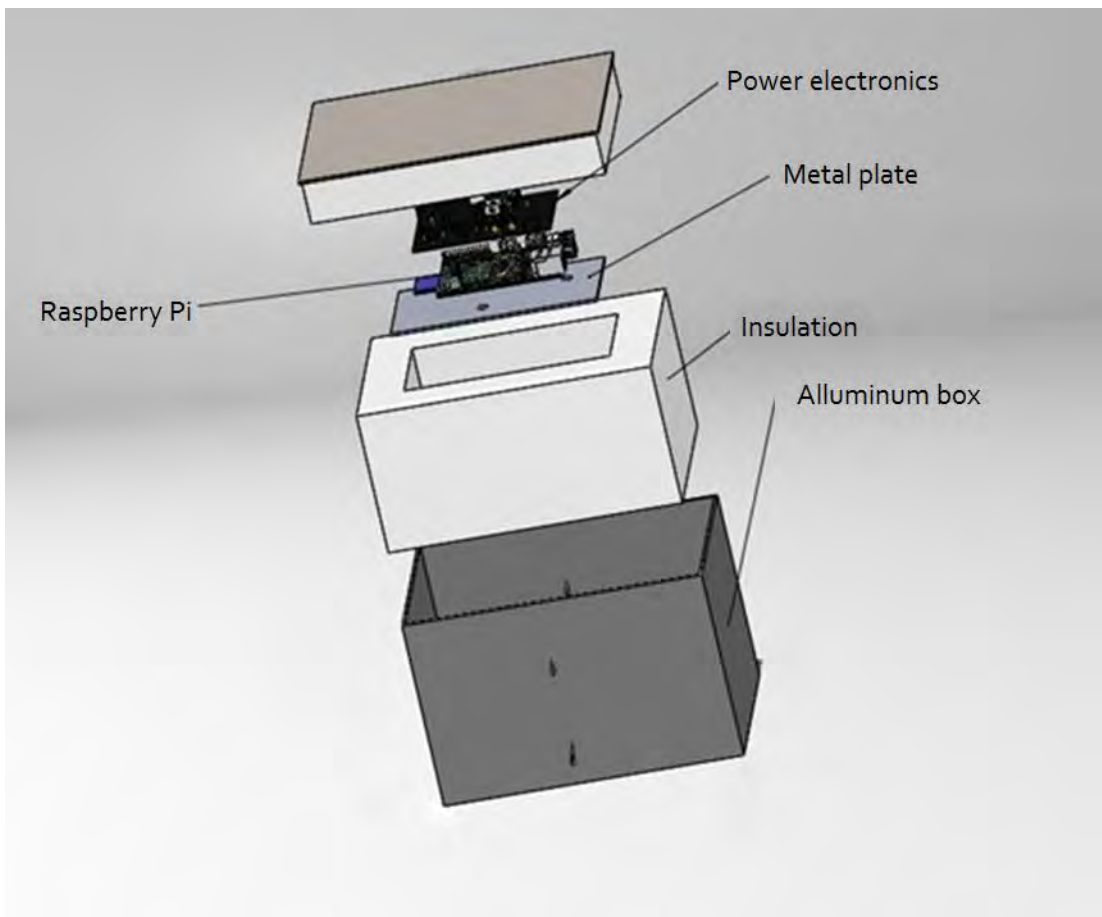


Figure 4-18 Inner box

The metal plate for support was held to the aluminium box as described in 4.2.1. All the elements inside this box were fixed to the metal plate for support using the mounting holes of the Raspberry Pi and the GPIO pin.

The Raspberry Pi was fixed to the metal plate through 2xM3 screws, nuts and washers. These screws passed through the Raspberry and were used to fix the power electronics. The power electronics were fixed by these screws and supported by the GPIO through an adaptor.

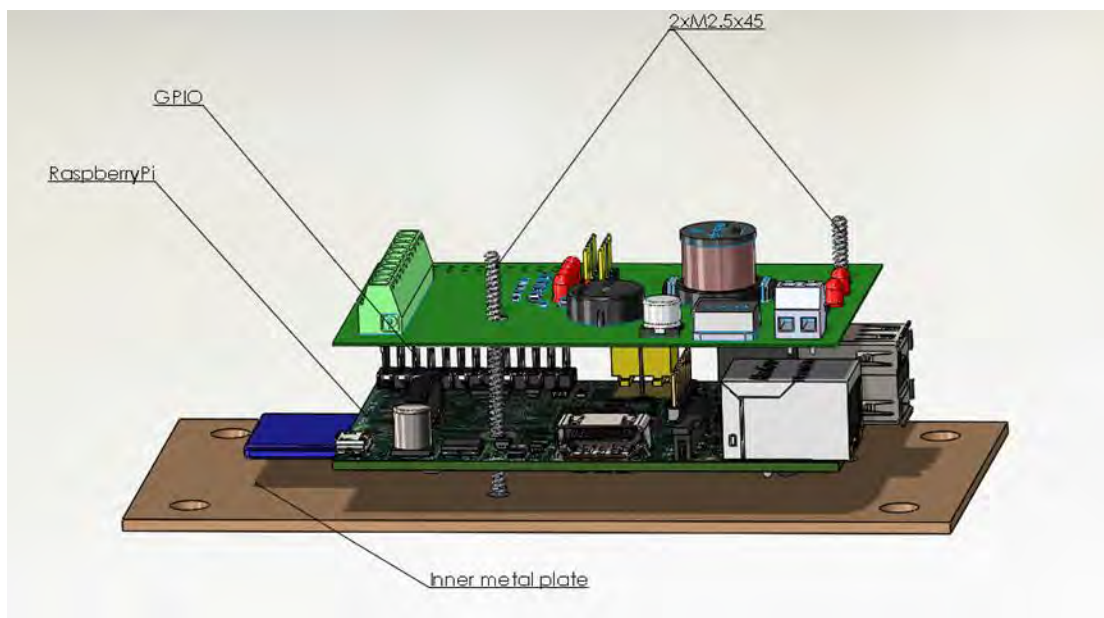


Figure 4-19 Raspberry Pi and power electronics fixation to inner box

4.4.2 Outer Box

The camera and a PCB that controls the magnetometer and which has two separate temperature sensors were inside this box.

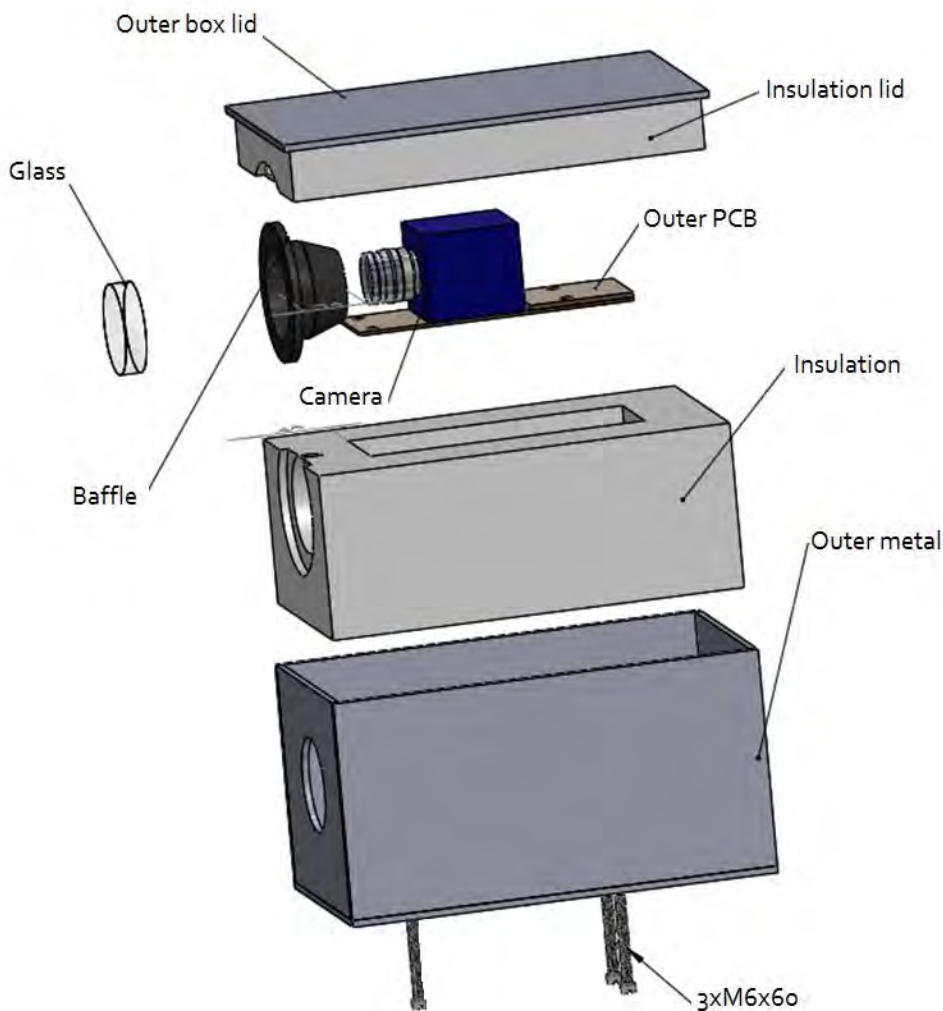


Figure 4-20 Outer box extruded view

As seen in the figure, a baffle was used to protect the camera from any possible damage to the lens and to stop sunbeams harming the pictures.

4.4.2.1 Baffle

To determine the length of the baffle, we used the following formula:

$$\frac{\phi_{PE}}{f} = \frac{1}{1.4} \quad (\text{Eq. 4-1})$$

which used data from the camera and lens manufacturer:

$$(1) f' = 12 \text{ mm} \pm 5\%$$



(2) Max. Aperture Ratio (A.R): 1:1.4

(3) Iris Range: F/1.4 to F/16

(4) Field of View: Vertical 21.88°, Diagonal 35.69° and Horizontal 28.91°

(5) Picture format: 6.4 × 4.8 mm

(6) Focusing Range Inf. to 0.25 m

(7) Back Focal Length: 11.50 mm

(8) Flange Back Length: 17.526 ± 0.05 mm

4xM4 were used with its corresponding nuts and bolts to fix it to the metal box. This glass was an IR filter. The glass was fixed inside the baffle by the pressure of the baffle against the box:



Figure 4-21 Baffle fixing



Figure 4-22 Baffle details



Figure 4-23 3D printed baffle

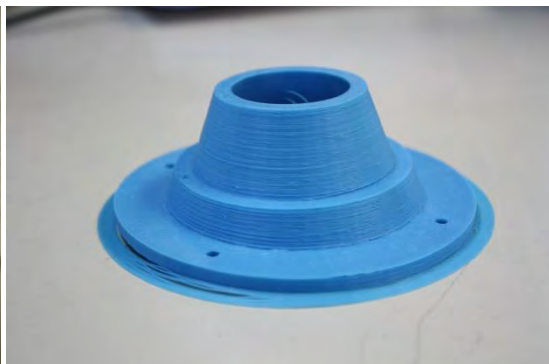


Figure 4-24 3D printed baffle

The baffle was covered to avoid dust, dirt and finger prints that were removed before flight as described in 6.1.4.2.

4.4.2.2 Camera Fixing

We used the four mounting holes available in the camera to fix it to the mounting plate:

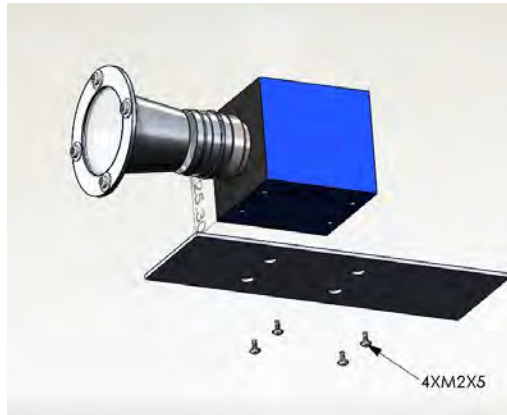


Figure 4-25 Camera fixing

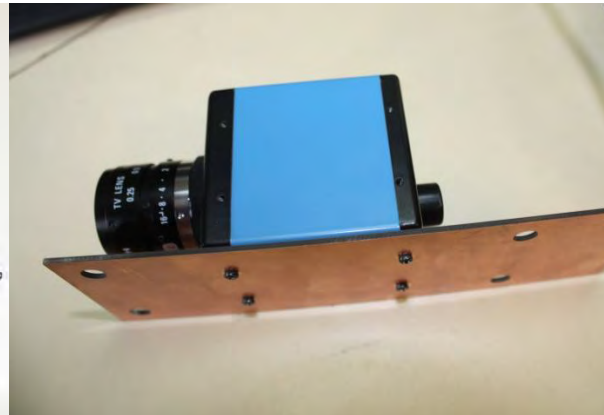


Figure 4-26 Camera fixed

4.4.2.3 PCB Fixing

3xM3x45 screws were used to attach the PCB to the metal support. By comparison with the box, the weight of the camera is small; it was designed to be attached using the mounting holes.

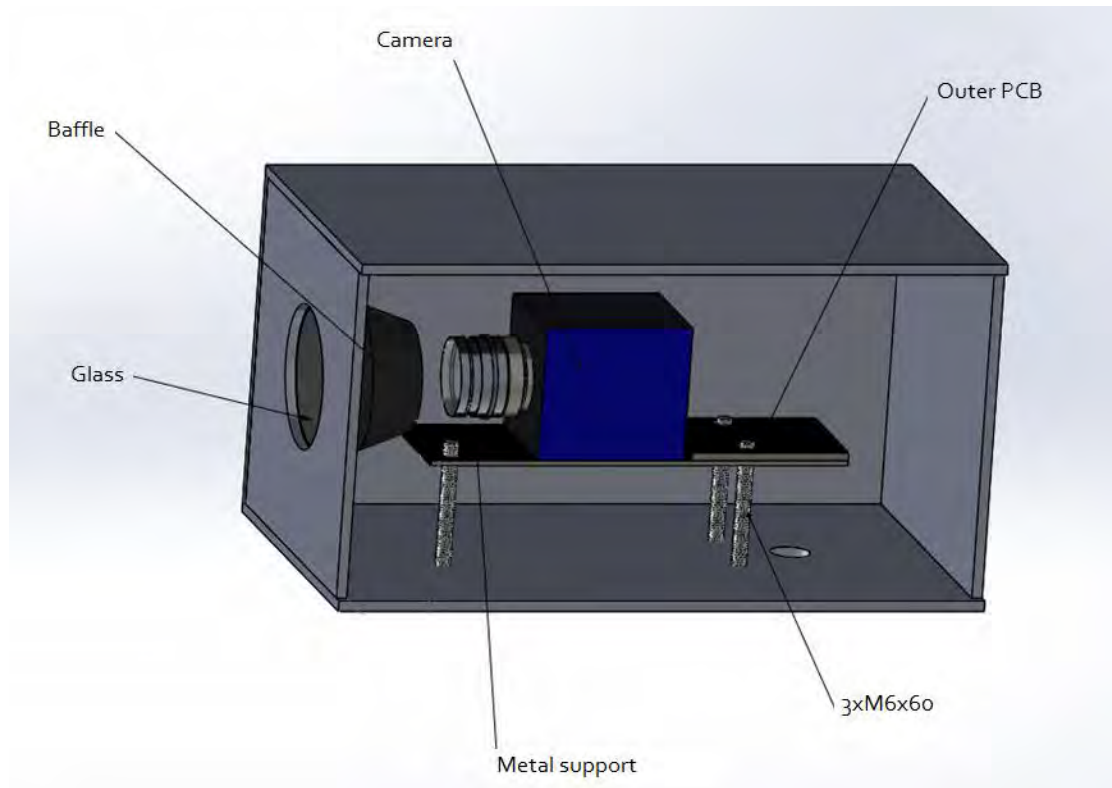
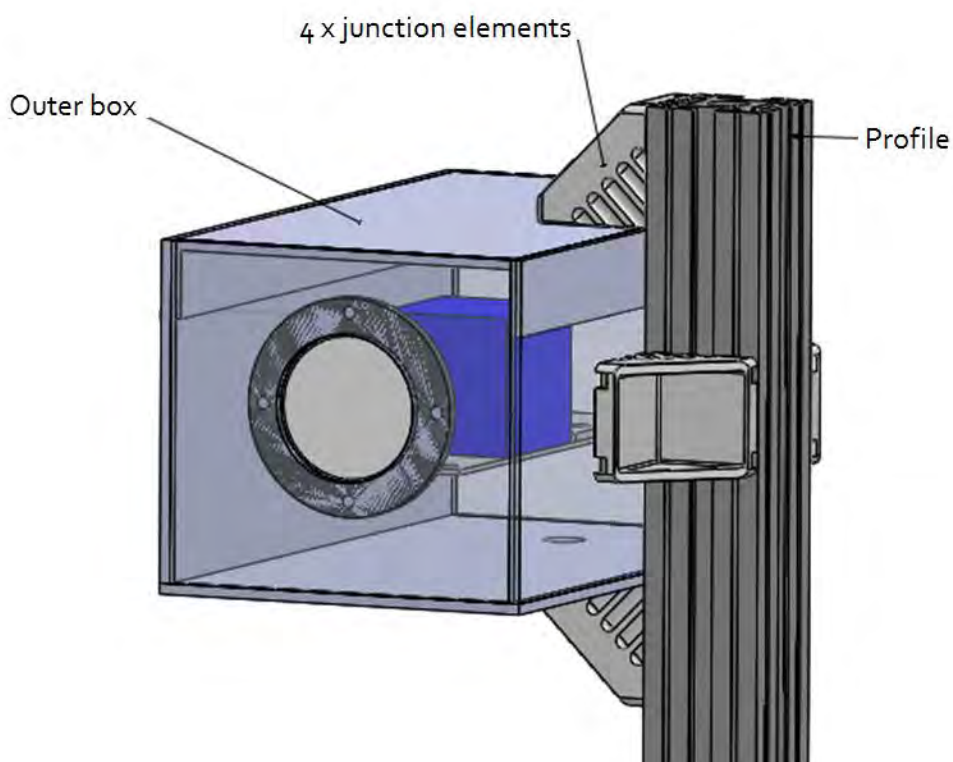


Figure 4-27 Outer box overview**4.4.3 Outer Box Assembly with the Profile**

To fix the outer box properly, we decided to use the approach followed in other BEXUS experiments. We decided to fix it on two points:

- 2 M6 screws attached it directly to the profile.
- 4 M6 junction elements connected the profile with the bottom of the aluminium box.

**Figure 4-28 Junction element****Figure 4-29 Outer box assembly with the profile**

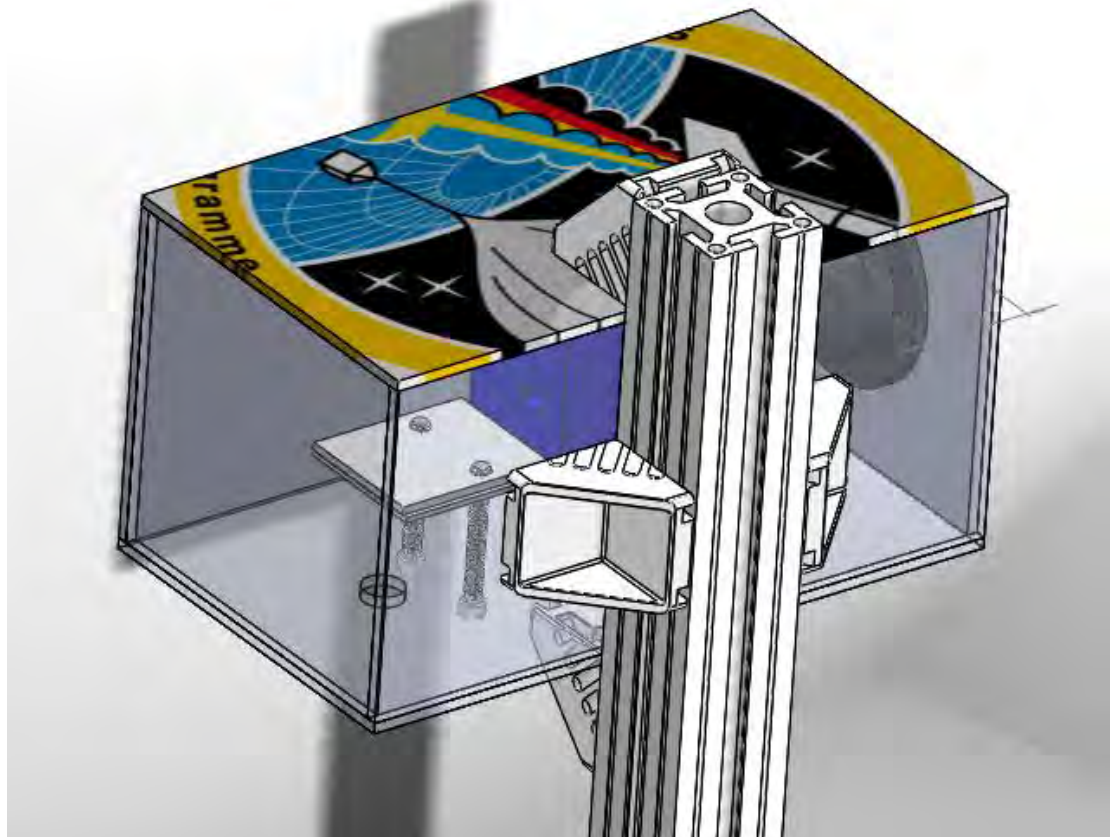


Figure 4-30 Details of the profile attachment with the outer box

After the discussions with the experts at the PDR sessions we decided to use this approach at two points.

An electricity tube was connected to the outer box through the element in Figure 4-31. This tube was fixed to the gondola with flanges and it had a thermal insulation. It was used to get the wires to the outer box.



Figure 4-31 Connection for the wires that go to the outer box

4.4.4 Box Closure

Six screws were used in order to fix the cover to the box. Methods used in both cases were the same. The nut of each bolt was fixed through welding to the cover, and when the box was closed, a screw passed through to close it completely. The closing method can be seen in the next figure:

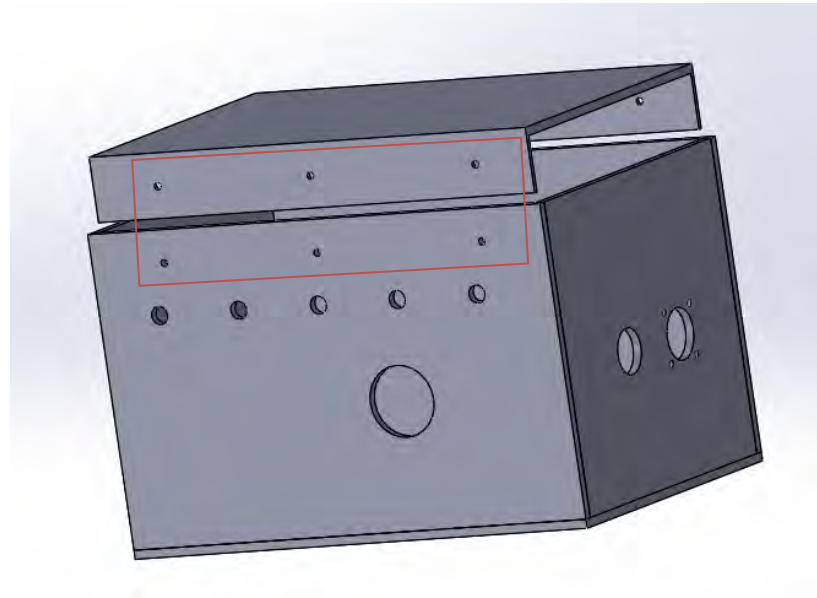


Figure 4-32 Holes to fix the cover

The closure was changed not long before the Launch Campaign and its performance needed to be checked. Instead of waiting for the vibration test results, we decided to do a fast analysis with SolidWorks Simulation. The model, shown in Figure 4-33, was

specifically designed for this study. Everything is made of aluminium except the bolts, which are made of steel.

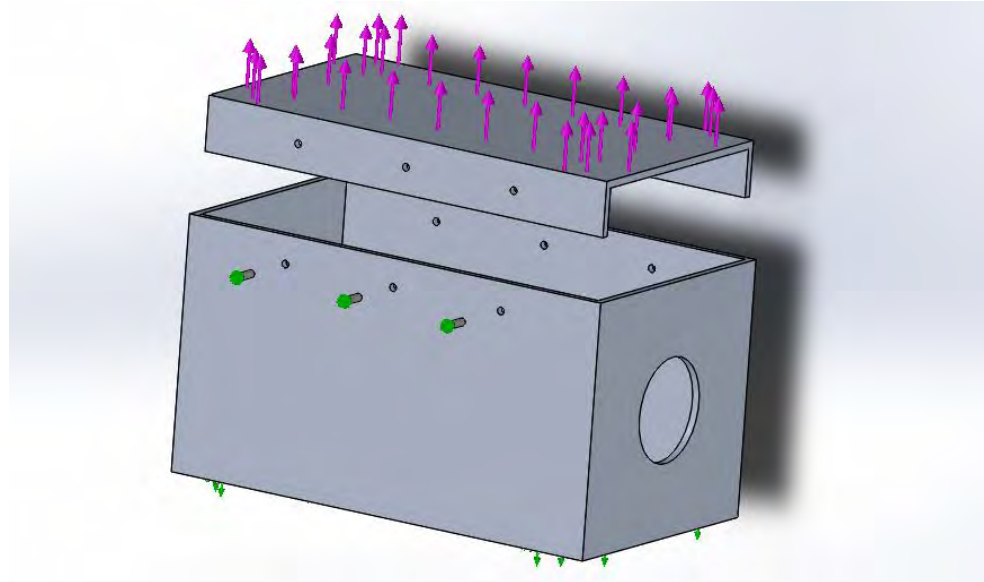


Figure 4-33 SolidWorks model of the outer box, lid and bolts

A force of 500 N was assumed to be applied on the lid, trying to open the outer box. This force is supposed to be produced by a great acceleration, up to 100 g. After the automatic meshing, stress distribution was calculated as it is depicted in Figure 4-34 and Figure 4-35.

The inside of the outer box is shown in Figure 4-34. The most stressed part there is the lid, in green colour, which is around 10 MPa. The aluminium yield stress is 27 MPa, thus there are no problems expected with this new lid. In addition, because of the linear process, it would take a force of 270 g to produce some damage to the box.

In Figure 4-35 we focussed on the bolts. In order to prevent the outer box from opening, there is a stress concentration on the bolts which is up to 20 MPa, very far from the steel yield stress, which is about 480 MPa. Therefore, we concluded we were not going to expect any kind of failure in the box closure.

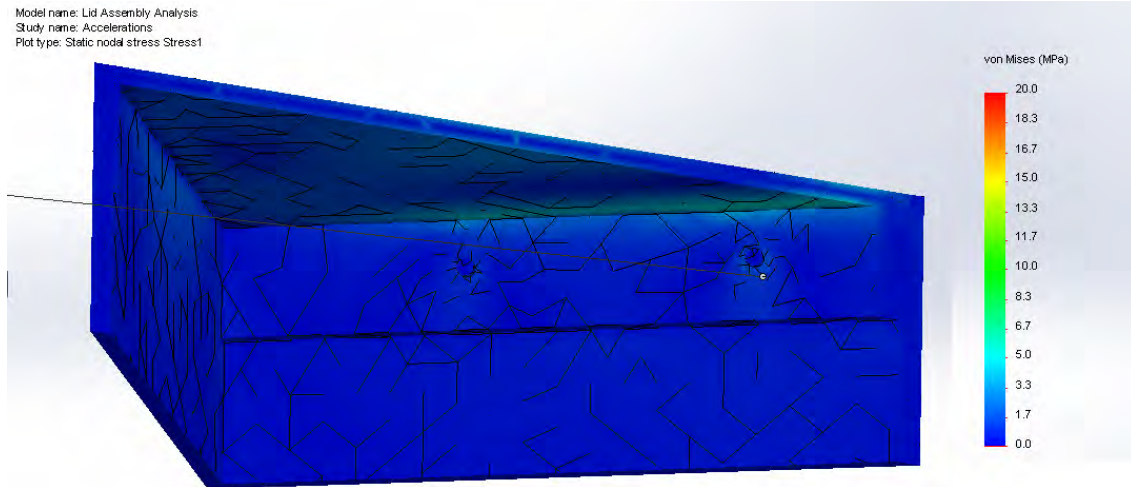


Figure 4-34 Stress distribution on the lid - inside of the box-

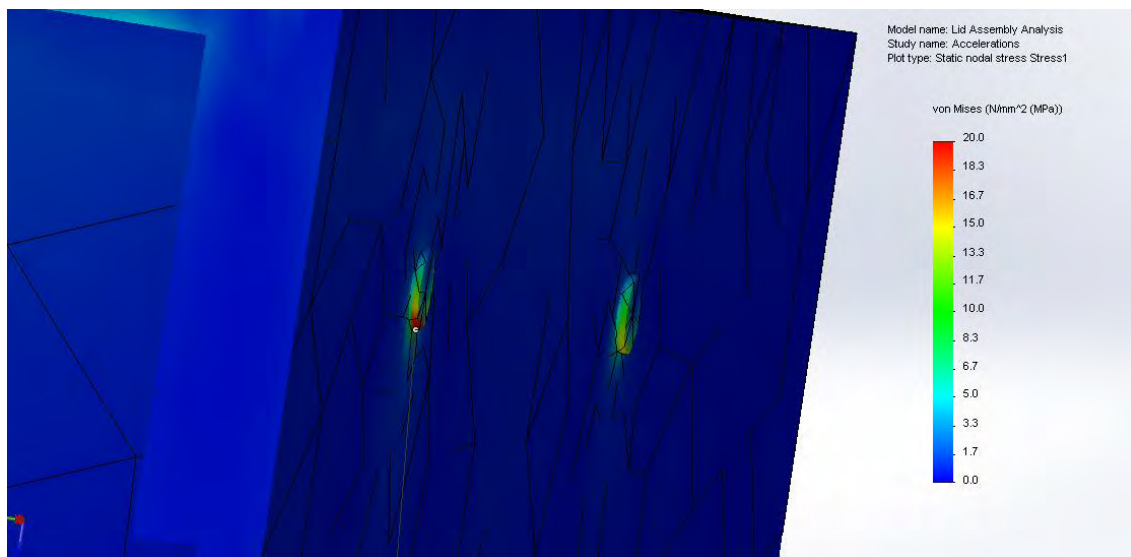


Figure 4-35 Stress distribution on the bolts

4.4.5 Mechanical Simulations

Using SolidWorks Simulation, we calculated stresses and displacements of both models in the following cases:

- We used a random vibration test to consider a wide range of loads during the flight: manipulation, aerodynamic turbulence and impacts, among others.
- A linear dynamics test where design loads correspond to accelerations of 10 g vertically and ± 5 g horizontally, because of the parachute opening.

In every simulation, we aim to prove that displacements are not so great as to damage the internal components and stresses are lower than the yield stress of the material.

A static load simulation was considered at first, but results were not as representative those of the other simulations.

4.4.5.1 Outer Box

The main characteristic of this assembly is the boom length; the longer it was, the better the magnetometer would work. However, if the boom length was too long, the outer box could have suffered small vibrations that would have made the camera useless because of the low stiffness. In addition, free space had to be left to fix the outer box properly.

Random vibrations:

We simulated a random dynamic test lead to the x-axis of the model, as a safety measure, it is the worst case scenario. The profile simulated is shown in Figure 4-36.

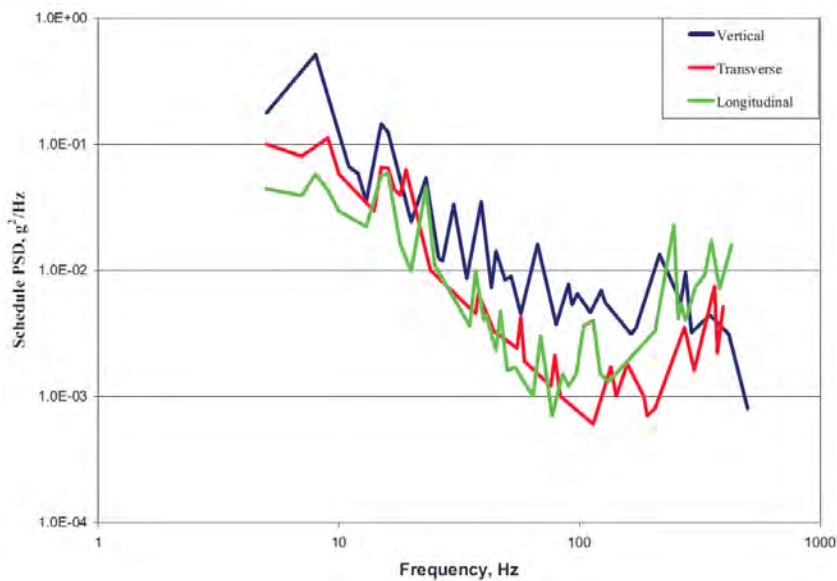


Figure 4-36 Random vibrations profile from a composite wheeled vehicle. The three profiles are used, each one for each axis.

Stresses displacements were calculated with a curvature based mesh. Results are shown in Figure 4-37 and Figure 4-38.

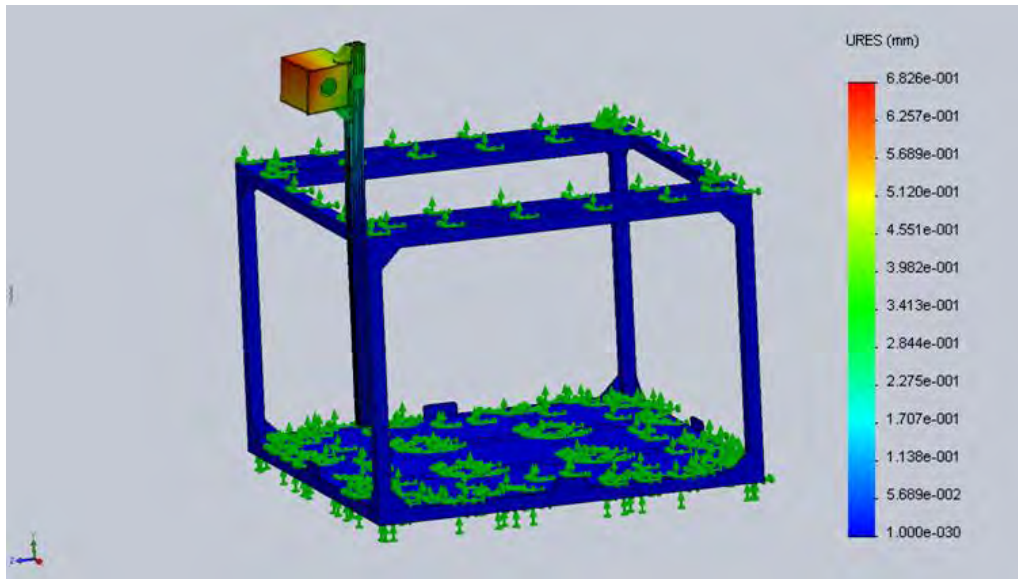


Figure 4-37 Displacements of the random vibration simulation

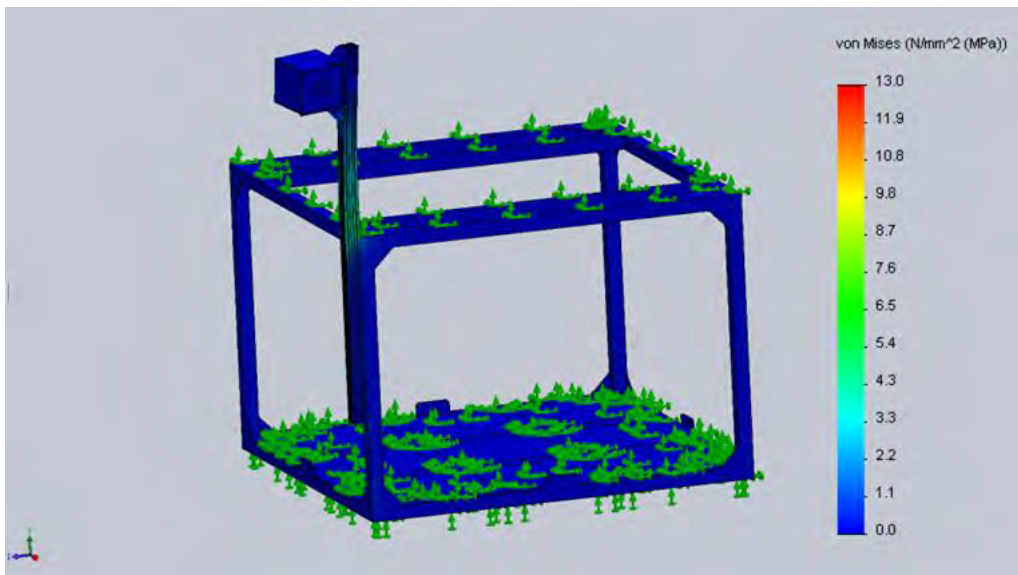


Figure 4-38 Von Mises' stresses, i.e., probability of elastic failure. The bluer is the colour, the lower is the stress

The maximum stress is produced where the profile is attached to the gondola, reaching near to 4.4 MPa. The aluminium yield stress is 28 MPa, so the outer box was safe as the von Mises' criterion stipulates.

To perform a 3σ confidence level is enough to multiply the maximum RMS stress 3 times, giving us 13.2 MPa stress.

Accelerations:

Parachute opening causes accelerations that must be considered in design stage. For vertical accelerations a force producing a 10 g force was considered. Since we could not assume that the gondola is a rigid body, it was hard to know how great the force must be to produce a 10 g acceleration. Being conservative, we assumed a force of 4,000 N applied in the upper side of the gondola, where the parachute is attached. Similarly, we assumed a force of 2,000 N for horizontal accelerations. Results are shown in Figure 4-39 and Figure 4-40.

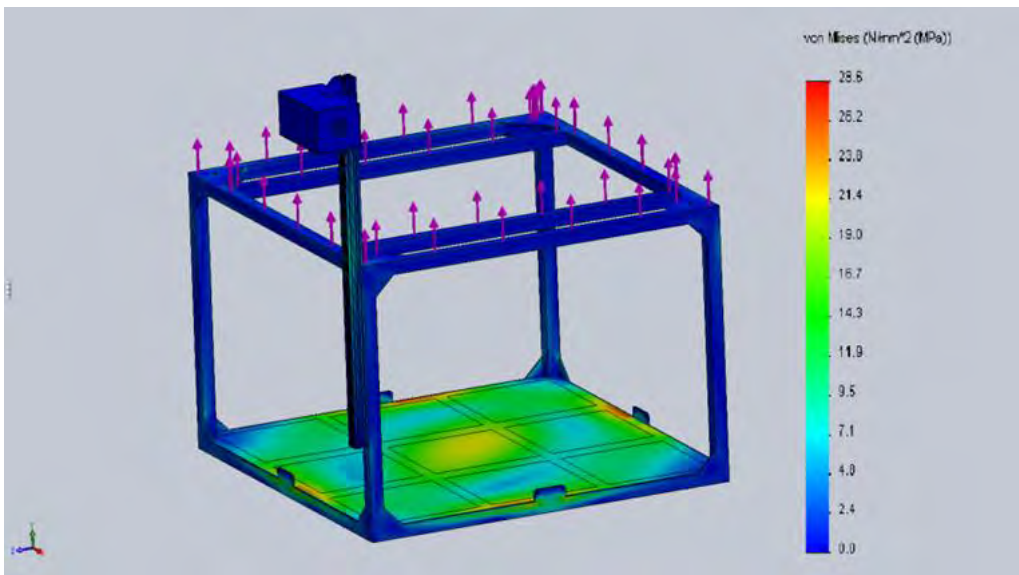


Figure 4-39 Von Mises' stresses of the 10 g acceleration simulation

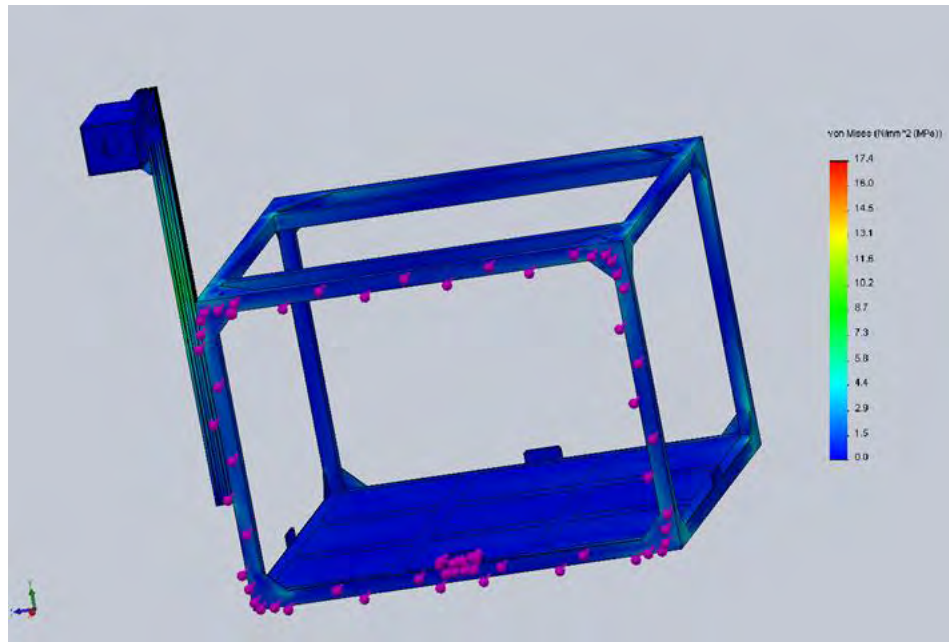


Figure 4-40 Von Mises' stresses of the 5 g acceleration simulation

Considering opposite signs of the forces, results were the same. Stresses in the outer box were negligible.

The evolution in time of max stressed node are shown in Figure 4-41.

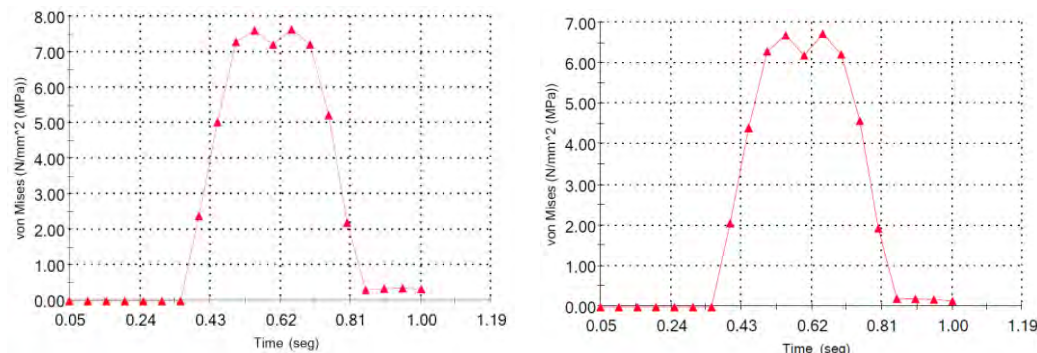


Figure 4-41 Time evolution of max stressed node with 10 g (left) and 5 g (right) accelerations

Modal analysis

In this analysis we wanted to study the dynamical response of the structure under vibrational excitation.

The frequencies of the first, second and third modes of vibration are 43.69 Hz, 50.89 Hz and 86.11 Hz respectively. Their simulation can be seen on the next three figures:

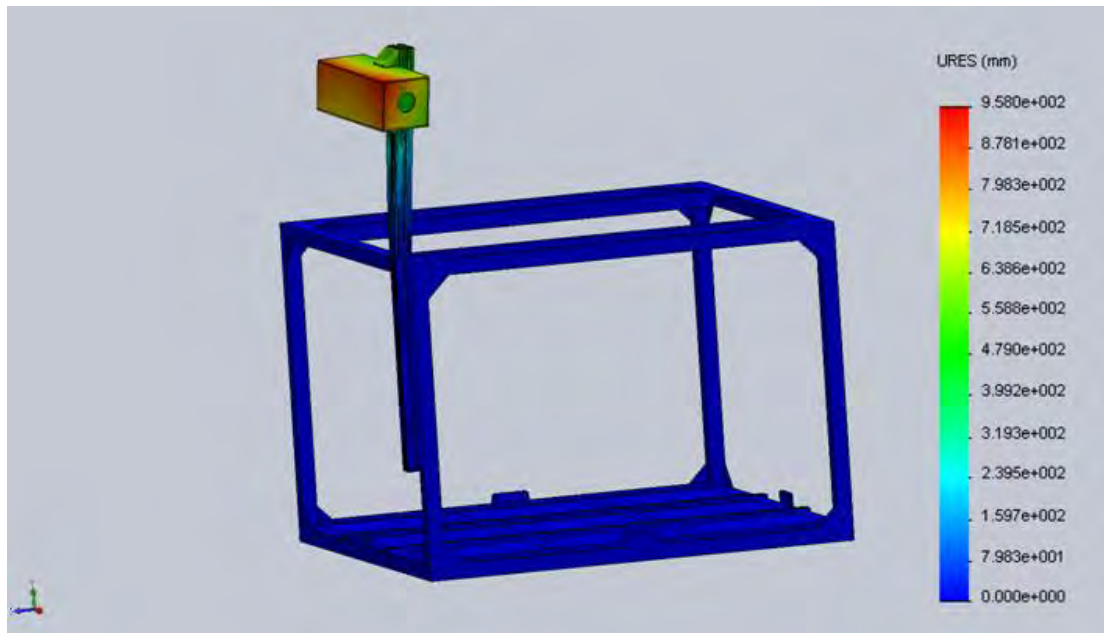


Figure 4-42 Shape of the first mode of vibration

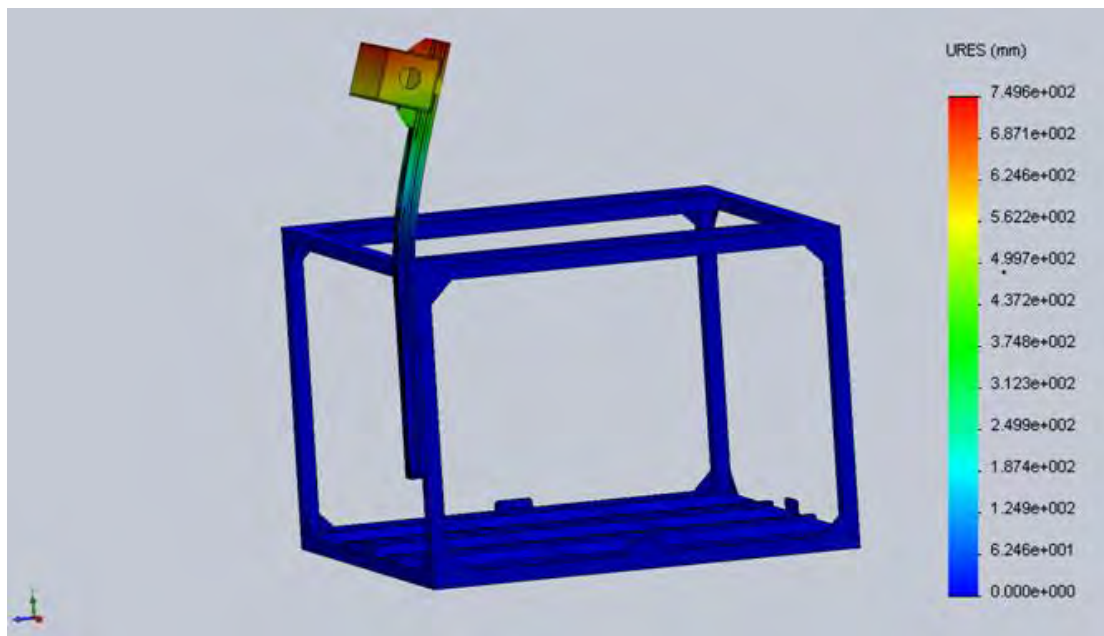


Figure 4-43 Shape of the second mode of vibration

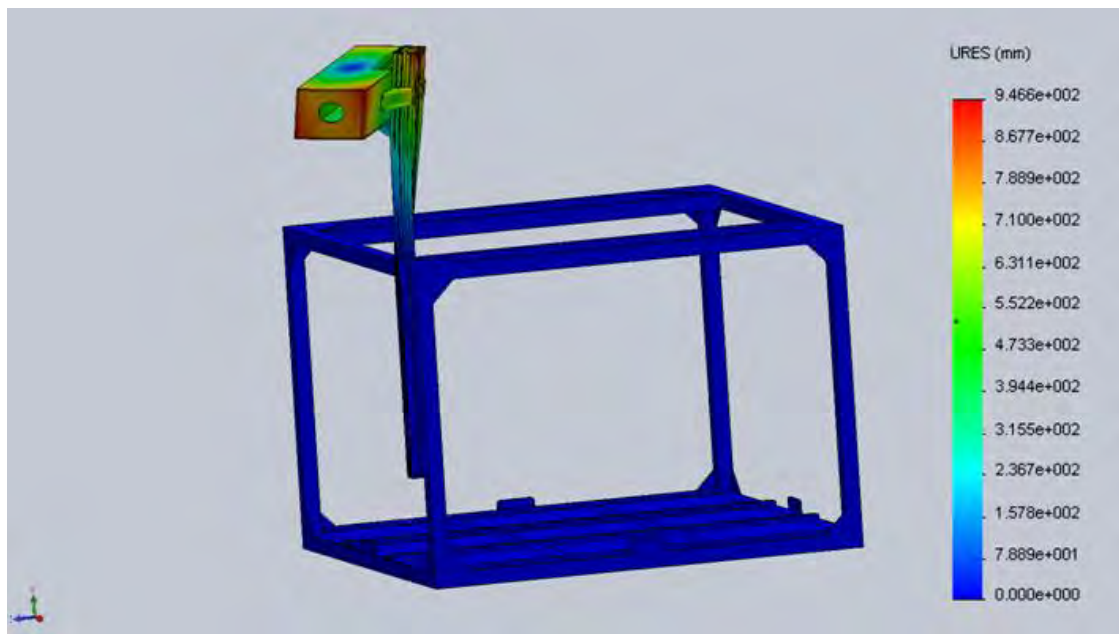


Figure 4-44 Shape of the third mode of vibration

Modal characterisation

Once all mechanical simulations were performed, assumptions and mechanical properties had to be verified. We decided to prepare a simple experiment to check the frequency of the first vibration mode and the damping ratio.

The outer box was attached to the boom and the boom was attached to a very rigid structure, maintaining the same orientation and distribution as if it were attached to the gondola in order to reproduce the flight conditions in the most realistic manner. Finally, an accelerometer was inserted into the outer box to register accelerations of free vibration movements and shaking.

We proceeded by starting the accelerometer recording, as shown on Figure 4-45, and by hitting and shaking the boom. With this, we could record the movement and made a simple Fourier analysis to calculate the frequencies that form the response.

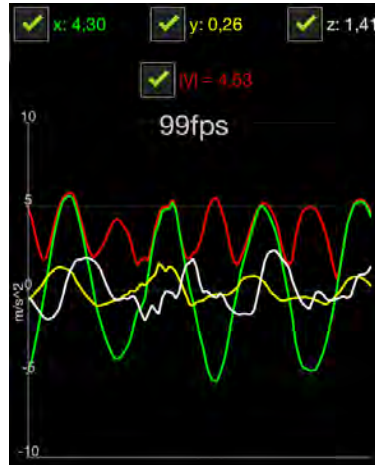


Figure 4-45 Screenshot of the accelerometer working

With the acceleration given in the three components x, y and z, and its modulus, and using MATLAB, Fast Fourier Transformation (FFT) can be performed easily. In Figure 4-46, a peak near to 20 Hz in x and y component can be observed. However, z component does not show any dominant frequency.

Instead of working with acceleration components, if the FFT of the acceleration modulus response was calculated, a peak near 40 Hz, which corresponds with the frequency of the first mode of vibration (43.67 Hz), would have been obtained. Greater modes could not be obtained since the sampling frequency was 100 Hz and, according to Nyquist-Shannon theorem, peaks over 50 Hz after FFT analysis cannot be found.

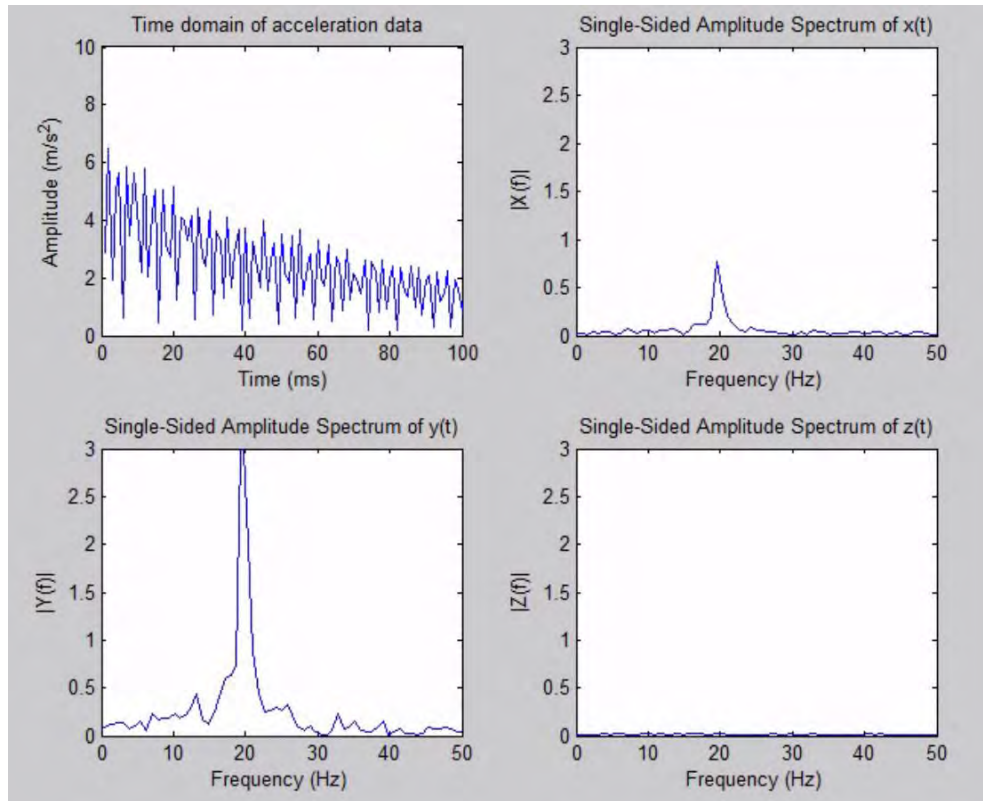


Figure 4-46 Acceleration modulus (up-left) and FFT of x, y and z components

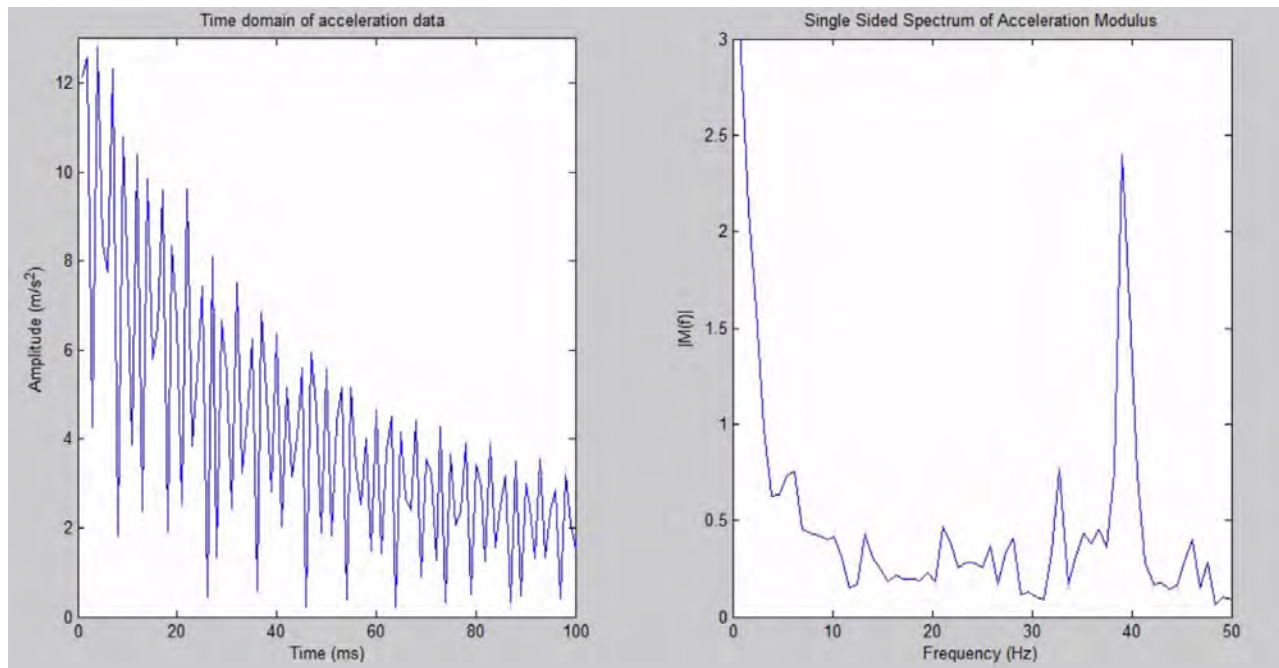


Figure 4-47 Acceleration modulus (left) and FFT of the acceleration modulus (right)

With acceleration samples, damping ratio can also be calculated. Using notions of damped vibrations the peaks of a damped free vibration have to be found. In Figure 4-48, there is an acceleration register that was used to determine the damping ratio of the system camera-boom.

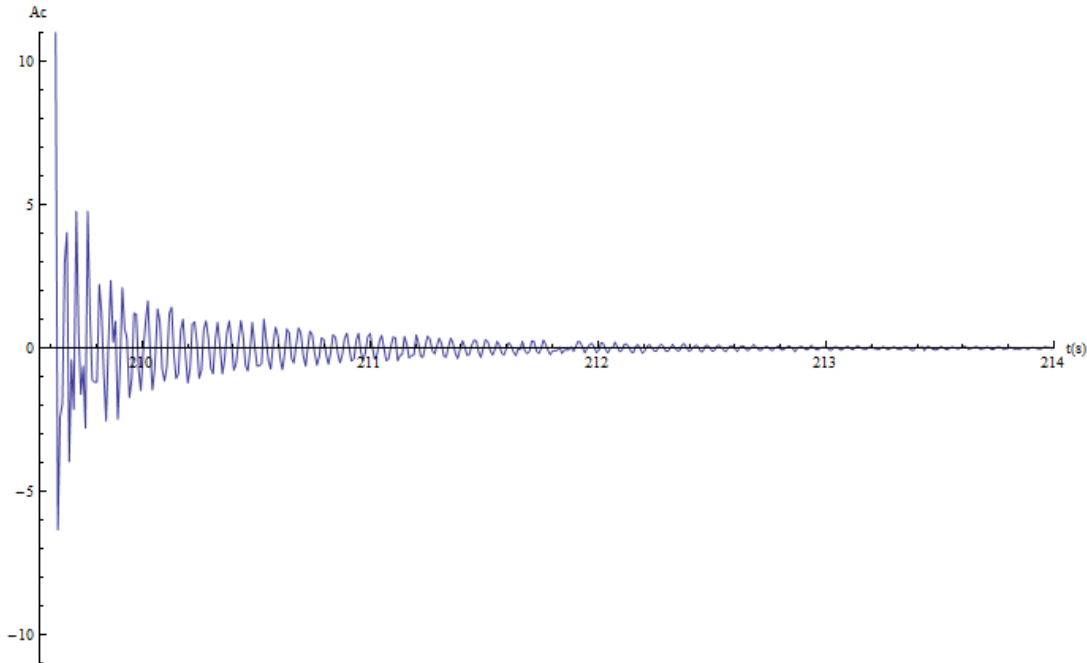


Figure 4-48 Acceleration register of a free vibration test

The relation between the ratio of two successive peaks of a damped vibration and the damping ratio is as follows:

$$\log\left(\frac{a_i}{a_{i+1}}\right) = \frac{2\pi\xi}{\sqrt{1-\xi^2}} \quad (\text{Eq. 4-2})$$

Where a_i represents the peaks and ξ is the damping ratio. These peaks should represent a decay of the motion. However, the sampling frequency was not high enough to ensure that the following peak is lower than the previous one. Thus, damping measurements have a great variance. In Figure 4-49, possible damping ratios are shown.

Assuming the arithmetic mean as a good estimator, damping ratio ξ is 6.66 %. During mechanical simulations a damping ratio of 5 % was considered and we assumed a close enough and conservative value.

In conclusion, our hypothesis on mechanical simulations were correct and our results were consistent.

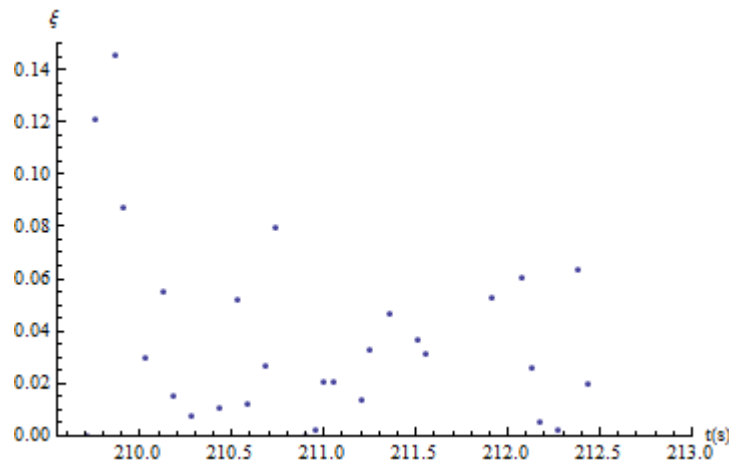


Figure 4-49 Possible damping ratios calculated from the free vibration test

4.4.5.2 Inner Box

Although the inner box was placed inside the gondola, meaning it is structurally safer, results were the same.

Random vibrations:

Using the same acceleration spectral density plot, fixations, damping ratio and mesh, results were produced as shown in Figure 4-50 and Figure 4-51:

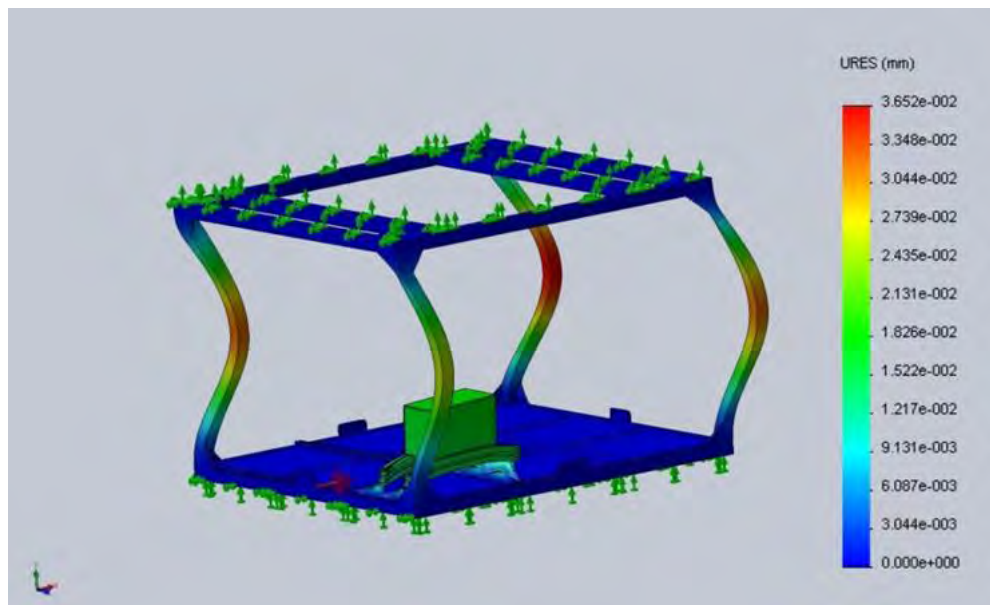


Figure 4-50 Displacements of the random vibration simulation

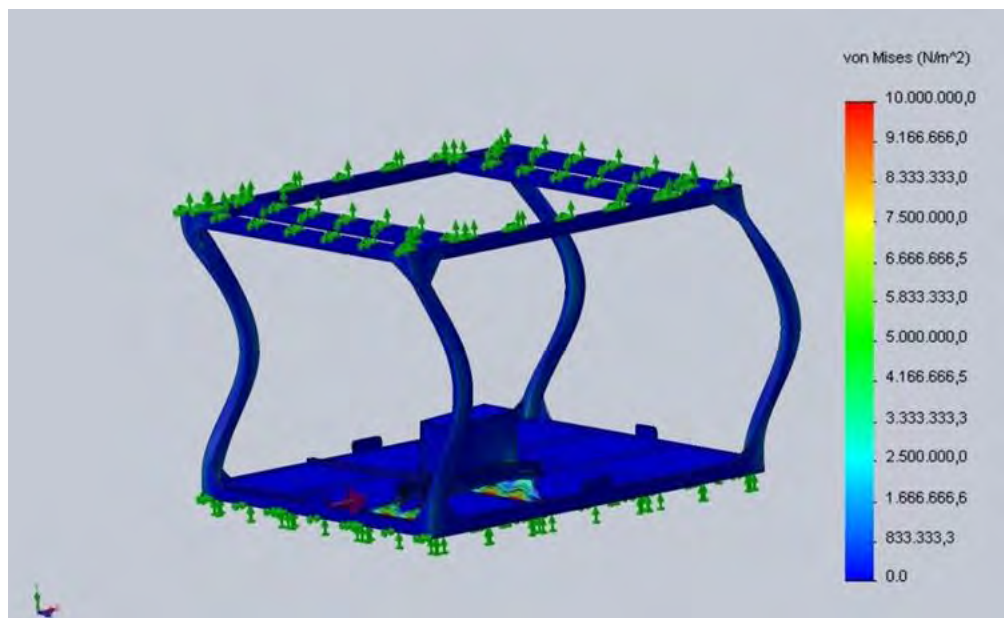


Figure 4-51 Von Mises' stresses of the random vibration simulation

In this case, displacements were lower calculated in random vibration simulation for the outer box. The maximum displacements for the inner box and the aluminium profiles are near to $2.5 \cdot 10^{-2}$ mm.

Moreover, stresses are lower but they approach 10 MPa on steel rails. There were no special safety measures to take as the maximum stress is very far from the yield stress, but we needed to take care of connections to avoid stress concentrations.

Accelerations:

Using the same time-force plot, fixations, damping ratio and mesh, results were produced as shown in Figure 4-52 and Figure 4-53.

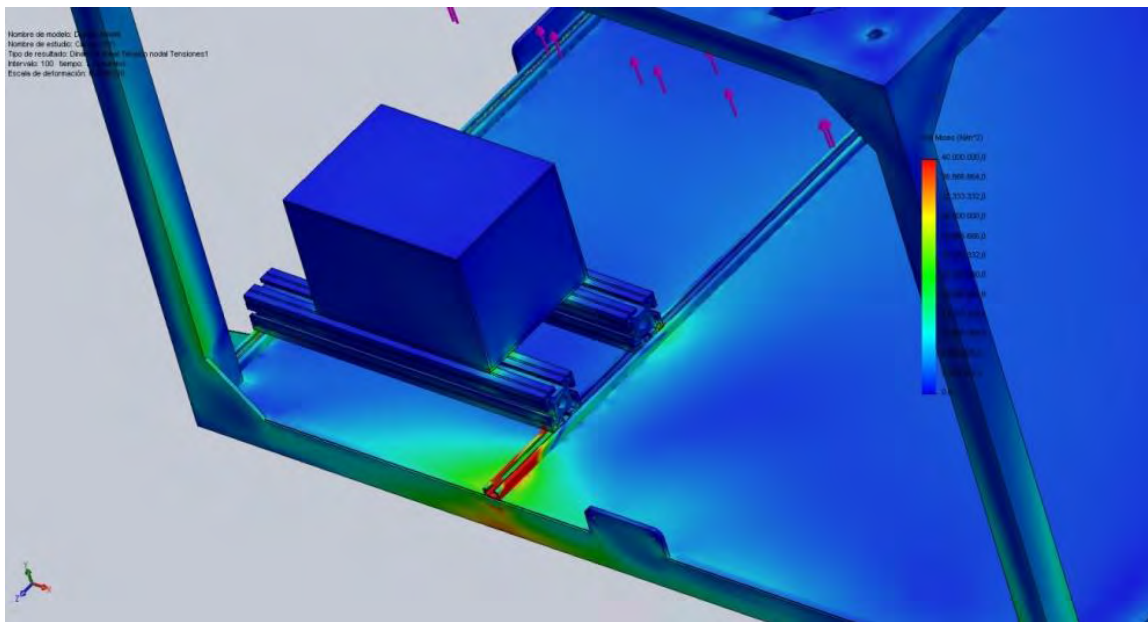


Figure 4-52 Von Mises' stresses of the 10 g acceleration simulation

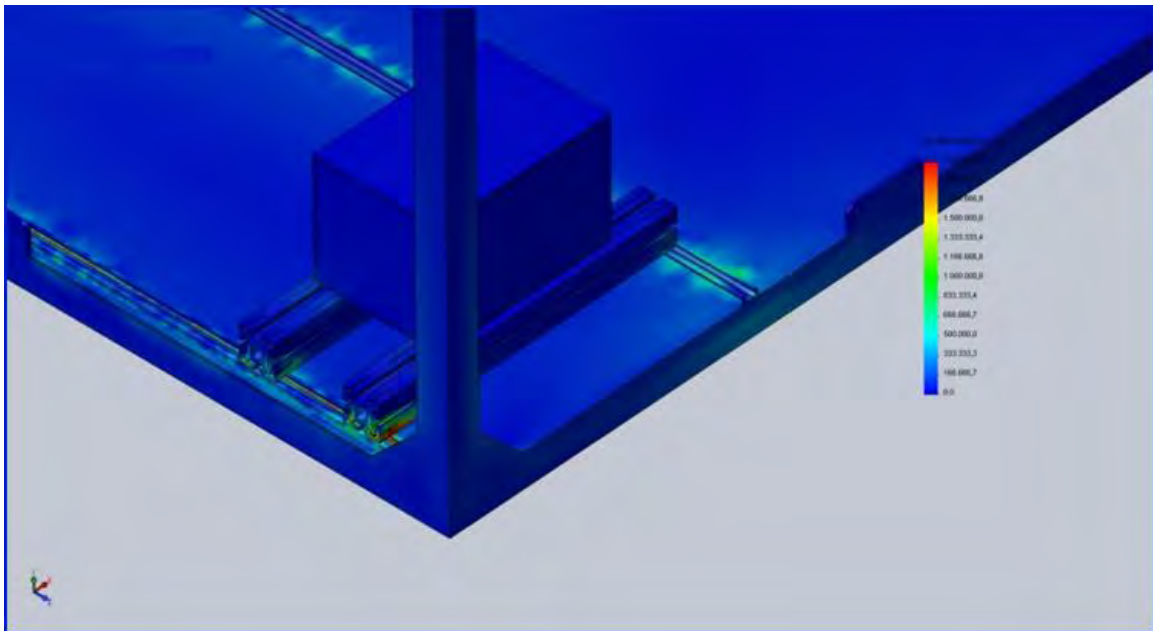


Figure 4-53 Von Mises' stresses of the 5 g acceleration simulation

Stresses in the box and aluminium profiles (near to 2.5 MPa maximum) are lower than the outer box case and extremely low when compared to the yield stress of aluminium. Steel stresses are higher but yield stress of steel is even higher (235 MPa).

In conclusion, the design would resist random vibrations and accelerations of 10 g vertically and ± 5 g horizontally.

4.4.5.3 PCB Hole Stress Analysis

To perform holes for the supporting bolts on PCBs did not affect the structural safety of the plates. Modelling the problem in SolidWorks Simulation we could predict the behaviour of the plate on any shake expected. For example, being pessimistic, a 10 g and a 5 g acceleration at a time could be assumed to get a representative result.

PCB material is known to be FR4 (sometimes written as FR-4), glass-reinforced epoxy laminate plate. SolidWorks does not have this material available in its databases. Thus, we had to introduce the FR4 characteristics ourselves. The FR4 was assumed as an isotropic material and a Young's Modulus of 25 GPa, a Poisson's Ratio of 0.12 and a yield stress of 30 MPa were considered. Hole dimensions near the edge are the shortest distances measures in every hole on the PCBs, around 1.5 mm and 2 mm.

Assuming the mass of the PCB and its components is 0.3 kg, forces due to expected accelerations are, distributed on the bolts, 15 N along X and 10 N along Y. After meshing a piece of the plate containing a bolt, stresses were calculated as it is shown in Figure 4-54.

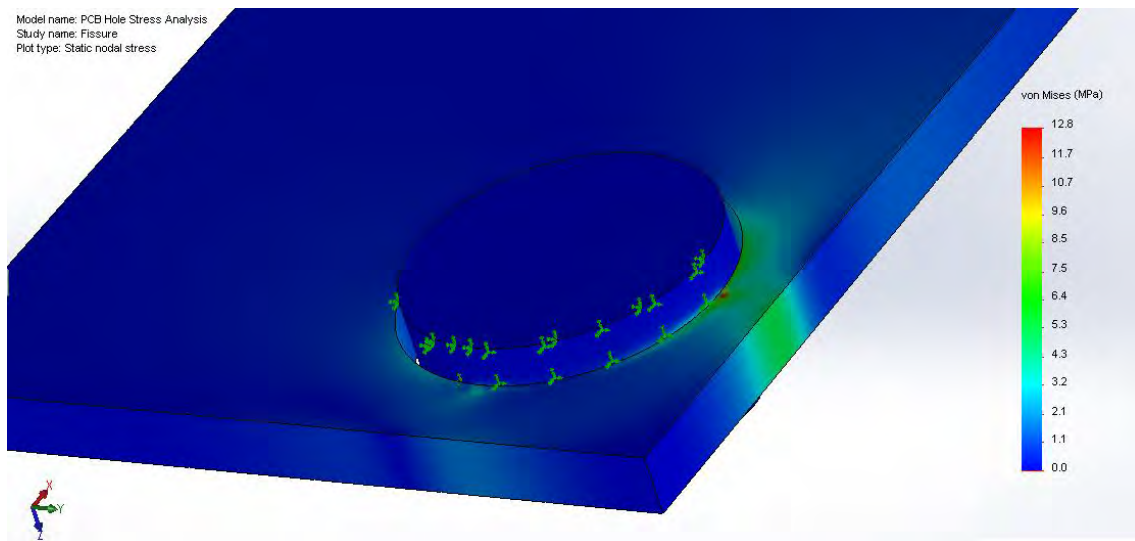


Figure 4-54 Stress distribution around a hole, assuming 10 g and 5 g accelerations

Skipping the mesh bug near the bolt (red), which is a frequent error in a normal FEA analysis, maximum stress on the plate is around 6 MPa, far from the yield stress (30 MPa). Thus, the holes near the edge would produce a stress concentration but they would not produce brittle failure or fissure phenomenon on the PCBs.

4.4.5.4 Mechanical Fixations

During the mechanical design, the number of bolts needed were thought in order to accomplish the following goals:

- Avoid any movement in every component. This implies to absorb any kind of force or torque in all directions (outer box and boom).

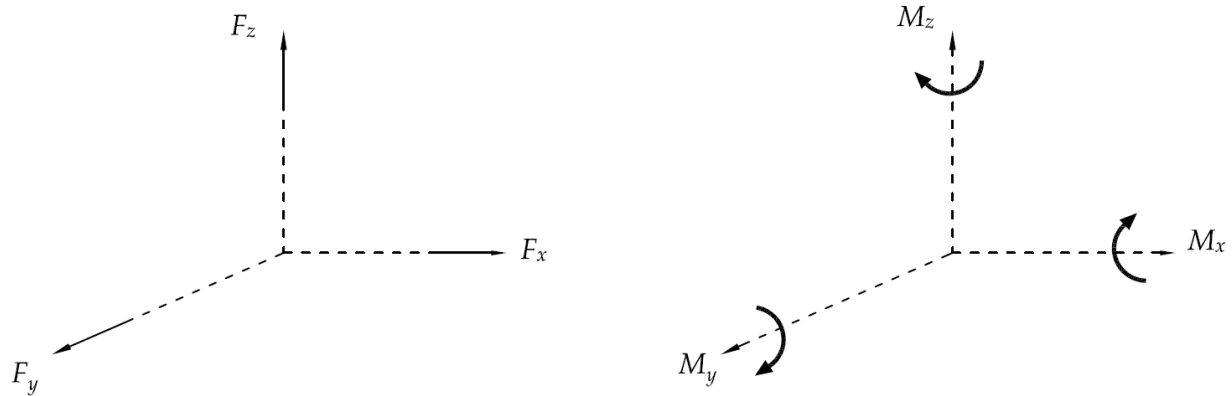


Figure 4-55 Forces and torques the experiment must absorb

- Resist the maximum tension stress (in the bolts).
- Resist the maximum shear stress (in the bolts).
- Resist the maximum stress (in the aluminium plates).

The fixation bolts for the outer box to the boom prevented all possible movements from occurring because there were four of them distributed on three different faces. In addition, bolts were attached to stiff junction elements that reinforced the joint. The following figures show how bolts were placed in the outer box:

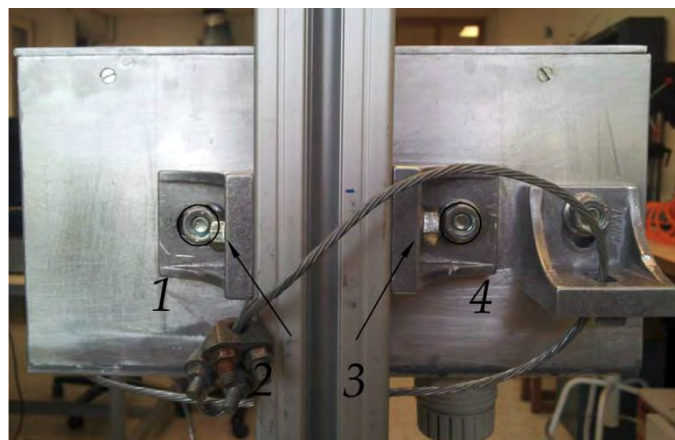


Figure 4-56 Front view of the outer box

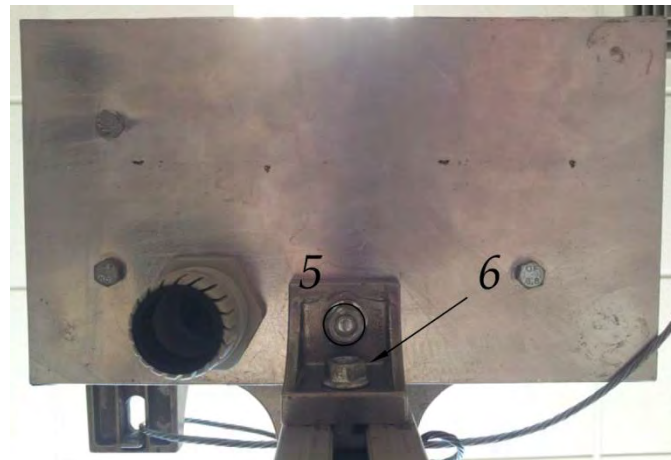


Figure 4-57 Top view of the outer box

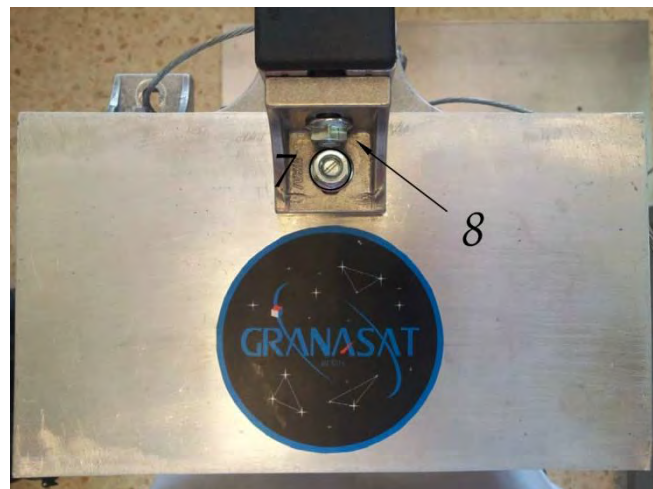


Figure 4-58 Bottom view of the outer box

Are the bolts strong enough to endure stresses? The minimum yield force is related to shear stress which can be calculated, to the smallest bolt used (yield stress of 640 MPa (8.8) and diameter of 8 mm), as follows:

$$F_{tension} = f_{yd} \cdot A = 640 \text{ MPa} \cdot 8^2 \text{ mm}^2 \approx 32,200 \text{ N} \quad (\text{Eq. 4-3})$$

$$F_{shear} = \frac{f_{yd}}{\sqrt{3}} A = \frac{640 \text{ MPa}}{\sqrt{3}} \frac{\pi}{4} 8^2 \text{ mm}^2 \approx 18,500 \text{ N} \quad (\text{Eq. 4-4})$$

Knowing that the mass of the outer box is around 2 kg, we are going to perform a systematic attachment compendium as follows:

- To endure F_x , the bolts 1, 4, 5, 6, 7 and 8 absorb shear stress and bolts 2 and 3 absorb tension stress and they can hold a force up to 8,800 g.
- To endure F_y , the bolts 2, 3, 5 and 7 absorb shear stress and bolts 1, 4, 6 and 8 absorb tension stress and they can hold a force up to 10,200 g.
- To endure F_z , the bolts 1, 2, 3, 4, 6 and 8 absorb shear stress and bolts 5 and 7 absorb tension stress and they can hold a force up to 8,800 g. However, it is true only if we do not consider that the bolts could slip through the boom. If it happens, there is a steel cable attached to the outer box that prevents it from disassembling.
- To endure M_x , the bolts 5 and 7 absorb shear stress and bolts 6 and 8 absorb tension stress. Considering a lever arm of 130 mm and a centre of mass distance of 120 mm, they can hold a force up to 5,500 g.
- To endure M_y , the bolts 1, 2, 3 and 4 absorb shear stress and bolts 5 and 7 absorb tension stress. Considering a lever arm of 70 mm and a centre of mass distance of 85 mm, they can hold a force up to 5,500 g.
- To endure M_z , the bolts 2, 3, 7 and 8 absorb shear stress and bolts 1 and 4 absorb tension stress. Considering a lever arm of 65 mm and a centre of mass distance of 65 mm, they can hold a force up to 7,000 g.

The supporting bolts for the PCBs are enough to constrain displacements in X, Y and Z axis and rotations in X, Y and Z axes. In the outer box joint, three bolts instead of four were used in order to interfere with the magnetometer as less as possible. However, they are completely functional, theoretically, if they are properly assembled.

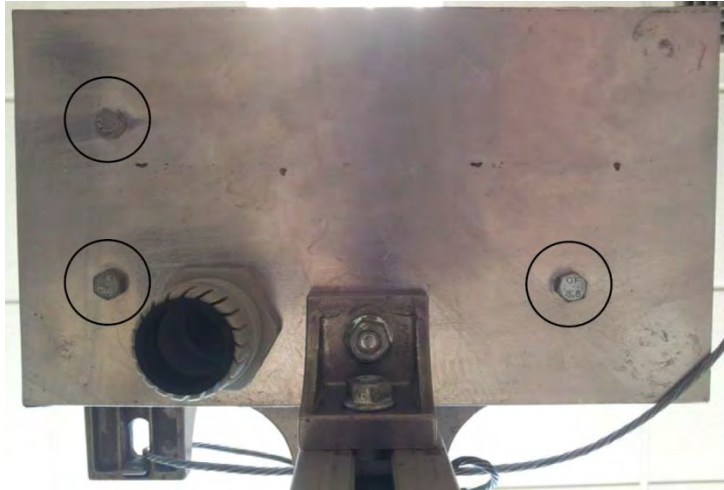


Figure 4-59 Bottom view of the outer box, PCB bolts are shown

How strong are the bolts to endure stresses? The minimum yield force is related to shear and tension stress which can be calculated, according to the bolt used (yield stress of 480 MPa (6.8) and diameter of 5 mm), as follows:

$$F_{tension} = f_y \cdot A = 480 \text{ MPa} \cdot 5^2 \text{ mm}^2 \cdot \frac{\pi}{4} \approx 10,000 \text{ N} \quad (\text{Eq. 4-5})$$

$$F_{shear} = \frac{f_y}{\sqrt{3}} \cdot A = 480 \text{ MPa} \cdot \frac{1}{\sqrt{3}} \cdot 5^2 \text{ mm}^2 \cdot \frac{\pi}{4} \approx 5,400 \text{ N} \quad (\text{Eq. 4-6})$$

Knowing that the mass of the PCB and the camera is 0.4 kg, we could proceed the same way we did with the bolts of the outer box. However, similar results will be obtained so, it is not necessary to calculate them again.

Are aluminium plates prevented from bearing? Maximum bear stress that aluminium can hold, assuming a yield stress of can be calculated as follows:

$$F_{bear} = 2.5 \cdot f_y \cdot d \cdot t = 2.5 \cdot 27 \text{ MPa} \cdot 5 \text{ mm} \cdot 4 \text{ mm} \approx 1,400 \text{ N} \quad (\text{Eq. 4-7})$$

Therefore, we can conclude that it is not likely that the outer box will break.

4.4.5.5 Shock Simulation

Performing a shock test would expose our components into a high risk of break or malfunction. Instead of a shock test, we decided to perform a shock simulation to predict what would happen in case of hard landing.

Using SolidWorks Simulation software, the outer box was programmed to be falling at 5 m/s, which is the expected gondola speed after the parachute opening. Surface landing was considered to be the smallest one of the box.

Material selected was, as usual, aluminium. However, instead of a Linear Elastic Isotropic analysis, a Plastic analysis was selected. This is because a ground shock on the box is not expected to happen in a normal flight. And if it happens, we do not consider essential to find it in perfect state. Some dents would be expected, but breaking is not admissible.

We obtain, as shown in Figure 4-60, that there are locations where yield stress is reached (27.6 MPa), near the camera hole. The rest of the outer box is safe to high stresses.

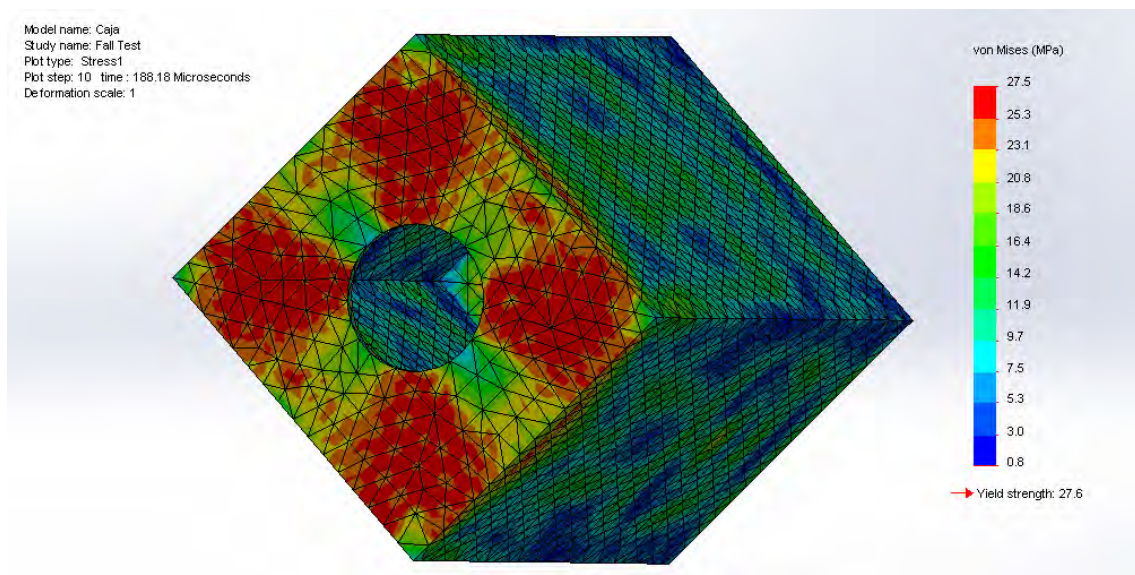


Figure 4-60 Stress distribution 188 μ s after landing

So, is reaching the aluminium yield stress a risk for the box? The answer is in Figure 4-61. When a plastic material reaches its yield stress, deformations increase greatly. However, maximum displacement is about 1 mm which is a very small displacement if we compare it with the outer box dimensions.

In conclusion, there is no failure expected in a possible shock.

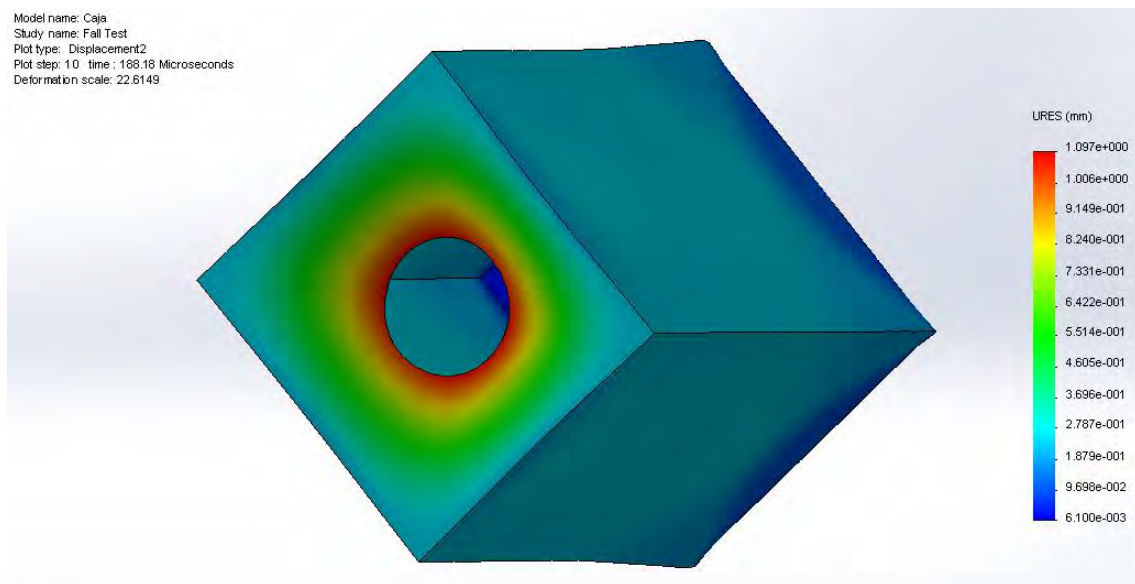


Figure 4-61 Deformed shape 188 μ s after landing

4.4.5.6 Gondola Attachment Analysis

Harming the gondola or its attachments is a common problem when teams overstress the elements trying to get adequate mechanical fixations, producing break or malfunction of them.

To avoid this, we are going to focus on the boom attachment to the gondola. As we do not have and cannot produce a profile similar to the gondola, we will use SolidWorks Simulation for a fast analysis instead of a real test. A model for this analysis is shown in Figure 4-62. Assuming that the gondola profile is made of steel, the boom is made of aluminium and the attachments are made of steel, a static force study will be used.

Through trial and error, we obtained that the minimum force on the bolts required to harm any part of the assembly is 1,000 N. In the same figure, stress distribution can be seen. Maximum torque applicable can be calculated using the equation:

$$T = k \cdot d \cdot F = 0.2 \cdot 10 \text{ mm} \cdot 1,000 \text{ N} = 2 \text{ Nm} \quad (\text{Eq. 4-8})$$

Where F is the force on the bolts, d is the diameter of the bolts and k is a coefficient that represents the friction between surfaces of the plates and the screw.

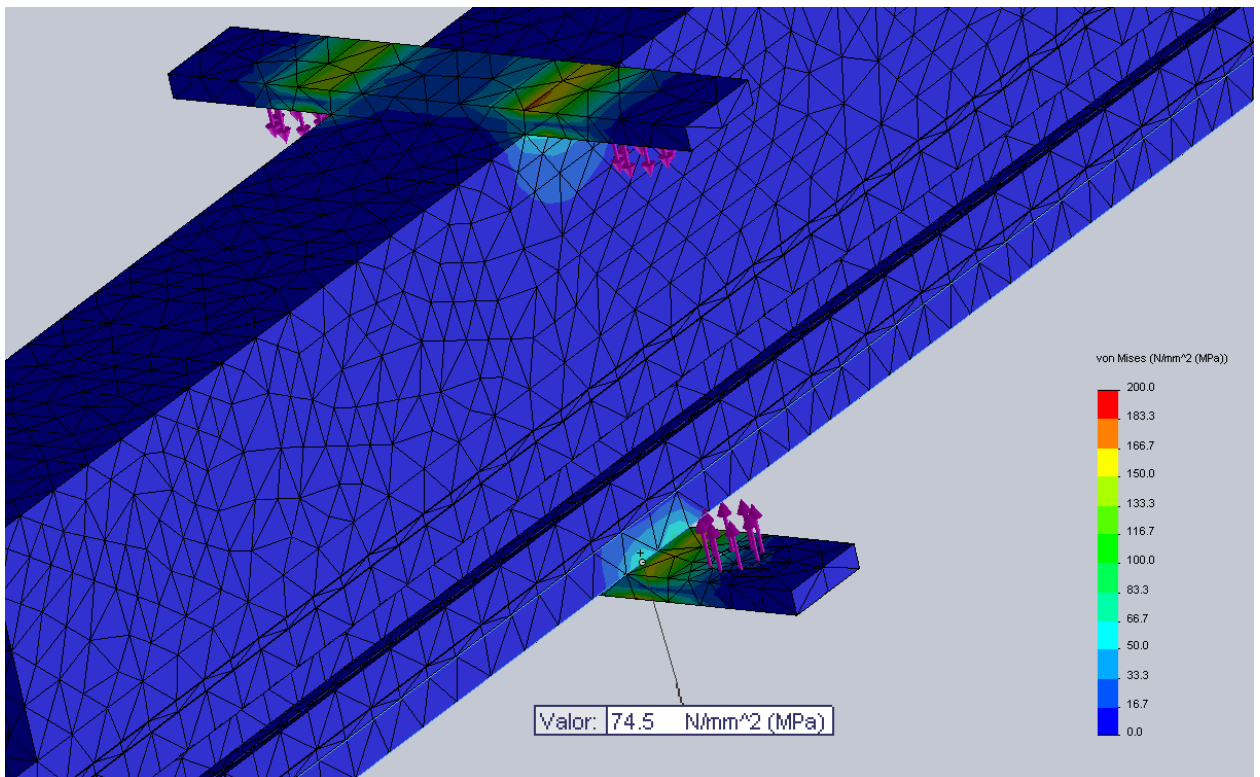


Figure 4-62 Stress distribution on boom, gondola profile and attachments

The maximum force that the bolts can hold is around 38,000 N. Therefore, we did not expect any problem with the bolts resistance.

In conclusion, if too much force is applied to the bolts, some parts of the boom and the connector will plastify nearly at the same time. In addition, the gondola would never be harmed at all. Maximum torque admissible is 2 Nm.

4.4.6 Static Load Test

In order to confirm the mechanical simulation results, we made a simple static load test.

In a parachute opening, accelerations of 10 g vertically and 5 g horizontally are expected. We cannot find a way to reproduce a parachute opening. Furthermore, performing a shock test is too risky for our experiment.

A reasonable way to check that the outer box can hold such accelerations is applying equivalent forces. These forces must be higher in order to consider side effects of a dynamic load.

A box full of tools and books was used as a weight. A scale gave us a force of 25 kp, over 12 times the mass of the outer box. That is enough to verify that it will withstand these parachute accelerations. Equivalent forces of 12 g were applied in each direction.



Figure C.7 1 Static load applied transversally

The outer box + boom system was attached to a desk, leaving the boom completely horizontal as shown on Figure C.7 1. We carefully left 400 mm from the edge of the desk to the outer box as specified in the mechanical design. The load box was placed on the top of the outer box and it was left still for ten minutes. When the load began, the system oscillated briefly but it was damped soon. No breaks, dents or loose bolts were seen after the load time.



Figure C.7 2 Static load applied vertically

After that, the outer box + boom system was placed vertically as shown on Figure C.7 2. Then, the load box was placed on the top of the outer box.

We made sure that the box did not touch the boom –see Figure C.7 3–, to let the outer box receive the whole load of 12 g. If the load had been touching the boom, a part of the force would have been absorbed by it.

There was no oscillation after the load box was placed. No breaks, dents or loose bolts were seen after a ten minute load time.



Figure C.7 3 The load box does not touch the boom

In conclusion, we can say that the outer box will successfully withstand the parachute accelerations of the BEXUS flight.

4.4.7 Camera Lens Characterisation

In order to protect the camera optics from extreme cold, we first attached a double filter in the baffle hole. However, following the advice given to us during IPR, we have decided to use only one lens. The results shown are the results of performing the tests with the double lens. If the results, such as light transmittance, are adequate when using two lenses, we can infer that when using only one its performance will be adequate as well. Nonetheless, further explanation about why we decided to remove one of the lenses can be found in Changes in the Camera Filters.

Double Lens Test

The double lens has an air layer between the two filters to reduce thermal conductivity. They are shown in Figure 4-63. These lens are supposed to filter UV radiations.



Figure 4-63 The two filters attached

We want to ensure that these filters do not insert optical aberrations or light intensity loss, because of the filter itself and because of open viewing angles, needed for star tracker for example. We have performed two tests to measure these issues.

The first one measures the characteristics of the filter itself, such as transmittance, thereby we want to know if filters produce light intensity loss. This is important because the camera exposure time will be related with light intensity.

To perform this test, we used a Spectrascan spectroradiometer (see Figure 4-64). This device allows us to know the wavelengths and intensity received. The spectroradiometer is calibrated with a reference blank and then the filters are placed and the measurements retaken. Comparing both spectrums and their intensity we can know if filters really filter the desired wavelengths and the amount of light intensity deducted.



Figure 4-64 Spectrascan spectroradiometer used in filter characterization test

Spectroradiometer screen shows directly the spectrum and its intensity. A screenshot can be seen in Figure 4-65.

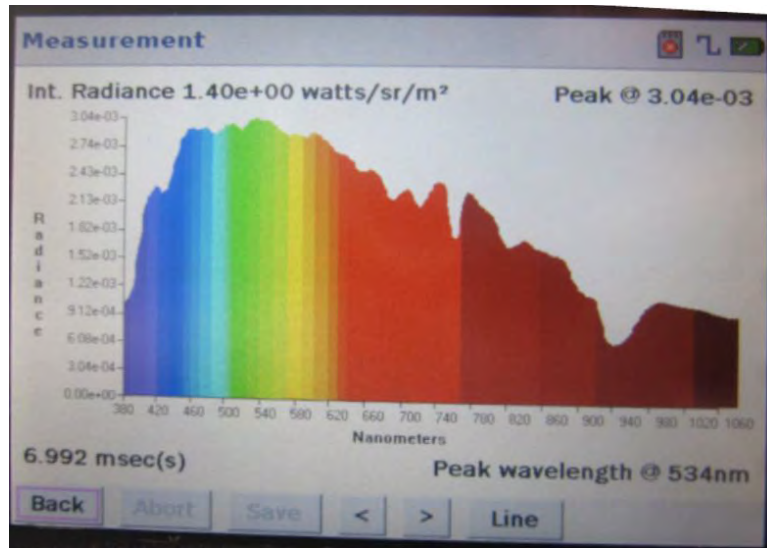


Figure 4-65 Screenshot of spectroradiometer while blank reference measurement

For this first test, we obtained the data points shown in Figure 4-66. As we can see, there is a reduction in light intensity with filters attached. Red discontinuous line shows the beginning of IR radiation, whereas blue discontinuous line shows the beginning of visible radiation:

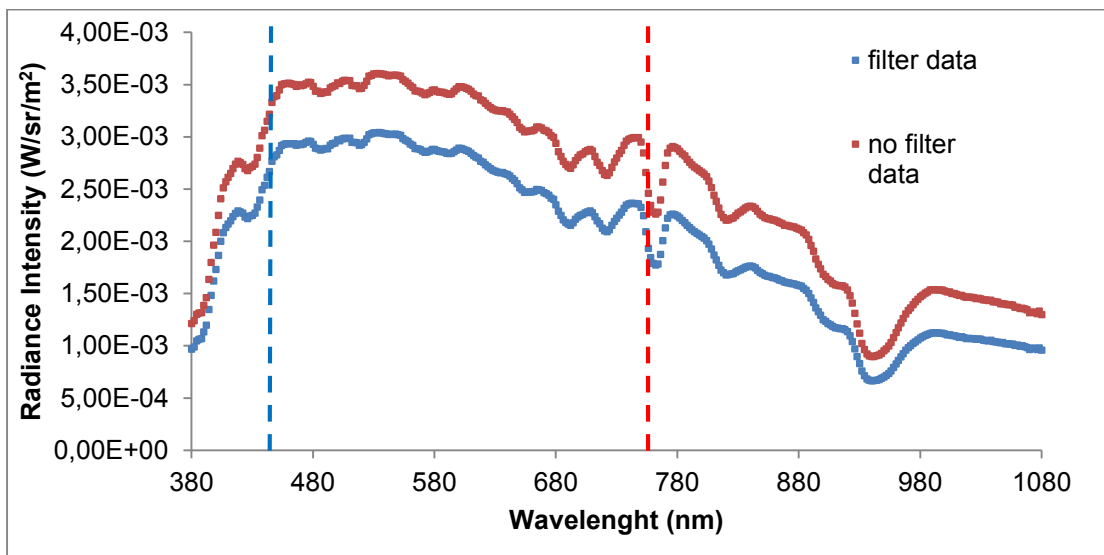


Figure 4-66 Radiance intensity detected by the spectroradiometer vs wavelength with no filters and with filters

To know the real transmittance, it is necessary to make the ratio between radiance intensity with and without filters. Results and discussions are shown in Figure 4-67.

As in Figure 4-66, blue discontinuous line shows the beginning of visible radiation and red discontinuous line shows the beginning of IR radiation

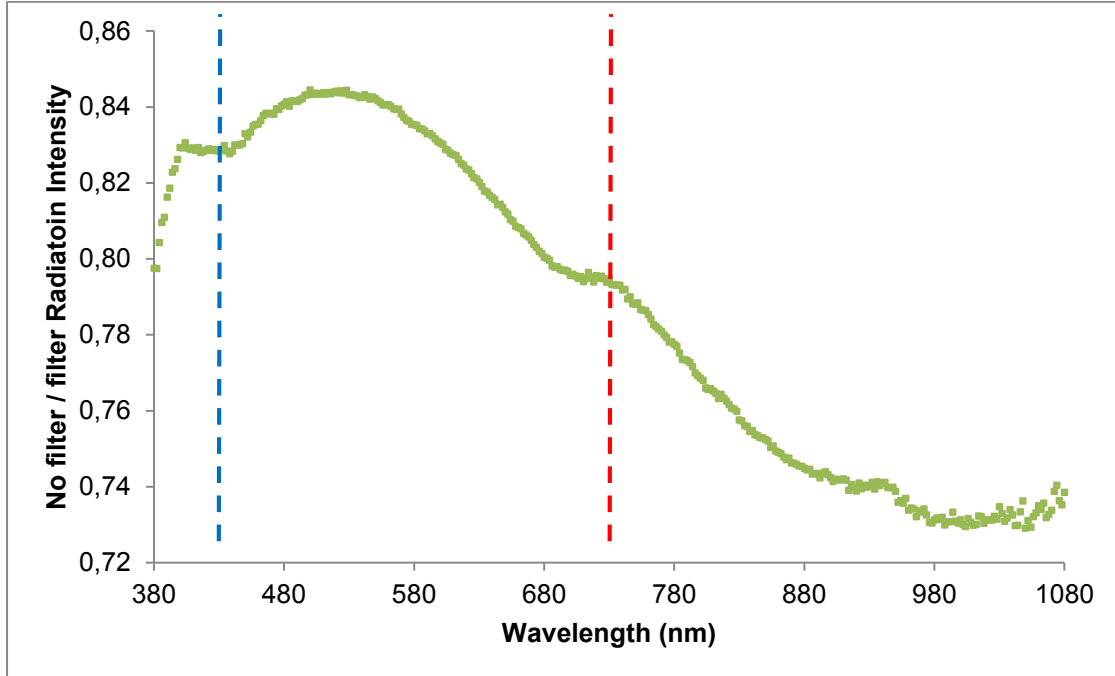


Figure 4-67 Ratio between no filter radiation intensity and filter radiation intensity

As shown in Figure 4-674, filters filter more in red and infrared spectrum (transmittance decays after ~ 500 nm peak). In violet/near ultraviolet zone we can see higher transmittance rates (about 0.83), whereas in red-infrared zone the transmittance is about 0.80 and decreasing. We expected to have a transmittance curve like the one shown in Figure 4-68.

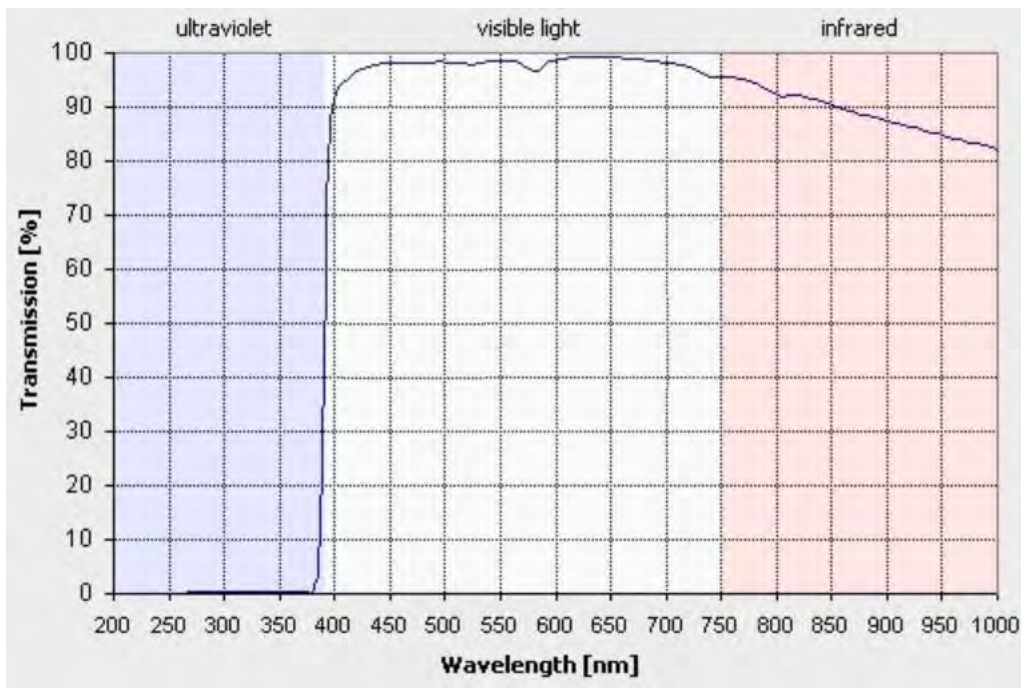


Figure 4-68 Transmittance vs wavelength in a quality UV filter - Blue zone represents UV wavelength and red zone represents IR wavelengths

Comparing both Figure 4-67 and Figure 4-68 we can see that the transmittance curve is not the same. Figure 4-68 shows that UV cut off is produced at ~ 380 nm, whereas transmittance in IR zone should be stable. This situation is not produced in Figure 4-67, where UV cut off at 380 nm is at $\sim 80\%$ and is very low at IR zone.

So we can say that this filter is not very appropriate to filter UV wavelengths because it deducts a big amount of IR wavelengths too.

Moreover, if we have a look at the camera datasheet, we can find the responsiveness curve vs wavelength, shown in Figure 4-69.

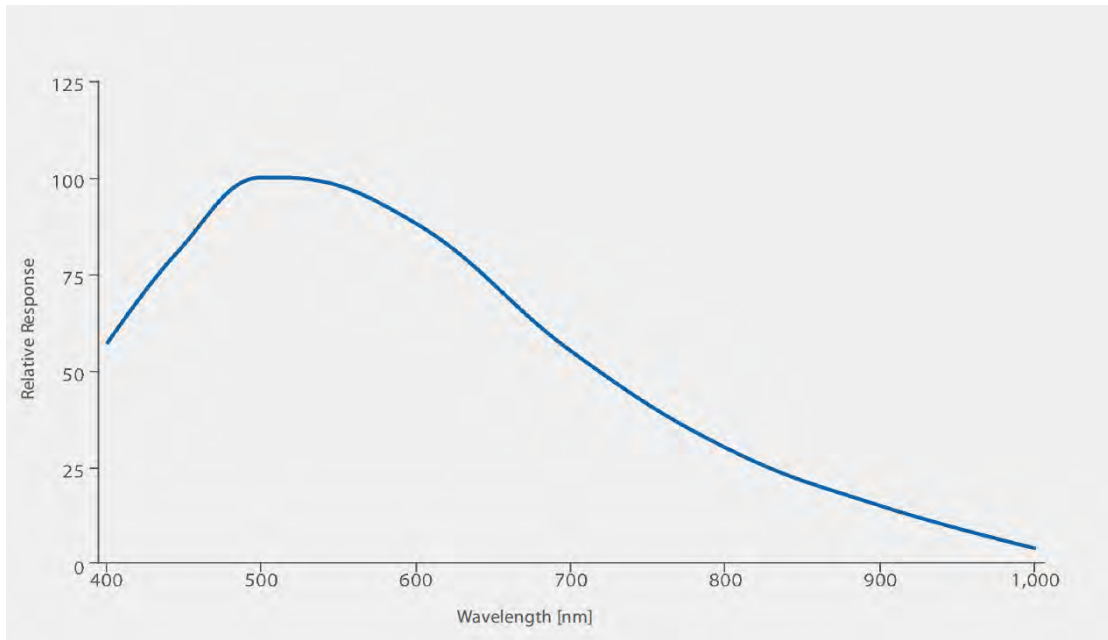


Figure 4-69 Relative responsiveness of the camera [7] as a function of wavelength

Despite all this, we do not have to be so obsessed with wavelengths filtered, but with total intensity. Namely, stars light are emitted in a wide range of wavelengths, so the parameter we should consider is total emissivity with and without filter. If we divide blue and red lines shown in Figure 4-66 in little rectangles and calculate the total area (namely, the total amount of light received), we can compare and see if these filters deduce a big quantity of light.

Surface under red line is $1.95 \cdot 10^{-2}$ u.a. (units area; it is not necessary to know the units, that means that normalized units are enough). Surface under blue line is $1.58 \cdot 10^{-2}$ u.a.

So finally we can say that filters reduce a total amount of

$$1 - \frac{1.58 \cdot 10^{-2}}{1.95 \cdot 10^{-2}} = \mathbf{18.82\%}$$

That means that filters do not deduce a big amount of light intensity. And despite of its reduction of light intensity in some wavelengths, the total quantity of light received with filter is enough to keep detecting the stars light and make the star tracker function.

The second test we performed with filters is related with their opacity according to the observation angle.

Because of some of the stars tracked have a wide view angle, we needed to ensure that light transmittance is good even in these wide angles.

To perform this test, we took 20 photos of a scene with filters and another 20 photos with no filters. If we calculate the ratio between the matrix values of scenes with filters and matrix values of scenes with no filters and analyse the results, we can see if there were any problems with light transmittance in extreme view angles.

In theory, if a filter works fine independently of the angle, we should see a field like the one shown in Figure 4-70. By contrast, if filter has problems with wide view angles, we should see a field like shown in Figure 4-71.

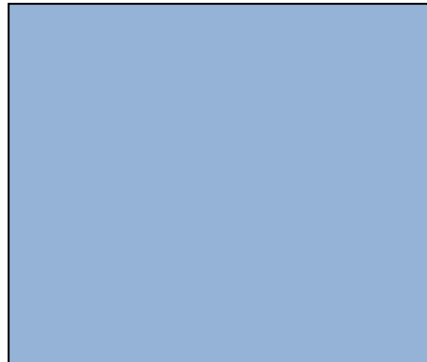


Figure 4-70 Filter transmittance has no dependency with view angle

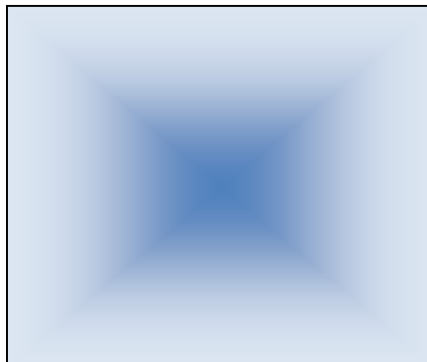


Figure 4-71 Filter transmittance has a high dependency with angles

We obtained the field show in Figure 4-72. In this image, the darker is the colour, the higher is the filter aberration.



Figure 4-72 Intensity light field related to view angles

As shown in Figure 4-72, there were some irregularities in the image, but there was no pattern related to angles (as shown in Figure 4-71). The data image is more similar to Figure 4-70, so in this second test, the filters had good angle behaviour.

In conclusion, here it is the qualification test:

- Filters filter more in red zone, but stars emit in other wavelengths, so that is not a problem.
- Intensity light reduction ws only an 18.82 %, quite good to keep the star tracker functioning.
- There were no angle aberrations. Quite good again.

4.4.8 Changes in the Camera Filters

After some research and simulations, we decided we are not going to use two lenses for the following reasons:

- There is no air circulation inside the outer box and low amounts of heat will be dissipated. Hence, it is not necessary to overprotect the camera optics against cold.

- The space between the lenses can become a pressure vessel. High pressured air compared with low pressures of outside could cause cracks in lens glasses. By removing one filter, we mitigate a safety risk and the quality of the pictures is not affected by any cracks.

Furthermore, another problem that we suspected we were going to have disappeared: if the air trapped between the lenses had different humidity conditions, it could cause condensation inside the lenses space. We needed to let the outside air come inside to level the humidity conditions and avoid condensation in one face of the remaining lens. With this change, we no longer have this condensation risk.

4.5 Electronics Design

4.5.1 General Electronic Design

We used the power of the gondola batteries that provided 28 V and 1 A. This voltage was converted by step-down voltage regulators, one per box.

We have chosen a LM2576 regulator, since it provides a 3 A load with an excellent line and load regulation. This device is available in a fixed output voltage of 5 V.

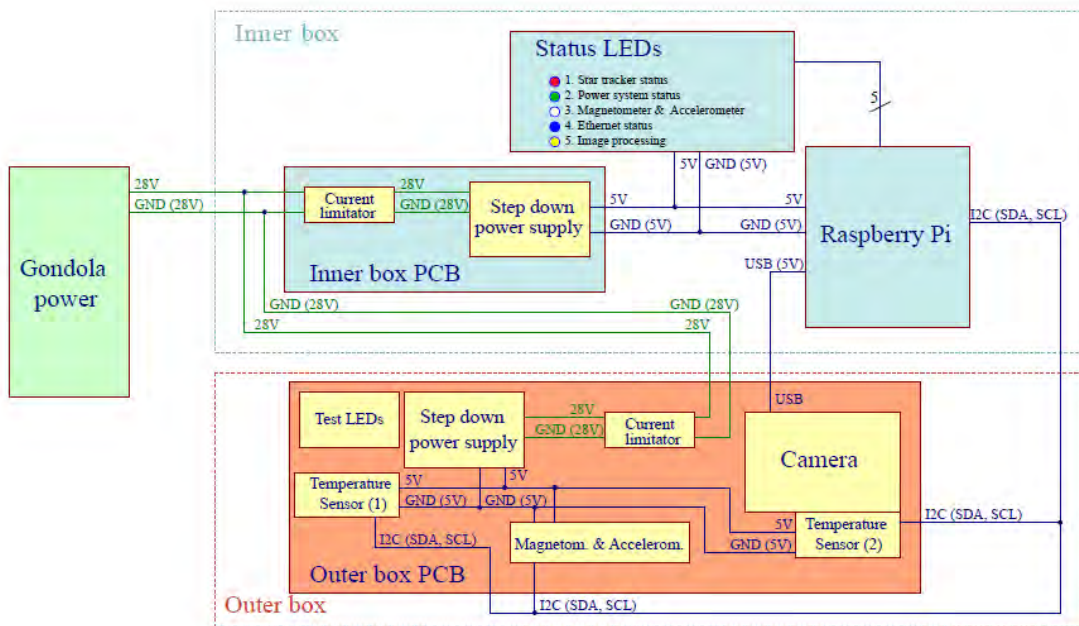


Figure 4-73 Electronics blocks

We placed the inner box PCB above the Raspberry Pi, as shown in Figure 4-19 in 4.4.1.

We had two PCBs. One controlled the power in the inner box, and the other controlled the magnetometer and accelerometer and measured the temperature inside the outer box with two temperature sensors.

To supply the current to the status LEDs we used MOSFETs, as the Raspberry Pi has a maximum output current of 16 mA from each GPIO and a maximum output current 50 mA from all GPIOs simultaneously. This is shown in Appendix C.1 Plans.

Current limiters system:

The image (see further information in Appendix C.1 Plans) shows the connection with the gondola batteries. In order to protect the inner box PCB and the outer box PCB, we used three current limiters. These current limiters are designed to stop the current in case of over current.



Figure 4-74 ITS4141N

Table 4-11 ITS4141N Characteristics

| Parameter | Value |
|---------------------------|-------------------|
| Model | ITS4141N |
| Power Load Switch Type | High Side |
| Maximum Input Voltage | 60 V |
| Current Limit | 700 mA / 1,100 mA |
| Operating temperature min | -30 °C |
| Operating temperature max | 85 °C |

I²C interface

In order to improve the communication between the outer box and the inner box, based in I²C interface, we used a component which extends the separation distance between the boxes securing a strong signal in the end of the wire.

The solution we designed consists in the use of the NXP P82B715 component [8], which is an I²C-bus extender.

By using a P82B715 component inside the inner PCB and another one inside the outer PCB we solved the problems related to the low level signals, such as the high noise environment and the long cable between the outer box and inner box. The implementation we developed is showed in Figure 4-75.

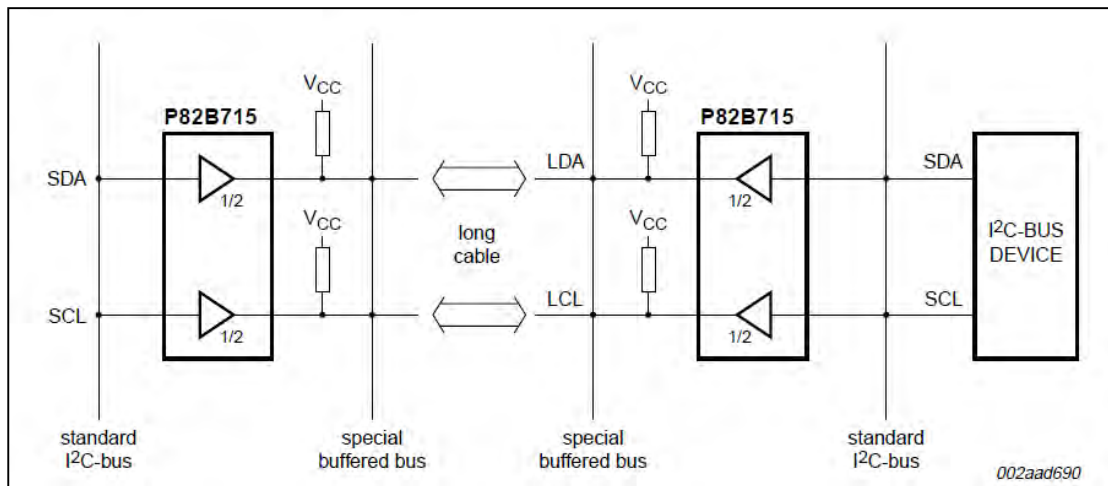


Figure 4-75 Use of I²C-bus extender by P82B715 between outer box and inner box

The P82B715 has a SO8 package. It can operate at bus speeds up to 1MHz.

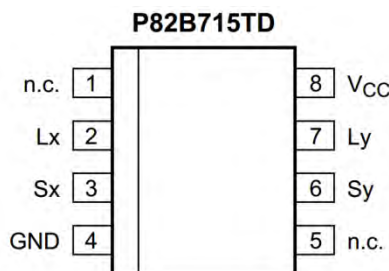


Figure 4-76 P82B715

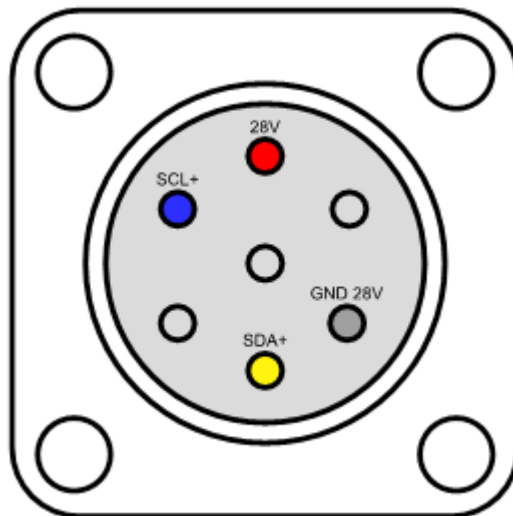
Table 4-12. P82B715 Characteristics

| Parameter | Value |
|----------------------------|---------|
| Model | P82B715 |
| Supply voltage typ. | 5 V |
| Voltage range buffered bus | 5 V |
| Maximum cable length | 50 m |
| Operating temperature min | -40 °C |
| Operating temperature max | 85°C |

Table 4-13. P82B715 Pins

| Pin | Description |
|-----|----------------------------------|
| 1 | Not connected |
| 2 | Buffered bus, LDA or LCL |
| 3 | I ² C-bus, SDA or SCL |
| 4 | Negative supply |
| 5 | Not connected |
| 6 | I ² C-bus, SDA or SCL |
| 7 | Buffered bus, LDA or LCL |
| 8 | Positive supply |

Link between the outer and the inner box:

**Figure 4-77 Link between the outer box and the inner box**

The link between the inner box and the outer box is presented in Figure 4-77. This link has 7 pins (three were not used), which have their own function.

The following table indicates the colour of every wire:

Table 4-14 Wires colour code

| | |
|--------|----------|
| Red | 28 V |
| Grey | GND 28 V |
| Yellow | SDA |
| Blue | SCL |

This connector is the model Amphenol MIL-DTL-26482 (7 pins). It is shown in Figure 4-78.



Figure 4-78 Amphenol MIL-DTL-26482 connector

The pins have these functions:

- SDA-SCL: To control I²C bus for DS1621, TC74 and LSM303DLHC sensors
- 28 V: To supply the voltage to the outer box
- GND (28 V)

There are 7 pins but only 4 were used because of the changes in the design during the several versions. Changing the connector was not of any use when these failures were discovered.

I²C lines

I²C bus is a two-wire interface used to interconnect components. The outer box sensors and the Raspberry Pi were connected through a shielded twisted pair in order to avoid interferences.

Outer box link

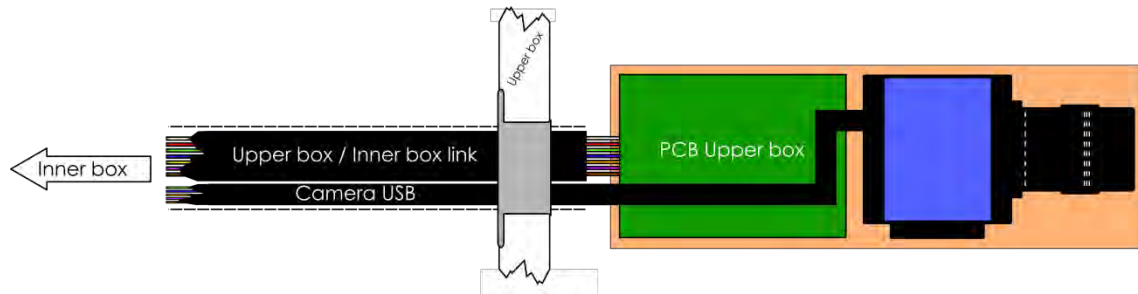


Figure 4-79 Outer box link

To enter the USB cable for the camera and the link into the outer box, a cable gland with thermal insulation was used.

More information about this design can be consulted in C.5 Electronics Schematics.

Cables

Calculating the proper sizing of an electrical cable is essential to guarantee that it can operate continuously under full load without being damaged, to avoid excessive voltage drops and to ensure operation of protective devices during a ground fault.

The wire has been considered like a resistance:

$$R = \rho \frac{L}{S} \quad (\text{Eq. 4-9})$$

And resistance in a circuit is the constant between the voltage applied and the current:

$$R = \frac{V}{I} \quad (\text{Eq. 4-10})$$

If we combine both equations we obtain:

$$\rho \frac{L}{S} = \frac{V}{I} \quad (\text{Eq. 4-11})$$

The value is doubled because of the double pass through the wire performed by the electrical particles:

$$S = \frac{2\rho LI}{\Delta V} \quad (\text{Eq. 4-12})$$

Where S is the section of the wire [mm^2]. L is the length of the wire [mm]; ρ is the electrical resistivity ($\Omega \cdot \text{mm}$, we use copper = $16.78 \text{ n}\Omega \cdot \text{m}$ at 20°C); R is the resistance [Ω], ΔV is the maximum permitted voltage drop and I is the current.

To calculate the maximum permitted voltage drop the following equation has been used:

$$5\% \text{ of Voltage} = 2 \cdot \Delta V \quad (\text{Eq. 4-13})$$

Table 4-15 Cables section

| Wire description | Length (m) | Voltage (V) | ΔV (V) | Current (A) | Section (mm^2) | Standard section (mm^2) |
|---------------------------------|------------|-------------|----------------|-------------|---------------------------|------------------------------------|
| Wire from the gondola batteries | 1.5 | 28 | 0.7 | 1 | $72 \cdot 10^{-3}$ | 0.25 |



| Wire description | Length (m) | Voltage (V) | ΔV (V) | Current (A) | Section (mm ²) | Standard section (mm ²) |
|--|------------|-------------|----------------|-------------|----------------------------|-------------------------------------|
| Wire between inner box and outer box (SDA, SCL) | 2 | 5 | 0.0825 | 0.05 | $40.6 \cdot 10^{-3}$ | 0.25 |
| Wire between inner box and outer box (28V and GND 28V) | 2 | 28 | 0.7 | 1 | $95.88 \cdot 10^{-3}$ | 0.25 |
| LEDs | 0.1 | 3.5 | 0.0875 | 0.02 | $0.76 \cdot 10^{-3}$ | 0.25 |

4.5.2 Grounding Diagram

The choice of earthing system is crucial since it can affect the safety and electromagnetic compatibility of the power supply.

To illustrate the concept of the ground distribution of the experiment Appendix C.1 Plans can be consulted.

A single-point grounding distribution is shown in the diagram.

4.5.3 Inner Box PCB Design

The schematic used to design the inner box PCB can be found in Appendix C.1 Plans.

The Raspberry Pi and the GPIOs are in the top left corner. They were used to control the sensors and status LEDs that are in the centre of the schematic. In the bottom left corner is the voltage regulator, a circuit that can be seen with greater definition in Appendix C.1 Plans too.

At the top of this image the connectors to the gondola power and two LEDs to test the circuit can be seen.

At the bottom of the Raspberry we will place a buzzer to test the circuit.

This is the final inner box PCB design:

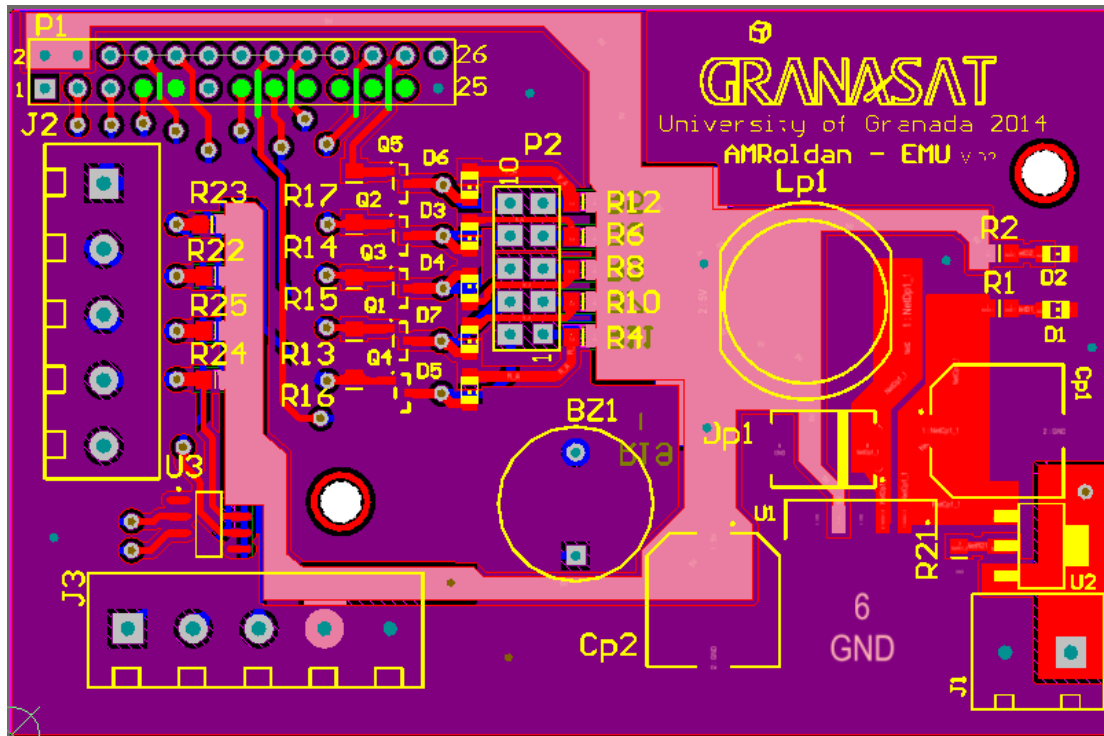


Figure 4-80 Inner box PCB design - top layer

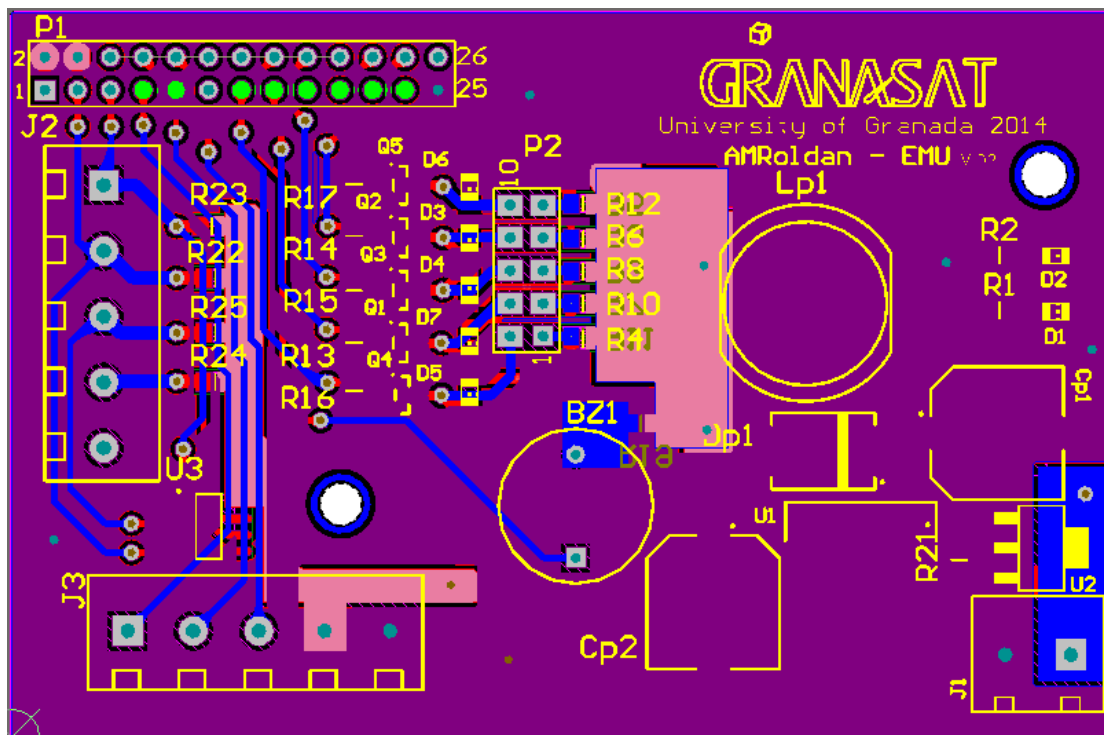


Figure 4-81 Inner box PCB design - bottom layer

The 3D model is the following image, where the components that were put in the circuit can be seen:

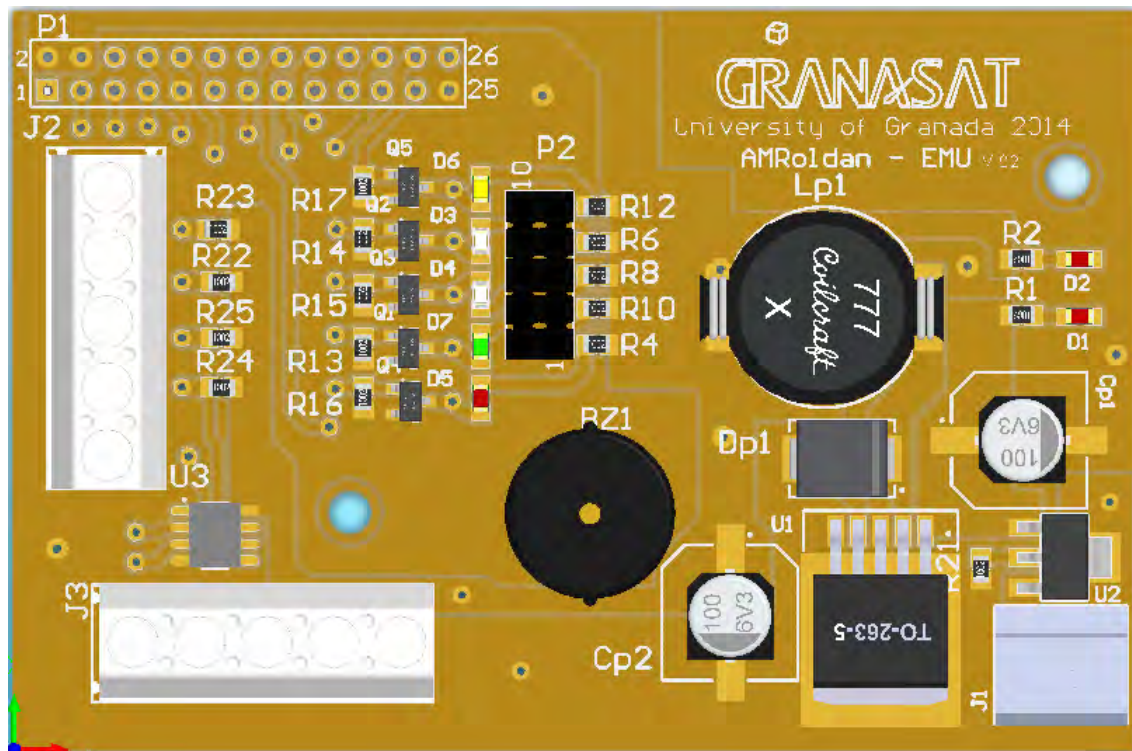


Figure 4-82 Inner box PCB 3D model (Top view)

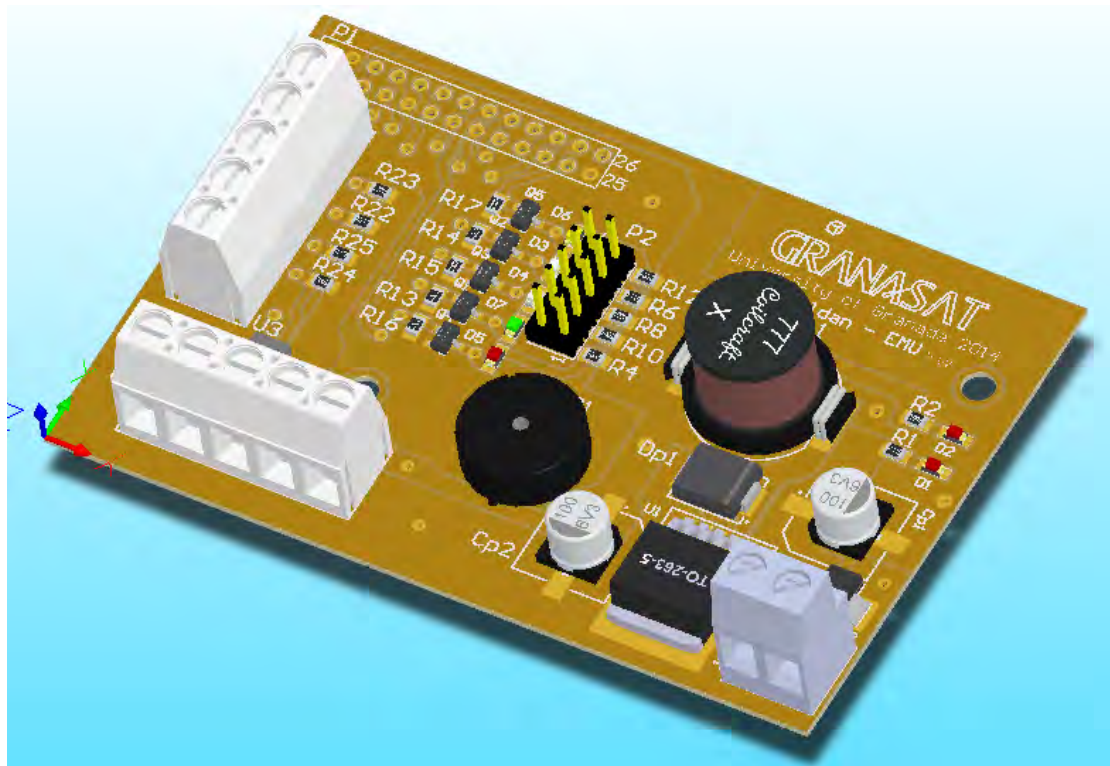


Figure 4-83 Inner box PCB design 3D model



Student Experiment Documentation

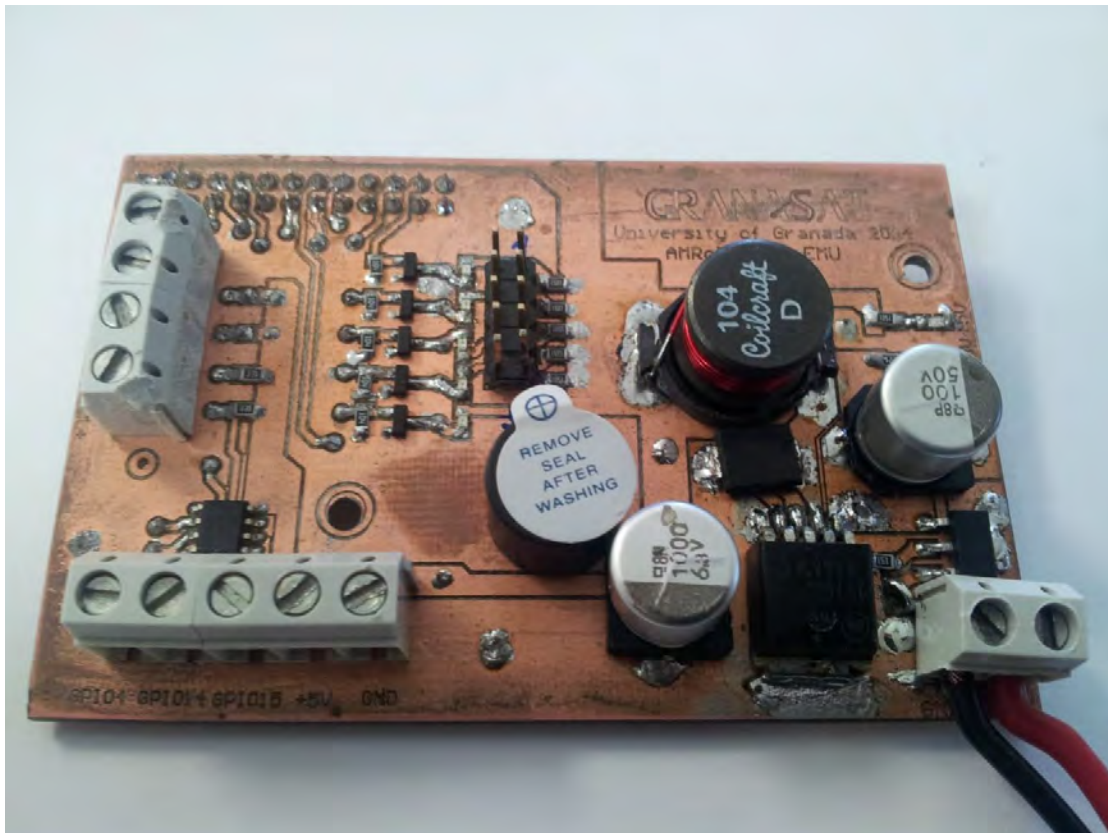


Figure 4-84 Second version of the inner box PCB - top view

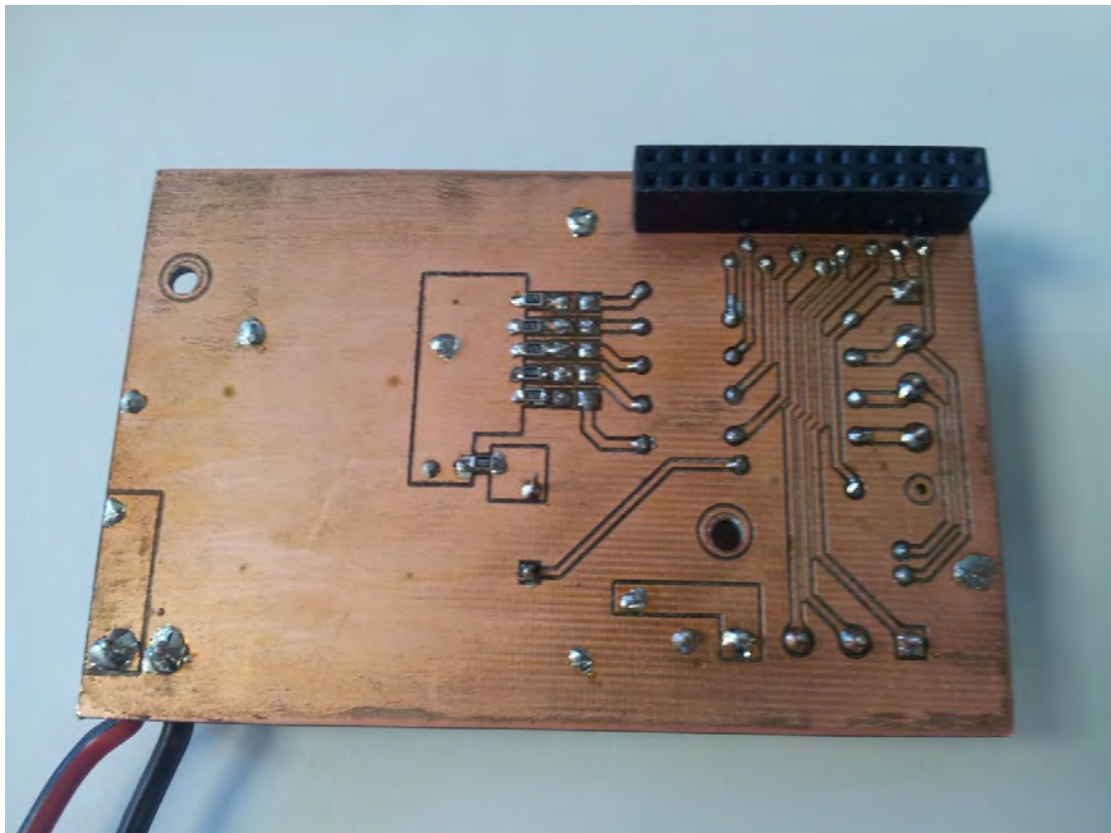


Figure 4-85 Second version of the inner box PCB - bottom view

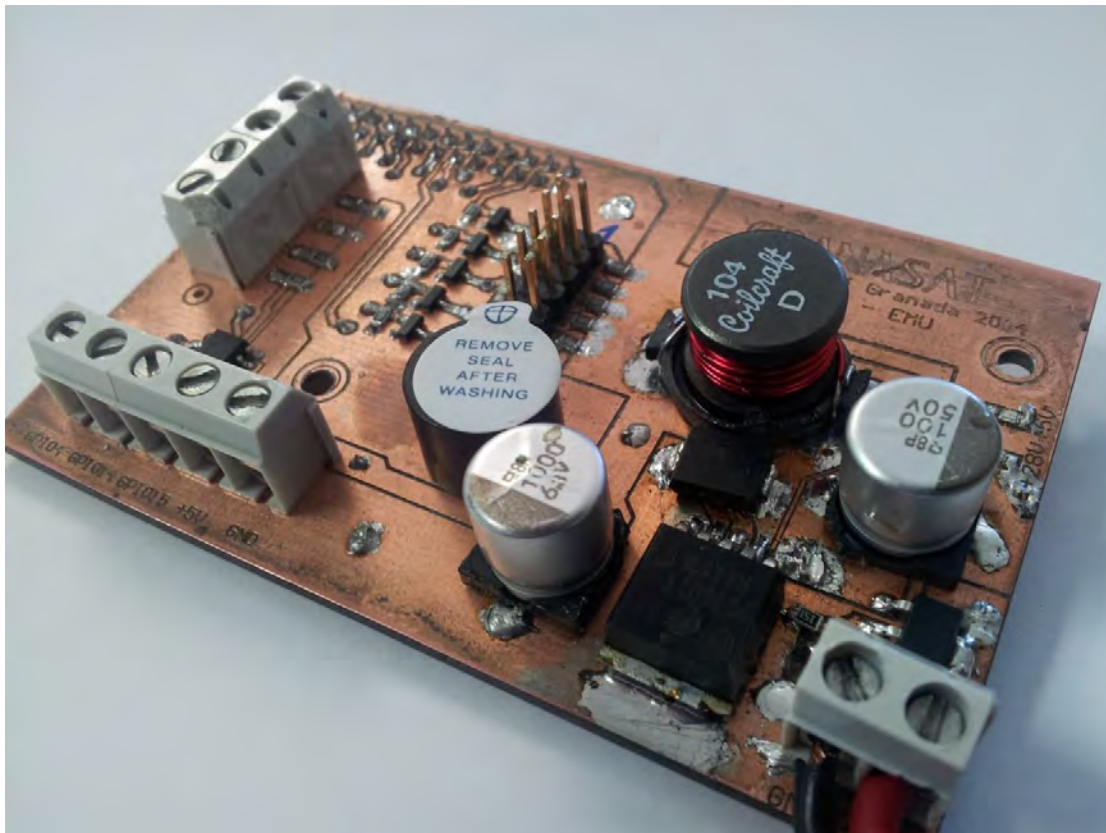


Figure 4-86 Second version of the inner box PCB

We faced some problems with the routing in the inner box. In the following pictures is depicted the before and after status of this box and its PCB:



Figure 4-87 Before solving the routing problems

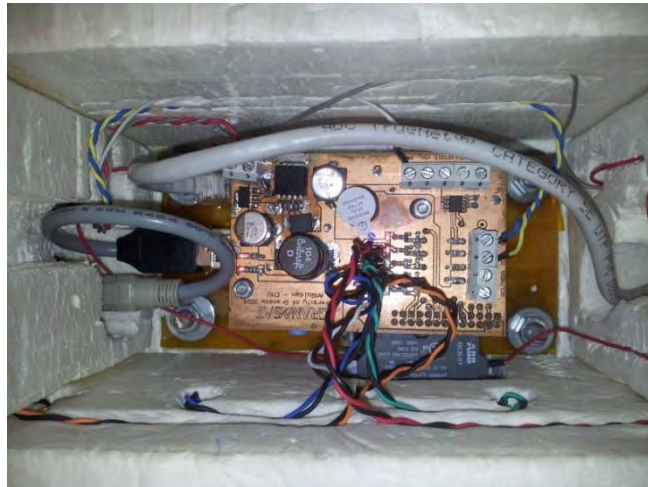


Figure 4-88 After solving routing problems

4.5.4 Outer Box PCB Design

The sensors in the outer box PCB, the magnetometer and the accelerometer, are in the schematic in Appendix C.1 Plans. Two temperature sensors were used because one had to be in contact with the camera.

The LEDs that can be seen in the schematic of this PCB were used to check if the external power is supplied and the DC/DC converter works.

This is the final design of the outer box PCB:

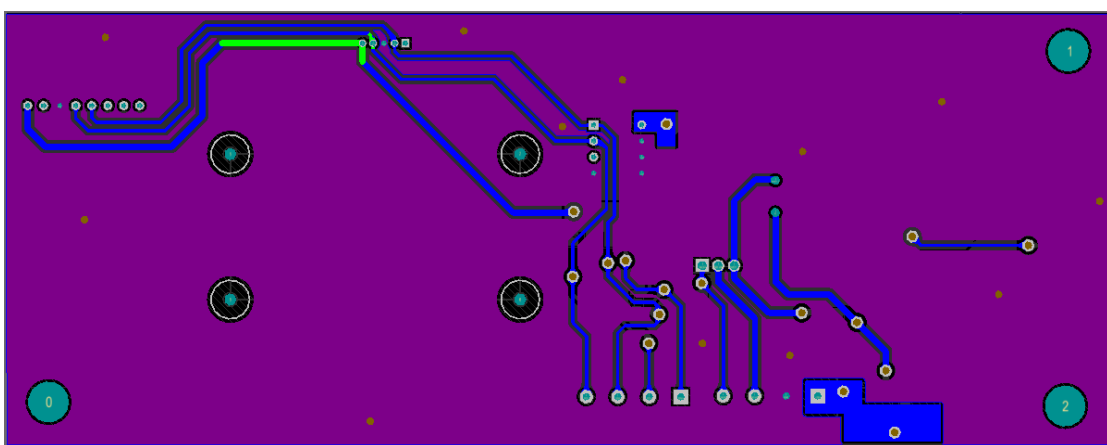


Figure 4-89 Outer box PCB design - bottom layer

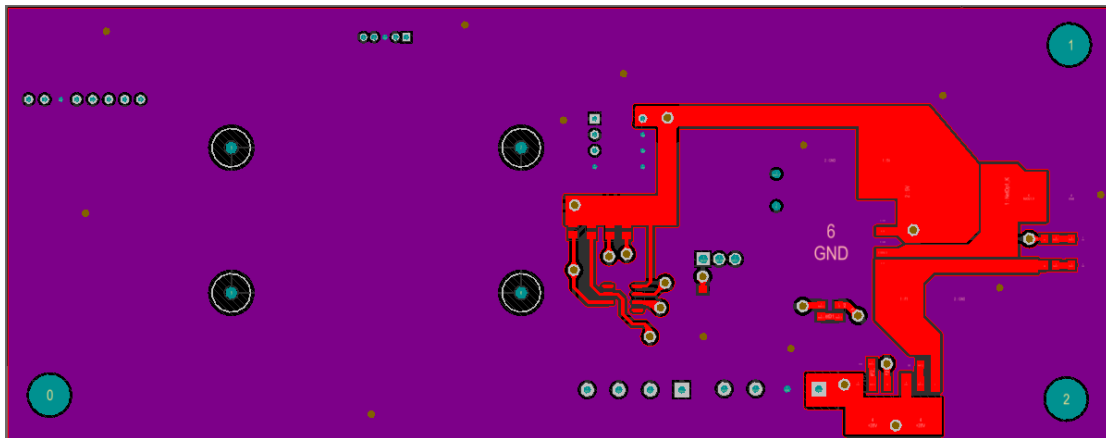


Figure 4-90 Outer box PCB design - top layer

The 3D model is:

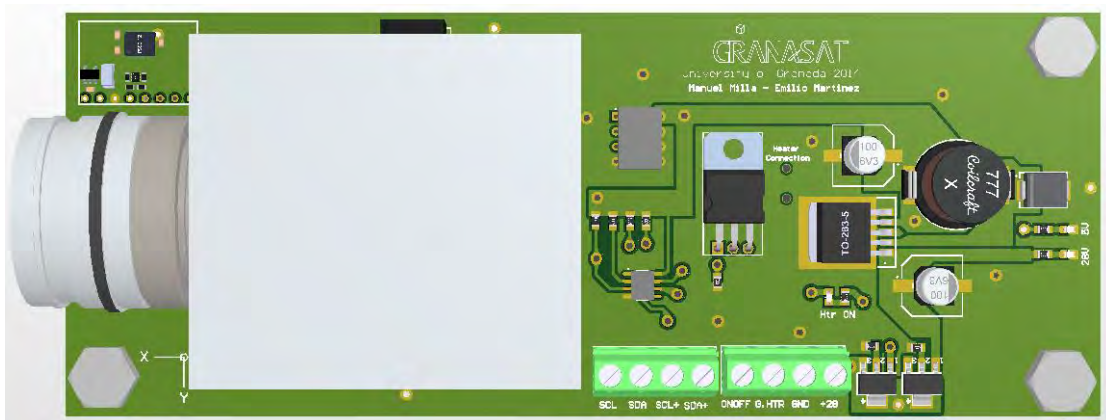


Figure 4-91 Outer box PCB design 3D model (Top View)

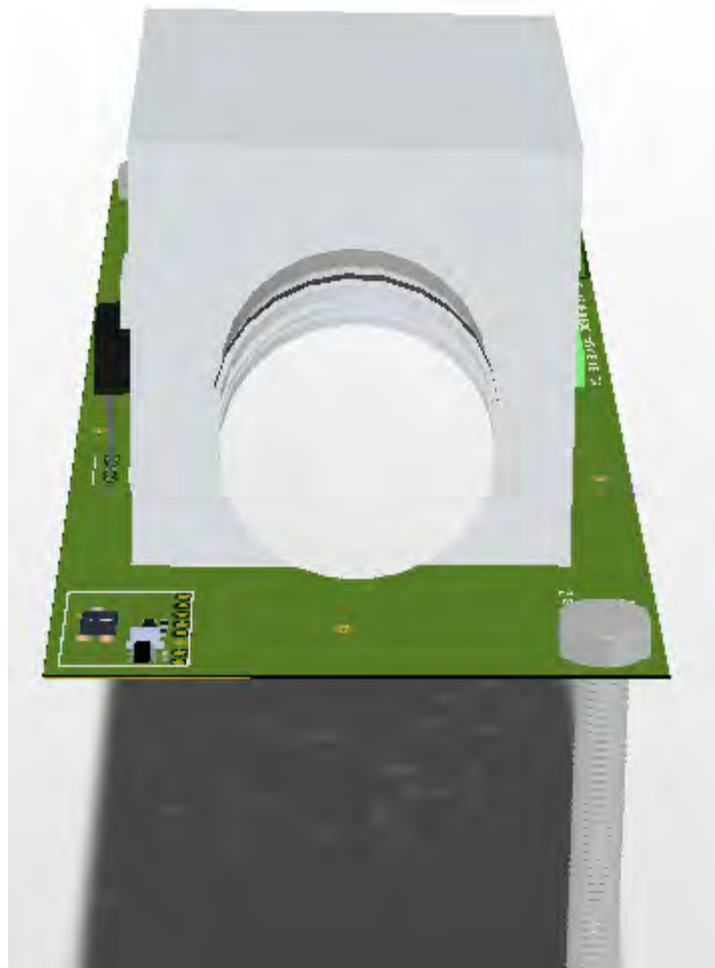


Figure 4-92 Outer box PCB design 3D model (Front View)

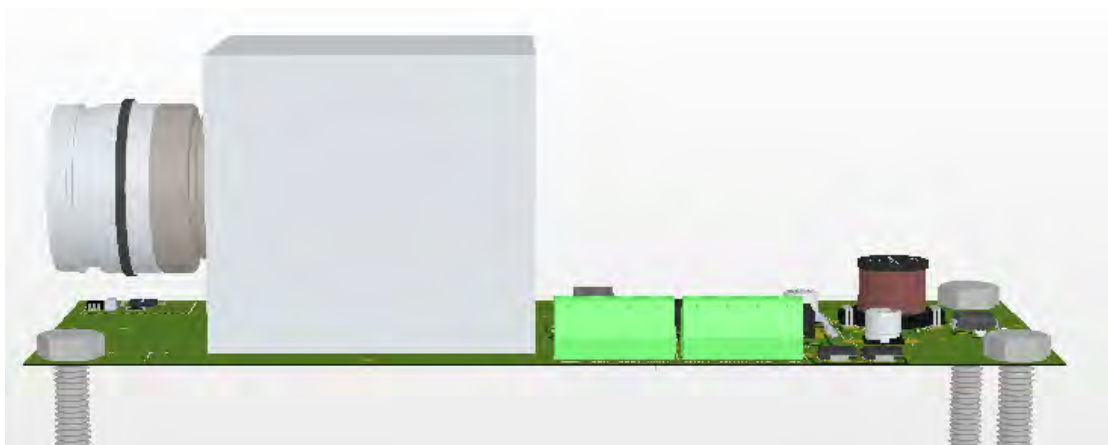


Figure 4-93 Outer box PCB design 3D model



Figure 4-94 Flight model of outer box PCB

4.5.5 Magnetometer & Accelerometer Sensor LSM303DLHC

We selected the LSM303DLHC, which is a system-in-package featuring a 3D digital linear acceleration sensor and a 3D digital magnetic sensor. It is often used in handheld compensated compass and position detection devices. We have bought a test board, shown in Figure 4-95 in order to characterize the 3D magnetometer and accelerometer. This breakout board is the GY-511 LSM303DLHC model.

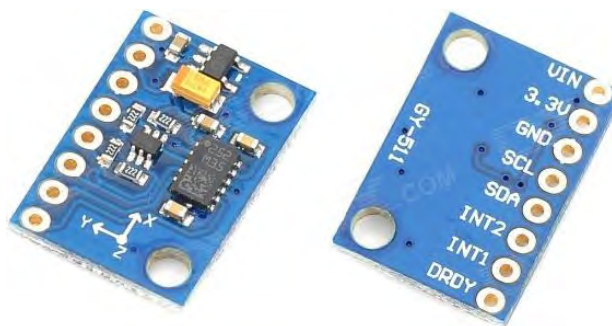


Figure 4-95 Magnetometer and accelerometer test board

The LSM303DLHC is available in a plastic land grid array package (LGA) (see Figure 4-96) and is guaranteed to operate over an extended temperature range from -40 °C to +85 °C. The thermal design has to take account of this thermal constraint.

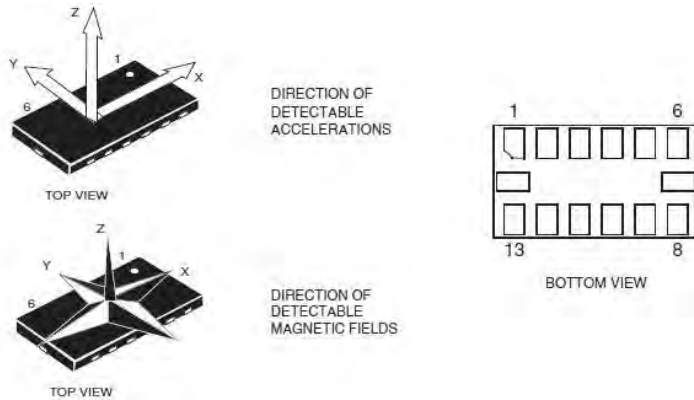


Figure 4-96 Pin connection LSM303DLHC

LSM303DLHC has full-scales linear acceleration of $\pm 2 / \pm 4 / \pm 8 / \pm 16$ g and a full-scale magnetic field of $\pm 1.3 / \pm 1.9 / \pm 2.5 / \pm 4.0 / \pm 4.7 / \pm 5.6 / \pm 8.1$ gauss. These ranges for acceleration and magnetic field measurements are enough for the functional and performance requirements, established in Experiment Requirements and Constraints.

LSM303DLHC includes a 3.3 V I²C serial bus interface that supports standard and fast mode 100 kHz and 400 kHz. The magnetometer and accelerometer can be enabled or put into power-down mode separately. The test board includes specific electronic devices to allow the 3.3 V – 5 V I²C serial bus. The pin out of the test board (Figure 4-95) is shown in Table 4-16.

Table 4-16 Pin function

| IMU | Pin function |
|-----|--------------|
| V+ | 3.3 V |
| GND | GND |
| SDA | A4 |
| SCL | A5 |

In order to enable and configure the LSM303DLHC sensor it is necessary to write in dedicated purpose 8-bit registers. Since we can obtain independent measurements from acceleration and magnetic field, it is required to repeat this process for both the accelerometer and the magnetometer registers.

For the accelerometer configuration, the registers are CTRL_REG1_A and CTRL_REG4_A. The first one allows to enable X, Y or Z axes measurements and



choose between standard or fast mode data rate. The second register sets up the measurement resolution to get a certain full-scale range.

Regarding the magnetometer configuration, the registers are MR_REG_M and CRB_REG_M. The first register enables or disables the magnetometer, but unlike the accelerometer, this sensor cannot choose independent axis measurements or data rate. The second register works in the same way it does in the accelerometer.

Finally, the LSM303DLHC lectures are written in the corresponding 8-bit output registers: OUT_X_L_A, OUT_X_H_A, OUT_Y_L_A, OUT_Y_H_A, OUT_Z_L_A and OUT_H_L_A for the acceleration data and OUT_X_H_M, OUT_X_L_A, OUT_Z_H_M, OUT_Z_L_M, OUT_Y_H_A and OUT_H_L_A for the magnetic field data. These X, Y or Z axis data are split into the least significant byte and the most significant byte.

Thus, we only needed to write a simple C function to read the output registers and, therefore, obtain the 3-axis vector components for both acceleration and magnetic field as shown in Figure 4-97.

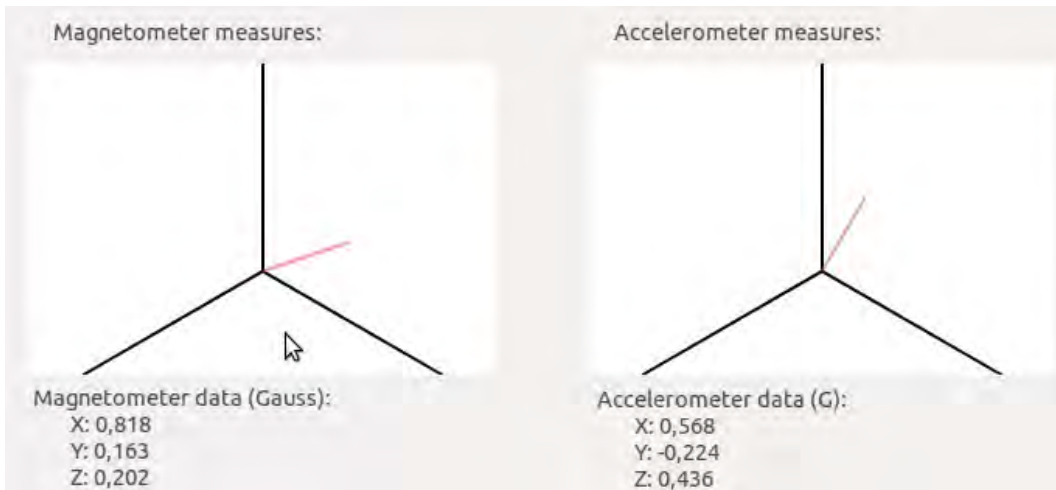


Figure 4-97 Measures read from LSM303DLHC

Further information of these registers is specified in LSM303DLHC documentation [9].

4.5.6 Temperature Sensor DS1621

Thanks to WiringPi library [10] it is easy to control the temperature sensor DS1621. This library allows us to communicate directly with the sensor without caring about the I²C ACK, addressing and clock signals. From our point of view, we had to configure

the DS1621 to be continuously converting data and this can be done with simple write and read C functions.

First, we have to acces the configuration register; to do this we send 0xAC (all information about the DS1621 commands and its purpose can be found in the device's datasheet p.10 [11]) Once we have done it, we will send the 0x00 and the 0xEE commands. These commands tell the DS1621 we need to convert temperature continuously. The 0xEE command is the start condition that the sensor needs to start converting temperatures.

Secondly, when this sensor is set up, we can ask it for a temperature value with the 0xAA command.

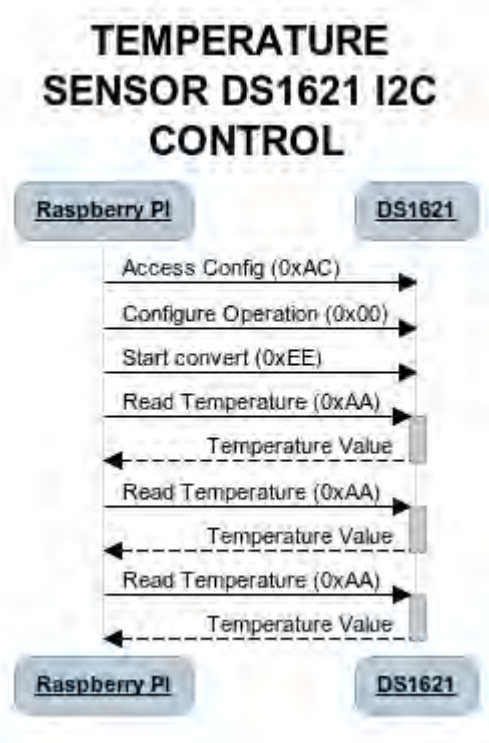
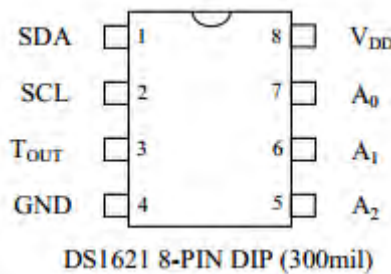


Figure 4-98 I²C message flow

The DS1621 will respond with a 2-byte value. The first byte contains the temperature value in two's complement with a resolution of 1 °C. The second byte can be used to get a resolution of 0.5 °C.

Table 4-17 Pin function DS1621

| | |
|-------------|----------------------------------|
| SDA | 2- Wire Serial Data Input/Output |
| SCL | 2 -Wire Serial Clock |
| GND | Ground |
| TOUT | Thermostat Output Signal |
| A0 | Chip Address Input |
| A1 | Chip Address Input |
| A2 | Chip Address Input |
| VDD | Power Supply Voltage |

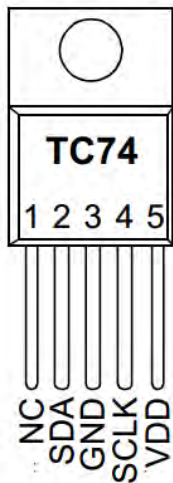
**Figure 4-99 Pin connection DS1621**

4.5.7 Temperature Sensor TC74

This second temperature sensor has been chosen because it can be placed in vertical position to come into direct contact with the camera, as shown in the 3D Model Figure 4-93.

In earlier versions, we had another sensor, but when the sensor was tested with a 2 meters wire in C.7.5 Thermal Test, the 1-Wire connection did not work well. To avoid this, the sensor was changed to an I²C sensor. The I²C signal works perfectly with the I²C extender.

The TC74 digital thermometer provides 8-bit Celsius temperature measurements. . This sensor is connected by two I²C data wires to the CPU. The other pins supply the power (VDD) and GND. The pins (one NC, Not Connected) are depicted in the following figure:

TO-220**Figure 4-100 TC74 Temperature sensor****Table 4-18 Pin function TC74**

| | |
|-------------|-------------------------------|
| NC | Wire Data Input / Output |
| SDA | Serial Data I ² C |
| SCLK | Serial Clock I ² C |
| GND | Ground |
| VDD | Power Supply Voltage |

Table 4-19 Temperature/Data relationship

| Actual Temperature | Registered Temperature | Binary Hex | |
|--------------------|------------------------|------------|------|
| +130.00°C | +127°C | 0111 | 1111 |
| +127.00°C | +127°C | 0111 | 1111 |
| +126.50°C | +126°C | 0111 | 1110 |
| +25.25°C | +25°C | 0001 | 1001 |
| +0.50°C | 0°C | 0000 | 0000 |
| +0.25°C | 0°C | 0000 | 0000 |
| 0.00°C | 0°C | 0000 | 0000 |
| -0.25°C | -1°C | 1111 | 1111 |
| -0.50°C | -1°C | 1111 | 1111 |
| -0.75°C | -1°C | 1111 | 1111 |
| -1.00°C | -1°C | 1111 | 1111 |
| -25.00°C | -25°C | 1110 | 0111 |
| -25.25°C | -26°C | 1110 | 0110 |



| | | | |
|----------|-------|------|------|
| -54.75°C | -55°C | 1100 | 1001 |
| -55.00°C | -55°C | 1100 | 1001 |
| -65.00°C | -65°C | 1011 | 1111 |

4.6 Thermal Design

Thermal design minimised the heat loss through passive actions to prevent the camera from freezing (DMK 41BU02.H [7]), as the camera is the most sensitive element in the outer box.

Table 4-20 Operating temperature range

| Instrument | T _{min} (°C) | T _{max} (°C) |
|------------------------------|-----------------------|-----------------------|
| Camera | -5 | 45 |
| CPU | 0 | 50 |
| Temperature Sensor (1) | -45 | 125 |
| Temperature Sensor (2) | -40 | 125 |
| Magnetometer & Accelerometer | -40 | 85 |
| Regulator | -40 | 125 |
| Buzzer | -40 | 85 |
| Fast Diode | -65 | 125 |
| Inductor | -40 | 85 |
| Capacitor (in) | -55 | 105 |
| Capacitor (out) | -55 | 105 |
| Current Limitator | -30 | 85 |
| I ² C Extender | -40 | 85 |

The insulation material chosen is extruded polystyrene (XPS), which is a very common closed cell insulation material, used in a wide area of applications as well as in some BEXUS experiments. We chose it because of its price and its insulation properties. It is available in many configurations in which thermal conductivity may vary from 0.03 W/mK to 0.04 W/mK [12] depending on the density of the specific model and differences between manufacturers. Both boxes (inner and outer box) were insulated with a 40 mm XPS panel. This configuration has demonstrated satisfactory performance during all flight stages in several BEXUS experiments, such as the one done by COMPASS team in BEXUS 9 campaign [13].

In addition, the XPS insulation works correctly under vacuum. It has been empirically shown that there is not expansion of the material after vacuum tests such as the one done by TORMES team [14] in their experiment.

It is necessary to take into account the heat loss due to the conduction between the outer box and the boom that attaches it to the gondola. In order to minimize this heat loss a plastic thermal bridge was used.

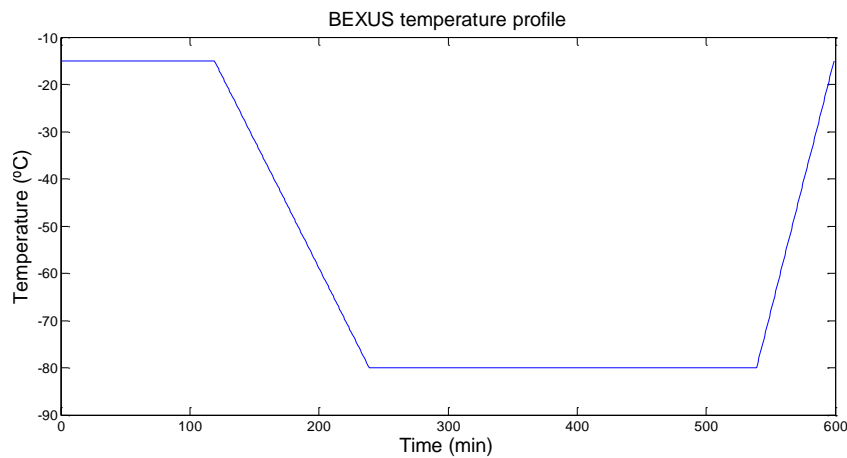


Figure 4-101 Temperature profile worst case scenario

Because of the difficulty in only calculating the performance of the insulation with equations, a thermal simulation of the system is necessary to provide an overview of its behaviour.



4.6.1 Thermal Simulations

As a requirement mentioned in section 2.3 Design Requirements, electronics must operate between -5 and 45 °C. Lower or higher temperatures could cause the malfunction or even damage the electronics components.

Using SolidWorks the worst case scenario was simulated to ensure the insulation works as intended.

In addition, we needed to know the power requirements of thermal elements to ensure batteries were not drained.

4.6.1.1 Outer Box

The worst case scenario for the temperature profile is shown in Figure 4-101, where we can notice that the lowest temperature we could reach is -80 °C.

In every test, we want to prove that external temperatures do not affect the outer box components and that we can protect them against extreme cold.

4.6.1.2 Inner Box

For this case, the lowest temperature outside the box is up to -40 °C because of the gondola insulation.

The elements placed inside the inner box are the Raspberry Pi and the PCB, which generate heat by its own.

Thermal parameters of materials placed in the inner box are similar to the ones of the outer box.

4.6.1.3 Simulation Results

Outer box

For the outer box, we simulated an outside temperature of -80 °C. The only heating component is the camera emitting 2.5 W from time 0 to final experiment time.

The results of the simulation are shown in Figure 4-102. As we can see, the bluer is the colour, the colder is the material. This screenshot taken simulates the outer box during the descent phase:

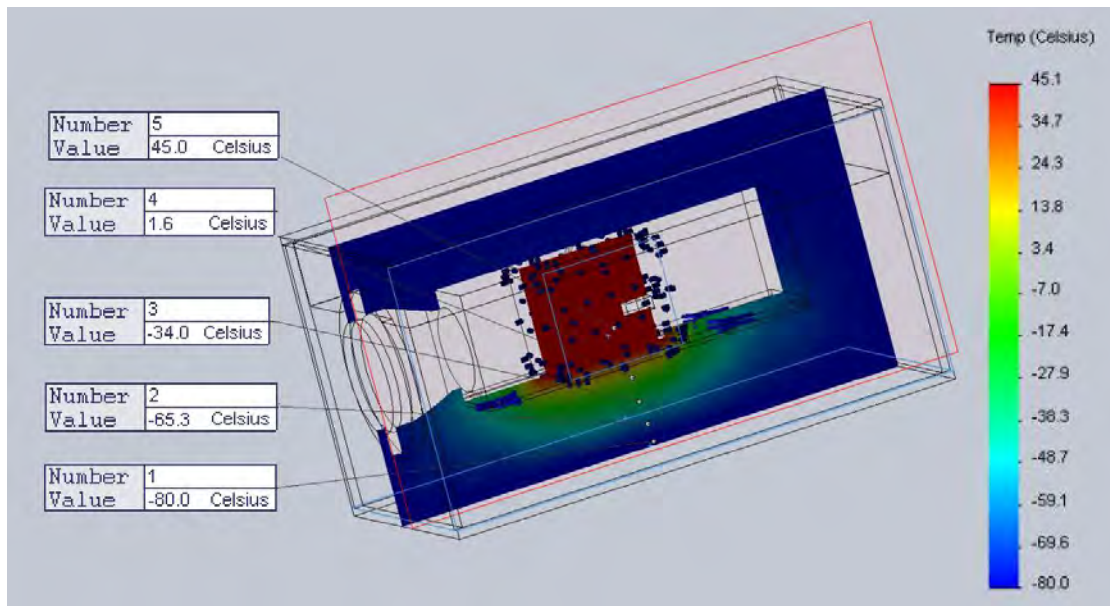


Figure 4-102 Thermal simulation for the outer box just before the re-entry of the experiment in the atmosphere (~ 8.5 hours after the start of the experiment)

Thermal behaviour of the experiment in general is good as we can see in Figure 4-102. The coldest temperature reached in the camera body (the most critical component) is about 2.2 °C, which is higher than the minimum operational temperature (-5 °C).

The temperature of the camera body and other parts of the insulation are shown in Figure 4-103, from time 0 to 9 hours. On this figure, yellow line corresponds to temperature in the camera body (point 5 in Figure 4-83); black line, to the temperature found at inner insulation surface (point 4); green line, to 1/3 depth (point 3); blue line,

to 2/3 depth (point 2) and red line corresponds to most external insulation temperature (point 1).

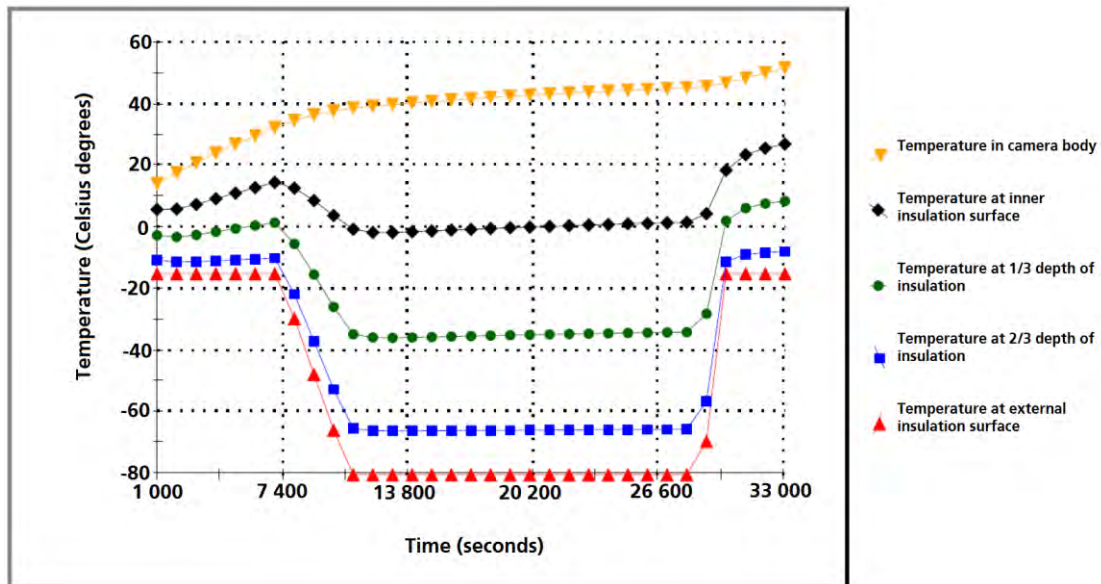


Figure 4-103 Temperature vs time for different parts of the outer box.

As shown in Figure 4-103, critical temperature for electronics (less than -5°C) is never reached inside the box. This means the insulation works as intended and protects the electronics from freezing.

To consider the hot case, thermal simulation was redone with the same characteristics, only changing some boundary conditions:

- External temperature before the launch and after the landing is 20°C .
- Minimum temperature during the flight is -60°C .
- Materials, flight time, initial temperature and heat power were the same.

The screenshot in Figure 4-104 shows the temperature distribution in a hot case, in the beginning of the descendant phase. Compared to the cold one, temperatures are up to 20°C higher.

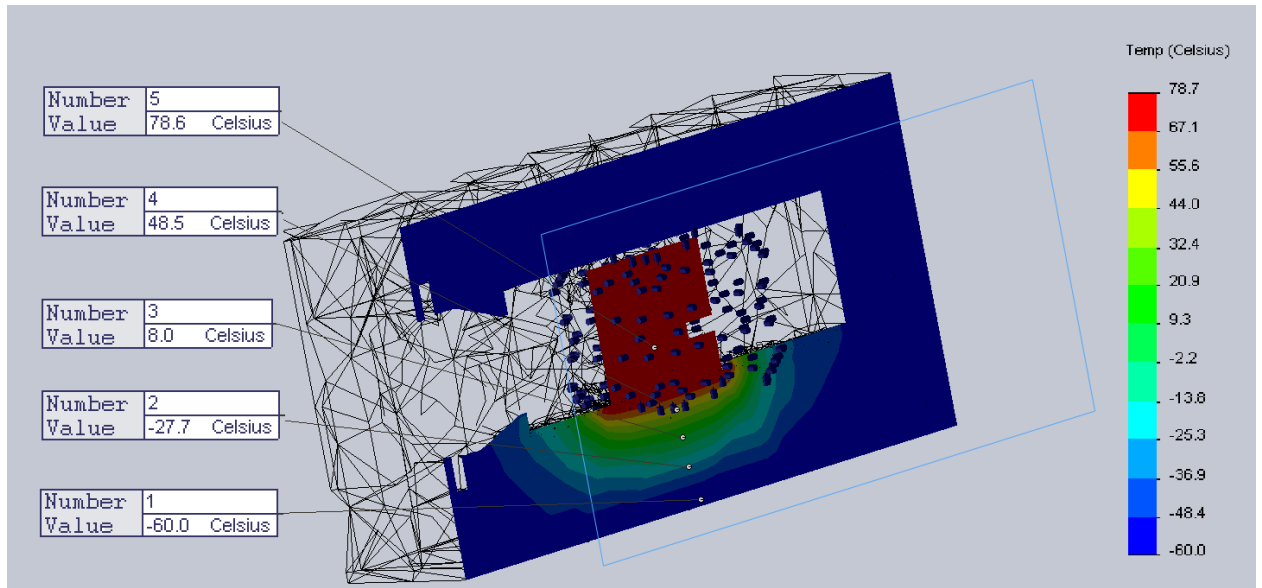


Figure 4-104 Thermal simulation result in a hot case

However, during the descendant phase, camera temperature increases until the end as shown in Figure 4-105. Maximum temperature is 90°C.

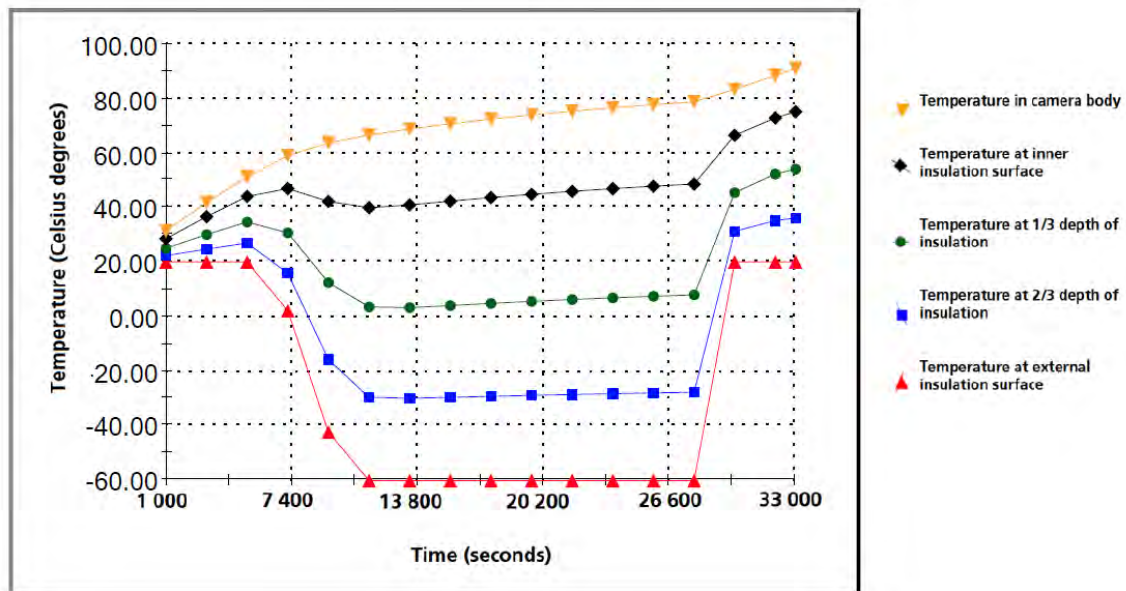


Figure 4-105 Temperature vs time plot of the outer box in the hot case

Inner box

For the inner box, results are shown in Figure 4-106. The image represents a two plane cut to better see the temperature profile at different depths of the insulation. The only emitting element inside the inner box is the Raspberry Pi, which generates 3.5 W of thermal power.

As we can see, the bluer is the colour, the colder is the material. The outside of the box is at -40 °C and the internal components are at \approx 17 °C, never reaching the critical temperature for the Raspberry (0 °C).

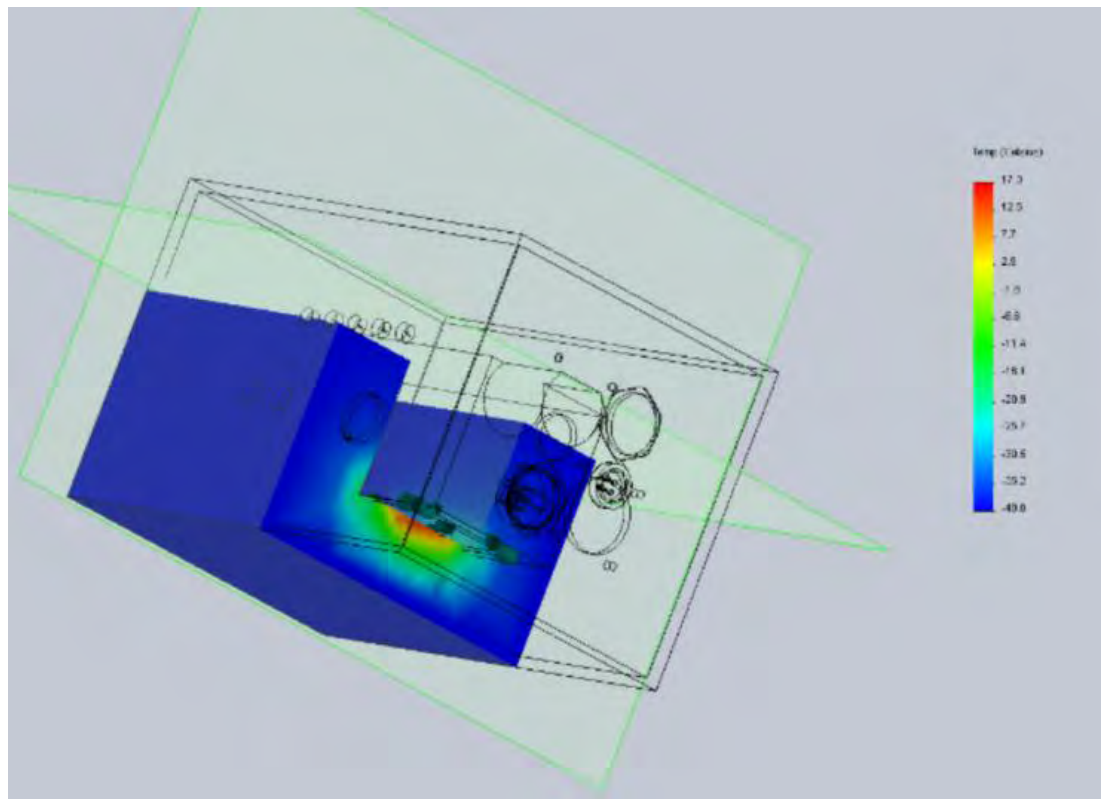


Figure 4-106 Thermal simulation after 8.5 hours for the inner box

In conclusion, thermal simulations showed that insulation and power were properly calculated so no extra precautions against cold were needed.

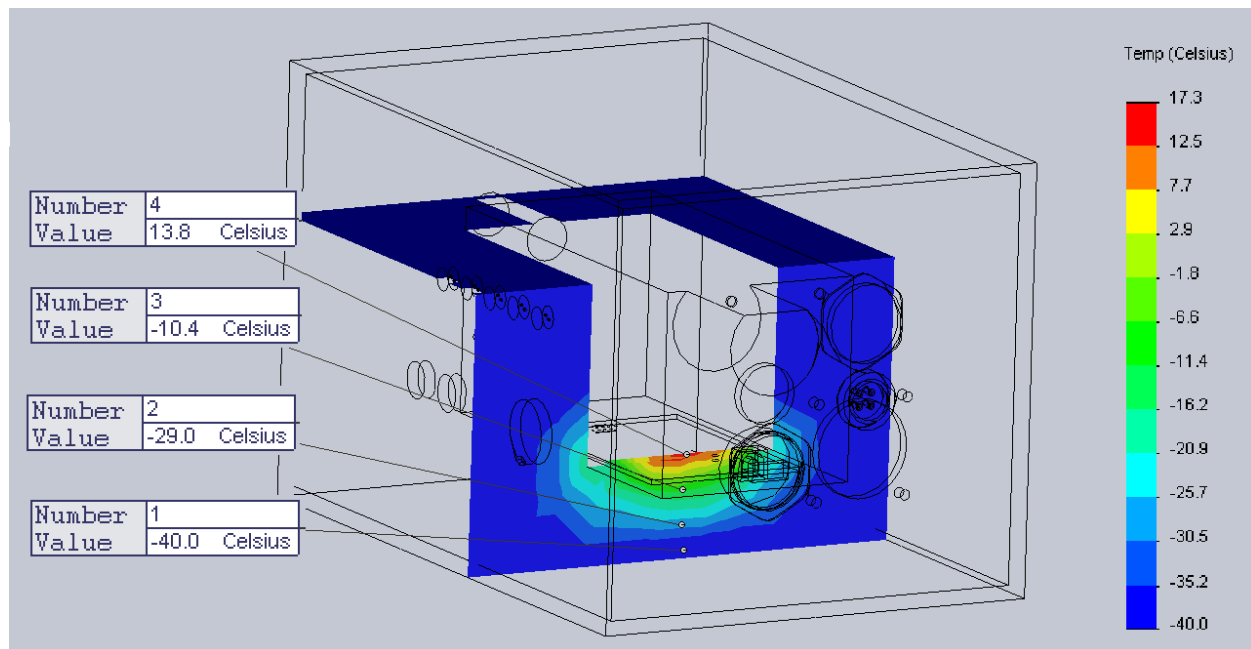


Figure 4-107 Temperature distribution of the inner box

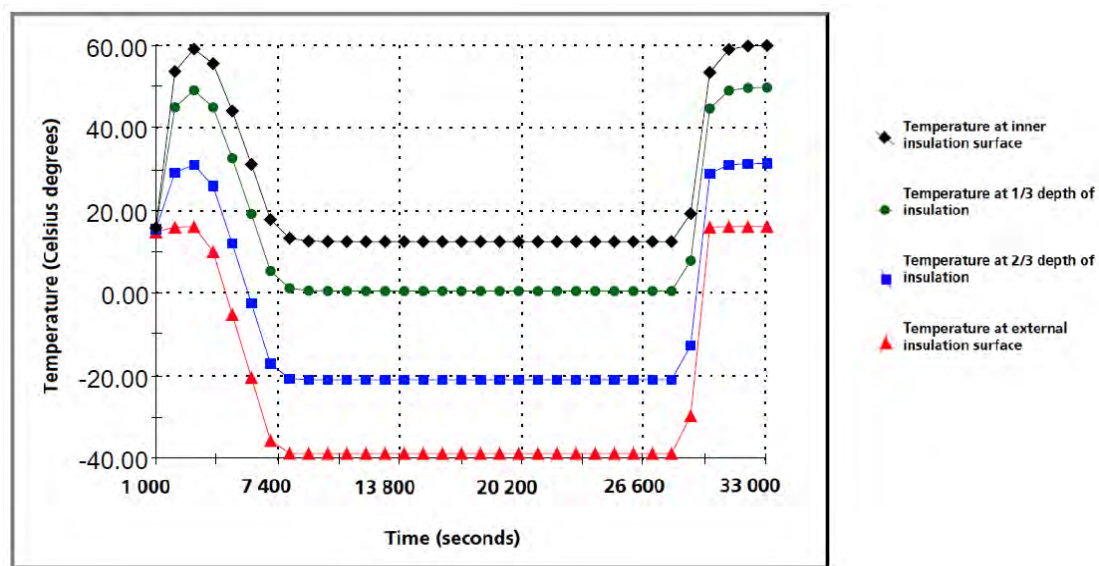


Figure 4-108 Temperature vs time distribution of the inner box

Further information about this can be found in C.8.1 Thermal Simulation.

4.6.1.4 Inner Box Heat Sink

After performing simulations and once test C.7.12. results (vacuum and thermal test) were known, it was clear that a hot case situation could be reached during the flight. These high temperatures can affect the electronics performance. For example, Raspberry Pi CPU is sensitive to heat, if high temperatures are reached (more than 85 °C), the CPU performance could decrease.

Electronics could be damaged permanently if high temperatures are not avoided. The worst case is damaging them in on board, which could result in the complete failure of the experiment.

We decided to attach a heat sink on the top of the Raspberry Pi CPU (as seen in Figure 4-109). This heat sink has a 14.29 cm² surface and the union as made with thermal glue.



Figure 4-109 Heat sink view

The decision of attaching this heat sink was based on the following evidences:

- There is not going to be air inside the boxes and there is not going be any air circulation to cool down the CPU.
- The XPS insulation is not going to protect, neither from heat or cold, because there is not air circulation and no transfer of energy is going to take place.
- The sole way to transfer energy in this environment is radiation.

- Concerning radiation, CPU surface is 1.44 cm^2 .
- By attaching a heat sink to the CPU, we change the surface from this value to 14.29 cm^2 .
- If the heat sink reaches 80°C , it could dissipate up to 1.59 J of energy.

After flight conclusion: with the heat sink the heating ratio was lower. It avoided the overheating of the Raspberry Pi and high, dangerous temperatures were not reached.

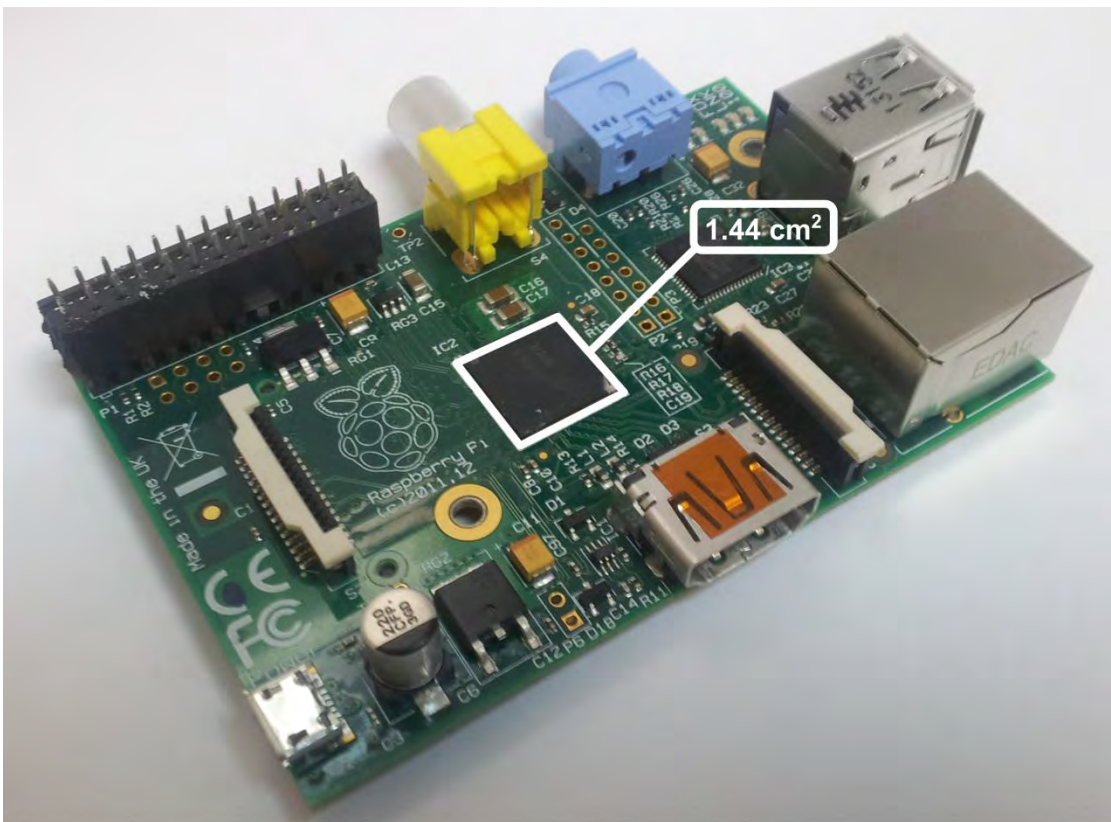


Figure 4-110 Raspberry Pi without the heat sink - ARM area is shown



Figure 4-111 Raspberry Pi with the heat sink attached

Concerning glue and possible de-gasification in a vacuum environment, in case it occurred, it would not have been a problem since the sensitive elements to gasification, camera and lens, are located in the outer box. No extra precautions were considered with respect to this.

4.6.2 Heat Transfer Substantiation

In the previous paragraph, we have supposed that the camera thermal power is 2.5 W because in its data sheet it is said that its electrical consumption is 2.5 W. However, we had to ensure that all this power is taken from the electrical network and transformed into heat after the camera data processing.

To test this, three temperature sensors were put to the camera sides (one up, and other two at each side). Another sensor was free to measure surrounding air temperature.

Using Newton's law of cooling we have

$$q[W] = \overline{h_c} \cdot A \cdot \Delta T$$

where $\overline{h_c}$ is the thermal convection conductivity, A is the area of the radiating object and ΔT is the difference of temperatures between the camera and the environment. This environment is supposed to be a thermal bath, so its temperature never changes.

Assuming a $\overline{h_c}$ value of 10, an area A equal to $1.5 \cdot 10^{-2} \text{ m}^2$ and $\Delta T = 39.9$ (camera surface average temperature) – 22.6 (surrounding air temperature) = 17.3 °C, we get a heat transfer power of **2.59 W**. Obviously, if the camera only consumes 2.5 W (according to data sheet), we have got a higher value due to error associated to assumptions done in camera surface, or thermal conduction conductivity value (in air, this parameter varies from 10 to 100).

In conclusion, we could say that was fine to take a camera thermal power equal to its electrical consumption, and that SolidWorks simulations were performed with known and substantiated parameters.

4.7 Power System

The GranaSAT experiment used the 28 V/1 A power supply from the BEXUS gondola [15].

During the connection process, the peak current was limited at a maximum level with a capacitor and a resistor. The PCB has a voltage regulator (LM2576), a 5 V and 3 A output.

GranaSAT theoretical power consumption is:

Table 4-21 Power consumption

| Instrument | Model | Supply min/max (V) | Current consumption (mA) | Power (W) |
|------------------------|--|--------------------|--------------------------|-------------------|
| Camera | DMK 41BU02.H | 5 | 500 | 2.5 |
| CPU | RPi B | 5 | 700 | 3.5 |
| Temperature Sensor (1) | DS1621 Digital Thermometer and Thermostat | 5 | 1 | $5 \cdot 10^{-3}$ |
| Temperature Sensor (2) | TC74 Digital Temperature Sensor I ² C | 2.7/5.5 | 0.2 | $1 \cdot 10^{-3}$ |



| Instrument | Model | Supply min/max (V) | Current consumption (mA) | Power (W) |
|------------------------------|----------------------|--------------------|-------------------------------|---------------------|
| Magnetometer & Accelerometer | LSM303DLHC | 5 | 0.11 | $5.5 \cdot 10^{-4}$ |
| Regulator | LM2576 | 28 | 23.6 (Output Leakage Current) | 0.66 |
| LEDs | SMD LEDs | 1.869 | 2 | $3.7 \cdot 10^{-3}$ |
| LEDs | High brightness LEDs | 3 | 20 | $60 \cdot 10^{-3}$ |
| I ² C extender | P82B715 | 5 | 14 | $70 \cdot 10^{-3}$ |
| Current Limitator | ITS4141 | $90 \cdot 10^{-3}$ | 0.6 | $54 \cdot 10^{-6}$ |

In the Raspberry Pi, we connected the accelerometer and the magnetometer (model LSM 303DLHC TR) using an I²C bus with a 2.16-3.6 V power supply, with a of 275 µW consumption. The I²C communication is further explained in Appendix C.1 Plans.

To connect the box with the BEXUS batteries, an MS3112E8-4P military connector was used, as defined in the BEXUS manual [15].



Figure 4-112 Gondola power system connector

The power strategy takes as a reference the power budget defined by the power consumption of the different experiment components and the design requirement. If flight duration is 6h, testing is 2h and countdown is 4h.

4.7.1 Power Consumption Timeline

This section describes the real power consumption throughout the flight campaign.

From the very beginning, all the subsystems were turned on; however, not all of them consumed maximum power from the start.

In the pre-launch phase, only some components were connected to check the correct operation: the on-board computer, the camera, the sensors and the losses in the step-down DC/DC regulator consumed power.

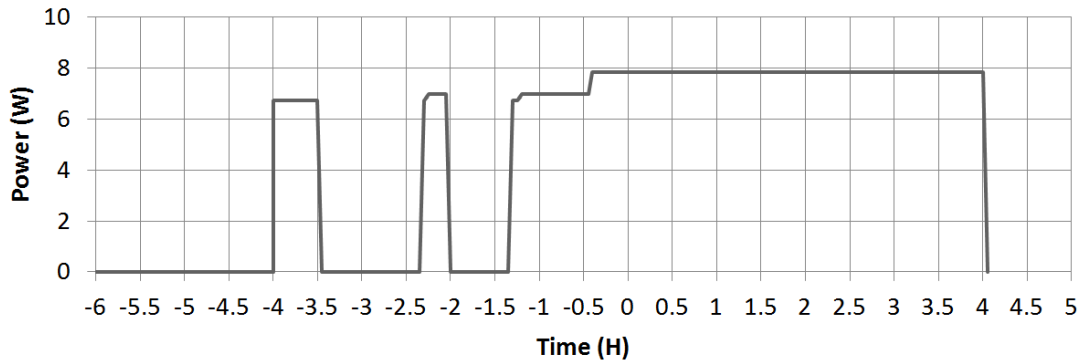
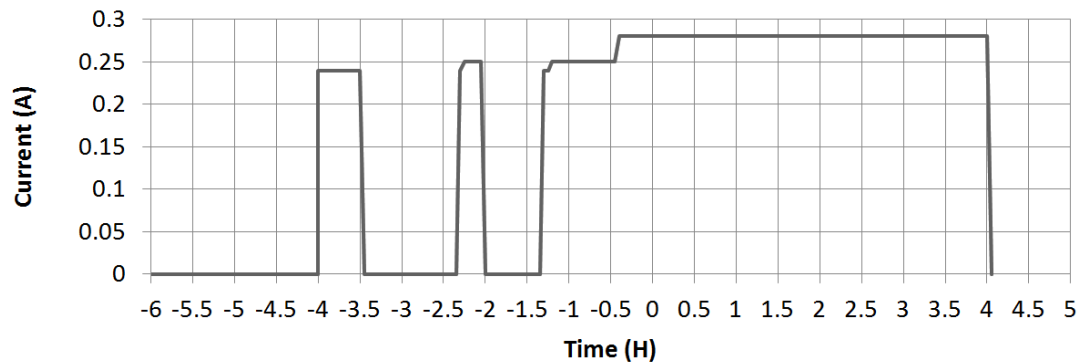
During the launch and the flight itself, the subsystems maintained their power consumption.

Just five minutes before the cut down, the experiment was turned off from the ground station, reducing the power consumption to zero.

After the flight, we could conclude that the assumptions made were right, and the power consumption of the experiment was as expected, without any issues during the flight.

Table 4-22 Current/Power consumption timeline

| TIME | | Current consumption(A) | Power consumption(W) |
|-------------|--------------|-------------------------------|-----------------------------|
| From | Until | | |
| T-6H00 | T-4H00 | 0 | 0 |
| T-4H00 | T-3H45 | 0.24 | 6.7 |
| T-3H45 | T-2H30 | 0 | 0 |
| T-2H30 | T-2H25 | 0.24 | 6.7 |
| T-2H25 | T-2H00 | 0.25 | 7.0 |
| T-2H00 | T-1H30 | 0 | 0 |
| T-1H30 | T-1H20 | 0.24 | 6.7 |
| T-1H20 | T-0H40 | 0.25 | 7.0 |
| T-0H40 | T4H00 | 0.28 | 7.8 |
| T4H00 | T>4H00 | 0 | 0 |

**Figure 4-113 Power comsumption timeline****Figure 4-114 Current consumption timeline**

More details can be consulted in Table 6-6.

These graphics were extracted from the data collected during the Power Electronics Test and component's datasheets. We obtained good results in the test: we got an average efficiency of an 80 % for power delivery of 2.5 A over 5 V.

4.7.2 Battery State of Charge (SoC)

To study the SoC of the experiment, the data shown in the previous section and Table 6-6 was used. This study proved whether one pack of the gondola batteries (LSH20) is sufficient for us.



Figure 4-115 Gondola batteries model (LSH20)

The capacity of the batteries during flight since T-2H25 is shown in the timeline below.

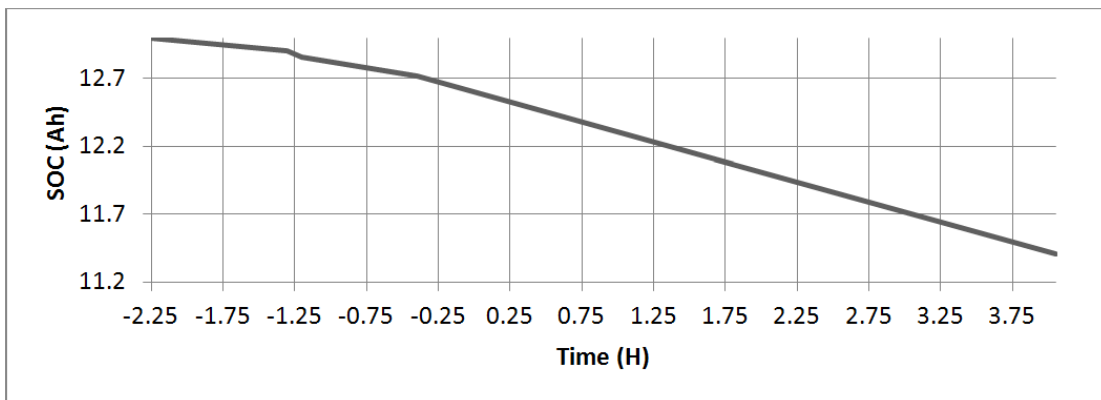


Figure 4-116 State of charge of gondola batteries

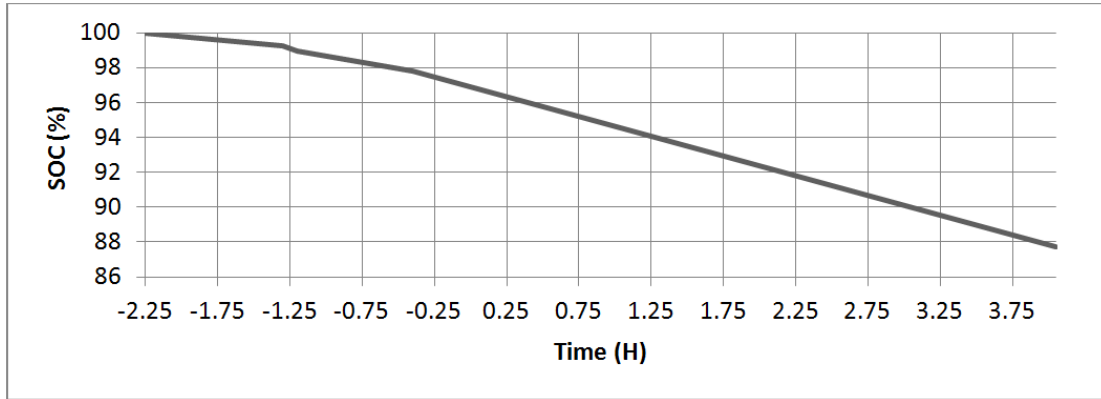


Figure 4-117 State of charge of gondola batteries in percentage

In the next table the results are shown with more details:

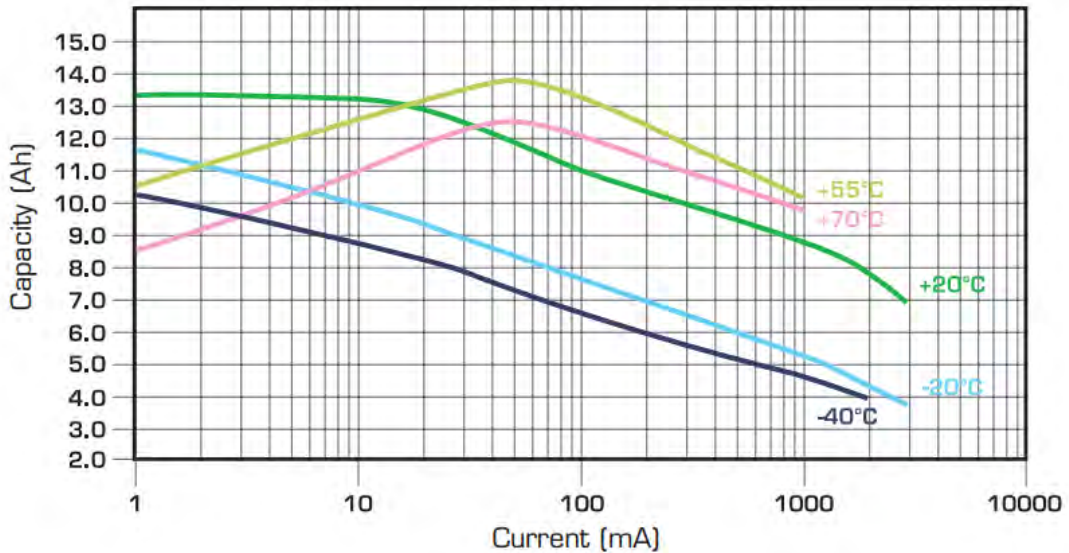
Table 4-23 Soc of the experiment

| TIME (H) | SOC(Ah) | SOC(%) |
|----------|---------|--------|
| -2.25 | 13.000 | 100.00 |
| -1.30 | 12.900 | 99.23 |
| -1.20 | 12.860 | 98.92 |
| -0.40 | 12.714 | 97.80 |
| 4.05 | 11.408 | 87.75 |

-2H25 is the time we started using the gondola batteries. Until this moment, we had been using the external power and Hercules power, as it can be seen in Table 6-6.

With this results we could prove that one pack of the gondola batteries are sufficient for the experiment. We would be able to use this batteries during more than 46 hours (using the maximum value of the consumed current).

In the next figure, the behaviour of this batteries against temperature and the consumed current is shown. This graphic was taken from the batteries datasheet.

**Figure 4-118 - Capacity against current and temperature of LSH20**

In addition, we proved that we were able to endure the losses of capacity in the batteries because of the extreme conditions during the flight.

4.8 Software Design

The handling of the data in this experiment is as important as data processing, so the architecture design, depicted in Figure 4-119, is critical.

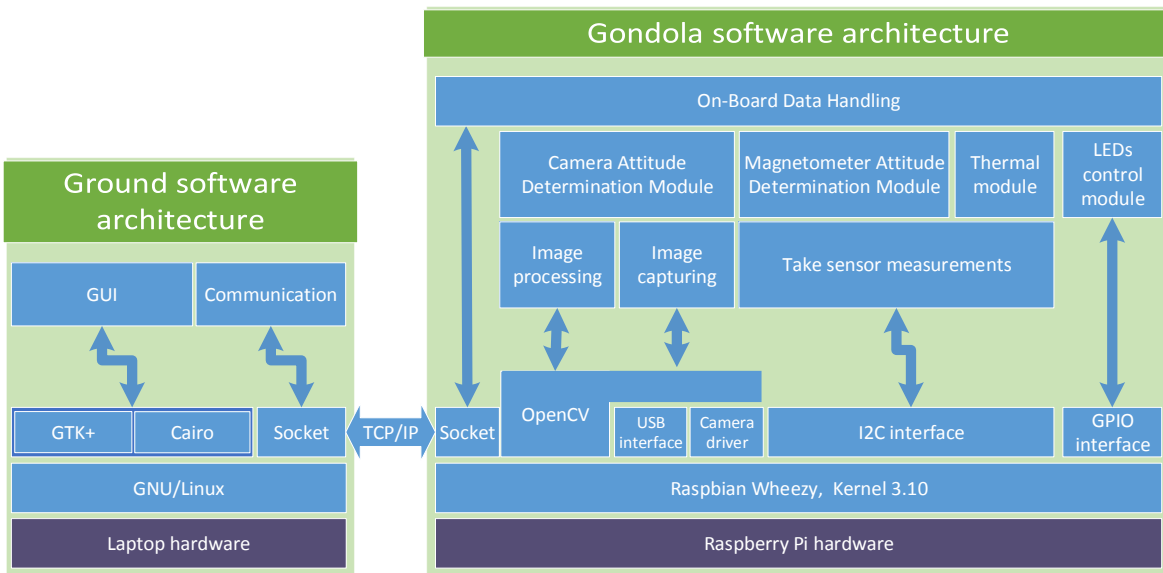


Figure 4-119 Top-level structure of the software architecture

The on-board computer is a Raspberry Pi, model B. The core software beneath our own code is an ARMv6 Linux distribution, Raspbian Wheezy. The programming language used in the whole software project (both the Raspberry software and the ground software) is C and the most relevant libraries used are OpenCV and V4L for the image processing and GTK+ and Cairo for the ground software GUI.

For the connection between the gondola and the ground software, the Raspberry acts as the server side of a TCP/IP connection that starts from ground, whose software acts as the client.

The on-board software is a hard image processing work to be done by the Raspberry Pi. In order to test whether the on-board computer could handle all the data, it is essential we know the performance requirements of the software itself (see Software Requirements).

The attitude determination processing was done both on-board and off-board. The following table shows this distinction:

**Table 4-24 On-board and off-board processing**

| | |
|----------------------------------|--|
| Measurements processed on-board | Images taken from the camera |
| Measurements processed off-board | Magnetometer and accelerometer measurements. Images taken from the camera |

4.8.1 Data Budget and CPU Timing Estimation

The software had to fulfil the requirements, so some tests and calculations were made to confirm that the on-board computer could handle these tasks.

The estimated data budget is shown in Table 4-25, which confirms that a 32GB SD can store the data produced according to the performance requirements during a 10 hour flight.

Table 4-25 Data budget

| | Measured data (B) | Measurement rate (Hz) | Data rate (B/s) |
|-------------------------------|--------------------------|------------------------------|------------------------|
| Magnetometer | 6 | 1 | 6 |
| Accelerometer | 6 | 1 | 6 |
| Temperature sensor | 2 | 1 | 2 |
| CPU temperature sensor | 2 | 1 | 2 |
| Camera | 1,228,800 | 0.5 | 614,400 |
| | | TOTAL (B/s): | 614,416 |
| | | 10 hour data (GB) | 20.6 GB |

Furthermore, a test running a code which reads images, prepares them for processing and saves them in the SD, was made to check the S.1 in Software Requirements. The results, shown in Table 4-26, confirm that it was fulfilled. The test is defined in Test Plan and is deeply covered in C.7 Test Details.

Table 4-26 Performance test results

| | Mean time (μs) | Max Frequency (Hz) |
|--|-----------------------|---------------------------|
| Read and allocate one image | 200,079.4101 | 4 (4.998) |
| Save one allocated image | 29,830.6521 | 33 (33.523) |
| Read, allocate and save one image | 268,119.9635 | 3 (3.730) |

4.8.2 Software Details

The whole source code, along with the source documentation, is hosted in GitHub under a GPLv2 license. See [16] and [5] for more details.

4.8.2.1 Data Handling

The software follows a simple producer-consumer paradigm. There are two main processes:

- A producer, which reads the data from all sensors and stores them in intermediate buffers, and which has two main threads: one for the images and another one for the magnetometer measurements. Its flowchart is shown in Figure 4-120.
- A consumer, which takes the data, processes them, stores them and sends them through the E-Link system. It also has two main threads, one focused on the image module and another one focused on the magnetometer. For reliability and security reasons, the raw data was stored before processing, in order to secure the measurements and to post-process them if any error occurred. Figure 4-121 describes its flowchart.

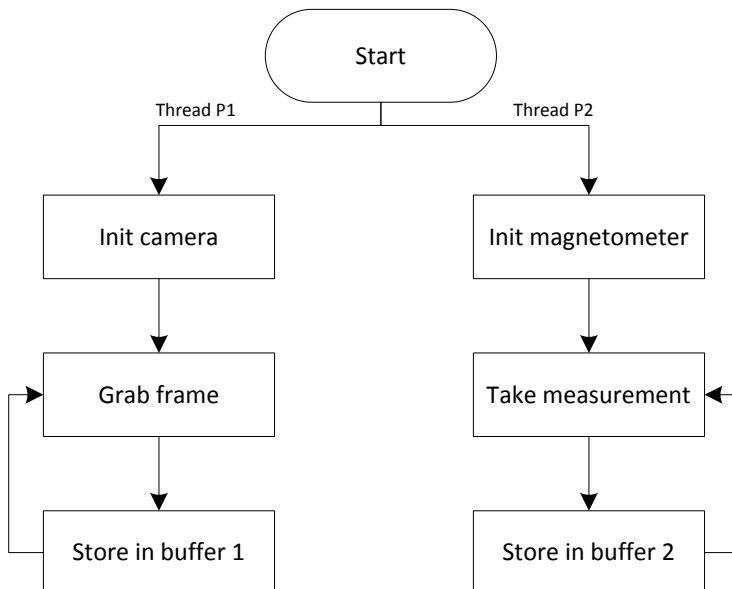
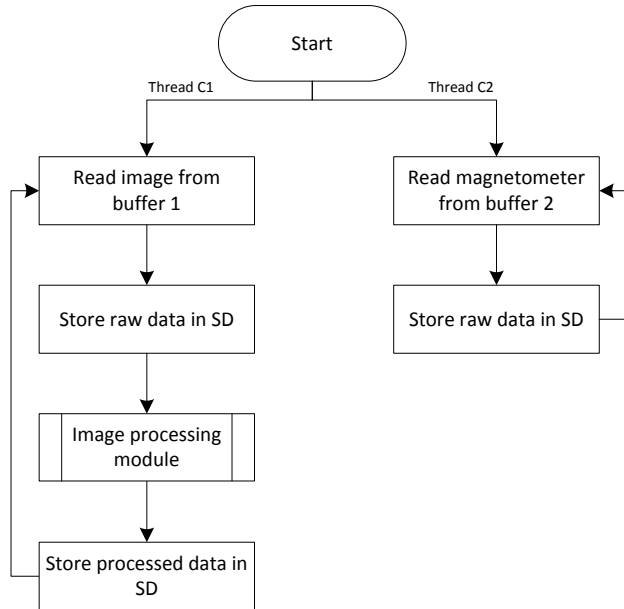


Figure 4-120 Producer**Figure 4-121. Consumer**

4.8.2.2 Image Processing Module

The image processing module is depicted with further information in Figure 4-122 and the two algorithms used in it, the star sensor algorithm and the horizon sensor algorithm, are shown in Figure 4-123 and Figure 4-124, respectively.

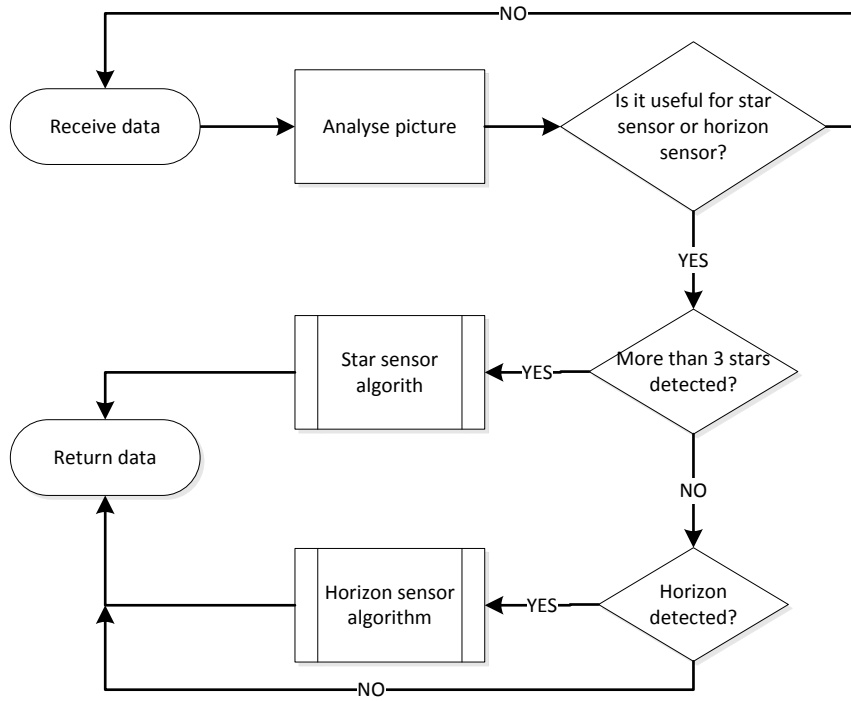


Figure 4-122 Image processing module

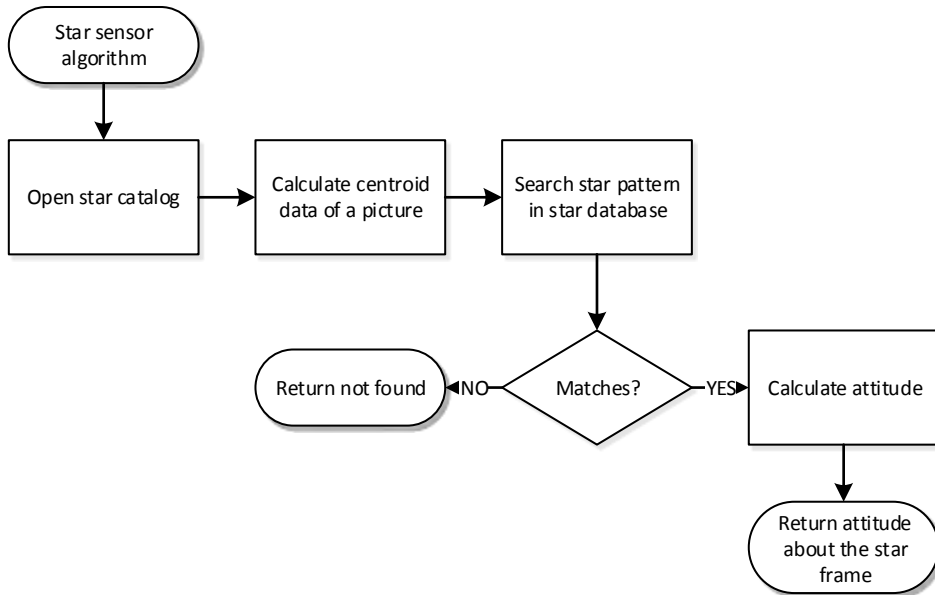
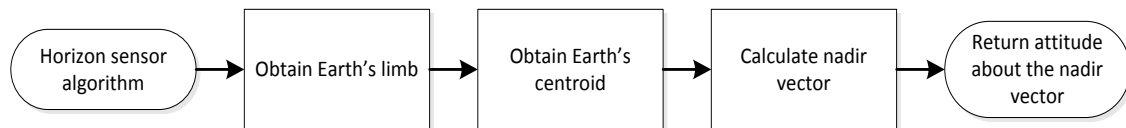


Figure 4-123 Star sensor algorithm

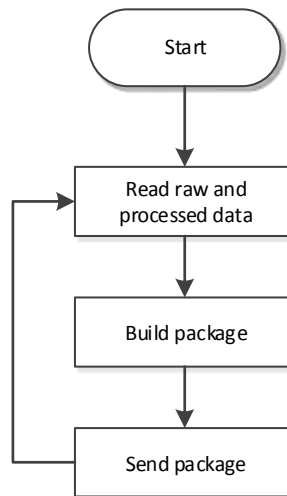
**Figure 4-124 Horizon sensor algorithm**

4.8.2.3 Connection Handling

The gondola software is the server side of the TCP/IP connection with the ground segment, so once the client contacts it, this module starts sending the data; each package sent includes:

- The raw records and the obtained attitude
- The temperature measurements
- The timestamp

This way, a snapshot of the experiment behaviour is received in the ground segment. The Figure 4-125 shows an overview of the simple connection module design.

**Figure 4-125 Connection module**

4.8.2.4 Flight Modes

Three flight modes for the image processing are designed to be handled by the Raspberry Pi:

- AUTO mode: The Raspberry Pi decides which algorithm will process each image taken from the camera, based on its histogram.
- STAR_TRACKER mode: All images taken are processed with the star tracker.
- HORIZON_SENSOR mode: All images taken are processed with the horizon sensor.

One of the main objectives of our experiment is to let the system decide which algorithm will process each image. Since there are a lot of connection losses in the flight because of the E-Link, a timeout loop was designed and implemented to get back to AUTO mode in case the system gets stuck in any of the other modes for more than 15 minutes.

To do so, a clock is initialised when a received command changes the mode from AUTO to STAR TRACKER or HORIZON SENSOR. If, in less than 15 minutes, there is no other command received to get back to AUTO mode, the system autonomously sets the mode to AUTO again.

4.8.2.5 Timestamp

In order to compare our attitude results with TORMES 2.0 data, it was necessary to synchronise the Raspberry Pi clock with some reference. To do so, the Raspberry Pi synchronises its clock with the Ground Station clock, which is synchronised with the GPS clock beforehand.

The client sends synchronisation messages in a regular way. Each time a synchronisation message is received in the server, it measures its own clock. This measurement was stored in a log file along with the client timestamp -sent just after the message-. Furthermore, another pair of clock measurements was stored in the client.

These files were used in the post processing in order to synchronise our measurements with a well-known reference, as the GPS clock.

4.8.3 Star Tracker Software

The following chapter will provide a familiarized reader with all the necessary steps to reproduce the star tracker program in any programming language.



During the development of the GranaSAT star tracker, it was necessary to build a Generated Catalog (GC) and a k-vector (k) [17]. This data was obtained only once before the flight, it was called pre-launch data and it will be detailed in section 4.8.3.1. The GC is the stellar database that appears in Figure 4-126. It contains relevant information of the selected guide stars from the Hipparcos Catalog (HP) [18]. The process to obtain these stars will be explained in section 4.8.3.1. Once the GC has been obtained, the vector k is generated through the angular distance d information of the stars in the GC.

Both the GC and k were generated and stored in text files using MATLAB [19] scripts as shown in Figure 4-126.

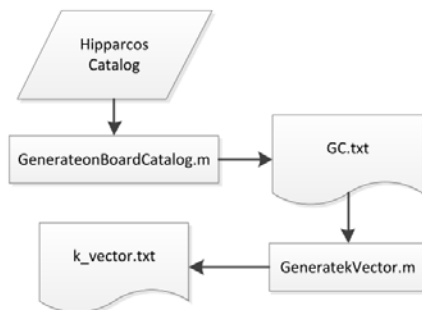


Figure 4-126 GC and k generation

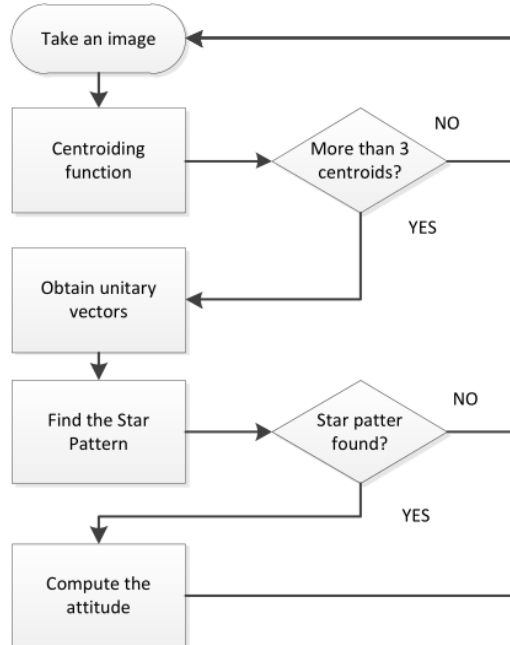
During the flight, the star tracker software ran always a set of C routines in the same order; these are called the Lost In Space (LIS) routine, because it seeks to find the stars appearing in the image and the attitude of the spacecraft without any previous information. Figure 4-127 shows the flow diagram of the LIS routine, which will be detailed in section 4.8.3.2

4.8.3.1 Pre-Launch Data

Building the Generated Catalog

We use the HP information to build the GC as well as to obtain the coordinates of the guide stars in the ECI reference frame.

We can use the VizieR web application [20] to download the whole HP. Every star in the HP has 67 fields, but only the following are useful for our purposes:

**Figure 4-127**

- **Hipparcos Catalogue Identifier** (HIP, Field H1): number between 1 and 118218 that uniquely identifies a star in the Hipparcos Catalog.
- **V magnitude** (Field H5): the V magnitude of the star.
- **Equatorial Coordinates** (Fields H8, H9): the Right Ascension (α) and Declination (δ) for the star in the ICRS for the J1991.25 epoch.
- **Trigonometric Parallax, π** (Field H11): the expected trigonometric parallax π , expressed in milliarcsec.
- **Proper Motions** (Fields H12, H13): the proper motion components for the equatorial coordinates in the ICRS J1991.25 expressed in milliarcsec per Julian year (mas/yr).

As the data in the HP is given for the J1991.25 epoch, we have to convert this data to the current epoch, which was the predicted date for the flight (October 8th, 2014). This operation can be done using NOVASv3.1 [21] software, which is available in [22].

The procedure to obtain the GC (Algorithm 1) is the same as it appears in [23] and its pseudo code is shown below:

Algorithm 1 GC procedure



```

1: for i=1:guideStars.Number-1 do
2:           [xi, yi, zi] = convertRADEC(guideStars(i).RA, guideStars(i).DEC)
3:           for j=i+1:guideStars.Number do
4:               [xj , yj , zj ] = convertRADEC(guideStars(j).RA,
guideStars(j).DEC)
5:               dij = acos(xixj + yiyj + zizj)
6:               if dij < FOV then
7:                   add2GC(guideStar(i).HIP, guideStar(i).HIP, dij)
8:               end if
9:           endfor
10:      end for
11: Short(GC)                                . Short in ascending order
according with dij

```

After this process, the GC can be seen as a shorted database of pairs of stars whose angular distance is smaller than a certain value, FOV. As shown in Table 4-27, the first two columns are the HIP for each star of the doublet. The third column is the angular distance in degrees between these two stars.

Table 4-27 GC overview

| HIP | HIP | d(°) |
|-------|-------|---------|
| ... | ... | ... |
| 82363 | 83153 | 6.0364 |
| 57399 | 58001 | 6.0414 |
| 20885 | 21402 | 6.0518 |
| ... | ... | ... |
| 30122 | 31685 | 13.5857 |
| 85696 | 90422 | 13.5858 |
| 85693 | 86032 | 13.5859 |
| ... | ... | ... |

The size of the GC depends on the number of guide stars chosen. Therefore, it is impossible to include all of the 118218 stars characterized in the HP as guide stars.

Usually, apart from discarding binary stars, the decision to include or not a star as a guide star is made considering its V magnitude (i.e. the apparent magnitude of a star, V mag) [24]. The size in number of entries in the GC grows nearly exponentially with the Vmag.

The Vmag selected depends mainly on the camera sensor. The greater the sensibility of the sensor is, the less bright the stars will appear in the image with less exposure time. After an analysis of sky covering (this is, Vmag vs FOV), the cutoff Vmag=4.5 was selected. The number of guide stars with Vmag < 4.5 in the HP is 909.

Once we have obtained an appropriate number of guide stars, we can build the GC following the steps described at the beginning of this section (Algorithm 1). We obtained a GC with 47477 entries. Finally, the following Figure 4-128 shows a representation of the guide stars in the Celestial Sphere for their coordinates in the ICRS at J1991.25.

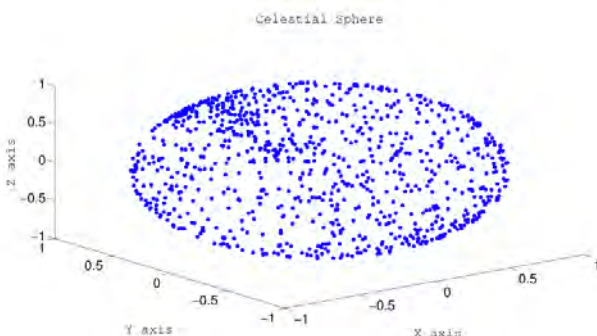


Figure 4-128 Celestial Sphere

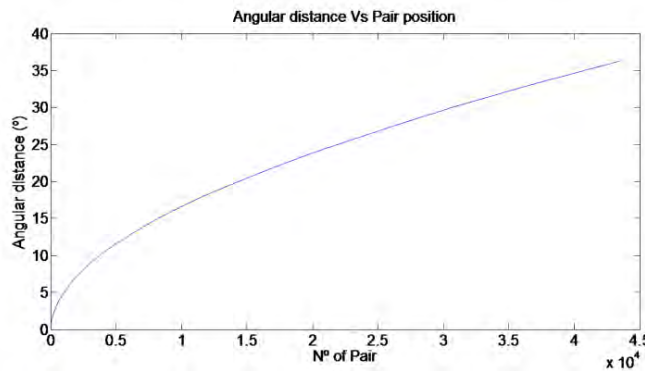
Building the k-vector

The k-vector searching technique [1] is used. This technique requires the generation of a n-long vector (k) where n is as equal as entries in the previous obtained GC. In our case, we obtained a n=43477 k-vector. The following Figure 4-130 shows the angular distance in degrees versus the pair index in our GC. As we can see, the greater the index is, the greater the angular distance between any two guide stars will be too. The vector k is created from the shorted GC as shown in the following pseudo-code:

```

1:  $m = \frac{y_{max} - y_{min}}{n-1}$                                  $\triangleright y_{max}, y_{min}$  are the maximum and  $d_{ij}$  in the GC
2:  $q = y_{min} - m$ 
3: for  $i \leq n$  do
4:    $z(i) = im + q$ 
5: end for
6:  $k(1) = 0$ 
7:  $k(n) = n$ 
8: for  $i = 2 : i \leq n - 1$  do
9:    $number = find(GC.d_{ij} < z(i))$ 
10:   $k(i) = number$ 
11: end for

```

Figure 4-129 K-vector Generation**Figure 4-130 Angular distance VS Index**

As it appears in the previous Figure 4-129, every position $k(i)$ of the k vector represents the number of GC entries below the $z(i)$ value. Once k has been generated, the following expressions are used for finding in the GC all entries whose angular distance is inside the range $[a, b]$.

$$j_a = \left\lfloor \frac{a - q}{m} \right\rfloor \quad Eq \ 1$$

$$j_b = \left\lfloor \frac{b - q}{m} \right\rfloor \quad Eq \ 2$$

Then, the values $k \ start = k(j_a)+1$ and $k \ end = k(j_b)$ defines the index of the range $[a, b]$ in the GC. This is graphically explained in Figure 4-131.

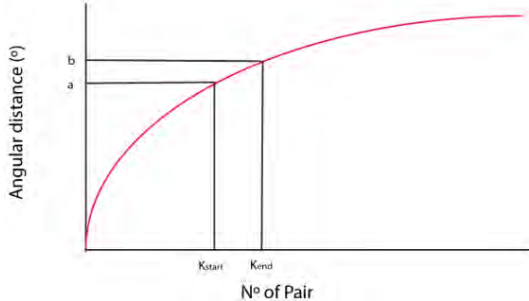


Figure 4-131 K-vector Range Searching Technique

4.8.3.2 Lost In Space Routine

Centroiding

Centroiding is the first sub-algorithm applied to an image after receiving it. The objective is to find the coordinates (x_{cm}, y_{cm}) in the image frame of each possible star. The algorithm used has been adapted from the one appearing in [25].

Considering the image as a matrix with n rows and m columns, the algorithm 5 seeks to find each star's coordinates (x_{cm}, y_{cm}) .

```

1: for i = 1 : n do
2:   for j = 1 : m do
3:     if image(i, j) ≥ Threshold then
4:       iBorder = computeIborder(ROI, n, m)
5:       DN = computeBrightness(ROI, n, m)
6:       xcm = computeXcm(ROI, n, m, DN)
7:       ycm = computeYcm(ROI, n, m, DN)
8:       centroid = [xcm, ycm, DN]
9:       append(listOfCentroids, centroid)
10:      end if
11:    end for
12:  end for
13: centroids = clusterCentroids(listCentroids)
14: centroids = shortCentroids(centroids)
```

Figure 4-132 Centroiding

The parameters used are:

- **Threshold:** as we are using grey color images, it is an integer between 0 and 255. It is used to discriminate between a noise pixel and star pixels.
- **Region Of Interest (ROI):** odd integer value that defines a square region.

Auxiliary functions and their functionality is explained below:

- `computeBorder()`

After detecting a pixel p which value is greater than the threshold, this function computes the average intensity of the pixels in the edge of the square region defined by ROI and centered in p . In Figure 10 we have dashed in red the edge pixel of a ROI=5. The reader must note that as we are using grey scale images, the closer the pixel is to pure white, the greater its value is.

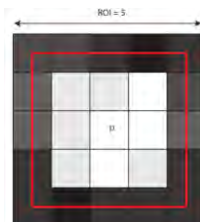


Figure 4-133 Region Of Interest

Finally, the average intensity iBorder is computed using Equation 3 :

$$iBorder = \frac{\sum \text{Pixels} \in ROI_{edge}}{4(ROI - 1)} \quad Eq. 3$$

- `computeBrightness()`

This function computes the brightness DN using equation 4:

$$DN = \sum_{x=\left(n-\frac{ROI}{2}\right)+1}^{\left(n+\frac{ROI}{2}\right)-1} \sum_{y=\left(m-\frac{ROI}{2}\right)+1}^{\left(m+\frac{ROI}{2}\right)-1} (image(x, y) - iBorder) \quad Eq. 4$$

- Computing x_{cm} and y_{cm}

Both coordinates are calculated through the `computeXcm()` and `computeYcm()` functions which implement Equations 5-6 respectively:

$$x_{cm} = \sum_{x=\left(n-\frac{ROI}{2}\right)+1}^{\left(n+\frac{ROI}{2}\right)-1} \sum_{y=\left(m-\frac{ROI}{2}\right)+1}^{\left(m+\frac{ROI}{2}\right)-1} x \frac{image(x, y)}{DN} \quad Eq. 5$$

$$y_{cm} = \sum_{x=\left(n-\frac{ROI}{2}\right)+1}^{\left(n+\frac{ROI}{2}\right)-1} \sum_{y=\left(m-\frac{ROI}{2}\right)+1}^{\left(m+\frac{ROI}{2}\right)-1} y \frac{image(x, y)}{DN} \quad Eq. 6$$

- `clusterCentroids()`

Quite often, a star will have more than one pixel with a greater value than the defined threshold. In this case, we need to cluster these centroids to be able to correspond each star with a unique centroid. In our case, we average the position of each centroid that belongs to the same star, eq 7-8:

$$x_{cm} = \frac{\sum_{x_i \in Star} x_i DN_i}{\sum_{x_i \in Star} DN_i} \quad Eq. 7$$

$$y_{cm} = \frac{\sum_{y_i \in Star} y_i DN_i}{\sum_{y_i \in Star} DN_i} \quad Eq. 8$$

- `shortCentroids()`: This function shorts the clustered centroids in descending order according with its brightness DN.

Getting the Unitary Vector

Once the centroids have been obtained, we can derive from them the unitary vector (\vec{v}) associated with each one. This is done assuming firstly that the camera optics can be simplified as a pinhole system. As it is shown in Figure 4-132, in a pinhole system every ray that comes from the infinity passes through the pinhole. The distance between this point and the image plane is F (optics focal length), x_0, y_0 are the image principal points, this is, the image centre [26].

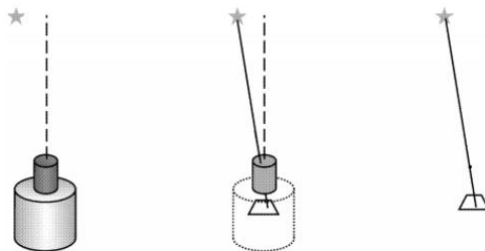


Figure 4-134 Pinhole system

Each centroid with coordinates x, y has an associated unitary vector $\vec{v} = \vec{i} + \vec{j} + \vec{k}$ that is computed using Equations 9, 10 and 11:

$$i = \cos(\text{atan2}(x - x_0, y - y_0)) \cos\left(\frac{\pi}{2} - \text{atan}\left(\sqrt{\left(\frac{x - x_0}{F}\right)^2 + \left(\frac{y - y_0}{F}\right)^2}\right)\right) \quad Eq. 9$$



$$j = \sin(\text{atan}2(x - x_0, y - y_0)) \cos\left(\frac{\pi}{2} - \text{atan}\left(\sqrt{\left(\frac{x - x_0}{F}\right)^2 + \left(\frac{y - y_0}{F}\right)^2}\right)\right) \quad Eq \ 10$$

$$k = \sin\left(\frac{\pi}{2} - \text{atan}\left(\sqrt{\left(\frac{x - x_0}{F}\right)^2 + \left(\frac{y - y_0}{F}\right)^2}\right)\right) \quad Eq \ 11$$

Finding the Star Pattern

The algorithm developed for identifying the stars in the image is a variation of the Matching Group algorithm [27]. After the previous steps, a list of unitary vectors, each one corresponding with a centroid, is available. With this information, we find the HIP number of each star in the image. In order to make this section more understandable, capital letters represent a unitary vector associated with a certain star.

The algorithm will be explained step by step:

1. Assume that we have a list of $\mathbf{N} \geq 3$ unitary vectors. Get the first three ones **A**, **B** and **C**.
2. Select the vector **A** as Kernel and compute its angular distance with the vectors **B** and **C**.
3. Use the k vector range searching technique to find in the GC the pairs of stars whose angular distance d_{xy} is inside the range $[d_{xy} - d_{xy}\varepsilon, d_{xy} + d_{xy}\varepsilon]$. This is done for both d_{AB} and d_{AC} . The ε value represents the relative error obtained when measuring angles, it depends on the camera calibration. The GC entries inside the range $[d_{xy} - d_{AB}\varepsilon, d_{xy} + d_{AB}\varepsilon]$ And $[d_{AC} - d_{AC}\varepsilon, d_{AC} + d_{AC}\varepsilon]$ are stored in separates structures S1 , S2.
4. For each star present in both S1 and S2 check if the other two star have an angular distance inside the range $[d_{BC} - d_{BC}\varepsilon, d_{BC} + d_{BC}\varepsilon]$. See Figure 4-135

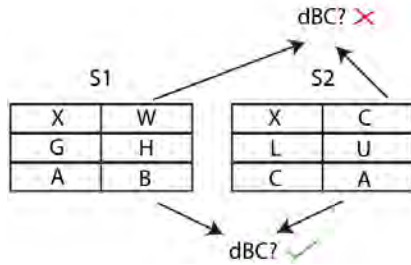


Figure 4-135 Step 4

If at least one triplet of stars **A,B,C** is found, store the triplet and proceed with step 5, otherwise, discard the image and process a new one.

5. Repeat steps from steps **2** to **4**, but selecting **B** as the kernel. If at least one triplet **B, A, C** is found, store the triplet and proceed with step **6**, otherwise, discard the image and process a new one.
6. Repeat steps from steps **2** to **4**, but selecting **C** as the kernel. If at least one triplet **C, A, B** is found, store the triplet and proceed with step **7**, otherwise, discard the image and process a new one.
7. At this point, it is possible to have the same three stars repeated three times with the only difference in its order, if that happens, chose these stars as the possible first three stars. Note that more than one possible triplet can be found due to the ε value.
8. If $N > 3$ proceed with step **9**, otherwise, if only one triplet is found, return this triplet as the stars appearing in the image. If more than one triplet is found and $N = 3$, the star field was not uniquely identified, in this case, discard the image and process a new one.
9. For each one of the remaining unitary vectors:

If $\exists \mathbf{D} \in [d_{AD} - d_{AD}\varepsilon, d_{AD} + d_{AD}\varepsilon] \in [d_{BD} - d_{BD}\varepsilon, d_{BD} + d_{BD}\varepsilon] \in [d_{CD} - d_{CD}\varepsilon, d_{CD} + d_{CD}\varepsilon]$ add **D** to the list of identified stars. Otherwise, discard **D** and proceed to **E**.

Note that if the list of identified stars grows, the number of ranges to check grows as well. Suppose that **D** has been found in the three ranges expressed above, now the star with unitary vector **E** has to be present in all ranges: $d_{AE} - d_{AE}\varepsilon, d_{AE} + d_{AE}\varepsilon] \in [d_{BE} - d_{BE}\varepsilon, d_{BE} + d_{BE}\varepsilon] \in [d_{CE} - d_{CE}\varepsilon, d_{CE} + d_{CE}\varepsilon]$

$[d_{DE} - d_{DE}\varepsilon, d_{DE} + d_{DE}\varepsilon]$ This makes the algorithm more robust against false stars with the more stars are added.

It is in this step when the possible multi-triplets found in step 7 are discarded since no new stars are added or its number is lower than the number of identified stars for the true match.

Getting the Attitude Matrix

In order to determine the attitude matrix of our spacecraft, we use the SVD method proposed by Markley [28]. Its procedure is described below:

- Suppose that it is available a set of n vectors (notated as \mathbf{b}) measured in the spacecraft frame. Their values \mathbf{r} in an inertial reference frame are available.
- The matrix B is constructed as it appears in Equation 12:

$$B = \sum_{i=1}^n \mathbf{b}_i \mathbf{r}_i \quad Eq. 12$$

- Applying the Singular Value Decomposition to the matrix B we can obtain:

$$B = USV^T \quad Eq. 13$$

- The current Attitude matrix is finally found:

$$A = U_+ V_+ \quad Eq. 14$$

Where:

$$U_+ = \begin{bmatrix} 1 & 0 & 0 \\ 0 & 1 & 0 \\ 0 & 0 & \det(U) \end{bmatrix} \quad Eq. 15$$

$$V_+ = \begin{bmatrix} 1 & 0 & 0 \\ 0 & 1 & 0 \\ 0 & 0 & \det(V) \end{bmatrix} \quad Eq. 16$$

4.8.4 Horizon Sensor Software

The horizon sensor consists in a simple image processing algorithm. However, there are some problems to face in its implementation.

As the algorithm works in the visible spectrum, the main problem lies in the horizon detection. The atmosphere, its albedo and the sunlight makes more difficult the Earth's limb isolation, so some assumptions and mathematical corrections are made.

Horizon Detection

The solution undertaken for the horizon detection is simple, and can be viewed in Figure 4-136.

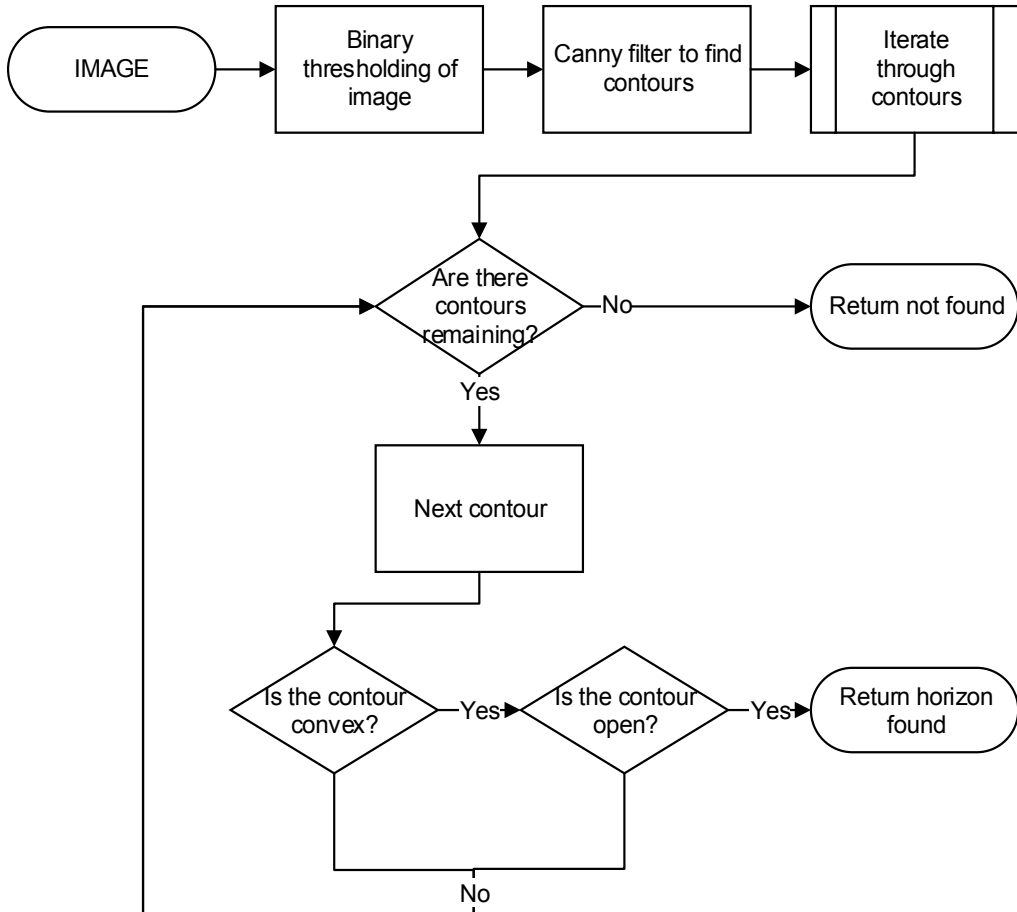


Figure 4-136 Horizon characterization

The horizon characterization is very simple. The algorithm makes the following assumption: a horizon in an image is a convex curve that fills the frame, i.e. a not closed contour.

Once a horizon has been detected in an image, the second problem to face lies in the approximation of the contour points by a circumference. The centre of this circumference represents the centre of the Earth, which is the point the algorithm looks for.

A geometric approach has been implemented to solve this problem. As three non-collinear points determine a unique circumference, the algorithm iterates through

all the contour points, tracing segments between every two adjacent points and obtaining their perpendicular bisectors. In an ideal situation, all the perpendicular bisectors would intersect in a single point. As this is not the case, an approximation has to be made between all the intersections in order to determine the centre of the Earth.

Earth Circumference Fitting

Once the horizon is detected, the collected data has to be processed in order to get the centre and the radius of the Earth's circumference.

There are several procedures to fit circles into data, most of them based in the least squares approach. After some research, mainly based in Dale Umbach and Kerry N. Jones paper [29], we decided to use the Modified Least Squares Method.

Its robustness against collinear points, the fact that downweights pairs of points that are close together, the ease of implementation and its fast performance lead us to choose MLS against any other proven method.

For further information about the advantages of this approach, see C.7.2 Horizon Sensor Test.

Testing

It was difficult to find images that fit the testing purposes of the algorithm, i.e. images in which the Earth limb was recorded from a high altitude. After some research, the team contacted with COMPASS, an experiment that flew in BEXUS 9 campaign. They provided us with eight videos taken with two different cameras that show the entire BEXUS 9 flight. As the conditions in which the videos were recorded are very similar to the conditions in which the algorithm will work, the team decided to use them as source of testing images.

The first approach of the horizon sensor algorithm running on the COMPASS videos can be seen in Figure 4-137.

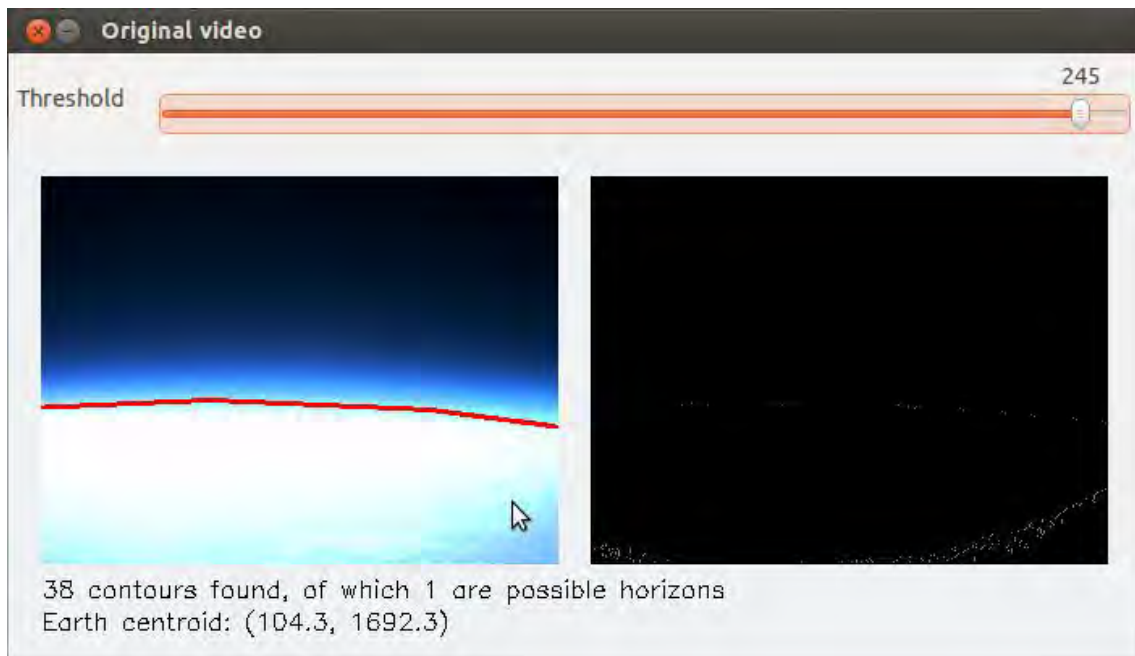


Figure 4-137 Horizon sensor test with COMPASS videos

Post-processing

The processing of the real images taken at BEXUS 19 flight showed two problems that were not expected: noisy images and low contrast images.

In order to solve them, two auxiliary methods were implemented:

1. A Gaussian blur filter, used just before the binary thresholding to smooth the images and get tractable contours.
2. Autonomously determined threshold -based in the overall luminosity of the image-, used in those cases where even the human eye cannot see the Earth's limb.

For more information, see section 7.3.2.

4.8.5 Magnetometer Attitude Determination Module

Before data recording begins, we have to configure the magnetometer software.

4.8.5.1 Operating Mode

First, we have to set the range of measures which will work for both the magnetometer and the accelerometer.

To set the range of the magnetometer, we have made a simulation of the magnetic field by taking the flight BX17 coordinates that we have been unable to locate. With these coordinates, we track the trajectory of the gondola, and we can obtain the magnetic field with a model IGRPF11 simulation. This simulation will provide us with the maximum and minimum values of the magnetic field and will help us choose the operating range of the magnetic sensor.

The graphs obtained from the simulation are shown in Figure 4-138, Figure 4-139 and Figure 4-140.

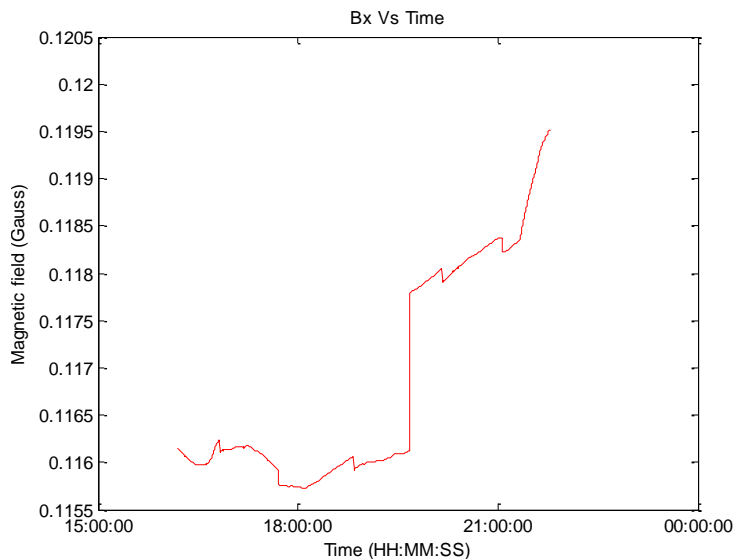


Figure 4-138 Simulated magnetic field on the X axis

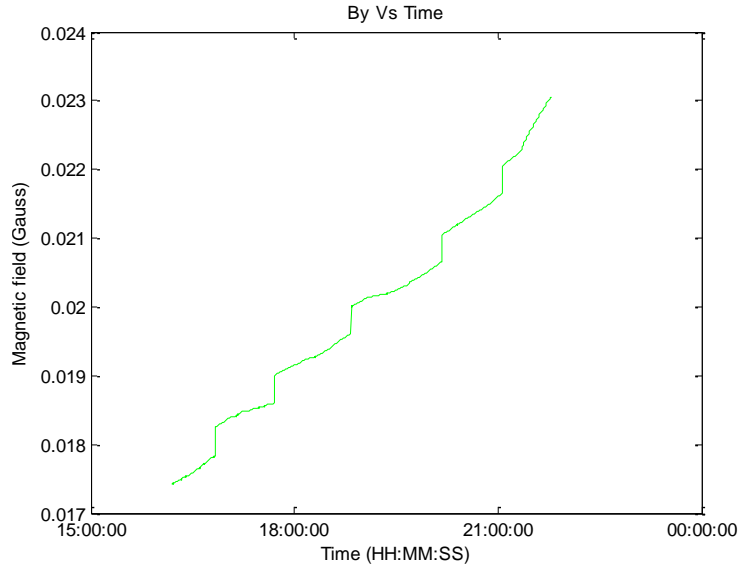


Figure 4-139 Simulated magnetic field on the Y axis

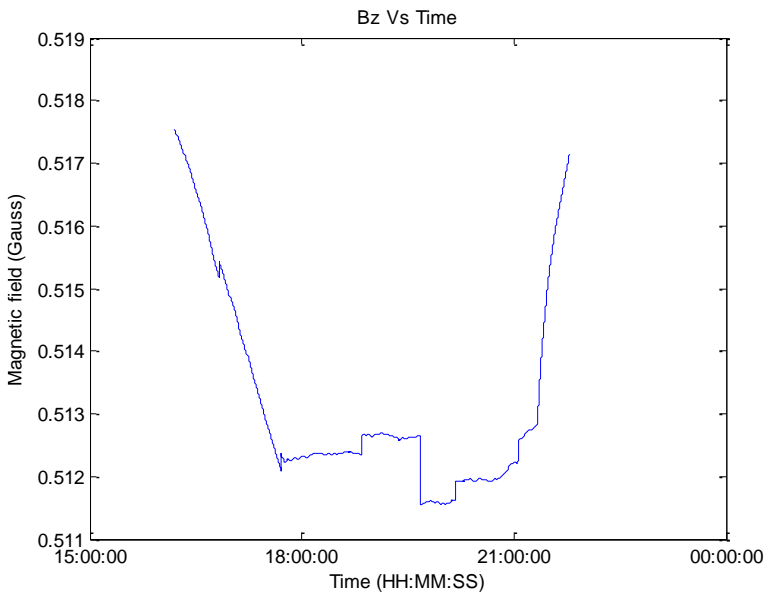


Figure 4-140 Simulated magnetic field on the Z axis

The maximum value of the Earth's magnetic field that we should measure will be 0.175 Gauss and the minimum 0.0174 Gauss.

Once we have done this, we configure the magnetic sensor to work in a ± 1.3 Gauss range, which is the minimum provided by the sensor.



To select the operating range of the accelerometer, we must bear in mind that the mechanical design shall provide protection for the possibility of 10 g vertical and 5 g horizontal. Hence, we are left with two possibilities in the accelerometer that meet these requirements and the maximum of G's we can measure:

- ± 8 g operating mode
- ± 16 g operating mode

If we choose ± 16 g operating mode, we would lose much precision, considering that 10 g is the maximum the mechanical design can support. Thus, we chose the ± 8 g operation mode.

Finally, the last thing to consider is the amount of measurements we will take from the accelerometer and magnetometer per second. Both will provide us with two measurements per second.

To configure all the aforementioned, we have to configure the registers included in the datasheet [9].

4.8.5.2 Magnetometer Calibration

To calibrate the magnetometer, we had to consider the two most important effects that we will face: hard and soft iron effects.

The magnetometer sensor was located in the outer box PCB, and calibrated it by following Talat Ozyagcilar's recommendations [30] [31] [32].

Hard iron magnetic fields are generated by permanently magnetized ferromagnetic PCB components. Figure 4-141 shows the modelling of the distortion of the geomagnetic field by three permanent magnets creating hard iron interference.

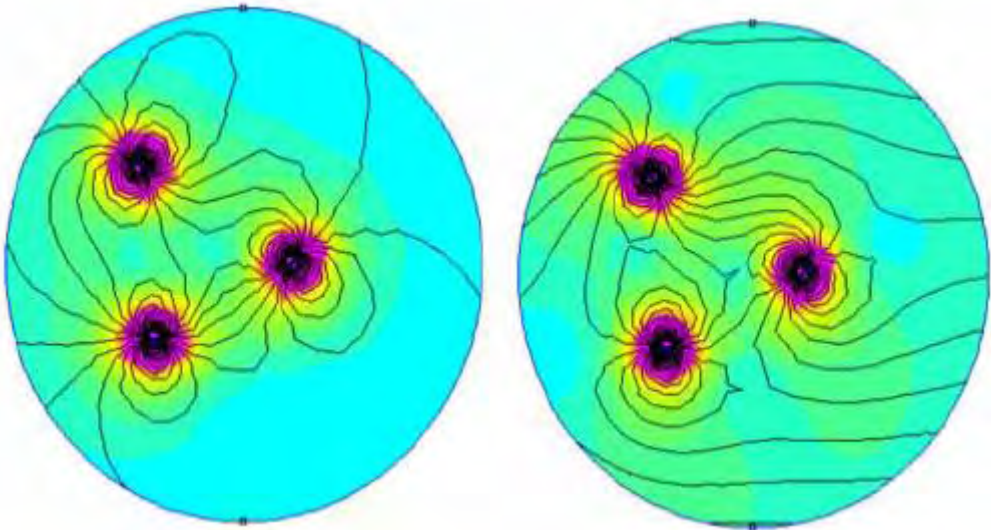


Figure 4-141 Hard iron disturbance of a uniform magnetic field (from [31])

Hard iron interference can be minimized avoiding strongly magnetized ferromagnetic components and placing the magnetometer as far away as possible from such components. In addition, since we cannot eliminate completely the hard iron effects, software compensation is required.

Soft iron interference is created by the induction of a temporary magnetic field into normally unmagnetized ferromagnetic components by the geomagnetic field, such as steel shields on the PCB.

To compensate the offset introduced by these effects, we had to take a number of measures, moving the magnetic sensor and, considering the move made by the accelerometer, build a sphere or an ellipse as is shown in Figure 4-142.

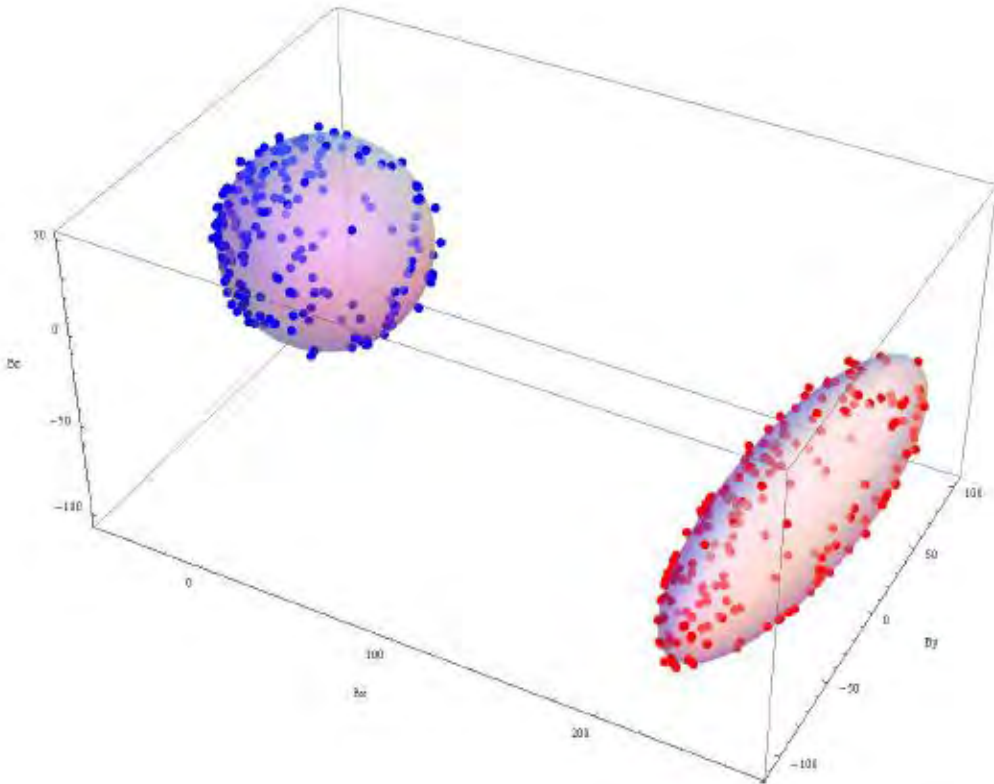


Figure 4-142 Calibrated and uncalibrated magnetometer measurements (from [30])

If we measure without hard and soft iron effects, we will obtain a sphere centred at zero. However, we took measurements under hard and soft iron effects. Hence, we obtained an ellipse shaped form as the gains of the axes are unbalanced. Therefore, we ran a calibration process at the beginning of the experiment to compensate with the software the measurement error.

4.8.6 Attitude Determination Using an Accelerometer

Due to difficulty for determining the inclination angle with a magnetometer –since magnetic field varies with altitude and we did not have a reference during flight-, we used an accelerometer/gravimeter to determinate the gondola inclination angle. The gravity acceleration is stable with elevation so no reference is needed –except knowing that gravity value is 9.8 m/s^2 .

The accelerometer is depicted in Figure 4-143.

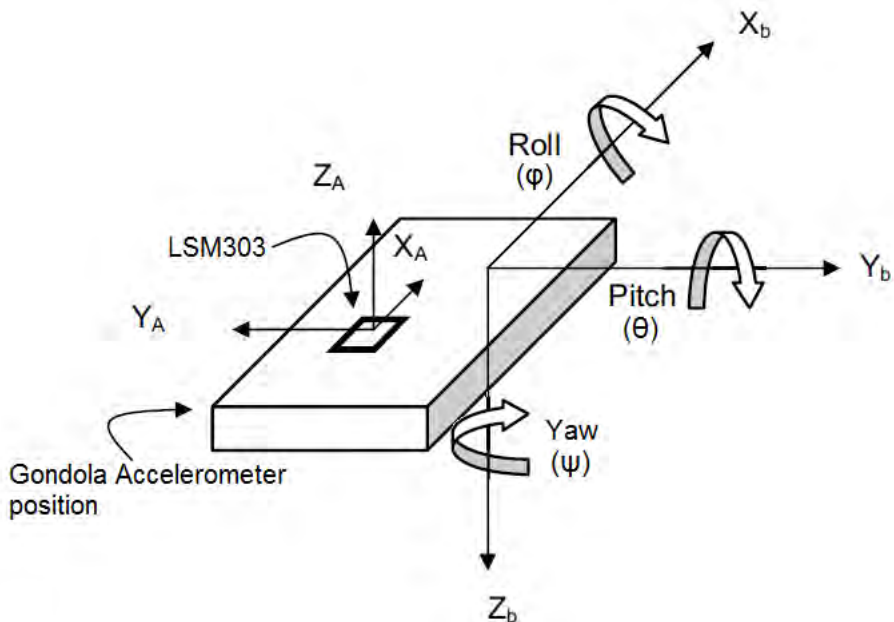


Figure 4-143 Accelerometer depiction. X_A, Y_A and Z_A shows the accelerometer sensors position, whereas X_b, Y_b and Z_b shows the different rotations that can be done

With accelerometer resting in any position, in general we read

$$\begin{pmatrix} X \\ Y \\ Z \end{pmatrix}$$

where X, Y, Z is the reading of gravity in each axis.

If our accelerometer rests in a horizontal position, the reading is

$$\begin{pmatrix} 0 \\ 0 \\ 1 \end{pmatrix}$$

where the measurements are done in g units (1 g = 9.8 m/s²).

But if we perform a α degrees roll clockwise rotation (referred to axis as shown in Figure 4-143), we measures a ξ_2 value in Y axis and a ξ_3 value in Z axis which means

$$\begin{pmatrix} 0 \\ \cos(\alpha) \\ \sin(\alpha) \end{pmatrix}$$

so solving $\arccos(\xi_2)$ or $\arcsin(\xi_3)$ we obtain the α angle rotated in pitch.



Extending this procedure to 3 dimensions rotation, using the same rotation matrix shown in 4.8.5.2, we obtain that given a reading of

$$\begin{pmatrix} \xi_1 \\ \xi_2 \\ \xi_3 \end{pmatrix}$$

we can undo the rotations applying

$$\widetilde{R_X^{-1}} \cdot \widetilde{R_Y^{-1}} \cdot \widetilde{R_Z^{-1}} \cdot \begin{pmatrix} 0 \\ 0 \\ 1 \end{pmatrix} = \begin{pmatrix} \xi_1 \\ \xi_2 \\ \xi_3 \end{pmatrix}$$

which simplifies the final result giving us the final solution:

$$\arcsin(-\xi_1) = \theta$$

and once known θ ,

$$\arcsin\left(\frac{\xi_2}{\cos(\theta)}\right) = \phi$$

$$\arccos\left(\frac{\xi_2}{\cos(\phi)}\right) = \psi$$

With this simple calculations implemented in the Raspberry Pi, we are able to track inclinations of the experiment, achieving our goal of determining the experiment attitude.

4.9 Ground Support Equipment

The ground segment consisted of two laptops, one of them as a backup solution if the other one failed.

The main activities accomplished by the ground software, which is written in C and whose GUI is built upon GTK+ and Cairo, are the following:

- Contact, via E-link system, with the experiment in the gondola and download all data sent by it. An Ethernet connection to the ground station is required. The ground software acted as the client side of the TCP/IP connection established with the gondola.

- Show all measurements acquired, with a GUI in which graphics obtained from the data received and the images downloaded were visible. Figure 4-145 shows the first tests of the window organization and data printing.
- Control through defined commands some critical aspects of the experiment in real time, such as the thresholds used to decide between algorithms or fatal errors that could be recovered: change_threshold, reset, power_off, power_on and recalibration commands were used.

The flow diagram for handling the received data is the following:

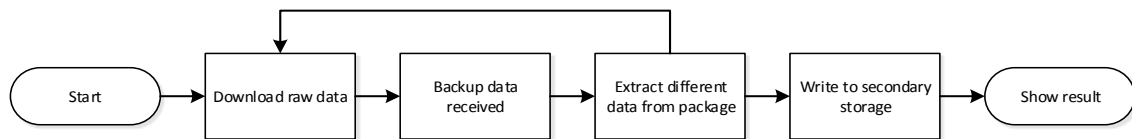


Figure 4-144 Ground software

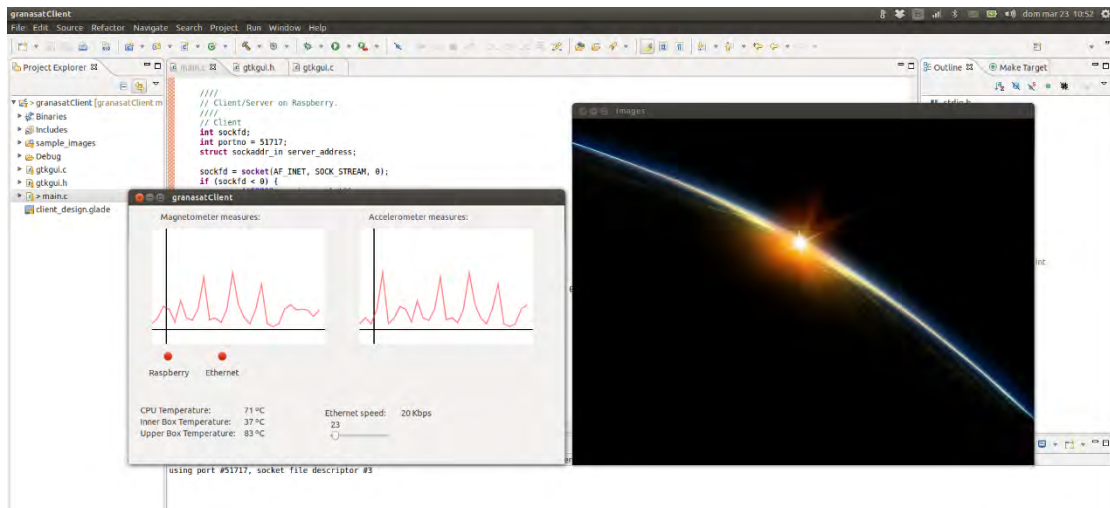


Figure 4-145 First GUI test



5 EXPERIMENT VERIFICATION AND TESTING

5.1 Verification Matrix

Table 5-1 Verification table

| ID | Requirement | Verification | Test number | Status |
|-----|---|--------------|-------------|--------|
| F.1 | The experiment shall obtain its orientation using the star sensor. | T | 1, 16 | ✓ |
| F.2 | The experiment shall obtain its orientation using the horizon sensor. | T | 2, 16 | ✓ |
| F.3 | The experiment shall obtain its orientation using magnetic field measurements. | T | 3, 16 | ✓ |
| P.1 | The output frequency of the star sensor shall be at least 0.5 Hz. | T | 1 | ✓ |
| P.2 | The output frequency of the horizon sensor shall be at least 0.5 Hz. | T | 2 | ✓ |
| P.3 | The maximum output frequency of the magnetic field measured shall be no greater than 5 Hz and the minimum shall be at least 0.1 Hz. | T | 3 | ✓ |
| P.4 | The star sensor shall be capable of at least 1 arcmin accuracy. | T | 1 | ✓ |
| P.5 | The horizon sensor shall be capable of at least 5° accuracy. | T | 2 | ✓ |



| ID | Requirement | Verification | Test number | Status |
|-----|---|--------------|-------------|----------------------|
| P.6 | The range of the magnetic field measured shall be of ± 1.5 to ± 8 gauss | V,A | - | ✓ |
| P.7 | The float altitude of the experiment shall be no lower than 11 Km because of the polar stratospheric clouds. | R | - | ✓ See CRP details |
| D.1 | The thermal subsystem shall guarantee a temperature between -5°C and 45 °C for the camera. | T | 5 | ✓ |
| D.2 | The mechanical design shall provide protection for the possibility of 10G vertical and 5G horizontal shocks with the ground. | A | - | ✓ |
| D.3 | The experiment shall not disturb or harm the gondola. | R,A | - | ✓ |
| D.4 | The experiment shall not disturb or harm other experiments. | R, A, T | - | ✓ |
| D.5 | The experiment shall not be disturbed or harmed by other experiments. | R, A, T | - | ✓ |
| D.6 | The experiment needs a box outside of the gondola that shall keep the magnetometer away from magnetic disturbances in order to avoid interferences. | I | - | ✓ |



Student Experiment Documentation

| ID | Requirement | Verification | Test number | Status |
|------|---|--------------|-------------|--------|
| D.7 | The insulation of the boxes shall work in low pressure environment, down to 10 mbar. | T | 12 | ✓ |
| D.8 | The insulation of the boxes shall work in low temperature conditions, down to -80 °C. | T | 5 | ✓ |
| D.9 | The outer box shall keep clear of humidity condensation in the lens | R, I | - | ✓ |
| D.10 | The link shall use a maximum of 500 Kbps of download rate. | T | 11 | ✓ |
| D.11 | The power system shall provide the necessary power to the instruments inside the boxes. | T | 6 | ✓ |
| D.12 | The thermal subsystem shall guarantee a temperature between 0 °C to 50 °C for the CPU. | T | 5 | ✓ |
| D.13 | The experiment shall operate in the temperature profile of the BEXUS balloon. | T | 5 | ✓ |
| D.14 | The experiment shall operate in the vibration profile of the BEXUS balloon (especially for shocks). | T | 13 | ✓ |



| ID | Requirement | Verification | Test number | Status |
|------|--|--------------|-------------|--------|
| D.15 | The horizon sensor and the star sensor shall use the same camera. | I | - | ✓ |
| D.16 | Energy consumption shall be lower than 28 W. | T | 4 | ✓ |
| D.17 | The experiment shall resist the vibrations during its transportation. | T | 13 | ✓ |
| D.18 | The experiment shall be easily assembled during the pre-launch preparation | R,I | - | ✓ |
| D.19 | The power system shall provide 5 V output voltage. | I | - | ✓ |
| D.20 | The link between the outer box and the inner box shall have low susceptibility to noise as the experiment has low voltage in some lines (I^2C) | T | 15 | ✓ |
| O.1 | The orientation shall be obtained autonomously by the CPU. | I, T | 16 | ✓ |
| O.2 | The experiment shall work autonomously after it has been turned on. | I, T | 16 | ✓ |

*Student Experiment Documentation*

| ID | Requirement | Verification | Test number | Status |
|-----|---|--------------|-------------|----------------------|
| O.3 | The flight duration shall not last less than 1 hour at the float altitude. | I | - | ✓ See CRP details |
| O.4 | The flight shall take place from 8:00 pm to 5:00 am. | I | - | ✓ See CRP details |
| O.5 | The measurements obtained (magnetic field, acceleration, and orientation obtained with the star sensor or the horizon sensor) shall be send to the ground segment to verify the good operation of the system. | I, T | 16 | ✓ |
| O.6 | The vertical gondola strut on which the boom is mounted shall be properly refurbished. | I | - | ✓ |
| S.1 | The system shall take and store images with a frequency of 0.5 Hz. | T | 7 | ✓ |
| S.2 | The system shall take and store magnetic measurements with a frequency of 1 Hz. | T | 8 | ✓ |
| S.3 | The system shall take and store acceleration measurements with a frequency of 1 Hz. | T | 8 | ✓ |

| ID | Requirement | Verification | Test number | Status |
|-----|--|--------------|-------------|--------|
| S.4 | The system shall take and store temperature measurements with a frequency of 0.5 Hz. | T | 9 | ✓ |
| S.5 | The system shall process the images with a frequency of 0.5 Hz. | T | 10 | ✓ |
| S.6 | The system shall send all the data measured through E-Link with a frequency of 0.1 Hz. | T | 11 | ✓ |

5.2 Test Plan

This table shows an overview of our experiment tests status tests. Every test is defined with further details in the following pages.

✗ Test failure

✓ Test completion

Table 5-2 Test plan summary

| Test number | Test type | Test completed | Test status |
|-------------|-------------------|----------------|-------------|
| 1 | Software | YES | ✓ |
| 2 | Software | YES | ✓ |
| 3 | Software | YES | ✓ |
| 4 | Power Electronics | YES | ✓ |
| 5 | Thermal | YES | ✓ |
| 6 | Power Consumption | YES | ✓ |
| 7 | Software | YES | ✓ |
| 8 | Software | YES | ✓ |
| 9 | Software | YES | ✓ |
| 10 | Software | YES | ✓ |
| 11 | Software | YES | ✓ |
| 12 | Vacuum | YES | ✓ |
| 13 | Vibration | YES | ✓ |
| 14 | Electronic | YES | ✓ |
| 15 | Signal Quality | YES | ✓ |

*Student Experiment Documentation*

| Test number | Test type | Test completed | Test status |
|-------------|----------------------|----------------|-------------|
| 16 | Full Functional Test | YES | ✓ |

| | |
|-----------------------------------|--|
| Test number | 1 |
| Test type | Software |
| Test facility | University of Granada. Higher Technical School of Information Technology and Telecommunications Engineering |
| Tested item | Star tracker software |
| Test level/procedure and duration | Use [33] software to simulate the night sky and test both the hardware (camera) and the star tracker algorithm |
| Test campaign duration | 3 days |
| Test campaign date | August (Week 34)* |
| Test completed | YES |

| | |
|-----------------------------------|--|
| Test number | 2 |
| Test type | Software |
| Test facility | University of Granada. Higher Technical School of Information Technology and Telecommunications Engineering |
| Tested item | Horizon sensor software |
| Test level/procedure and duration | Test several methods for fitting circle to data. Determine the most accurate one in order to know the accuracy of the horizon sensor |
| Test campaign duration | 3 days |
| Test campaign date | May (Week 22) |
| Test completed | YES |



| | |
|-----------------------------------|---|
| Test number | 3 |
| Test type | Software |
| Test facility | University of Granada. Higher Technical School of Information Technology and Telecommunications Engineering |
| Tested item | Magnetometer software |
| Test level/procedure and duration | Using a homemade 3D Earth's magnetic field simulator |
| Test campaign duration | 1 day |
| Test campaign date | August (Week 34)* |
| Test completed | YES |

| | |
|-----------------------------------|---|
| Test number | 4 |
| Test type | Power Electronics |
| Test facility | University of Granada. Faculty of Sciences |
| Tested item | Power supply |
| Test level/procedure and duration | Test the Step-Down Voltage Regulator in order to check the efficiency of the LM2576 |
| Test campaign duration | 6 days |
| Test campaign date | February (Week 8) |
| Test completed | YES |

| | |
|--------------------|--------------------------------------|
| Test number | 5 |
| Test type | Thermal |
| Test facility | Universitat Politècnica de Catalunya |
| Tested item | Whole experiment |

*Student Experiment Documentation*

| | |
|-----------------------------------|--|
| Test number | 5 |
| Test level/procedure and duration | The experiment will be placed inside of a thermal chamber and tested during 5 hours down to -80° |
| Test campaign duration | 1 day |
| Test campaign date | September (Week 37)* |
| Test completed | YES |

| | |
|-----------------------------------|---|
| Test number | 6 |
| Test type | Power Consumption |
| Test facility | University of Granada. Faculty of Sciences |
| Tested item | Whole experiment |
| Test level/procedure and duration | Measure the power consumption of the whole experiment |
| Test campaign duration | 1 day |
| Test campaign date | May (Week 20) |
| Test completed | YES |

| | |
|-----------------------------------|---|
| Test number | 7 |
| Test type | Software |
| Test facility | University of Granada. Higher Technical School of Information Technology and Telecommunications Engineering |
| Tested item | Raspberry Pi |
| Test level/procedure and duration | Intensive reading from the camera, memory allocation and storage in the SD of images |
| Test campaign duration | 2 days |
| Test campaign date | March (Week 11) |



| | |
|--------------------|-----|
| Test number | 7 |
| Test completed | YES |

| | |
|-----------------------------------|---|
| Test number | 8 |
| Test type | Software |
| Test facility | University of Granada. Higher Technical School of Information Technology and Telecommunications Engineering |
| Tested item | LSM303DLHC and Raspberry Pi |
| Test level/procedure and duration | Accuracy test from both the magnetometer and accelerometer sensors in the module |
| Test campaign duration | 1 day |
| Test campaign date | August (Week 34)* |
| Test completed | YES |

| | |
|-----------------------------------|---|
| Test number | 9 |
| Test type | Software |
| Test facility | University of Granada. Higher Technical School of Information Technology and Telecommunications Engineering |
| Tested item | DS1621 and Raspberry Pi |
| Test level/procedure and duration | Accuracy test from the temperature sensor |
| Test campaign duration | 1 day |
| Test campaign date | September (Week 37)* |
| Test completed | YES |

*Student Experiment Documentation*

| | |
|-----------------------------------|---|
| Test number | 10 |
| Test type | Software |
| Test facility | University of Granada. Higher Technical School of Information Technology and Telecommunications Engineering |
| Tested item | Raspberry Pi |
| Test level/procedure and duration | Test the computational capability of the Raspberry Pi to handle the image processing |
| Test campaign duration | 4 days |
| Test campaign date | June (Week 26) |
| Test completed | YES |

| | |
|-----------------------------------|---|
| Test number | 11 |
| Test type | Software |
| Test facility | University of Granada. Higher Technical School of Information Technology and Telecommunications Engineering |
| Tested item | Raspberry Pi |
| Test level/procedure and duration | Test the computational capability of the Raspberry Pi at the bandwidth offered to fulfil S.6 requirement |
| Test campaign duration | 4 days |
| Test campaign date | June (Week 26) |
| Test completed | YES |

| | |
|--------------------|--------------------------------------|
| Test number | 12 |
| Test type | Vacuum |
| Test facility | Universitat Politècnica de Catalunya |



| | |
|-----------------------------------|---|
| Test number | 12 |
| Tested item | Outer and inner box |
| Test level/procedure and duration | Test the whole experiment in a vacuum climatic chamber down to 4E-6 mbar during 2 hours |
| Test campaign duration | 1 day |
| Test campaign date | September (Week 37)* |
| Test completed | YES |

| | |
|-----------------------------------|--|
| Test number | 13 |
| Test type | Vibration |
| Test facility | University of Granada. Faculty of Sciences |
| Tested item | Outer box with profile and inner box |
| Test level/procedure and duration | Test with different frequencies of vibrations if any frequency has resonance with the system |
| Test campaign duration | 1-2 days |
| Test campaign date | September (Week 36)* |
| Test completed | YES |

| | |
|-----------------------------------|--|
| Test number | 14 |
| Test type | Electronic |
| Test facility | University of Granada. Faculty of Sciences |
| Tested item | ITS4141N |
| Test level/procedure and duration | Use a breadboard to probe the circuit chosen to solder it later to the PCB |
| Test campaign duration | 1 hour |
| Test campaign date | July (Week 28) |

*Student Experiment Documentation*

| | |
|----------------|-----|
| Test completed | YES |
|----------------|-----|

| | |
|-----------------------------------|---|
| Test number | 15 |
| Test type | Signal quality |
| Test facility | University of Granada. Faculty of Sciences |
| Tested item | I ² C-bus extender P82B715 |
| Test level/procedure and duration | Measure the quality of I ² C signal using the I ² C-bus extender across 3 meter twister pair shielded wire while a DS1621 sensor is working |
| Test campaign duration | 1 day |
| Test campaign date | June (Week 25) |
| Test completed | YES |

| | |
|-----------------------------------|--|
| Test number | 16 |
| Test type | Full functional test |
| Test facility | University of Granada. Faculty of Sciences |
| Tested item | Whole system |
| Test level/procedure and duration | System level. Simulate a whole flight to test the function of every subsystem working in a real scenario |
| Test campaign duration | 2 days (1 day set-up, 1 day testing) |
| Test campaign date | August (Week 35)* |
| Test completed | YES |

*These tests have a different scheduling after IPR.

5.3 Test Results

5.3.1 Star Tracker Test

Test 1 in Test Plan proved the robustness and accuracy of the star tracker software with the suitable output frequency.

The conditions of the test, its procedure and all the results obtained can be seen in C.7 Test Details.

100 test images were analysed. The absolute error per axis after the attitude determination was found is -22.94 arcsecs, -11.92 arcsecs and -6.41 arcsecs in the x,y,z axis respectively.

The output frequency was 0.5 Hz

These results confirmed that the P.1, F.1 and P.4 requirements were fulfilled.

5.3.2 Horizon Sensor Test

Test 2 in Test Plan simulated the circle fitting method in order to decide which is the best one in terms of accuracy and ease of implementation. Two methods were tested: a Modified Least Square method [29] (MLS) and the Kåsa [34] method.

The conditions of the test, its procedure and all the results obtained can be seen in C.7.2 Horizon Sensor Test.

Given a set of points from a circle, each method returns a centre, whose distance to the real centre of the circle has been measured. The methods were tested with generated points from circles of radius from 100 to 10,000, with an error of measurement that varies from 0 % to 10 % of each radius.

For each circle and error of measurement, the differences between Kåsa and MLS centres were calculated. Since the greatest difference between them is $6.72 \cdot 10^{-4}$, we concluded that, in terms of accuracy, both methods are similar.

As Kåsa method requires complex matrix operations, we concluded that the best method, in terms of accuracy, ease of implementation and computational complexity is MLS.



5.3.3 Magnetic Field Test

To simulate the conditions that we found in Kiruna, the magnetic field is as shown in Figure 5-1. In this figure, we can see the entire magnetic field, and the magnetic field experienced by each of the axes.

These data have been obtained from the NASA website for the magnetic field that we found in Kiruna in 2014, according to the IGRF model [35].

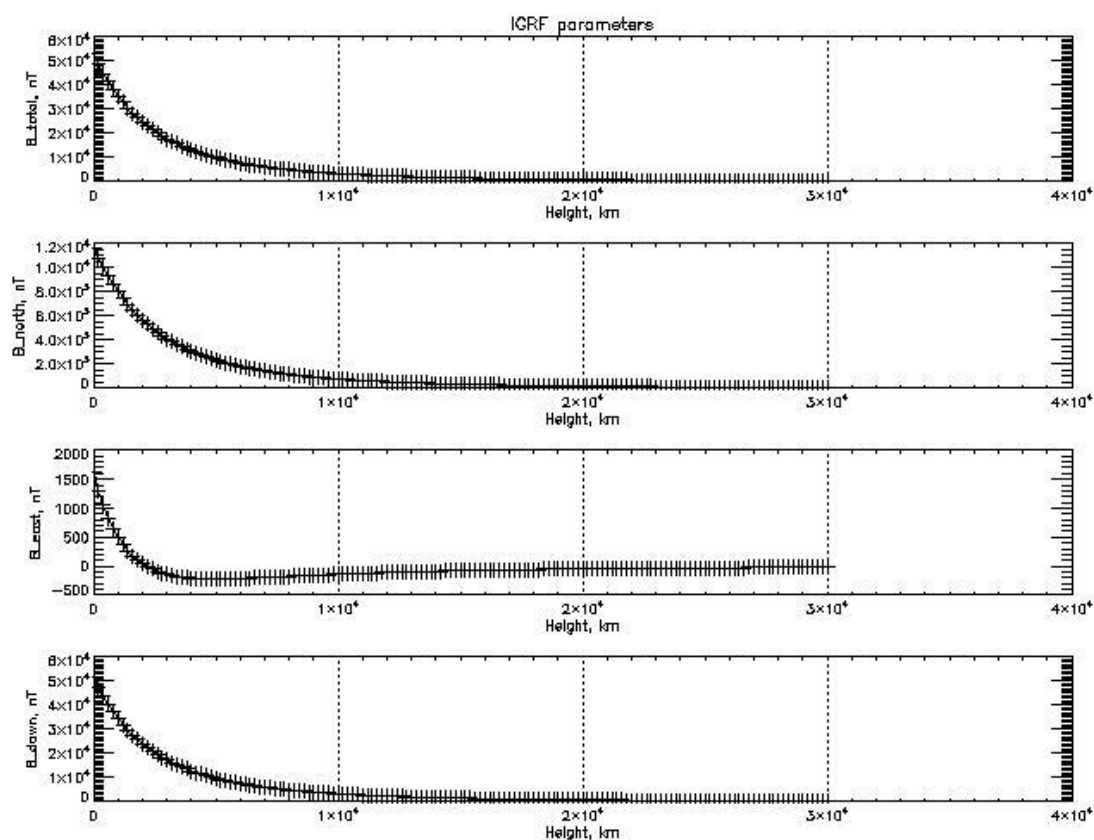


Figure 5-1 Magnetic field in Kiruna according to IGRF model

To simulate the magnetic field in the laboratory, we built a Helmholtz coils. Further information about this can be found in C.7.3 Magnetic Field Test.

5.3.4 Power Electronics Test

We tested the experiment in order to check its total current and power consumption. For this test, we needed a power supply generator, which has an ammeter. This test

gave us an idea of this consumption and the timeline consumption during the launch campaign. We want to check if the experiment will need to use another gondola battery. The results are shown in the following figure (please notice this test was performed before we decided not to use the heaters):

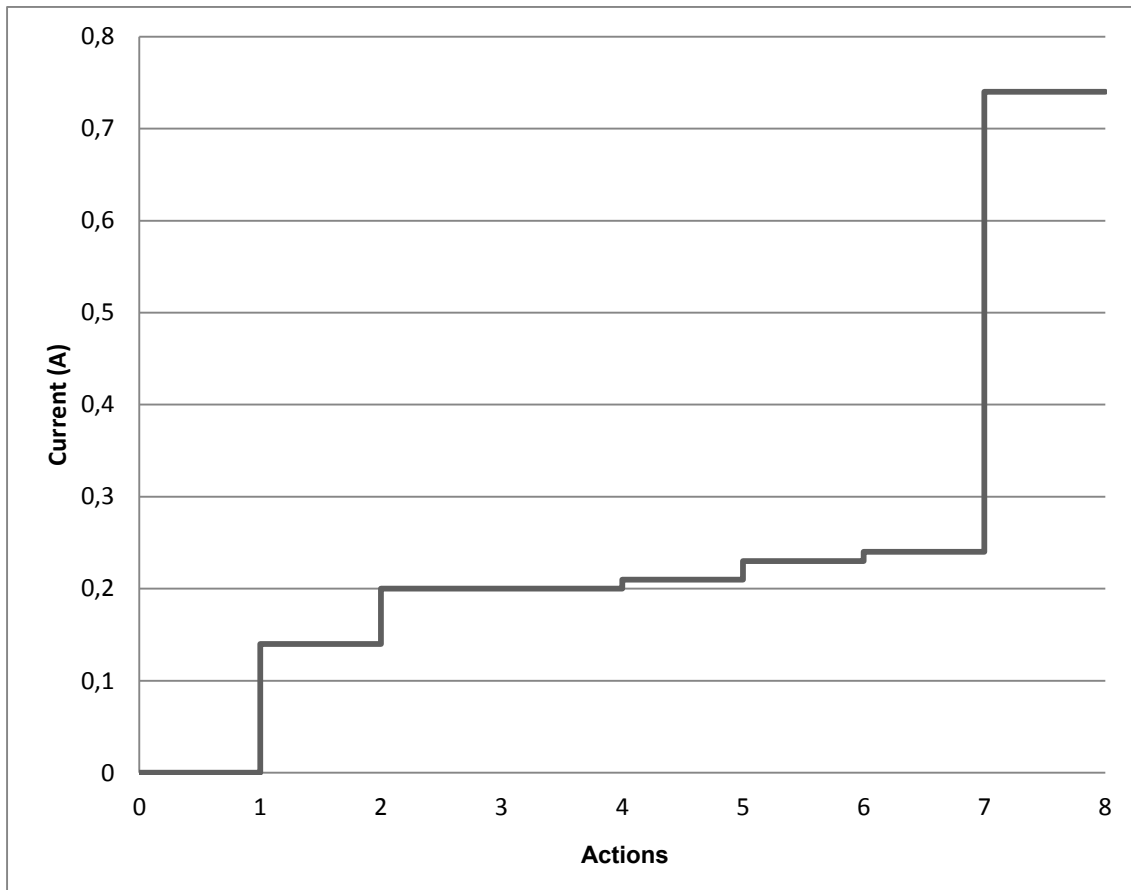


Figure 5-2 Current consumption test

Key for this figure:

1. Raspberry Pi off. Only the inner box PCB is on.
2. Raspberry Pi on (standby). Inner box PCB and Raspberry Pi are on.
3. LEDs on: All status LEDs are on in addition to CPU and inner box PCB.
4. Client connection: TCP connection established between the ground software and the Raspberry Pi.
5. Taking pictures: The camera is taking pictures.
6. Algorithm working: The image processing algorithm and the sensors start to work.



7. Algorithm working.

To sum up, we obtained good results in the test. We got a maximum current consumption of 0.75 A. This test indicates that the batteries design (one gondola pack batteries) is sufficient, because we have an efficiency of 80 % in the regulator, as shown in the other test.

5.3.5 Thermal Test

In order to achieve a successful flight, we must make sure that our components withstand the low temperatures reached in a BEXUS flight.

To perform a test as similar to the flight as possible, it was performed simultaneously with the vacuum test.

The experiment was placed in a TVAC chamber while working as in the flight. In order to check the hot case, the experiment was tested in vacuum conditions at room temperature. Later, in order to verify electronics will not freeze, the temperature decreased at -80 °C.

As expected, there were hot spots: both the camera and the Raspberry Pi CPU reached higher temperatures than the ones established on their datasheets. As the camera performance, along with the images produced, was not affected by the high temperatures, we are not worried about these results. However, the Raspberry Pi reached a temperature of 100 °C, which could be dangerous to the experiment. Although the CPU performance was not affected, 100°C can be considered as a high temperature if we compare it with the maximum working temperature recommended: 85 °C. Despite that, the experiment did not show low performance due to high temperature during the whole test.

We considered performing thermal bridges and reducing the XPS insulation thickness; however, the former is a complex solution and the effectiveness of the latter is hard to verify. We finally decided to install a heat sink on the Raspberry Pi CPU. For further information of the heat sink, see 4.6.1.4. Inner Box Heat Sink section.

The results of this test can be seen in C.7.5 Thermal Test section.

5.3.6 Power Consumption Test

We tested the Step-Down Voltage Regulator in order to check the efficiency of the LM2576 [36]. Before the test, we followed the selection guide of the design procedure as described on page 12 of the datasheet.

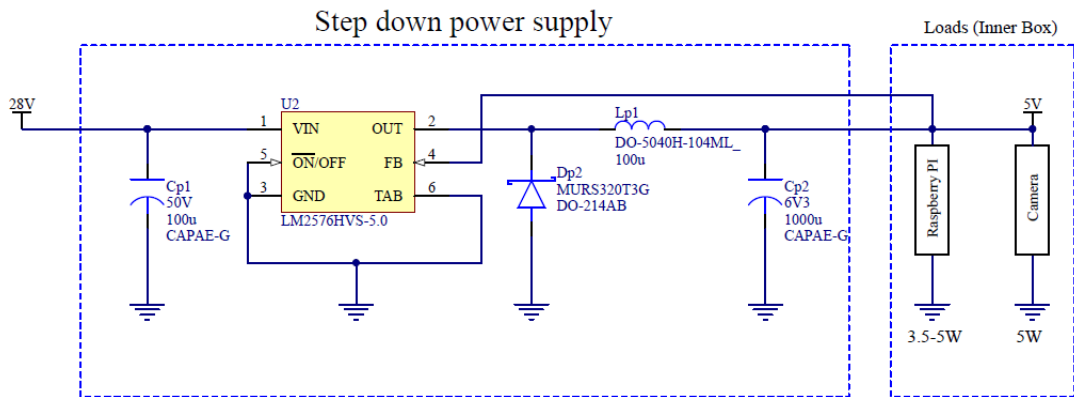


Figure 5-3 Step-Down power supply

For this test, we chose the input capacitor ($100 \mu\text{F}/50 \text{ V}$), the high frequency switching inductor ($100 \mu\text{H}$ -M104 Coilcraft), an electrolytic output capacitor ($1,000 \mu\text{F}/6.3 \text{ V}$) and a catch diode (MURS320t3g from Onsemi) to check the load regulation as described on page 1 of the datasheet.



Figure 5-4 PCB Power supply test

In the image above a cooling fin can be seen. This cooling fin has been used just for the test and we will not use it during the flight. The obtained values of current and

voltage measured in the prototype depicted in Figure 5-4 are shown in Figure 5-5 and Figure 5-6. With them we fulfil the requirements.

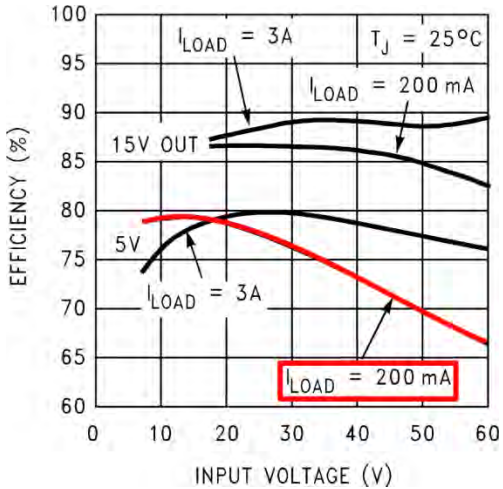


Figure 5-5 Theoretical efficiency of LM2576HVS

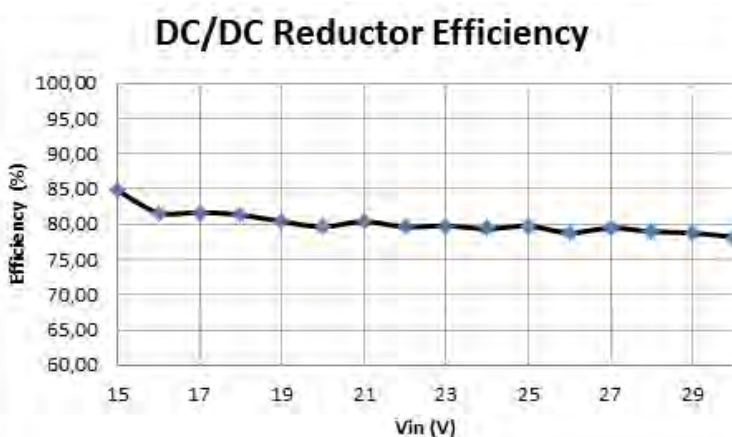


Figure 5-6 Experimental efficiency of LM2576HVS

We obtained good results in the test. We recorded 80 % efficiency for power delivery of 2.5 A over 5 V.

5.3.7 Raspberry Pi Test

Test 7 in Test Plan measured the time spent in reading from the camera, memory allocation and SD image storage. The conditions of the test, its procedure and results can be seen in C.7.7 Raspberry Pi Test.

Some sample results and the final values obtained are shown in the following table and confirm that the performance requirement S.1 in Software Requirements is fulfilled.

Table 5-3 Test 7 results

| | Reading and memory allocation (s) | Storing in the SD (s) | Reading, memory allocation and storing in the SD (s) |
|----------------------------|--|------------------------------|---|
| 01 – 1,000 Images | 200.243 | 31.018 | 267.786 |
| 05 – 1,000 Images | 199.915 | 30.859 | 267.226 |
| 10 – 1,000 Images | 199.974 | 31.351 | 268.166 |
| 15 – 1,000 Images | 200.045 | 29.003 | 268.368 |
| 20 – 1,000 Images | 200.044 | 28.722 | 266.957 |
| Mean - 1 image (μs) | 200,079.4101 | 29,830.6521 | 268,119.9635 |
| Max frequency (Hz) | 4 (4.998) | 33 (33.523) | 3 (3.730) |

5.3.8 Magnetometer Calibration Test

Test 9 in Test Plan checked the calibration of the magnetic data provided by LSM303DLHC sensor in order to ensure the data provided help us to find our attitude. The details of this test can be found in section C.7 Test Details . Basically, we rotated our experiment, then we took the data and finally we made the calibration.

Represented results pass from an ellipse to a circle shape (see figures 5-7 below)

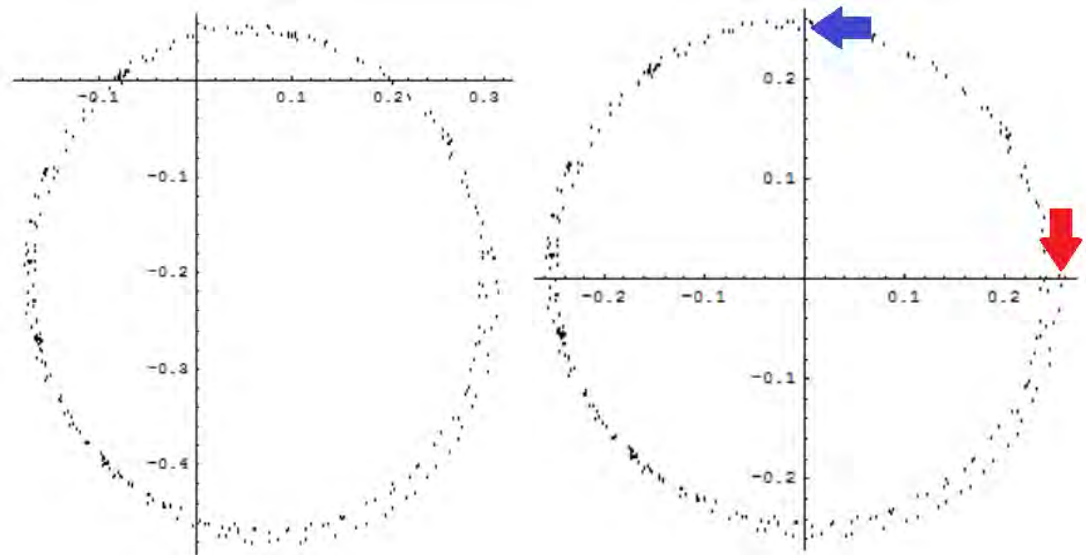


Figure 5-7 Data measures un-calibrated (left) and calibrated (right)

As we can see, the shape of the represented data changes its form as expected.

As a final detail, it is remarkable to say that when X axis of magnetometer points to North, then the value obtained in figure 5-7 right corresponds to the point signalled by the red arrow; whereas if Y axis points to North, the value obtained in figure 5-7 right is signalled by the blue arrow.

5.3.9 Temperature Sensor Test

Test 9 in Test Plan proved the accuracy of the experiment temperature sensors.

The conditions of the test, its procedure and all the results obtained can be seen in C.7.9 Temperature Sensor Test.

Several temperature measurements were taken. Having a calibrated temperature sensor as a reference, the error in the experiment temperature sensors did not exceed from 5 %. An offset of about 2 °C was found in the test.

The temperature measurements were taken with a frequency of 1 Hz.

These results confirm that the S.4 requirement is fulfilled.

5.3.10 Computational Capability Test

Test 10 in Test Plan measured the time spent in the processing of each image taken by the camera. The computational workload of the Raspberry Pi while processing the images in the test has been the same as in the real experiment.

The conditions of the test, its procedure and all the results obtained can be seen in C.7.10 Computational Capability Test.

2,500 times were measured, each of them as the mean of 5 execution of *obtainAttitude()* function. Some of them, as well as the final mean are shown in the following table:

Table 5-4 Times measured

| Iteration – Number of images | Mean time per image (s) |
|------------------------------|-------------------------|
| 0001 – 5 | 0.320448994 |
| 0500 – 5 | 0.302668449 |
| 1000 – 5 | 0.337983548 |
| 1500 – 5 | 0.257142526 |
| 2000 – 5 | 0.370227360 |
| 2500 – 5 | 0.210931629 |

| | |
|-------------------------|--------------|
| MEAN TIME PER IMAGE (s) | 0.3232118138 |
| Max Frequency (Hz) | 3 (3.0934) |

As the maximum processing frequency is 3, we concludes that the S.5 requirement is fulfilled.

5.3.11 Connection Bandwidth Test

Test 11 in Test Plan measured the time spent in sending the heavier of the connection loads -the images taken by the camera- through a TCP connection restricted to 500 KiB/s at download and 1 KiB/s at upload. The conditions of the test, its procedure and all the results obtained can be seen in C.7.11 Connection Bandwidth Test.

The mean results obtained for every set of images (2^i images, with $i \in \{0,1,\dots,9\}$) are shown in the following table and confirm that the performance requirement S.6 in Software Requirements is fulfilled.

**Table 5-5 Test result**

| | Time spent in receiving (s) | Mean – 1 image (s) |
|------------|------------------------------------|--|
| 1 Image | 2.398404272 | 2.398404272 |
| 2 Images | 4.803129015 | 2.401564508 |
| 4 Images | 9.605837094 | 2.401459274 |
| 8 Images | 19.21184405 | 2.401480506 |
| 16 Images | 38.42397230 | 2.401498269 |
| 32 Images | 76.84874043 | 2.401523138 |
| 64 Images | 153.6940238 | 2.401469122 |
| 128 Images | 307.7323954 | 2.404159339 |
| 256 Images | 614.7860329 | 2.401507941 |
| 512 Images | 1229.563592 | 2.401491390 |
| | | Mean - 1 image (s) 2.401455776 |
| | | Max frequency (Hz) 0.4 |

5.3.12 Vacuum Test

We must check that every component is completely stable at pressure variations. In a BEXUS flight, pressure drops to 5 mbar and up to the atmospheric pressure at the end.

Also, as there was a chance that a hot spot may appear during the flight, it was performed with the thermal test in a TVAC chamber.

During the test, every component held a much lower pressure than the one predicted for the flight, down to 10^{-5} mbar. The experiment worked as in the flight during the whole test, encountering no performance decrease or component malfunction.

However, a deposit from the outgassed baffle paint appeared on the inner side of the lens -in the outer box-. In order to avoid this problem in the flight, we prepared another baffle without paint, ready to replace the tested one.

The results of this test can be seen on C.7.12 Vacuum Test.

5.3.13 Vibration test

In order to face the launch in Kiruna successfully, we need to perform a vibration test, 13 in Test Plan.

We used our head academics' van to emulate the conditions of the experiment during the crane transport and other pre-launch procedures. The ride was a consecutive acceleration and braking driving followed by a regular driving through the city. All systems (camera, accelerometer, etc.) were fully functional at every moment and there were no signs of damage, excessive strain, loss of elements, etc. With all data recorded during the test, a power spectral density plot was obtained and compared with the one used in the random vibration simulation. Our results confirmed that the experiment is safe facing random vibrations and will work normally.



Figure 5-8 Experiment preparation

During the entire ride all systems were working smoothly. We were even able to record a nice monochromatic photography sequence of the trip through Granada. With the van stopped, we checked our experiment trying to find any sign of failure or damage in the mechanical design but, fortunately, all remained nearly intact: welding was not harmed, bolts were not loose, every cable was still connected, etc.

Therefore the test can be marked as passed under conditions related in Table C.7 13 Qualification test.



Figure 5-9 Picture taken by the camera during the trip through Granada

5.3.14 Fusible Test

Test 14 in Test Plan measured the voltage in some points of this sensor to ensure the correct operation of the new component in the PCB.

The circuit chosen is the following:

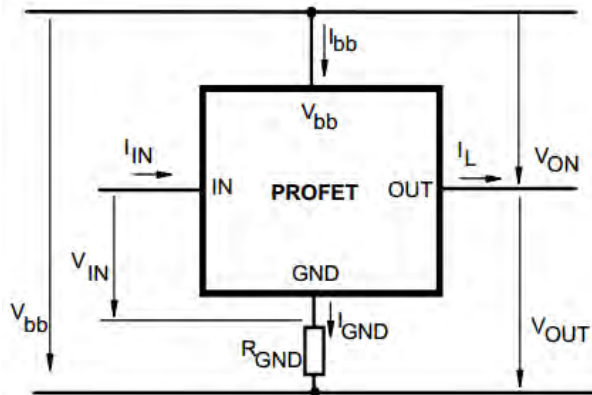


Figure 5-10 Schematic of the circuit chosen

In this circuit you can see a resistor (R_{GND}) whose value is $150\ \Omega$. This resistor reduces the V_{IN} and so that we can use the same V_{bb} and V_{IN} (27-28V).

To test this circuit we measured some of its points. The following images show the results:



Figure 5-11 Voltage V_{bb}



Figure 5-12 R_{GND} voltage

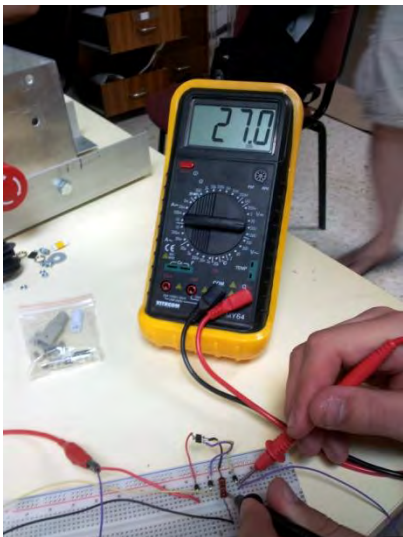


Figure 5-13 Voltage V_{IN}

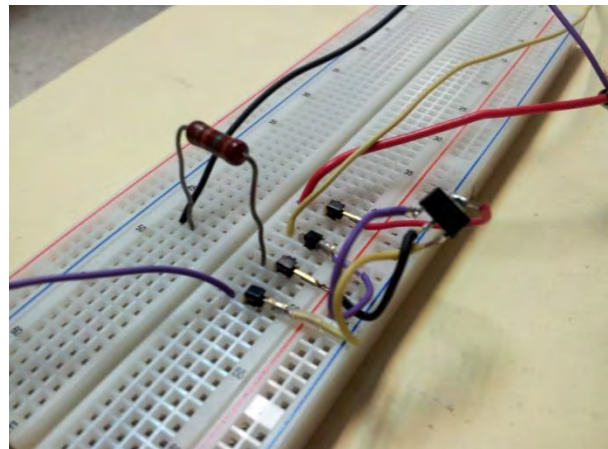


Figure 5-14 Breadboard circuit

The results are shown in Table 5-6.

Table 5-6 Test results

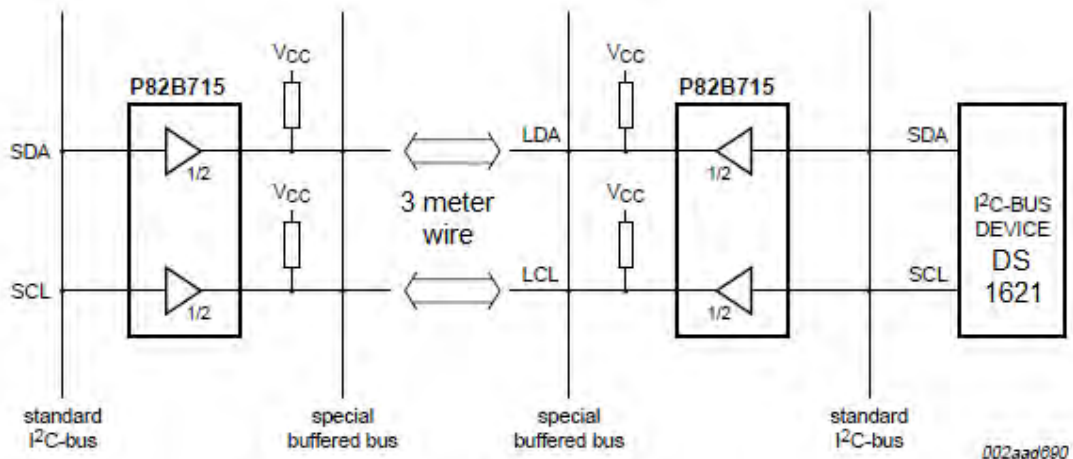
| | |
|-------------------|--------|
| V_{bb} | 27.1V |
| R_{GND} voltage | 90.7mV |
| V_{IN} | 27V |

5.3.15 I²C Bus Extender Test

Test 15 was made to secure the signal integrity of the I²C communication signal. We checked the good operation with the P82B715 component (more details in General Electronic Design).

The conditions, its procedure and others details are described in C.7.15 I²C Bus Extender Test.

The first step was to connect the DS1621 sensor to the I²C-bus extender with a 3 metre wire and to measure the signal quality in the master part. The schema mounted is shown in Figure 5-15.

**Figure 5-15 Values measured during test**

When the DS1621 was ready for work, we started the communication and we read the SDA and SCL channel with an oscilloscope. The Figure 5-16 show the values measured on SDA channel.

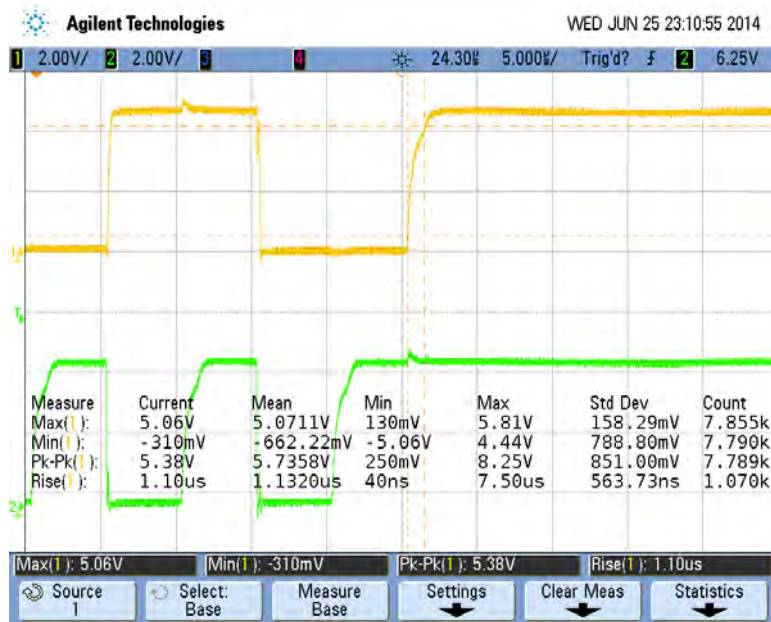


Figure 5-16 Values measured during test with the I²C bus extender

The next step was to remove the P82B715 and the 3 metre wire and to connect the DS1621 sensor directly to the Raspberry Pi with 10 cm twister pair wire. This connection enabled to know how the signal under a normal operation was and we decided if the I²C-bus extender improves the quality signal.

We measured again with the oscilloscope. The result is shown in Figure 5-17.

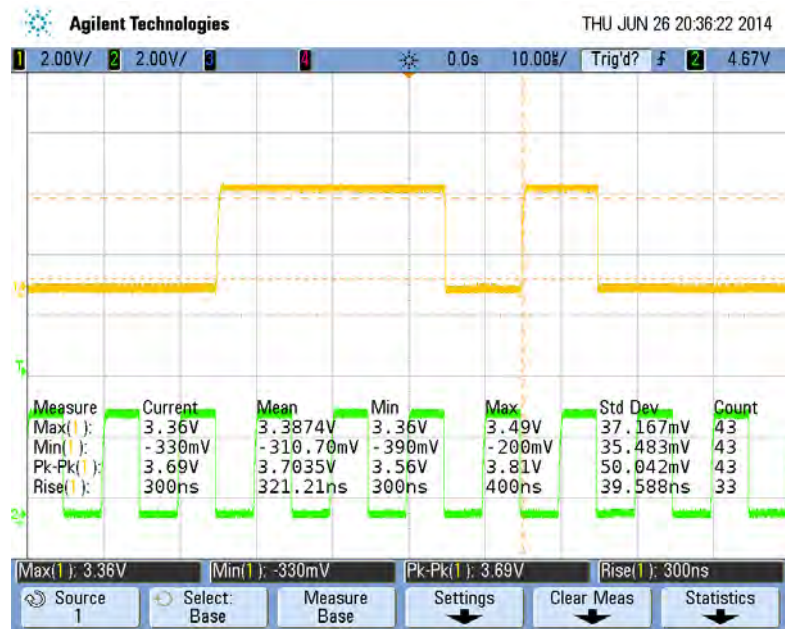


Figure 5-17 Values measured during test with standard I²C bus

Results can be compared in Table 5-7.

Table 5-7 Values measured during test

| Component under test | Link used between master-slave | Peak-to-peak voltage (V) | Rise time (μs) |
|----------------------|------------------------------------|--------------------------|----------------|
| DS1621 + P82B715 | 3 metre twister pair shielded wire | 5.38 | 1.1 |
| DS1621 | 10 cm twister pair wire | 3.36 | 0.3 |

We concluded that the I²C-bus extender component P82B715 improves the signal quality increasing the peak-to-peak voltage and keeping the rise time under operational conditions. In addition, the component enables a long wire communication, which is necessary to communicate the inner box and the outer box.



Therefore, the test was marked as passed under conditions related in Table C.7 14 Qualification test.

5.3.16 Full Functional Test

Test 16 in Test Plan tested the whole functionality of the experiment in a simulated scenario.

The conditions of the test, its procedure and all the results obtained can be seen in C.7.16 Full Functional Test.

The test was performed twice, leading to a failure the first time. The second time, it was completely successful. As all the steps were successfully accomplished, we concluded that the F.1, F.2, F.3, O.1, O.2 and O.6 requirements are fulfilled.



6 LAUNCH CAMPAIGN PREPARATION

6.1 Input for the Campaign / Flight Requirement Plans

6.1.1 Dimensions and Mass

Table 6-1 Experiment summary

| | | |
|--|--------------|--|
| Experiment mass (in kg): | Outer box | 2.195 |
| | Inner box | 2.630 |
| | Profile | 1.643 |
| | Attachments | 1.546 |
| | Total | 8.014 |
| Experiment dimensions (in m): | Outer box | 0.142 x 0.128 x 0.248 |
| | Inner box | 0.157 x 0.144 x 0.228 |
| | Profile | 0.045 x 0.125 x 0.045 |
| Experiment footprint area (in m ²): | Outer box | $35.216 \cdot 10^{-3}$ |
| | Inner box | $35.796 \cdot 10^{-3}$ |
| | Profile | $2.025 \cdot 10^{-3}$ |
| | Total | $73.037 \cdot 10^{-3}$ |
| Experiment volume (in m ³): | Outer box | $4.508 \cdot 10^{-3}$ |
| | Inner box | $5.155 \cdot 10^{-3}$ |
| | Profile | $2.531 \cdot 10^{-4}$ |
| | Total | $9.916 \cdot 10^{-3}$ |
| Experiment expected COG (centre of gravity) position (in m): | Outer box | X = -0.005 Y = 0.018 Z = 0.013 |
| | Inner box | X = -0.480 Y = -0.430 Z = 1.620 |
| | Profile | X = 0 Y = 0 Z = 0 |

6.1.2 Safety Risks

There was a risk of the beam detaching from the outer box. This was mitigated by static load test, good clamp design and a safety cable.

As we were not dealing with any hazardous substances or moving parts in the design, we considered that if the fixations to the gondola were adequate, the experiment would be safe for the personnel.

6.1.3 Electrical Interfaces

Table 6-2 Electrical interfaces applicable to BEXUS

| BEXUS Electrical Interfaces | | |
|---|---|------------|
| E-Link Interface: E-Link required? Yes | | |
| | Number of E-Link interfaces: | 1 |
| | Data rate - downlink: | 500 Kbit/s |
| | Data rate – uplink | 0.1 Kbit/s |
| | Interface type (RS-232, Ethernet): | Ethernet |
| Power system: Gondola power required? Yes | | |
| | Peak power (or current) consumption: | 7.8 W |
| | Average power (or current) consumption: | 7.0 W |
| Power system: Experiment includes batteries? No | | |

6.1.4 Launch Site Requirements

6.1.4.1 Materials

This table shows the materials that each department needed to operate at the launch of the experiment and the reason for using this material.

**Table 6-3 Materials needed during the launch campaign**

| Department | Material | Reason |
|------------|---------------------|-----------------------------|
| Mechanical | Screwdrivers | Tighten screw if necessary |
| | T-bolts | For gondola fixation |
| | Cutter | Unexpected event |
| | Electrical tape | Unexpected event |
| | Nuts | Unexpected event |
| | Screws | Unexpected event |
| | Washer | Unexpected event |
| | Wrench | Tighten screw if necessary |
| | Adjustable wrench | Unexpected event |
| | Screen cleaner | Clean lens if necessary |
| Software | Torque wrench | For gondola attachments |
| | Crimp | Unexpected event |
| | Pliers | Unexpected event |
| | Table | For the ground station team |
| Electronic | Chairs | For the ground station team |
| | Power supply | Test the experiment |
| | Multimeter | Test the experiment |
| | Banana connectors | Test the experiment |
| | Stripping tool | Unexpected event |
| | Flexible cable 2 mm | Unexpected event |
| | Heat shrink cable | Unexpected event |
| | Tweezers | Unexpected event |
| | Scissors | Unexpected event |

6.1.4.2 Remove Before Flight

Before the Count Down a ‘Remove Before Flight’ label was fixed on the glass of the outer box. This label avoided accidental disturbances on our experiment, such as undesirable spots caused by dust or any other kind of dirt.



Figure 6-1 Remove Before Flight label

6.1.4.3 Flight Conditions

We would like to test the horizon sensor and the star tracker on the same flight. To do so, we would like to test the experiment on a flight when we could take pictures during both day and night. For example, when simulating the sky in Kiruna on the 21st of September, the star tracker will work properly from 8 pm to 5 am.

- Float altitude and duration required (at least): 11 km for 3 hours

Example for 7th of October 2014:

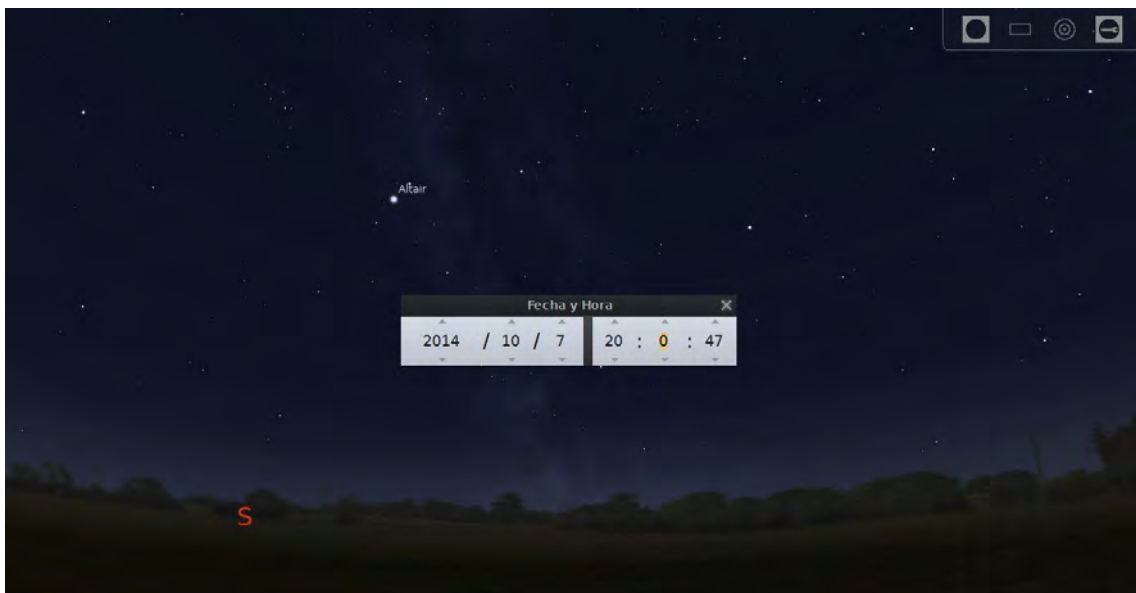


Figure 6-2 Example for 7th of October 2014

Aurora

We have considered as a risk the fact that the aurora may occur during the flight and interfere with the performance of the star tracker. However, we will not have problems with this as long as the aurora brightness is similar that the one of the Milky Way. If that is not the case, the performance of the star tracker will be affected.

After-flight update: During the entire flight an aurora occurred. It blocked images for the star tracker and the magnetic measures varied depending on the aurora's intensity.

Strobe light

After intensive research, we found that the strobe light might be a problem because of the back scattering effect. However, if the dust particles floating in the ambient were small enough, we would not have reflection effect so the strobe would not disturb us. If that was not the case, the performance of the star tracker would be affected. We submitted a Request for Waivers form and discussed the question with the Payload Manager of the campaign and the strobe light was definitely turned off when the gondola reached 20 km altitude.

Other requirements

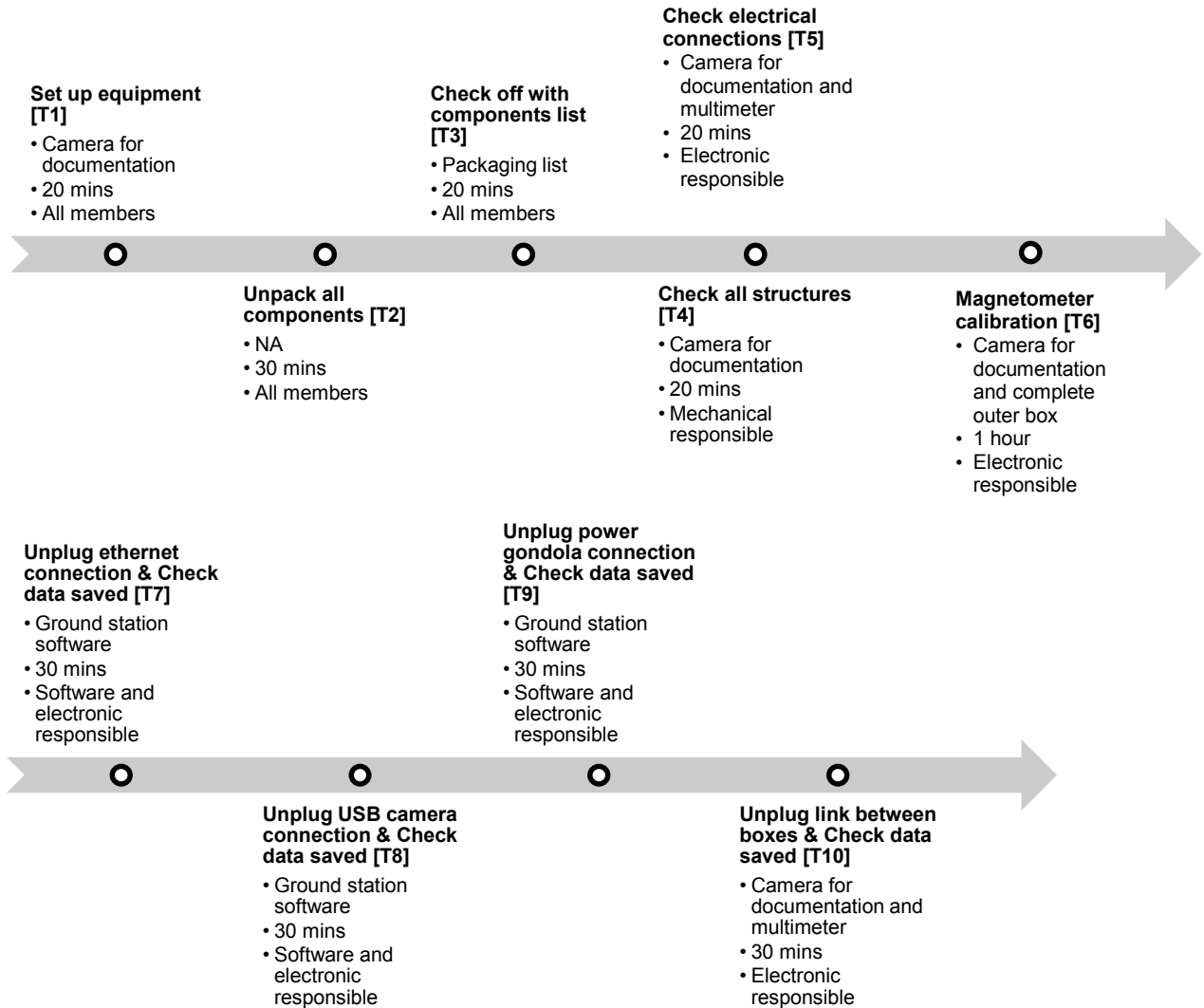
Some requirements, already mentioned in Experiment Requirements and Constraints, were highly important and were included again in this section:

- The float altitude of the experiment shall be no lower than 11 Km because of the polar stratospheric clouds.
- The flight shall take place from 8:00 pm to 5:00 am.
- The measurements obtained (magnetic field, acceleration, and orientation obtained with the star sensor or the horizon sensor) shall be sent to the ground segment to verify the good operation of the system.

We have agreed with TORMES 2.0 to coat the boom, rear facing the gondola and bottom face of the outer box with neoprene.

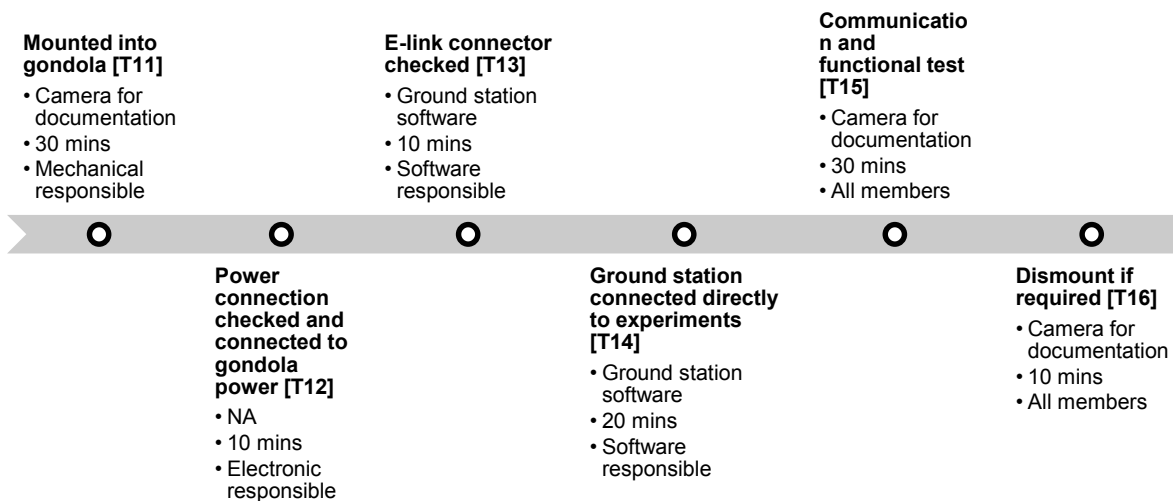
6.2 Preparation and Test Activities at Esrange

Day 1 – Unpacking, mounting and basic test

Experiment preparation:**Start of individual test:**



Student Experiment Documentation



T0 is a very important task. The person responsible for this task has to monitor all data gathered during preparation and test activities and support other team members.

Table 6-4 Who, when and what? – Day 1

| | 20 mins | 30 mins | 20 mins | 20 mins | 60 mins |
|-------------|---------|---------|---------|---------|---------|
| Electronics | T1 | T2 | T3 | T5 | T6 |
| Mechanics | | | | T4 | T0 |
| Software | | | | T0 | T6 |
| Coordinator | | | | | T0 |

| | 30 mins | 30 mins | 30 mins | 30 mins |
|-------------|---------|---------|---------|---------|
| Electronics | T7 | T8 | T9 | T10 |
| Mechanics | | | T0 | |
| Software | T7 | T8 | T9 | T10 |
| Coordinator | | | T0 | |

Table 6-5 Who, when and what? – Start of individual test – Day 1

| | 30 mins | 10 mins | 10 mins | 20 mins | 30 mins | 10 mins |
|-------------|---------|---------|---------|---------|---------|---------|
| Electronics | T0 | T12 | T13 | T14 | T15 | T16 |
| Mechanics | T11 | | | T0 | | |
| Software | T0 | T12 | T13 | T14 | T15 | |
| Coordinator | T0 | | | T0 | | |

Task list:



- T1** Choose workspace and setup equipment
- T2** Unpack all components
- T3** Check off components list
- T4** Check all structures
- T5** Check electrical connections
- T6** Magnetometer calibration
- T7** Mounted into gondola*
- T8** Power connection checked and connected to gondola power
- T9** E-link connector checked
- T10** Ground station connected directly to experiments
- T11** Communication and functional test
- T12** Dismount if required
- T13** Unplug Ethernet connection & Check data saved
- T14** Unplug USB camera connection & Check data saved
- T15** Unplug power gondola connection & Check data saved
- T16** Unplug link between boxes & Check data saved

*With this task, we have to ensure the inner box has been properly placed in the gondola to avoid Risk VE. 3.

Day 2 – Individual test

Main tasks scheduled on Day 2 are:

- Continue with individual test if not finished in day 1

Day 3 – Gondola Interference Test

Main tasks scheduled on Day 3 are:

Part I: Hardline



Student Experiment Documentation

Experiment connected to the E-Net and gondola power supply [T16]

- NA
- 20 mins
- Software and electronic responsible

Communication and functional test: Experiment by experiment [T18]

- Experiment
- 30 mins
- All members

G/S set up in ground station area [T17]

- NA
- 30 mins
- Software and electronic responsible

Communication and functional test: All experiments [T19]

- Gondola
- 30 mins
- All members

Part II: E-Link

Experiment connected to the E-Link [T20]

- NA
- 20 mins
- Software and electronic responsible

Magnetometer calibration [T22]

- Camera for documentation and complete outer box
- 1 hour
- Software and Electronic responsible

Communication and functional test: One by one [T24]

- Gondola
- 30 mins
- All members

RF interference check with E-link (low power) [T21]

- NA
- 30 mins
- Software and electronic responsible

Communication and functional test: Experiment by experiment [T23]

- Experiment
- 30 mins
- All members

Communication and functional test: Whole gondola [T24]

- Gondola
- 30 mins
- All members

Table 6-5 Who, when and what? – Day 3

| | 20 mins | 20 mins | 30 mins | 30 mins | 2h and 50 mins |
|-------------|---------|---------|---------|---------|----------------------------|
| Electronics | T17 | T18 | T19 | T20 | T21, T22, T23, T24 and T25 |
| Mechanics | | T0 | | | T0 |
| Software | T17 | T18 | | | T21, T22, T23, T24 and T25 |
| Coordinator | | T0 | | | T0 |

Task list:

- T17** Experiment connected to the E-Net and gondola power supply
- T18** G/S set up in ground station area
- T19** Communication and functional test (One by one)

- T20** Communication and functional test (Whole gondola)
- T21** Experiment connected, to the E-Link
- T22** RF Interference check with E-Link
- T23** Magnetometer calibration
- T24** Communication and functional test (One by one)
- T25** Communication and functional test (Whole gondola)

A task checklists with pictures that help follow the activities can be found in D.1 Launch Campaign Checklists in APPENDIX D – Launch campaign additional information.

6.3 Timeline for Countdown and Flight

This table shows the procedures that were followed before and during launch and the approximate duration of each. We consider T = 0 as the time of launch.

Table 6-6 Procedures to be followed before and during launch

| Time | Task | Duration | Comments |
|-------------------------------|--|----------|--|
| T-6H00 | Confirm Ready for start of Count-down | - | - |
| T-6H00 | Pre-pickup checks. | 10 min | No power necessary. Gondola in DOM. |
| T-4H00 Start of Count-down | Experiment turned on and LEDs checked. | 15 min | BEXUS Gondola on external power. |
| T-4H00 | Confirm Ready for Pick-up | - | - |
| T-2H30 Gondola Pick-up | Experiment turned on and LEDs checked. | 15 min | BEXUS Gondola on Hercules power. |
| T-2H30 | Confirm Ready for Sweet spot tests | - | - |
| T-2H25 Sweet spot Tests | Telecommand checkout | 15 min | Connection Ground Station - Gondola Required |
| T-1H35 | Confirm Ready for Line up | - | - |
| T-1H30 | LEDs checked | 1 min | Access required |
| T-1H30 | Camera RBF | 1 min | |



| Time | Task | Duration | Comments |
|-------------------|--|----------|--------------------------|
| T-1H30 | Lens cleaning | 1 min | |
| T-1H30 Line-up | Test images | 2 min | |
| T-1H30 | Command Start Ethernet connection from ground | - | - |
| T-1H30 | Command Start capturing images | - | - |
| T-1H30 | Command Start measuring data | - | - |
| T-1H30 | Start recording data | - | Altitude: 0km |
| T-0H40 | Start of inflation | - | Altitude: 0km |
| T-0H00 | Balloon release | - | Altitude: 0km |
| T+~1H00 | Floating altitude expected; best images expected | - | Expected altitude:~25km |
| T+~4H00 | Command cut down* | - | Expected altitude: ~25km |
| T+~4H05 | Command experiment turn off | 1 min | Expected altitude: |

*We need at least 10 minutes notice before balloon cut-down.

6.4 Post-Flight Activities

6.4.1 Recovery Instructions

When the gondola is falling down, the software responsible will turn off the Raspberry Pi to avoid the error in some subsystems of the experiment. The magnetometer and accelerometer will be turned off as well. In case the experiment has not been turned off during the descent phase, the recovery team will have to turn it off manually.

How do we know if GranaSAT experiment has not been turned off?

The experiment is turned on if, and only if, the green LED placed in the inner box is blinking –at 1 Hz–.

How do we turn off GranaSAT experiment?

Only in case of E-Link loss, the recovery team should switch off the experiment by turning the mushroom switch when the gondola is on the ground.

If the experiment has been successfully turned off, the green led will be switched off as well.

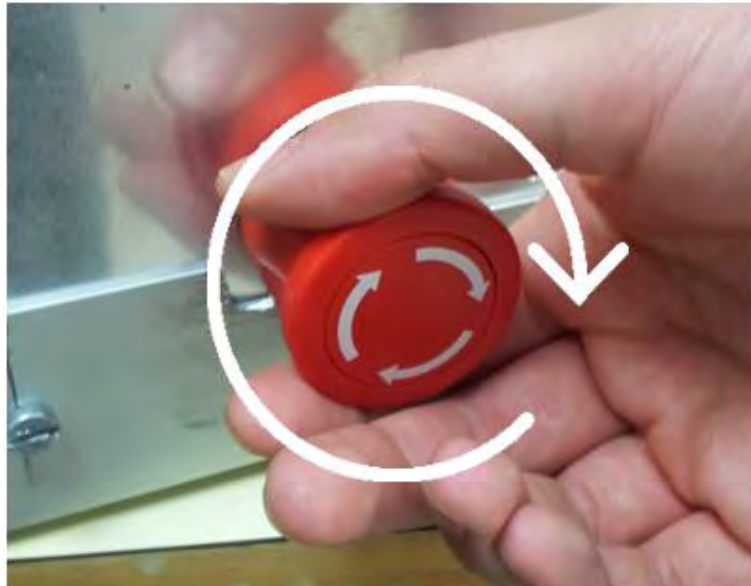


Figure 6-3 ON/OFF mushroom switch

Analysis and evaluation of experiment data

Back up of SD data storage was the first action, and, later, the software engineer read-out these data. Once we had the data, we analysed whether it was usable. The back-up procedure is further explained in D.2 Data Recovery Procedure.

We used this analysis to know if the attitude determination system is appropriate for our pico satellite.

6.4.2 Presentation during Post-Flight Meeting

After launch campaign, GranaSAT team presented the first results obtained during the flight thanks to the E-Link and those obtained from the SD card collected data.

If the system failed during the flight, in this meeting we would discuss with other teams and the organisers and experts about the issues that have led us to failure.

Some points about the Lessons Learned were discussed in this meeting too.

6.4.3 Input to Campaign Report

A Campaign Report was issued with the results obtained.

This report contained the followings points:

- The experiment operations that took place during the launch campaign.
- Some preliminary results obtained during and after the launch campaign.
- Data analysis plan explained in Data Analysis And Results and the next actions to be taken by the team.
- Pictures during the launch campaign: team working, experiment in the gondola, experiment mounting, etc.

6.4.4 Final Experiment Report

About 3 months after the Launch Campaign, the Final Experiment Report was issued with more detail and all the results obtained. All data from the star tracker, horizon sensor and magnetometer were processed and analysed (see section 7.3 for further information)

These data and results helped us to improve our experiment for the future GranaSAT pico-satellite.

6.5 System Success

Table 6-7 System success

| Subsystem | Level of Success |
|--|--------------------------------|
| Star tracker | Contribution of subsystem in % |
| Star tracker obtains an attitude with an error greater than 1 arcminute. | 15 % |
| Star tracker obtains a correct attitude with a maximum error of 1 arcminute. | 37.5 % |
| Horizon sensor | Contribution of subsystem in % |
| Horizon sensor obtains an attitude with an error greater than 5°. | 15 % |
| Horizon sensor obtains a correct attitude with a maximum error of 5°. | 27.5 % |



| Magnetometer and Accelerometer | Contribution of subsystem in % |
|--|--------------------------------|
| Magnetometer and Accelerometer obtains measurements of the magnetic field with errors greater than ± 1.5 to ± 8 gauss. | 5 % |
| Magnetometer and Accelerometer obtains corrects measurements (± 1.5 to ± 8 gauss) of the magnetic field. | 15 % |
| Power system | Contribution of subsystem in % |
| - | 0 % |
| All components receive the power necessary to operate correctly. | 5 % |
| Mechanical system | Contribution of subsystem in % |
| Boxes do not resist g forces but components stay inside. | 1 % |
| Mechanical components resist g forces and temperatures. | 5 % |
| Thermal system | Contribution of subsystem in % |
| Thermal system maintains the temperature but it is not recorded by the temperature sensor. | 3 % |
| The correct temperature is maintained inside the boxes thanks to the insulation material. | 5 % |
| Ground station | Contribution of subsystem in % |
| Data is correctly received by the ground station but the commands do not work perfectly. | 4 % |
| Data is correctly received by the ground station and the commands work perfectly. | 5% |

7 DATA ANALYSIS AND RESULTS

7.1 Data Analysis Plan

The data analysis mainly focused on comparing the attitude we inferred with the results obtained from the gondola once the flight is finished. We compared the measurements from the magnetometer with the Earth's magnetic model. We compared as well the efficiency of the horizon sensor with that of the star tracker to be able to choose a device for our pico satellite.

We checked the accuracy from the devices by cross-correlating the results between all the sensors. Moreover, we have contacted TORMES 2.0 team and we would have exchanged the data collected by both experiments if no failures were experienced.

7.1.1 Horizon Sensor Analysis

The horizon sensor module produced two types of data:

- Raw data: The camera images used by the horizon sensor to determine the attitude. These data are matrix of 1,280 x 960 monochrome pixels.
- Processed attitude: The obtained attitude after have processed the images with the horizon sensor algorithm. The attitude will be given as the nadir vector between the experiment and the Earth's centre. Furthermore, the obtained circumference and the centre calculated by the algorithm will help to visualize all data.

The analysis of these two types of data, along with the attitude obtained by the star tracker and magnetometer, proves, or disproves, that the horizon sensor algorithm is robust, reliable and precise. We were also in contact with TORMES 2.0 team in order to exchange the attitude data from both experiments and compare them.

The analysis plan for horizon sensor data was the following:

- Visually compare the Earth's circumference given by the algorithm and the real visible horizon inspecting each used frame. Obtain deviation from the real horizon and the obtained circumference and study extreme cases.

- Compare obtained circumference with more accurate circle fitting methods, whose complexity could not be handled by the Raspberry Pi. Study accuracy loss due to computational constraints.
- Compare obtained attitude with star tracker and magnetometer data. Estimate the absolute accuracy of the proposed algorithm.
- Compare obtained attitude with TORMES 2.0 experiment attitude. Estimate the absolute accuracy of the proposed algorithm.
- Detect errors in the image processing in order to improve the robustness of the detection routine.
- Detect errors in the Earth's centre calculation in order to improve the robustness of the circumference fitting routine.
- Obtain the algorithm efficiency using the timestamps provided by the main software module.

7.1.2 Star Tracker Data Analysis

The star tracker module will produce two types of data:

- Raw data: The camera images used by the star tracker to determine the attitude. These data are matrix of 1280 x 960 monochrome pixels.
- Processed attitude: The obtained attitude after having processed the images with the star tracker algorithm. This attitude will be computed on-board with the single value decomposition proposed by Markley [37].

The analysis of the data generated proves or disproves if the star tracker software designed is robust, reliable and precise. In particular, the aspects that we considered were the following:

- Ratio of correct identified stars in an image.
 - Relative error in the angle between stars measurements.
 - Absolute error in the attitude determination axes.
- Ratio of false stars identified.
- Capability to detect aberrations.
- Algorithm efficiency measured in correct identified stars/time.



7.1.3 Magnetometer and Accelerometer Data Analysis

This module will give us two types of measures. Three values of the magnetic field and another three of the accelerometer, each of them for the different axes (X axis, Y axis and Z axis).

These sensors therefore resolve the earth magnetic field vector in the experiment and the earth gravity gradient vector. This leads to resolve the vector-matching problem to estimate the Euler angles.

Two general procedures, with a huge number of derived solutions, have been proposed to the problem of spacecraft attitude determination historically:

- Deterministic solution: The attitude is estimated point by point based on two different data vector from a same point.
- Filter: The measured data is filtered by a recursive stochastic estimator combined with a theoretical model in order to converge into an estimation of the attitude.

We are going to use a deterministic solution. Our solution will use only the magnetic vector and accelerometer vector to achieve a point by point attitude estimation. This solution was the first used in aerospace and allows an easy development without complex algorithm training and/or parameters tuning. On the other hand, this solution is more sensitive to non-ideal deviations and noisy measurements. For this reason, more uncertainty will be expected in the attitude estimation.

The solution based on matching two non-zero and non-collinear vectors to obtain a point estimation was proposed in 1965 by Wahba [38] and requires at least two vector measurements. Therefore, a three-axis attitude determination cannot be estimated when only a single vector measurement is available.

The solution we used [39] is based in Wahba solution and provides the reference of the body frame $\{X_b, Y_b, Z_b\}$ into the Earth-fixed Cartesian coordinate system. Then, our camera orientation is the direction of the Earth's Magnetic field $B \{X_m, Y_m, Z_m\}$. In other words, we calculate the attitude referencing the magnetic north.

The step to provide the navigation in an earth-fixed Cartesian reference frame $\{X_n, Y_n, Z_n\}$, like the geographic north or any other reference, remains for a future work.

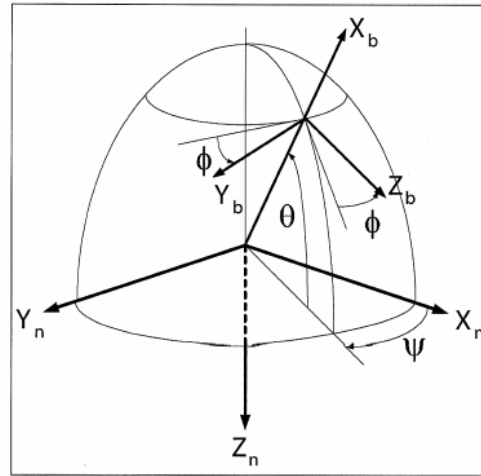


Figure 7-1 Euler angles

Figure 7-1 shows the coordinate systems and the relation between them with the Euler angles. These angles are Yaw (Φ), Roll (θ) and Pitch (Ψ), which are related to each set of vector measurement values, H_b and A_b , as follows:

$$\Phi_{m \rightarrow b}(t) = \arctan\left(\frac{H_{b,y}(t)}{H_{b,x}(t)}\right)$$

$$\theta_{m \rightarrow b}(t) = \arcsin(-H_{b,z}(t))$$

By using only one vector match (Magnetic Field in this case), we can only determine without ambiguity the Yaw and Roll angles. However, Pitch angle could be estimated by recursive method using the accelerometer sensor measurements.

Let $p(t)$ and $q(t)$ be the angular velocity of the X_b and Y_b axes about Z_b axis, and the angular velocity of X_b and Z_b axes about Y_b axis, respectively, estimated from the accelerometer measurements.

Then, the pitch angle is estimated as:

$$\Psi_{m \rightarrow b}(t) = \Psi_{m,0} + \int_{\tau=0}^t \frac{q(t)\sin(\Phi_{m \rightarrow b}(t)) + r(t)\cos(\Phi_{m \rightarrow b}(t))}{\cos(\theta_{m \rightarrow b}(t))} dt$$

Note that it is necessary to obtain the initial pitch angle in the magnetic coordinate system Ψ_m , 0



Calibration and correction procedure

Before performing the attitude determination procedure above explained and to ensure a good accuracy in our attitude estimation, several potential sources of errors are needed to be considered and corrected: [40]

- Calibration: Magnetometers are nonlinear devices and need to be calibrated. An on-earth data measurement calibration and an in-flight calibration will be performed to measure the error in each procedure. Magnetometer bias and misalignments are fixed as well with the calibration.
- Magnetic cleanliness: The spacecraft needs to be correctly designed to minimize magnetic disturbances, like hard or soft iron disturbances. The calibration procedure allows to reduce the external magnetic field effects.
- Time stamp: in order to correlate both accelerometer and magnetometers measurements, accurate timing is needed.
- Perturbations to the main field: The Earth's Magnetic Field is not regular in the time due to perturbations which may vary from a few nanoTeslas (nT) to thousands of nT. [41]. This source of error cannot be reduced by deterministic solution, but filter solution is needed as it is not affected by this phenomenon.

IGRF Model

An attitude estimation based on filter solution requires an estimation of the next measurement to reduce deviations in the field vector, which are cause by the sensor noise or other perturbations. This estimation is usually performed by a theoretical model independent to the sensor. In this case, in a magnetometer field based attitude determination, the International Geomagnetic Reference Field 11th generation (IGRF-11) model is widely accepted as the best option.

For future improvements, an IGRF-11 estimation of the magnetic field values can be implemented while tracking the balloon path during flight. Then, an error estimation from the real measurement can be carried out to analyse if it is appropriate for future use.

Once we have the path that has taken our experiment during the flight by processing the measured magnetic field, we can compare the results with the information provided



by the star tracker and the horizon sensor. In addition, we will be able to compare it by exchanging our flight data with team TORMES 2.0.

7.2 Launch Campaign

The launch campaign of BX18 and BX19 started the 3rd of October and ended the 13th of October 2014 at ESRANGE Space Center, Sweden. This section summarizes the activities that GranaSAT team performed during those days, as planned in Preparation and Test Activities at Esrange and in APPENDIX D – Launch campaign additional information.

Table 7-1 Launch campaign summary

| Day | Date | Activity | Notes |
|-----|---------|--|---|
| 0 | 03 Oct. | Arrival at ESRANGE | |
| 1 | 04 Oct. | Unpacking and checking of all components | |
| | | Assembly of inner and outer boxes | |
| | | Inner box mounted into gondola | |
| | | Individual test to inner box | |
| 2 | 05 Oct. | Outer box vacuum test | Test successful |
| | | Outer box mounted into gondola | |
| | | GranaSAT pre-flight test | Test successful |
| 3 | 06 Oct. | Magnetometer calibration | |
| 4 | 07 Oct. | Gondola Interference Test | Test successful |
| | | Flight Compatibility Test | Test failed |
| | | Investigation and fix of the failure | |
| 5 | 08 Oct. | Flight Compatibility Test | Test successful |
| | | BX19 flight | Launch at LT2000. Landed after 2H45 of flight |
| 6 | 09 Oct | Spare day | |
| 7 | 10 Oct. | BX18 flight | |
| 8 | 11 Oct. | BX18 and BX19 recovery | |
| | | Post-flight check | |
| | | Preliminary flight data evaluation | |
| 9 | 12 Oct. | Post flight meeting | |
| | | Packing | |
| 10 | 13 Oct. | End of launch campaign | |

7.2.1 Flight Preparations

Day 1

All experiment components, parts and tools we carried by ourselves, as well as the parts we delivered by postal mail to ESRANGE, were not damaged during the travel. Thus, the assembly of the instrument started immediately after the arrival.

After the assembly, we were able to mount the inner box to the gondola and perform several individual tests: the experiment was powered on to check the communications between the experiment and the Ground Station.

Day 2

We carried two baffles to the launch campaign -one painted in black, which caused some issues in the TVAC test (see C.7.5 Thermal Test), and one without paint-. After consulting to the SSC experts which baffle was more appropriate to avoid outgassing, we chose the one with no paint, to reduce the probabilities to have any particle on the lenses during the flight.

In addition, because of the organic properties of ABS plastic used in the 3D printing of the baffle, the SSC experts suggested to perform a fast vacuum test in SSC facilities, in order to ensure a completely outgassing in this piece.



Figure 7-21 Outer box vacuum test performed in SSC facilities

After the vacuum test, we were ready for assembling the outer box and the boom to the gondola. We fixed the boom at the proper distance and finished the link between the two boxes. Then, we ensured the experiment with a steel security cable to avoid a free fall in case of failure with the fixations during the flight. To avoid reflected signals

that may interfere to TORMES 2.0 experiment, one side of the outer box was coated with neoprene.



Figure 7-3 Final assembly of GranaSAT experiment into gondola

After the final assembly, we performed a pre-flight test to ensure the experiment worked according to the plan and without any malfunctions.

Day 3

During day three, the rest of the teams finished their experiments assembly into the gondola. At the end of the day we performed, together with TORMES 2.0 team, the calibration of our magnetometer instruments: while the gondola was spinning around with all the experiments switched on, we collected data from the magnetometer. This was made in order to correct the offset and magnetic disturbances.

Day 4

On day 4, the Gondola Interference Test and the Flight Compatibility Test on BX19 experiments were scheduled.



During the Gondola Interference Test, no problems were found. Specifically, communications with the experiment went fine.

During the Flight Compatibility Test we found a problem in our communication implementation: we were not able to modify the experiment parameters correctly.

To explain the error it is necessary to explain the communication procedure structure: the change of the experiment parameters from the Ground Station was made with a message whose syntax was the following:

- `<command>+<value>`, when the parameter accepted a value.
- `<command>`, in any other case.

Both `<command>` parameters and `<value>` data were codified as integer numbers.

A later inspection showed that the most probable cause of the problem was a failure in the communication protocol. The server expected a `<command>+<value>` message while the client had sent only a `<command>` message. As a result, the next sequences sent were misunderstood: the server interpreted some `<value>` as `<command>` and vice versa. With this failure the experiment became blocked frequently every time the experiment parameters were modified.

The change of the parameters, specifically of the camera parameters, was critical in our experiment, as it was the only way to obtain properly exposed images. For this reason, fixing this issue was mandatory. The organisation gave us three hours to test the modifications with the E-Link enabled. Furthermore, because of the problems TORMES 2.0 and TamaOS teams experienced, the organisation decided to repeat the Flight Compatibility Test the next day.

To solve our problem, we decided to disable the implemented communication, to connect directly to the Raspberry Pi by SSH connection and to modify directly the parameters.

Although we solved the problem, we lost the capability to synchronise the Raspberry timestamps with UTC time. Fortunately, after the flight, we found several marks to obtain a synchronisation by a semi-automated process.

Day 5

In the morning of day 5, a second Flight Compatibility Test was performed. This time the whole experiment, including the change of the parameters and the rest of the communication, worked fine.

At 1600LT launch countdown began.

7.2.2 Flight Performance

BEXUS 19 was launched at 2000LT, 08 October 2014. This section summarises the data gathered during flight.

7.2.2.1 Environmental conditions

In this part, we are going to analyse in which conditions our experiment flew. First of all, the most interesting part is the one related with temperatures. During the flight, we collected the data shown in Figure 7-4, from the EBASS data projected in the screen at Esrange and from our own sensors.

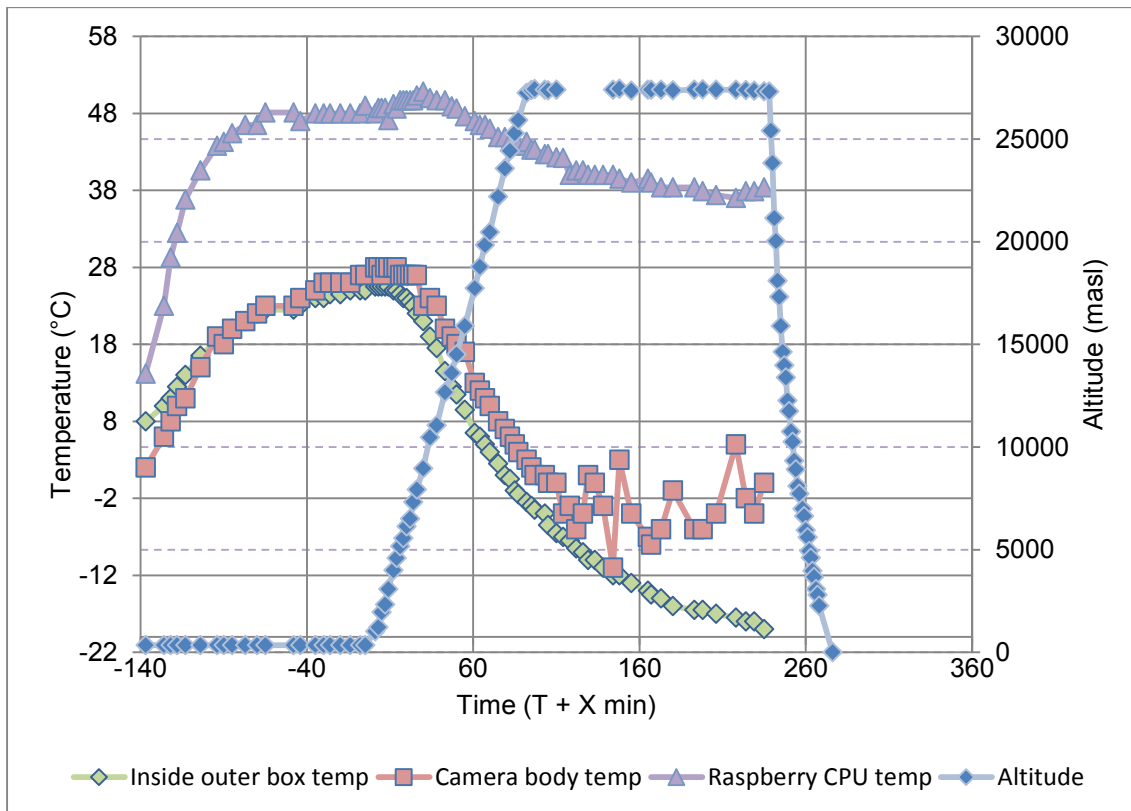


Figure 7-4 Data gathered during the flight

In the left side, the scale for temperature is shown, whereas the scale for altitude is in the right side.

Green dots represent the temperature in the sensor from the outer box. Temperature increased from T-140 to T0 because the experiment was situated in the ground during



this time. As the temperature was not too cold, the heat produced in the camera was enough to keep warm the inside of the outer box. When BEXUS 19 was launched, at T0, the outer temperature began to decrease, leading to a freezing of the inside. Critical temperature for the working experiment (-20 °C) was reached in the final phase. Despite of this temperature, the camera worked with no issues (no condensation and no failure of electronics due to low temperatures).

Red dots in Figure 7-4 show the temperature of the camera body. As we can see, when -2 °C temperature is reached, the sensor began to malfunction. This lead to a wrong record of data (the result is that measurements began to oscillate). From T+110, we are not sure about the real temperature of the camera body. The cause of the problem is still unknown, as in the test we performed to the same sensor we had no malfunction and no failures were encountered after the recovery.

Purple dots show the Raspberry Pi CPU temperature (located in the inner box). In this case, we got high temperatures even during flight time (near 50 °C), but finally the temperature was stabilised around 38 °C, even with -60°C outside the gondola. These temperatures were reached for two main reasons:

- The Raspberry CPU was doing a heavy processing work.
- The inner box was more protected inside the gondola because of the blankets that covered it.

Finally, blue dots show the balloon altitude. This data was collected from the EBASS measurements shown in the projected screen at Esrange.

We can conclude that the range of temperatures was ideal in the inner box but extreme in the camera. Maybe a thermal patch would have avoid the under zero temperatures. If the flight would have last more time, it is possible we would have had an electronics failure due to extreme cold temperatures.

7.2.2.2 Experiment behaviour

The behaviour of the experiment was in general really good. The main issue we had was a software failure. It gave us some problems during FCT –see 7.2.1 for more information–, but a solution was found and all the flight requirements were fulfilled.

Concerning the camera, we got really good pictures. We were able to modify the image parameters to get more detail in horizon or stars as required. The only issue was a little white spot in the right side of the images, whose cause is unknown; probably, it was just a dot of dirt.

The magnetometer had a good performance too. The calibration was successfully done and readings were as expected –even with the distortions because of the iron mine situated near Kiruna–.

7.2.2.3 Related issues

In the ground station, the data was received every two seconds, rate which remained constant during the whole flight. However, the solution we took to the problem experienced during the FCT had a side effect: it was necessary to restart the experiment every 12 minutes, approximately. Each restart took around 30 seconds, in which we were not able to collect any data.

Another issue related was the aurora, which appeared in the floating phase. Despite the beauty of the phenomenon, its brightness produced some unusable images. However, as the gondola spun slowly in 360°, we were able to take properly exposed images while the aurora was in the back of our camera.

7.2.3 Recovery

BEXUS 19 landed west of lake Porttipahta in Finland on the night of 08 October. It was a hard landing in a forest area. The gondola landed sideways; luckily for GranaSAT, the side in which the camera was mounted remained up.

BEXUS 19 spent one and a half day in the woods, as both of the gondolas were recovered at the same time: 10 October in the afternoon. The recovery team brought the gondolas back to Esrange on 11 October, when we were given access to inspect and dismount our experiment.

The recovery procedure was carefully followed, examining the whole experiment, checking its integrity and finally dismounting it.

A first visual inspection of the outer box showed that its status was perfect. The main weak point, the external filter, was not damaged at all, as seen in Figure 7-5.



Figure 7-5 Undamaged filter

A later inspection of the inside showed that the electronics and the camera were undamaged and reusable.

A first visual inspection of the inner box showed that its status was nearly perfect. Two minor mechanical failures were encountered; as shown in Figure 7-6, two solderings were damaged. However, the integrity of the box was undamaged and it was proved that the mechanical design fulfilled all the requirements.



Figure 7-6 Damaged solderings

A later inspection of the inside showed that the Raspberry Pi and the electronics were undamaged and completely reusable.

7.2.4 Post-flight activities

After the receiving of the experiment, GranaSAT team performed the following actions:

- The critical task was the recovery of the experiment SD. The SD card did not lose any kind of data.

- Disassembly of the experiment components for their transport back to Granada.
- Inspection of strange anomalies in the image. An example of these kind of anomalies is shown in Figure 7-7



Figure 7-7 Image anomaly

These anomalies were constant over all the images taken. As at the moment of the recovery they did not appear in the image taken in the Dome, its source could not be determined.

- A cloud backup of the data obtained during the flight was done to ensure the integrity of all the information.
- A preliminary study of the experiment logs was performed. First inspection of the data obtained during the flight by the Star Tracker algorithm.
- A 10 minutes presentation was performed in order to show the preliminary results of the experiment.

7.3 Results

Table 7-2 summarises the system final success. All sub-systems have achieved its maximum success, except for the horizon sensor subsystem (its accuracy has not been fully determined) and for the ground station (the failure experienced with the communication caused the commands not to work perfectly).

The final system success has been of 86.5 %.

**Table 7-2 System final success**

| Subsystem | Level of Success |
|---|--------------------------------|
| Star tracker | Contribution of subsystem in % |
| Star tracker obtains a correct attitude with a maximum error of 1 arcminute. | 37.5 % |
| Horizon sensor | Contribution of subsystem in % |
| Horizon sensor obtains an attitude with an error greater than 5°. | 15 % |
| Magnetometer and Accelerometer | Contribution of subsystem in % |
| Magnetometer and Accelerometer obtains corrects measurements (± 1.5 to ± 8 gauss) of the magnetic field. | 15 % |
| Power system | Contribution of subsystem in % |
| All components receive the power necessary to operate correctly. | 5 % |
| Mechanical system | Contribution of subsystem in % |
| Mechanical components resist g forces and temperatures. | 5 % |
| Thermal system | Contribution of subsystem in % |
| The correct temperature is maintained inside the boxes thanks to the insulation material. | 5 % |
| Ground station | Contribution of subsystem in % |
| Data is correctly received by the ground station but the commands do not work perfectly. | 4 % |

7.3.1 Star Tracker Results

Table 7-3 shows the relevant events of the BEXUS 19 flight from the Star Tracker point of view. This table is graphically shown in Figure 7-8. As we can see, four constellations were observed. In Figure 7-8, the constellations' location over the Earth's horizon during the flight is shown, green colour means satisfactory results while red colour



means unsatisfactory results. The unsatisfactory results will be discussed in section 7.3.1.1.

Table 7-3 Flight events

| Event | UTC Time |
|--|---------------------------|
| Launch | 17:55:47 |
| First Image Registered | 17:59:11 |
| End of Ascending Phase | 19:28:58 |
| E-Link Turned OFF | 19:36:02 |
| E-Link Turned ON | 19:39:50 |
| Aquarius and Capricorn Constellation Observed | 19:55:56 - 20:01:22 |
| Capricorn Constellation Observed | 20:09:36 - 20:21:29 |
| Aurora's Activity | 20:21:29 - 21:03:26 |
| Capricorn Constellation Observed | 21:03:26 - 21:14:05 |
| Aurora's Activity, Cancer Constellation Observed, Jupiter Observed | 21:14:05 - 21:38:29 |
| Orion Constellation | 21:38:26 - 21:52:29 |
| Experiment Turned OFF | 21:52:29 |
| Beginning of Descend Phase | 21:55:15 |
| Last Data Registered by the EBASS | 22:24:11 |

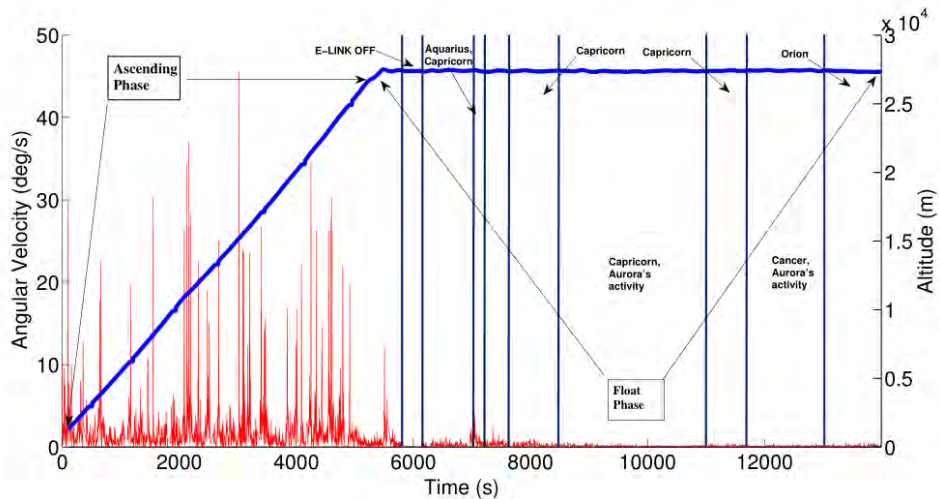


Figure 7-8 BEXUS 19 flight summary



Figure 7-9 Constellations observed

From Table 7-4 to Table 7-7 the general results are shown for each one of Aquarius, Capricorn and Orion constellations for its periods of times, which appear in Table 7-3. Once an image had been taken, it was analysed by the Star Tracker LIS routine as it appears in the Earth's Horizon was removed for all images taken from Capricorn and Aquarius constellations, since the brightness of the horizon was comparable to the stars' brightness because of the high exposition time and gain value required to properly capture stars. Figure 7-10 shows an image of Capricorn constellation where the horizon makes this image impossible to be analysed by the LIS routine, the left-sided image shows the same picture but the horizon removed.

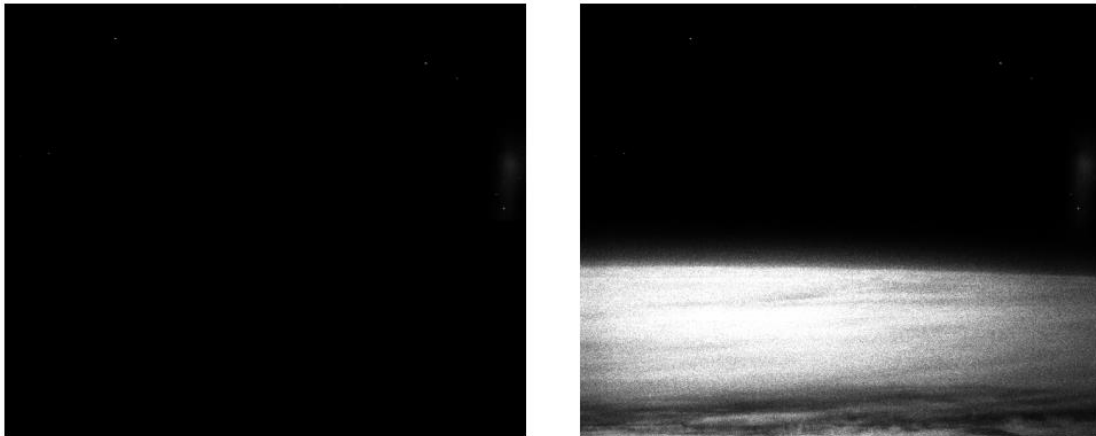


Figure 7-10 Removing horizon



Table 7-4 Aquarius Capricorn images and camera parameters

| | |
|---|------|
| Total Images | 94 |
| Stellar Fields Uniquely Identified | 38 |
| Correct / Incorrect Stellar Fields | 34/4 |
| Not Enough Centroids | 27 |

| | |
|--------------------------|------|
| Brightness | 1 |
| Gamma | 20 |
| Gain | 1023 |
| Exposure Time (s) | 0.63 |

Table 7-5 Capricorn images and camera parameters

| | |
|---|-------|
| Total Images | 176 |
| Stellar Fields Uniquely Identified | 154 |
| Correct / Incorrect Stellar Fields | 154/0 |
| Not Enough Centroids | 9 |

| | |
|--------------------------|------|
| Brightness | 1 |
| Gamma | 20 |
| Gain | 1023 |
| Exposure Time (s) | 1 |

Table 7-6 Capricorn images and camera parameters

| | |
|---|------|
| Total Images | 129 |
| Stellar Fields Uniquely Identified | 93 |
| Correct / Incorrect Stellar Fields | 87/6 |
| Not Enough Centroids | 9 |

| | |
|--------------------------|-----------|
| Brightness | 1 |
| Gamma | 35 |
| Gain | 1023 |
| Exposure Time (s) | 1.2 – 1-7 |

**Table 7-7 Orion images and camera parameters**

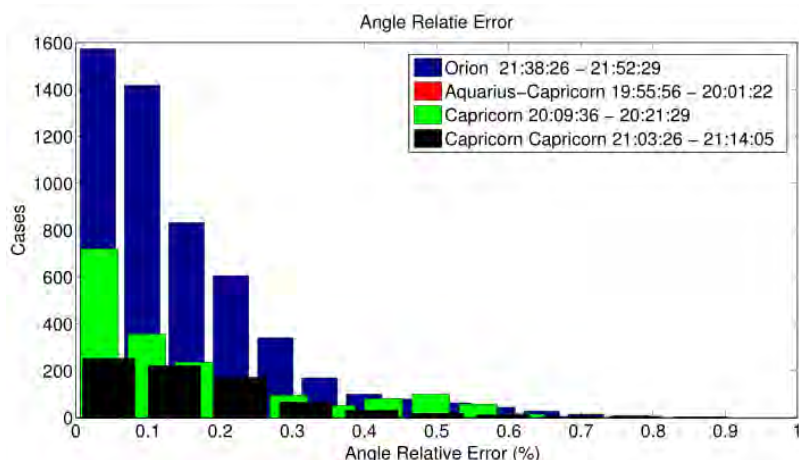
| | |
|---|-------|
| Total Images | 172 |
| Stellar Fields Uniquely Identified | 170 |
| Correct / Incorrect Stellar Fields | 170/0 |
| Not Enough Centroids | 2 |

| | |
|--------------------------|-----|
| Brightness | 1 |
| Gamma | 50 |
| Gain | 923 |
| Exposure Time (s) | 0.8 |

Table 7-8 Data summary

| | |
|---|---------------|
| Total of Images Analysed | 571 |
| Total of Uniquely Identified Star Fields (Correct / Incorrect) | 455 445/10 |
| Total of Not Uniquely Identified Star Fields | 74 |
| Total of Images Discarded (Not Enough Centroids) | 42 |

As a summary, Table 7-8 shows the statistics of the accuracy for the LIS routine developed. The LIS routine was able to identify uniquely the 91.5 % of the images not discarded because of the absence of enough centroids in the image. The 97.80 % of these uniquely identified star fields were correctly matched. Consequently, the performance of the LIS routine for the Star Tracker is considered a success in absence of non-stars objects. The histogram of the angle relative error measured in each constellation validates our calibration, since the error obtained is always below 1 % (see Figure 7-11).

**Figure 7-11 Angle relative error measured**

The attitude error for each star field was obtained once the stars appearing in the image had been identified. As explained in section 4.8.3, the attitude matrix, A, is obtained using the SVD procedure. Figure 7-12 shows the histogram of the error in arcsecs obtained for each one of the constellations analysed. It have been computed for each correctly identified stars as it appears in the following equation.

$$e_i = 3600|\cos(r_i \cdot Ab_i)| \quad Eq\ 1.1$$

Where e_i is the error obtained, r_i are the coordinates of a star in the ECI reference frame, A is the attitude matrix and b_i are the coordinates of the star in the camera frame.

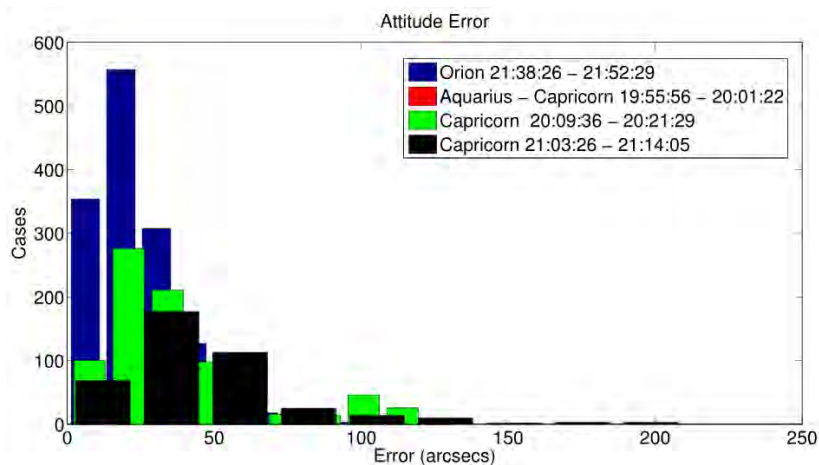


Figure 7-12 Histogram of the attitude error

Even though these results validate our design, we outlined in Figure 7-9 that an entire constellation (Cancer) could not be matched properly. In section 7.3.1.1 we will analyse these situations which makes our LIS routine to fail.

7.3.1.1 Failure Analysis

During the flight, two main reasons made the Star Tracker software to fail in the identification of the star field in the image. The first one is due to the gondola motion, in figure 7-14 we can see the angular velocity for an approximated time of 7 minutes for each one of the previous constellations analysed above.

Table 7-7 shows the mean of the angular velocity for each period in Figure 7-15. As we can extract from it, the two periods of time with the larger angular velocity coincide with the two constellations in section 5.6.1 with incorrect identified stellar fields. As an



example of how the gondola motion affects the quality of the images taken, Figure 7-13 shows a picture of Orion constellation, as we can see the stars are quite well defined. In contrast, Figure 7-14 shows an image of Capricorn constellation with blurred stars.

The LIS routine proposed did not fail with all the blurred images, but we found that 59 out of 74 not uniquely identified star fields were blurred.



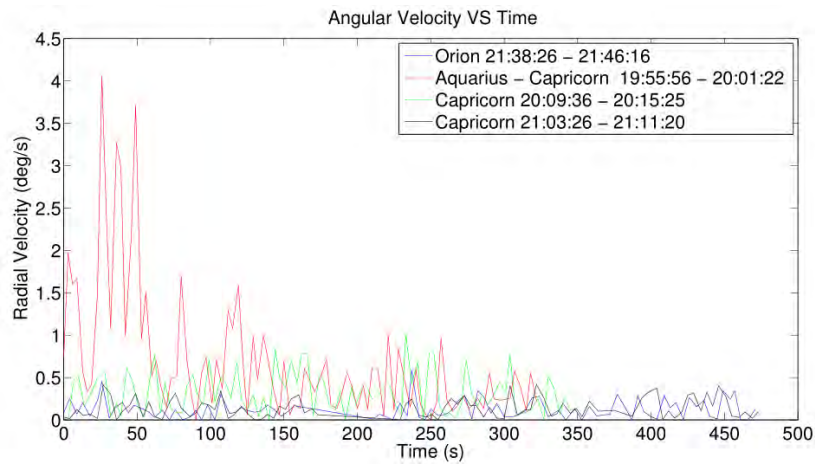
Figure 7-14 Capricorn image



Figure 7-13 Orion image

Table 7-9 Mean of the angular velocity

| Period | Mean of Angular Velocity (deg/s) |
|---------------------|-------------------------------------|
| 19:55:56 – 20:01:22 | 0.69 |
| 20:09:36 – 20:15:25 | 0.13 |
| 21:03:26 – 21:11:20 | 0.27 |
| 21:38:26 – 21:46:16 | 0.13 |

**Figure 7-15 Periods**

The routine to identify the stars proposed in section 4.8.3 implies that the three most bright stars in the image have to be present in the GC. Otherwise the star identification will fail. The biggest example of this weakness was found from 21:14:05 -21:38:29 when Cancer constellation could be observed. However, as it is shown in Figure 7-16, Jupiter was right in the middle of this constellation as the "the brightest star". For this reason, the algorithm was unable to identify properly none of the Cancer images.

**Figure 7-16 Jupiter**

Finally, during the flight we experimented long periods of time with high aurora activity (see Figure 7-8). In this case, its position in the image is impossible to predict as we did in the case of the Earth's Horizon. Figure 7-17 shows a beautiful, but useless image for the Star Tracker as the Aurora brightness is too high.



Figure 7-17 Aurora

7.3.1.2 Conclusions

As discussed in this section, all the star tracker requirements have been fulfilled and the sub-system behaviour has been really successful.

Then, the star tracker sub-system success has been maximum: 37.5 %

7.3.2 Horizon Sensor Results

This section covers the conclusions obtained after the processing of all gathered data related with the horizon sensor algorithm.



Figure 7-18 One of the images processed

Although the night conditions of the flight have been ideal to test the star tracker performance, they have been the main cause of the failures encountered by the horizon sensor. Then, we cannot give a final answer to the question regarding if the proposed algorithm is suitable for a picosatellite, as further tests in day conditions should be done. This is not critical for the experiment success as the star tracker have been fully tested. From a technical point of view, the use of only one sensor for both algorithms has been successfully proved, as we have been able to collect attitude data from both of them.

In the other hand, the accuracy of the horizon sensor cannot be fully determined because of the loss of the synchronisation signal, which would have been used to synchronise our attitude determination with TORMES 2.0 data. As EBASS attitude data is not reliable, we do not have a reference to compare with, which forces us to determine the accuracy with the simulations and tests done before the flight.

Concerning the flight conditions, it is important to remark the weather we faced that night:

-
1. All the flight area was covered by a thick layer of clouds.
 2. There was a nearly full moon.

We did not expect to test the horizon sensor algorithm in a dark night situation, but the combination of the previous two factors gave us the possibility to do it –see Figure 7-19–, as the contrast between the limb and the sky was visible. However, we have never faced those conditions on the tests, and some problems appeared.

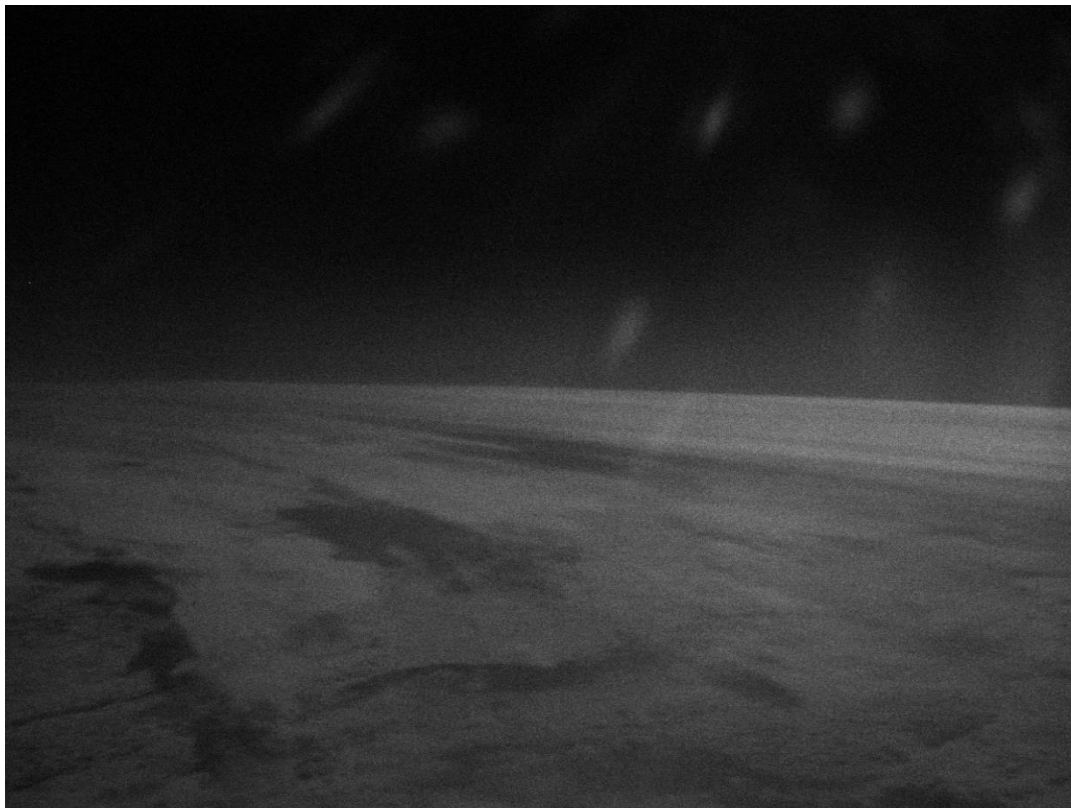


Figure 7-19 The moon light reflected in the clouds

7.3.2.1 Failure Analysis

Noisy images

The images used in the tests -taken from COMPASS [13] footage- were filmed in a clear day flight and no noise was visible.



Given that, our algorithm was not completely ready to deal with highly noisy images, like the ones our camera took in the flight.

This noise disturbed the proper function of the limb detection algorithm. In order to solve it, an auxiliary method has been added.

Before the binary threshold, a Gaussian blur filter has been used. The image smoothing helped the next steps to perform as they did in the tests. See Figure 7-20 and Figure 7-21.



Figure 7-20 Binary result from noisy image; thousands of undefined contours.

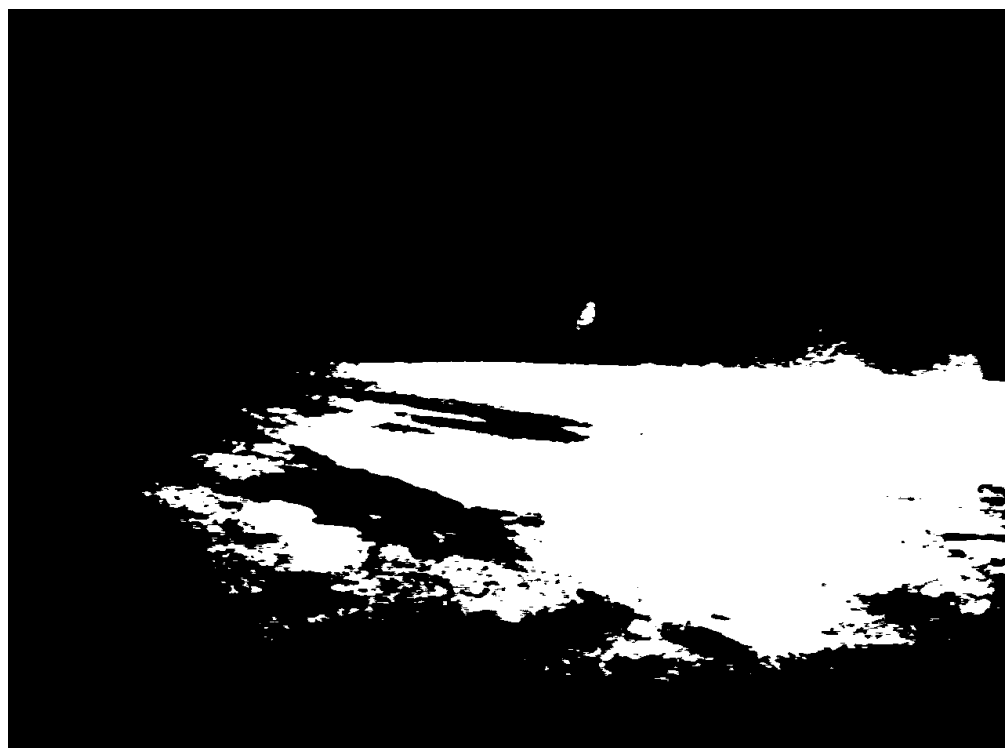


Figure 7-21 After the smoothing, the noisy image is tractable

Even if this solution solved the problem in many cases, some really noisy images were discarded by the algorithm, ignoring the presence of the faded limb.

Low contrast images

Also as a result of the night conditions, a lot of the images taken have a very low contrast, as in Figure 7-22. This fact has hindered the performance of the limb detection algorithm, as it relies a lot in the threshold used to convert the photograph taken into a binary image.



Figure 7-22 Example of a very low contrast image

The threshold was thought to be determined manually in the flight. However, to test those low contrast cases, we have developed an algorithm to determine it autonomously. As an example, one of these tests can be seen in Figure 7-23 and Figure 7-24, which are the result of processing the image from Figure 7-22 with the manual way and the autonomous method, respectively.

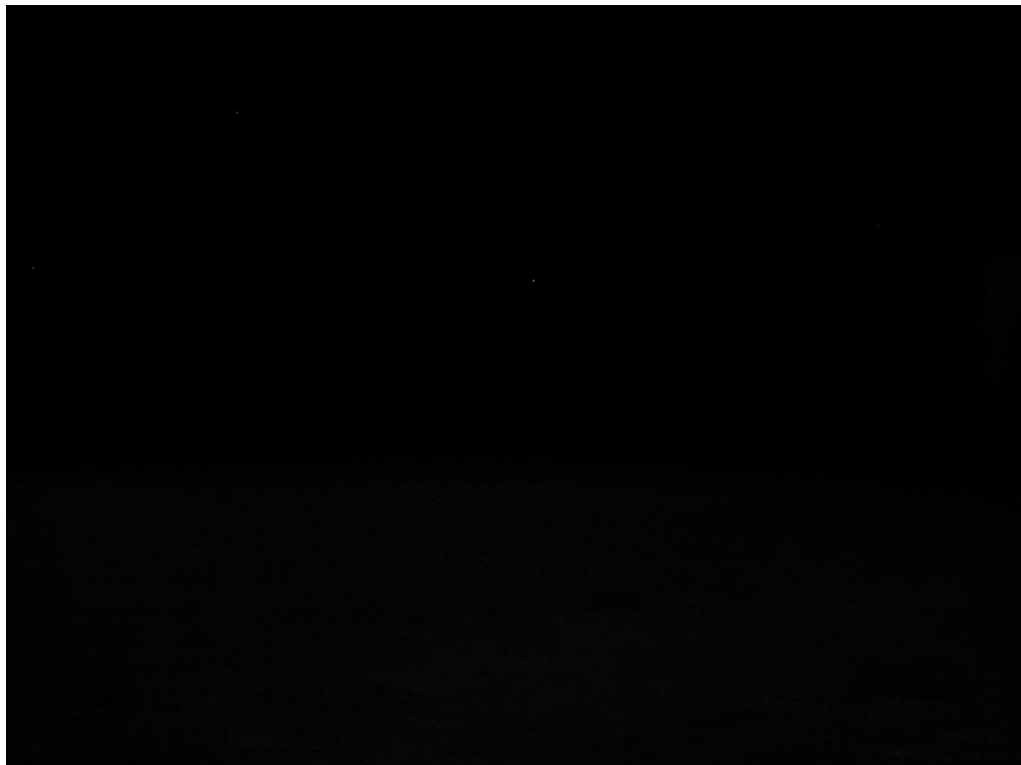


Figure 7-23 Threshold obtained manually

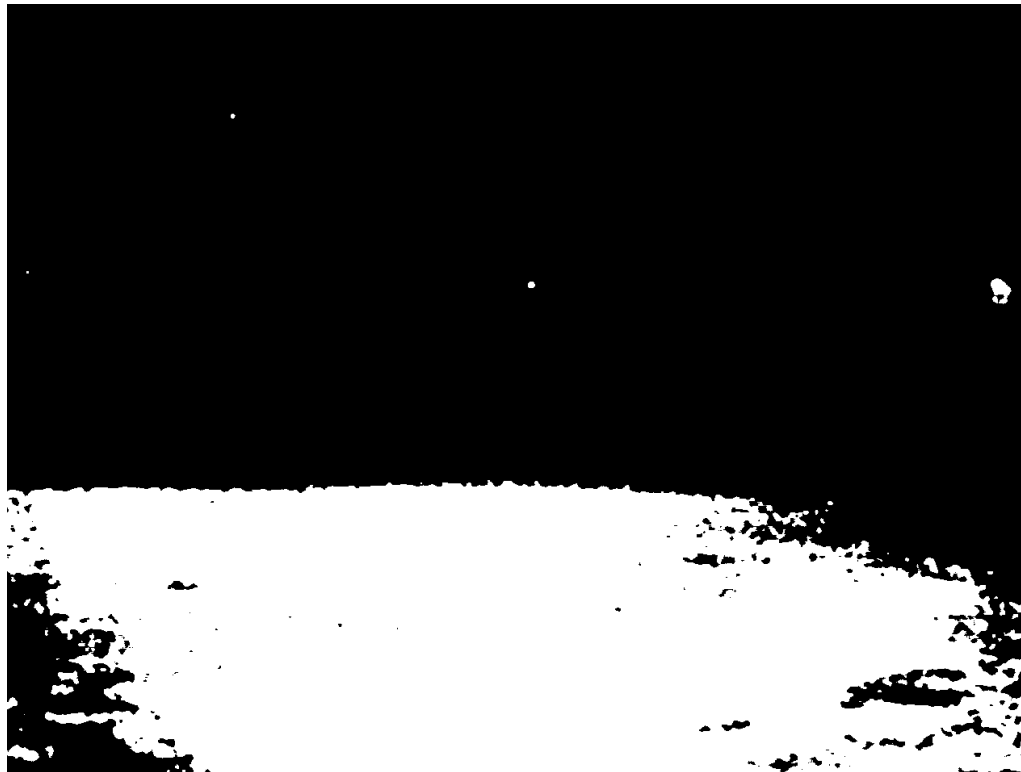


Figure 7-24 Threshold obtained autonomously

Synchronisation

The worst failure we faced during the launch campaign was the loss of the synchronisation signal. The problems we had during the FCT were all solved except for that feature: the protocol we have designed to synchronise the data gathered in the Raspberry with a global time server was finally unusable. The reason of the failure was not on the protocol itself but in the communication channel, which was messed with unordered packets.

Because of that, we lost the possibility of synchronising our processed data with TORMES 2.0 GPS attitude. Although we have been able to synchronise the data in a rough way with the EBASS timestamps -just to correlate the temperatures, altitudes and positions-, we needed a higher accuracy in order to compare our processed attitude with a reliable frame.

This was not possible. Hence, we can only rely on the conclusions obtained from test 2, which proves only the accuracy of the circle fitting method, but not the limb detection method.

7.3.2.2 Conclusions

The horizon sensor algorithm performed better than expected. We did not design it to work in completely dark conditions, but the reflected moon light from the clouds was enough to let the algorithm determine the horizon in the vast majority of images.

Although some unexpected problems appeared, simple solutions were made to solve them.

Finally, the accuracy of the algorithm has not been determined, as no fixed reference is available. Even if no rigorous conclusion can be given, we can estimate that requirement P.2 is fulfilled because of the two following reasons:

1. The visual inspection of the algorithm performance conclude that the limb detection method worked as expected, with the exception of the highly noisy images.
2. From test 2 we can conclude that the fitting circle method is reliable.

The sub-system success has not been the maximum possible, as the accuracy has not been fully determined.



As we cannot conclude if the horizon sensor error has been lower or greater than 5°, the horizon sensor sub-system final success has been of 15 %.

7.3.3 Magnetometer and Accelerometer Results

7.3.3.1 Summary

During the flight we gathered enough data to obtain a reconstruction of the Earth's magnetic field vector. However, concerning the accelerometer, a measurement failure arose at T+1H40 and it got worse during the rest of the flight.

As explained in section 7.2, we experienced an error with the E-Link connection during the Flight Compatibility Test. As we lost the capability to synchronise the Raspberry timestamps with UTC time, we had to perform a semi-automated process to synchronize the data. Despite this, we were able to process all the data gathered and to synchronize Raspberry timestamps with UTC time.

Flight data exchanging with TORMES 2.0 team was not necessary for the post processing of this sub-system. All additional required data was provided by EBASS data.

Due to the accelerometer failure, three axis attitude determination was not achievable, but two axis attitude determination was reached with the uncertainties detailed in Table 7-10.

Table 7-10 Uncertainties on the Euler angles

| Angle | Uncertainty (deg) |
|-------|-------------------|
| Roll | 4 |
| Pith | Unresolved |
| Yaw | 3 |

7.3.3.2 Accelerometer Module

The acceleration sensor module did not work as expected during the flight. Figure 7-25 shows the acceleration measurements gathered along the flight as well as the Z axis acceleration from EBASS.

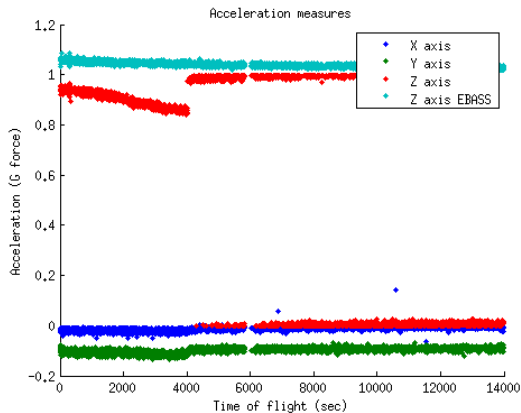


Figure 7-25 Acceleration measurements

After approximately 4,000 seconds of flight, there was a discontinuity in the accelerometer measurements: the measurements from X, Y and Z axes experienced a sudden rise; the increase was bigger in Z axis. It is clear the accelerometer had a malfunction during the flight, making these data useless for the attitude determination estimation.

Despite this malfunction, an interesting value to determine the sensor misalignment was obtained. Observing the difference between X and Y axes acceleration, and if we assume X axis is not misaligned, we can calculate that Y axis is rotated 5.9 degrees with respect to the horizontal plane. This information is useful to minimize the error assumed in the estimation of Euler angles.

Figure 7-26 shows three sets of data: the Z axis acceleration measurements, the temperature from the sensor into the outer box and the external temperature provided by EBASS sensors. When internal temperature reached 4 °C two events occurred: the rise of the acceleration measurements and an acceleration fluctuation between 0 g and 1 g. This behaviour got worse with the descent of the temperature. However, given that the operating temperature range of the sensor is from -40 °C up to +85 °C, and observing that the malfunction started at 4°, we conclude this failure was not caused by the low temperatures.

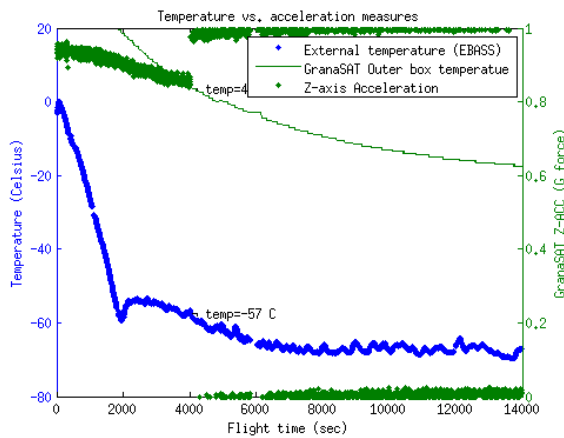


Figure 7-26 Temperature vs. Z axis acceleration

Furthermore, the measurements gathered did not exceed in any case 1 g, shifting to 0 g when they should be bigger than 1 g. The sensor Full Scale (FS) chosen in the mission was the minimum provided by the sensor, ± 8 g, which cannot explain this weird behaviour.

We assume the sensor, which was a low cost one, was defective. In addition, it seems to have an operating temperature range lower than the specified one.

This discussion concludes a part of the secondary mission of our experiment: to analyse the behaviour of a very cheap instrument like LSM303DLHC and to determine if it is appropriate for an aerospace mission. We can conclude that LSM303DLHC is not a good option for an accelerometer that will be used under hard conditions.

7.3.3.3 Magnetometer Module

The first step in the process of determining the minimum error in the magnetometer is the calibration. Two calibration processes were realised: on-earth and in-flight.

On-Earth calibration

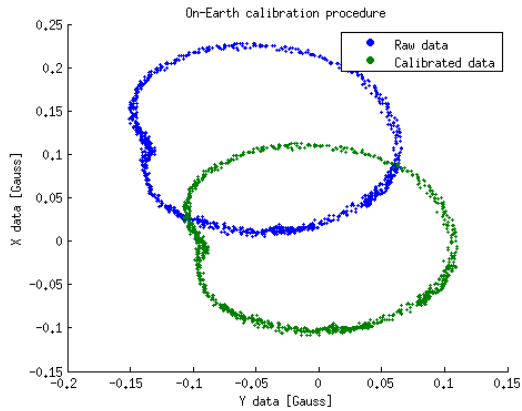


Figure 7-27 On-earth calibration

The process of calibration is detailed in C.7.8 Magnetometer calibration Test.

The magnetic field measured in Kiruna before the flight is shown in Figure 7-27. The calibration procedure was successful: the offset was removed and the soft and hard iron disturbances were attenuated.

It is easy to see a big disturbance that come from the East. This disturbance is due to the iron mine in Kiruna. Checking the satellite map shown in Figure 7-28, we confirm that the relative positon of the mine with respect to Eesrange is consistent with the data obtained.

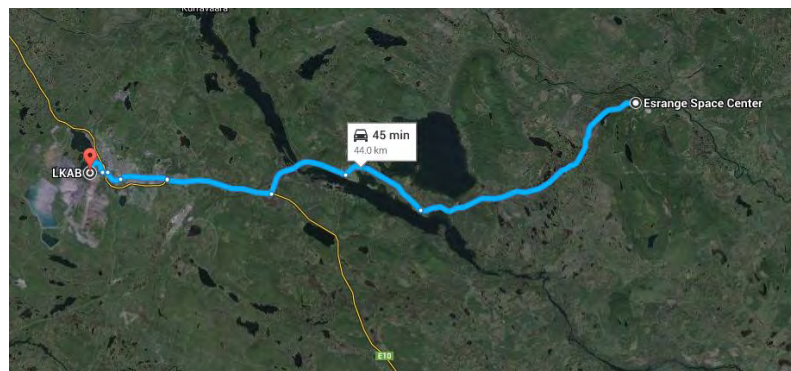


Figure 7-28 Esrange and Kiruna mine

After have obtained the calibration parameters we performed the calibration to the flight data gathered. The result was not satisfactory—the offset of the sensor was not removed and the circumference was not centred—as the calibration was performed with parameters that differed from the real data measurements.

In-flight calibration

To avoid this problem, an in-flight calibration was performed: measurements from the real flight were used to obtain the calibration parameters.

Figure 7-29 shows the result. A circumference and two of its diameters are drawn to see the matching of the centre of the circumference with the (0, 0) reference.

The calibration was performed with all the magnetic field measurements, although a single spin is enough to achieve a good result.

Figure 7-30 shows the differences between both calibration procedures. The in-flight calibration procedure is clearly much better than the on-earth one.

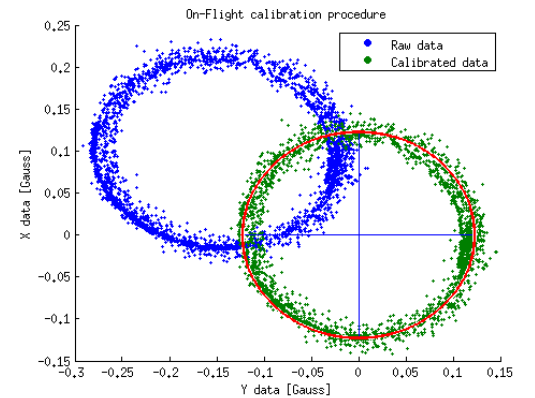


Figure 7-29 Flight data in-flight calibration

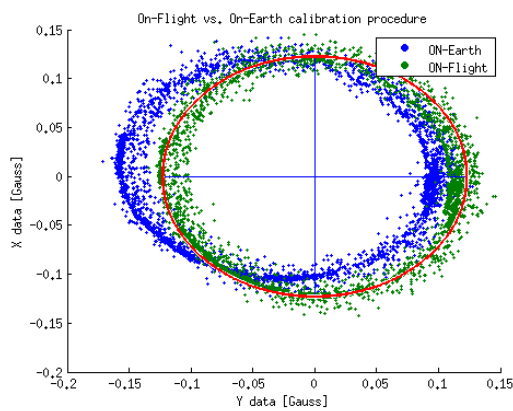


Figure 7-30 On-earth vs. in-flight calibration

All the following representations and operations concerning the Earth's magnetic field are done with the measurements calibrated with the in-flight procedure.

Sensor misalignment correction

The error assumed in our calculations depends on how the sensor is physically placed. Then, before performing the estimation of the attitude, the alignment of the sensor has to be determined.

The misalignment is easy to see in Figure 7-31, where the magnetometer value scatter measured during the flight is shown. Note the toroid-form scattering should be parallel to the horizontal plane, as long as the sensor and the gondola—nearly all the flight time—were level. However, we obtained a rotated toroid-form. This is due to the misalignment of the sensor and the rest of the experiment, like the boom or the outer box attachment.

Taking the orthogonal projections of these values we can calculate, by lineal regression, the angle of deviation in each Euler angle. Then, through an isometry operation, we can spin the measurements to the adequate angle.

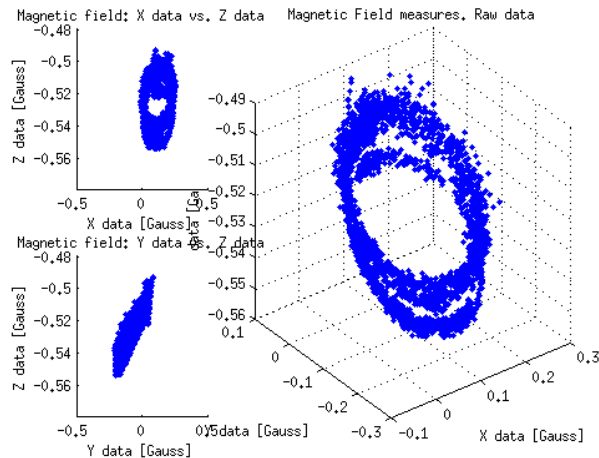
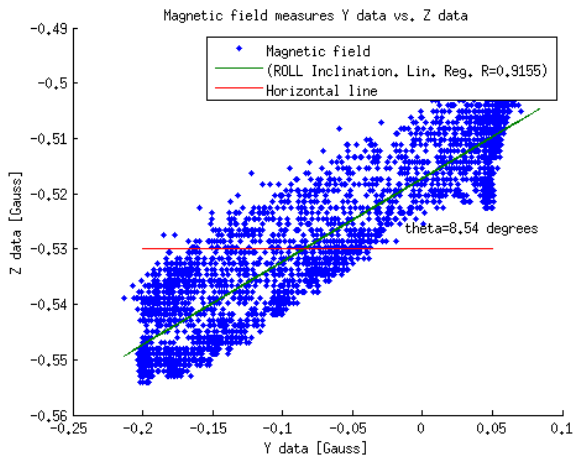
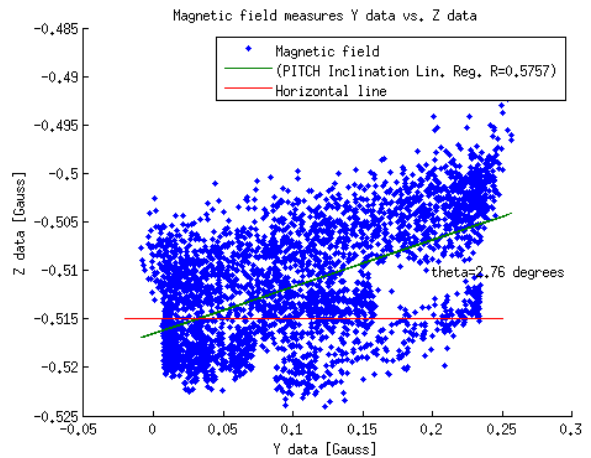


Figure 7-31 Magnetometer values with angle deviation

Figure 7-33 and Figure 7-32 show the Roll and Pitch angle deviation of the sensor. The estimated angle of deviation is shown in Table 7-11.

Table 7-11 Estimated deviation angles

| Angle | Deviation (deg) |
|---------------|-----------------|
| Roll θ | 8.54 |
| Pitch Ψ | 2.76 |

**Figure 7-33 Roll angle deviation: 8.54 degrees****Figure 7-32 Pitch angle deviation: 2.76 degrees**

Once the angle deviation is estimated, we just need to perform an Isometry to obtain a matrix with the fixed and corrected values of the magnetic field.

$$\vec{B}_{Fixed} = A \vec{B}_{Raw}$$

$$A = \begin{bmatrix} \cos\Psi & 0 & -\sin\Psi \\ 0 & 1 & 0 \\ \sin\Psi & 0 & \cos\Psi \end{bmatrix} \begin{bmatrix} 1 & 0 & 0 \\ 0 & \cos\theta & \sin\theta \\ 0 & -\sin\theta & \cos\theta \end{bmatrix}$$

After this operation, the fixed magnetic field measurements are ready to be used to estimate the attitude of our experiment. After the correction, if we perform again this process we can ensure the alignment is fulfilled. In a new iteration the deviation angles shown in Table 7-12 were obtained.

Table 7-12 New estimated deviation angles

| Angle | Deviation (deg) |
|-------|-----------------|
| Roll | 0.014 |

| Angle | Deviation (deg) |
|-------|-----------------|
| Pitch | 0.012 |

An iterative method to tune this alignment could be a nice-to-have improvement for a future work. As the operations performed are isometries, no difference exists between the calibration of raw magnetic field measurements and the calibration of the fixed magnetic field measurements.

In addition, this rectification of the three Euler angles should be performed at laboratory before the flight, and with the whole spacecraft structure mounted, to perform a reliable correction of the measurements.

Sensor measurement error

In order to establish a minimum value of the error we can achieve with our instrument, it is necessary to perform a measure of the Earth's Magnetic Field with the sensor still. This allows us to analyse the precision of our sensor and therefore a value of standard deviation can be obtained.

The values of standard deviation for each axis are shown in Table 7-13. These values were calculated performing this process several times and with different configuration, trying to avoid a magnetic noisy environment.

Table 7-13 Magnetic field sensor precision

| Standard deviation | Value: Gauss (nT) |
|--------------------|-------------------|
| σ_x | 0.0013 (130) |
| σ_y | 0.0014 (140) |
| σ_z | 0.0014 (140) |

We are now able to calculate the minimum angle we can measure without doubt. The angles obtained are shown in Table 7-14. This result does not mean these sigma values are the error achieved in our attitude estimation, but indicates the minimum value of uncertainty we can reach with this specific magnetic field sensor.

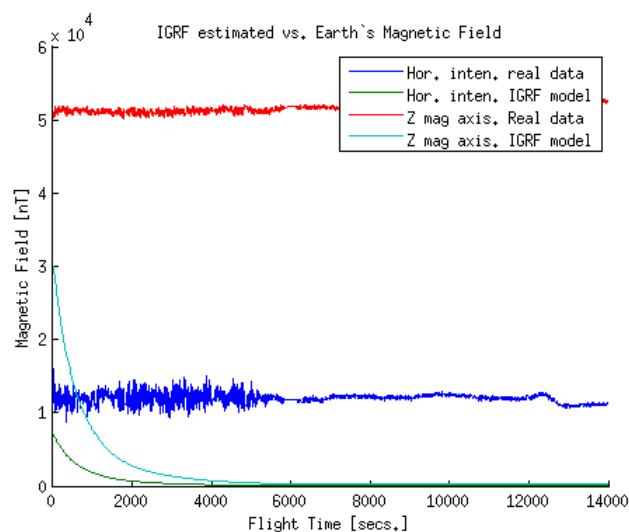
Table 7-14 Minimum standard deviation in Euler angles by precision sensor

| Standard deviation | Value (degrees) |
|-------------------------|-----------------|
| σ_{yaw} | 0.66 |
| σ_{roll} | 0.09 |
| σ_{pitch} | 0.09 |

7.3.3.4 IGRF Model

An attitude determination based in Filter Solution, like the Kalman filter, requires a model which can deduce a theoretical value of the magnetic field in order to estimate the value of the actual attitude. The IGRF model is widely accepted to develop this function.

We have used the Drew Compson's IGRF functions [42] to estimate the magnetic field in the path followed by the gondola during the flight. These values are shown in Figure 7-34, along with the Earth's magnetic field measured during the float altitude phase. Note the rapid fall of the magnetic field with the increasing altitude. These values match the ones of the NASA website (see section 5.3.3). However, after comparing them with the data obtained during the flight a big difference was seen. Then, a horizontal intensity conversion was required for X and Y axes.

**Figure 7-34 IGRF values and magnetic field measured during the flight**

Nevertheless, keeping the GPS coordinates and assuming an altitude of 0 meters we achieve a better fit, as shown in Figure 7-35.

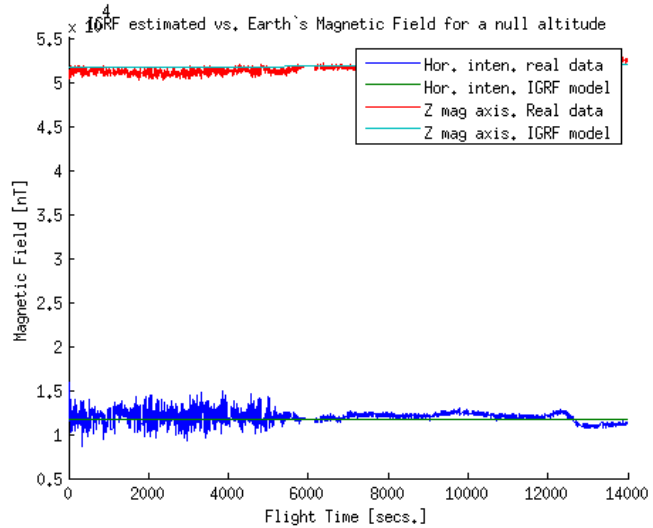


Figure 7-35 IGRF value for a null altitude scenario and magnetic field measured

The values are smoother in the floating phase than in the ascending phase. We can determine the error and deviation values focusing on those measurements. The results are shown in Figure 7-36 and in Figure 7-37.

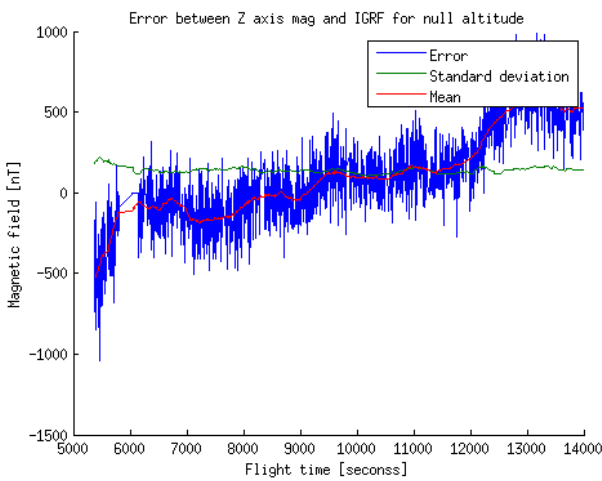


Figure 7-36 Z axis error between IGRF and magnetic field measured

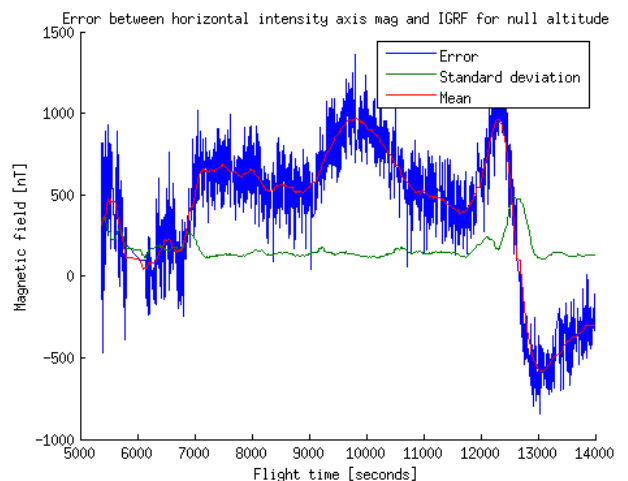


Figure 7-37 Horizontal intensity error between IGRF and magnetic field measured



Concerning Z axis, the maximum mean error experienced is about 500 nT, being lower than 100 nT for a considerable part of the flight. Concerning horizontal intensity, the nominal mean error is no lower than 500 nT.

Further investigations are needed for understanding the IGRF behaviour and why the flight measurements does match when we assume a null altitude instead of the real value.

7.3.3.5 Attitude Reconstruction:

After the process of calibration and correction of the measured data, we are able to perform the attitude reconstruction of the experiment during the flight. As briefed in section 7.1, the attitude will be estimated with respect to the Magnetic North.

We obtained the estimation of Yaw and Roll attitude angles by the procedure justified in 7.1.3. As predicted, we were not able to estimate the Pitch angle due to the failure of the accelerometer. Therefore, because of the lack of the second vector measurement, we did not the direct vector matching.

Yaw angle attitude estimation

The Yaw Euler vector estimation for the whole flight is shown in Figure 7-38. It is clear how the angular movement is bigger during the ascending phase, while in the floating phase the spin is smoother and slower.

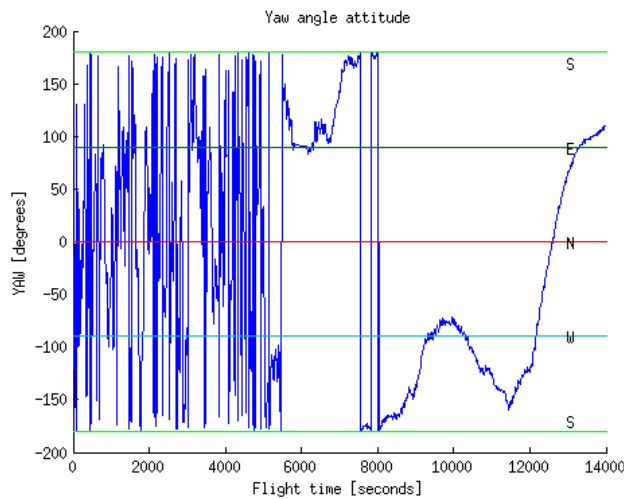


Figure 7-38 Yaw angle attitude for the whole flight

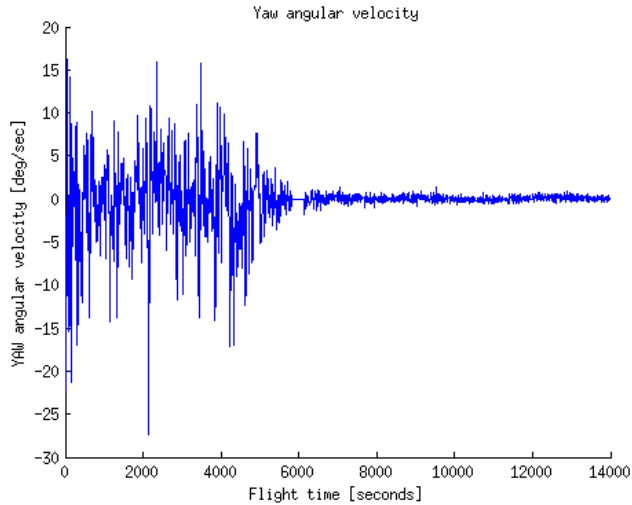


Figure 7-39 Yaw angle angular velocity for the whole flight

Indeed, if we also estimate the angular velocity for the Yaw angle—see Figure 7-39—we can see the movement behaviour: during the ascending phase the angular velocity for Yaw angle was about 5 degrees per second, while in the floating phase the value decreased to about 1 degree per second or lower.

Roll angle attitude estimation

The estimation of the Roll Euler angle attitude has been calculated by reference to the vertical axis. As shown in Figure 7-40, we have obtained a noisy result, due to the noisy measurements of the Z axis magnetic field. Despite this fact, the process we have done is capable to detect the inclination in the experiment produced by the misalignment during the experiment mounting. This is the reason because the estimated angle is over 90 degrees in nearly all the flight.

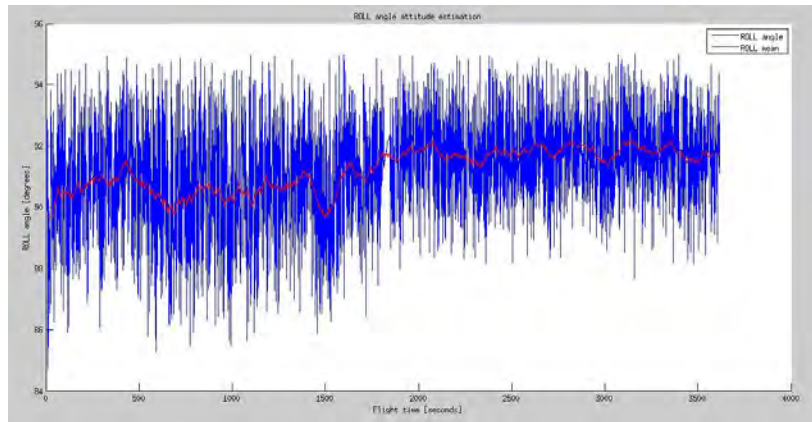


Figure 7-40 Roll angle attitude for the whole flight

Error in attitude estimation

For obtaining the error in our attitude determination estimation we should know the real attitude data. As this is impossible, we have isolated the sets of photographs which are still for a period of time for each Euler angle; then, we have obtained the attitude estimation to check if they are still too. The uncertainty obtained by this process is shown in Table 7-15

Table 7-15 Uncertainties on the Euler angles

| Angle | Uncertainty (deg) |
|-------|-------------------|
| Roll | 4 |
| Pitch | Unresolved |
| Yaw | 3 |

For both Yaw and Roll angles the maximum uncertainty obtained is lower than 5 degrees. These values are enough for small satellite missions that need a less accurate attitude determination.

7.3.3.6 Conclusions

Although we did not have gathered good accelerometer measurements because of the malfunction experienced, the magnetometer has worked correctly and the post-processing of the data has gone better than expected.

The maximum value of 5 degrees of uncertainty is, usually, the minimum requirement for ADCS from small satellites, secondary ADCS or missions with a lower requirement in this system. Our results are then better than acceptable, taking into account that the second field vector could not be used in our analysis, and in addition by using a direct method for the estimation.

Also we have compared the magnetic field measurements with IGRF model. Although the behaviour of the IGRF model with the altitude parameter has been unexpected, now we understand better the model and its use in the future Magnetometer Attitude System is feasible.

The analysis of the misalignment deviation of the sensor has been very important for achieving a good result. Therefore, this procedure will be mandatory in future electronics design, in order to avoid future corrections of the measured data.

Regarding the method of the attitude determination, the use of a better method for determining the attitude angles is mandatory if a better accuracy is needed. To design a Kalman filter instead of a Direct Method is now the next step for future improvements. Also, the use of an inertial sensor like a gyroscope or angular rate is preferable to an accelerometer, because it obtains directly the magnitude the attitude determination method needs.

In the other hand, the use of a low cost integrated sensor (less than \$ 4) has been half satisfactory: the magnetometer has worked perfectly but the accelerometer has not. This could be because of the use of a lower cost test circuit instead of a good quality LSM303DLHC sensor. The choice of the sensor and his manufacturer must be done more carefully the next time.

Finally, due to the good results provided by this sub-system, and because the magnetometer has obtained the measurement from the magnetic field under the requirements, the sub-system has fulfilled their objectives and the contribution to the whole experiment is 15 %, the maximum possible.

7.4 Lessons Learned

Special experiences and problems



In the next list, we summarise some lessons learned and problems that appeared during the design of the experiment and the organisation of the project.

1. The team leader role is critical to the whole team behaviour; the project management is crucial.
2. Money makes the world go round and the REXUS/BEXUS programme is expensive from a student's point of view. Sooner or later your team will most likely face economic problems. Look for sponsorship from the very beginning. Good marketing management is highly relevant in order to obtain a good economic support.
3. Good organisation is essential to avoid overtasking and unexpected problems.
4. All the meetings should be scheduled at least three days in advance. Short periodic meetings are also very important.
5. English is a very important skill.
6. Design is never trivial, even if it looks like it.
7. A thermal and mechanical expert in the team is essential.
8. Working face to face is much better than virtual meetings. As technology improves, communication at work becomes easier, to the point that doing almost all of your tasks without seeing each other is feasible. However, working individually and far from your team mates reduces the exchange of ideas, making solving problems and improving yourselves more unlikely to happen.
9. The problems, both technical and personal, have to be faced as soon as possible.
10. Time spent in improving your work is time well spent.
11. Each member in the team must be responsible of their own tasks and should never expect the team leader to always help or even solve the problems by himself.
12. Even if you have a task assigned, and only in case you are not neglecting it, it could be useful to collaborate with other colleagues in other tasks. When you collaborate, you can contribute with original ideas or give a different point of view not seen before by others.
13. Do not underestimate any person just because he or she is not an engineer or a scientist. You will have to execute many tasks that are not technical or scientific that will be crucial for the success of your experiment. An expert in

these tasks will be a great help and will provide suggestions and new thoughts that may improve your work.

14. Documentation is a big and relevant task. Take your time to decide how to organise the documentation workflow. Schedule deadlines at least a week before the official review deadlines and save some days just to check all the text written. A member with really good writing skills should be responsible of this work; the rest of the team should follow his/her instructions, which should be agreed in advance. Any lack of organisation in the writing of the documentation has to be resolved as soon as possible.
15. The outreach is as important as time consuming; having a member with this task as his/her only responsibility would be perfect.
16. It is hard to make up for a lost day of work without causing any delay.
17. Be professional: if you think that something is poorly done or can be improved, say it; this is the only way to achieve all the experiment objectives. Also, expect the other team members to criticise your work and listen to their advices.
18. Be prepared to receive requests and, sometimes, even orders. One must always have disposition to keep working, the BEXUS group does not have to be a friends group, but a work one. Motivation and work must go on.
19. Human relationships are also important. When possible, it is nice and relaxing to have some free time with your colleagues, or to organise reunions to talk, drink and eat with the others. Ideas flow better and you get to know more deeply the problems of your colleagues. The ambient inside a lab may be tense some days! Any lack of communication between the team members has to be resolved as soon as possible.
20. It is important to give manufacturers good CAD drawings and detailed descriptions of what you want and when.
21. A good planning must consider the time needed to learn about design CAD tools.
22. A good knowledge of a CAD tool does not always result in a good design.
23. Put pressure on suppliers so they get what you need on time.
24. Software implementation, not just the design, has to be started from the very beginning.
25. Objectives have to be defined from the start and should not be over-ambitious.



26. Avoid having students switching between one task to another during the development of your experiment. Stability means productivity and it will be increased if you can focus on just one or two tasks.
27. The PCB design is critical for the experiment, which is why it has been changed frequently because of the modifications in other departments.
28. Mechanical simulations software requires time. Representative results cannot be achieved fast.
29. Having at least two students in the core tasks is almost mandatory.
30. The software should be designed and coded by at least two members of the team. Keep in mind that you will have to code different pieces of software for the tests, the simulations or the post processing, not only for the experiment itself.
31. Document every line of code from the very first moment. To put off the documentation of the software is a very bad decision, both for you and for the other programmers.
32. A version control system such as Git is the best decision for the development of the code and for the collaboration between the programmers.
33. Think about the license of your software. REXUS/BEXUS is an educational programme: a free or open source license can help future teams to easily access your code and learn from your work.
34. Spare electronic components must always be available for a good PCB design and implementation.
35. Try to have a minimum quality level by the beginning in your work. Otherwise, future improvements or nice to have implementations will be hard to achieve in the future.
36. Media do not understand much about science, you must provide them with accessible and understandable information for all audiences.
37. The electronic department needs to have every hardware in their own hands to test the circuits in the critical moments.
38. Every department should be together when an important test starts, since each member has the know-how for their part.
39. Every test has to be completely planned and detailed. The more detail the test plan has, the more successful the test will be.



40. A detailed test schedule is critical.
41. Any test delay has to be fixed as soon as possible.
42. The tests are not independent. Some of them may depend on the success of other tests.
43. The actions to be taken after the success or failure of any test have to be ready before performing the test. Both scenarios—success and failure—have to be contemplated, and the team should know what to do regardless of the test result.
44. The electronic tests can damage some elements. Spare PCBs and components have to be ready before any dangerous test.
45. A system is not finished unless it has passed a phase test successfully.
46. It is cheaper, when possible, to verify the experiment behaviour through simulation and analysis rather than through test.
47. The scientific production is more important than the experiment itself. It is the purpose of the project.
48. A good early data analysis plan could prevent many concept mistakes in the design.
49. An after launch campaign plan is mandatory to achieve a successful final report.



8 ABBREVIATIONS AND REFERENCES

8.1 Abbreviations

| | |
|------------------|--|
| ACK | Acknowledgement |
| ADC | Analog to Digital Converter |
| CAD | Computer-Aided Design |
| CADS | Camera Attitude Determination Subsystem |
| CCD | Charge Coupled Device |
| CCS | Central Control Subsystem |
| CDR | Critical Design Review |
| COG | Centre of Gravity |
| CPU | Central Processing Unit |
| DC | Direct Current |
| DEC | Declination |
| DLR | Deutsches Zentrum für Luft- und Raumfahrt |
| DQ | Data Queue |
| EP | Exit Pupil |
| EBASS | ESRANGE Balloon Service System |
| ESA | European Space Agency |
| ETSIIT | <i>Escuela Técnica Superior de Ingenierías Informática y de las Telecomunicaciones</i> , Higher Technical School of Information Technology and Telecommunications Engineering. |
| FFT | Fast Fourier Transformation |
| FOV | Field Of View |
| GCS | Ground Communication Subsystem |
| GND | Ground |
| GPIB | General-Purpose Instrumentation Bus |
| GPIO | General Purpose Input Output |
| GSS | Ground Segment Subsystem |
| GTK | GIMP Tool Kit |
| GUI | Graphical User Interface |
| H/W | Hardware |
| I ² C | Inter-Integrated Circuit |
| ID | Identification |
| IGRF | International Geomagnetic Reference Field |
| IPR | Interim Progress Review |
| IR | Infrared |

| | |
|--------|---|
| LCD | Liquid-Crystal Display |
| LCL | Line CLock |
| LCS | LEDs Control Subsystem |
| LDA | Linear DAta |
| LIS | Lost In Space |
| LED | Light-Emitting Diode |
| LGA | Land Grid Array |
| MADS | Magnetometer Attitude Determination Subsystem |
| MLS | Modified Least Square |
| MOSFET | Metal-Oxide-Semiconductor Field-Effect Transistor |
| NASA | National Aeronautics and Space Administration |
| NMOS | Negative-channel Metal-Oxid Semiconductor |
| PCB | Printed Circuit Board |
| PDR | Preliminary Design Review |
| PSD | Power Spectral Density |
| QUEST | QUaternion ESTimator |
| RA | Right Ascension |
| RBF | Remove Before Flight |
| RMS | Root Mean Square |
| ROI | Region Of Interest |
| RPI | Raspberry Pi |
| SCL | Serial Clock |
| SD | Secure Digital |
| SDA | Serial DAta |
| SED | Student Experiment Documentation |
| SMD | Surface Mount Device |
| SoC | State of Charge |
| S/W | Software |
| T | Time before and after launch noted with + or – |
| TBD | To be determined |
| TCP/IP | Transmission Control Protocol/Internet Protocol |
| TS | Thermal Subsystem |
| UGR | University of Granada |
| USB | Universal Serial Bus |
| UV | Ultraviolet |
| VROS | Vice-Rector's Office for Students |
| V4L | Video for Linux |
| WBS | Work Breakdown Structure |
| XPS | Extruded Polystyrene |



8.2 References

- [1] C. McBryde, "A Star Tracker Design for CubeSats", Master Thesis, The University of Texas at Austin, 2012.
- [2] e. a. Mohamed Nazree, "Modular CMOS Horizon Sensor for Small Satellite Attitude Determination and Control Subsystem," in *20th Annual AIAA/USU Conference on Small Satellites*.
- [3] C. C. Liebe, «Star Tracker for attitude determination,» *IEEE AES Systems Magazine*, vol. 10, n° 6, pp. 10-16, June 1995.
- [4] ECSS Secretariat, "ECSS-M-ST-10C Rev. 1," ECSS, Noordwijk, The Netherlands, 6 March 2009.
- [5] M. Román García, «GranaSAT client repository in GitHub,» [En línea]. Available: <https://github.com/M42/granasatClient>.
- [6] European Cooperation of Space Standardization ECSS: Space Engineering, "Star sensors terminology and performance specification," 15 Nov 2008.
- [7] The Imaging Source, *DMK 41BU02.H Monochrome Camera*, Charlotte, United States, 2013.
- [8] NXP B.V., "P82B715 I2C-bus extender," 9 November 2009. [Online]. Available: http://www.nxp.com/documents/data_sheet/P82B715.pdf. [Accessed 14 07 2014].
- [9] STMicroelectronics, "LSM303DLHC," April 2011. [Online]. Available: <http://www.adafruit.com/datasheets/LSM303DLHC.PDF>. [Accessed 28 05 2014].
- [10] "Software PWM Library," [Online]. Available: <https://projects.drogon.net/raspberry-pi/wiringpi/software-pwm-library/>.
- [11] Maxim integrated, *DS1621 Digital Thermometer and Thermostat*, San Jose, United States, 2005.



- [12] M. A.-S. J. K. E. PlacidO, "Thermal properties predictive model for insulating foams," vol. 46, no. 3, p. 219–231, January 2005.
- [13] R. Ravaglia, S. Donati, T. Cardona and G. P. Candini, *C.O.M.P.A.S.S. Student Experiment Documentation*, 2009.
- [14] H. Carreno-Luengo, J. Querol, G. Forte, R. Onrubia, R. Díez, F. Fabra and R. Jové, *TORMES Student Experiment Documentation*, 2013.
- [15] EuroLaunch, *BEXUS User Manual*, 2014.
- [16] A. García Montoro and M. Milla Peinado, "GranaSAT server repository in GitHub," [Online]. Available: <https://github.com/agarciamontoro/granasatServer>.
- [17] D. & N. B. Mortari, «k-vector range searching techniques,» de *AAS 00-128, AAS/AIAA Space Flight Mechanics Meeting*, January 2000.
- [18] ESA, «The Hipparcos and Tycho Catalogues,» *ESA SP-1200*, 1997.
- [19] I. The MathWorks, «MATLAB 2013b,» Natick, Massachusetts, United States..
- [20] UDS/CNRS, «VizieR Service,» [En línea]. Available: <http://vizier.u-strasbg.fr/viz-bin/VizieR>. [Último acceso: 20 December 2014].
- [21] J. P. W. K. G. B. J. H. W. F. a. A. M. Banguert, «User's Guide to NOVAS Version C3.1,» USNO, 2011.
- [22] USNO, «Naval Observatory Vector Astrometry Software (NOVAS) Version 3.1 Fortran, C, and Python Editions,» USNO, [En línea]. Available: http://aa.usno.navy.mil/software/novas/novas_info.php. [Último acceso: 20 December 2014].
- [23] M. P. S. S. I. a. L. M. Kolomenkin, «Geometric voting algorithm for star trackers.,» *Aerospace and Electronic Systems*, vol. 44, nº 2, pp. 441-456, 2008.
- [24] A. a. H. D. Wu, «Stellar inertial attitude determination for leo spacecraft.,» de *Decision and Control, 1996., Proceedings of the 35th IEEE Conference on Volume 3, pp. 3236–3244*, Kobe, 1996.

- [25] C. Liebe, « Star trackers for attitude determination,» *Aerospace and Electronic Systems*, vol. IEEE 10, nº 6, pp. 10-16, 1995.
- [26] C. Liebe, «Accuracy performance of star trackers - a tutorial,» *Aerospace and Electronic Systems*, vol. 2, nº IEEE Transactions on 38, p. 587–599, 2002.
- [27] R. W. H. van Bezoijen, «True-sky demonstration of an autonomous star tracker.,» *Tracking, and Pointing*, vol. 2221, nº VIII, p. 156–168, 1994.
- [28] F. L. Markley, «Attitude determination using vector observations and the singular,» *The Journal of the Astronautical Sciences* , vol. 3, nº 36, p. 245–258, 1988.
- [29] D. Umbach and . K. N. Jones, “A Few Methods for Fitting Circles to Data,” *IEEE Transactions on Instrumentation and Measurement*, vol. XX, no. Y.
- [30] T. Ozyagcilar, «Calibrating an eCompass in the Presence of Hard and Soft-Iron Interference,» 02 2012. [En línea]. Available: http://cache.freescale.com/files/sensors/doc/app_note/AN4246.pdf. [Último acceso: 06 07 2014].
- [31] T. Ozyagcilar, “Layout Recommendations for PCBs Using a Magnetometer Sensor,” 02 2012. [Online]. Available: http://cache.freescale.com/files/sensors/doc/app_note/AN4247.pdf. [Accessed 03 07 2014].
- [32] T. Ozyagcilar, “Implementing a Tilt-Compensated eCompass using Accelerometer and Magnetometer Sensors,” 01 2012. [Online]. Available: http://cache.freescale.com/files/sensors/doc/app_note/AN4248.pdf. [Accessed 06 07 2014].
- [33] Stellarium, “<http://www.stellarium.org/es/>,” [Online]. Available: <http://www.stellarium.org/es/>.
- [34] I. Kåsa, «A circle fitting procedure and its error analysis,» *IEEE Transactions on Instrumentation and Measurement*, vol. 25, 1976.



- [35] "IGRF," [Online]. Available: http://omniweb.gsfc.nasa.gov/vitmo/igrf_vitmo.html.
- [36] "LM2576/LM2576HV Series SIMPLE SWITCHER® 3A Step-Down Voltage Regulator," [Online]. Available: <http://www.ti.com/lit/ds/symlink/lm2576.pdf>.
- [37] F. Markley, "Attitude determination using vector observations and the singular value decomposition," *J. Astronaut. Sci.*, vol. 38, no. 3, pp. 245-258, 1988.
- [38] G. Wahba, «A Least Squares Estimate of Spacecraft Attitude,» *SIAM review*, vol. 7, n° 3, pp. 409-409, 1965.
- [39] M. J. Wilson, «Attitude Determination with magnetometers for gun-launched munitions,» ARL-TR-3209, 2004.
- [40] T. Bak, «Spacecraft Attitude Determination: A magnetometer approach,» Aalborg Universitetsforlag, Aalborg, 1999.
- [41] R. A. Langel, «The main geomagnetic field.,» de *Geomagnetism*, J.A. Jacobs, pp. 249-512.
- [42] D. Compston, «International Geomagnetic Reference Field (IGRF) Model. Matlab Central,» [En línea]. Available: <http://es.mathworks.com/matlabcentral/fileexchange/34388-international-geomagnetic-reference-field--igrf--model>. [Último acceso: 28 12 2014].
- [43] J. Heikkilä and O. Silvén, "Calibration procedure for short focal length off-the-shelf CCD cameras," in *Proc. 13th International Conference on Pattern Recognition*, Vienna, Austria, 1996.
- [44] J. Bouguet, "Camera Calibration Toolbox for MATLAB," 2 December 2013. [Online]. Available: http://www.vision.caltech.edu/bouguetj/calib_doc/.
- [45] Institute of Environmental Sciences and Technology, *MIL-STD-810G: Test Method Standard for Environmental Engineering Considerations and Laboratory Tests*.
- [46] Infineon Technologies AG, "ITS 4141N," 09 03 2006. [Online]. Available: <http://docs->



- europe.electrocomponents.com/webdocs/1074/0900766b810743a3.pdf.
[Accessed 19 07 2014].
- [47] R. Kandiyil, *Attitude Determination Software for Star Sensor*, Department of Robotics and Telematics, JMUV, 2009.
- [48] Minco, *Flexible heaters design guide*, Minneapolis, United States, 2007.
- [49] NXP Semiconductors ,
“http://www.nxp.com/documents/data_sheet/PCA9616.pdf,” 2014. [Online]. Available: http://www.nxp.com/documents/data_sheet/PCA9616.pdf. [Accessed 28 05 2014].
- [50] A. Harper, M. Ryschkewitsch, A. Obenschain and A. Day, "General Environmental Verification Standard," [Online]. Available: <https://standards.nasa.gov/documents/viewdoc/3315858/3315858>.
- [51] Maxim Integrated, "DS18B20 Programmable Resolution 1-Wire Digital Thermometer," 2008. [Online]. Available: <http://datasheets.maximintegrated.com/en/ds/DS18B20.pdf>. [Accessed 4 07 2014].
- [52] J. Bouguet, «Camera Calibration Toolbox for MATLAB,» [En línea].
- [53] Wilson, «Attitude Determination with magnetometers for gun-launched munitions,» *ARL*, 2004.



APPENDIX A – EXPERIMENT REVIEWS

- PDR
- CDR
- IPR
- EAR



REXUS / BEXUS

Experiment Preliminary Design Review

Flight: BX19

Payload Manager: tbd

Experiment: GranaSAT

Location: SSC, Esrange Space Center, Sweden

Date: 05 March 2014

1. Review Board members

Alexander Kinnaird, SSC

Olle Persson, SSC

Koen deBeule, ESA

Natacha Callens, ESA

Nora Newie, ESA

Lucio Scolamiero, ESA

Dieter Bischoff, ZARM

Simon Mawn, ZARM

2. Experiment Team members

Alejandro González Garrido

Manuel Milla Peinado

Teresa Lucía Aparicio Jiménez

Alejandro García Montoro

Victor Burgos González

Pedro Manuel Vallejo Muñoz

3. General Comments

- Presentation
 - Team should start with overall overviews
 - Good presentation & style
 - Don't stand in front of the screen
 - WBS slide could have just been shown, reading the slide is not so useful
- SED
 - Not PDR level yet
 - Pictures (esp. exploded views) were very good
 - Use bookmarks
 - It would be helpful if internal links actually link to this part (e.g. in ch 3.4 link to app B)
 - Use same font type (consistency)
 - Needs to be approved by someone who's not from team (e.g. professor)
 - Use hyphen '-' between version and issue in the filename and doc ID
 - Be sure to reference your sources (table 1-1)

4. Panel Comments and Recommendations

- Requirements and constraints (SED chapter 2)
 - Mission statement should be more precise
 - Primary objective needs to be clearer and more precise too (star tracker/horizon

- sensor + magnetometer).
 - “As lot as possible” not verifiable, needs numbers
 - Some requirements are too obvious
 - Performance requirements are under developed.
 - D3 & D16 are the same
 - most operations requirements are actually design requirements
 - a requirement on wavelength might be good - will the horizon sensor only operate in visible? IR is much better. 2 degs accuracy in visible could be difficult, especially in the polar regions.
 - for IR you might need lower angle requirement for horizon sensor
 - split D6, D15
 - Do you have a height and flight duration requirement?
 - Budget is a constraint
 - The objective of integration with a pico satellite does not seem to have fed into your requirements.
 - Design of the component for use in the satellite should at least restrain its mass and dimensions but also its thermal requirements.
 - Power of the ‘gondola’ should be clarified to be the power requirement of the experiment – and changed to Ah or Wh.
- Mechanics (SED chapter 4.2.1 & 4.4)
- Boom on top of gondola – there is E-Link which could disturb your system even more
 - Boom needs safety line
 - Upper box is prone to vibrations whilst on the pad, enhanced vibration testing is recommended.
 - Rather use rails than plates for attachment for gondola
 - Modal characterisation for boom mount important (make sure small vibrations don’t vibrate you enough to make images blurry)
 - Consider shock absorber etc. for camera mount on boom
 - Camera on boom can be ruined during landing
- Electronics and data management (SED chapter 4.2.2, 4.2.3, 4.5, 4.7, 4.9)
- How much power do use from gondola battery and when?
 - Power section is confusing – present total power budget
 - Expand on chapter (data budget, power budget, cables..), needs more specifics
 - Control loop for heater power missing (should have hysteresis)
- Thermal (SED chapter 4.2.4 & 4.6)
- Rather state results than the “how”
 - “How” can be in appendix if you think it’s important
 - Convection usually not an issue at BX
 - Double glass vacuum might escape – try to use dry gas
 - Make conservative assumptions for boundary conditions to be on save side
- Software (SED chapter 4.8)
- Very good flow charts (precise and focused)
 - Good choice of microcontroller and language
 - You need performance requirements for software to see if Raspberry pi can handle your image processing and storage
 - Team clarifies they use will not use C for GUI for ground software
 - Team clarifies they save measured data (raw) before processing too - good storage is needed
 - Parts of star tracker algorithm developed
 - Intermediary data (raw – before PADS/SADS s/w) should also be stored on board for reconstruction after flight/fault finding.
 - working image processing software due at CDR
 - Prototype software should be available at CDR, this is critical for your experiment.
- Verification and testing (SED chapter 5)
- You should verify all requirements

- Find a facility for testing asap
 - Wrong classification in verification matrix (often you can't verify by analysis)
 - Static load test for the beam is required.
 - According to your test plan D3 is verified by test (Test 4).
 - Vibration test should be driven on the end of the beam for upper box mounting
- Safety and risk analysis (SED chapter 3.5)
 - Severity 5 is harming people - be careful to use
 - A risk could be that you won't get full dark night
 - Include risk of detachment of upper box, mitigated by static load test, good clamp design and a safety cable
 - Include risk of condensation, temperature for electronics, project management risks (budget, communication, persons unavailable, schedule....)
 - TC.1 is not a severity 5.
 - TC.4 - have spare components.
 - MS.1 look at thermal control design concepts and control in more detail to avoid this.
 - MS.2 Watchdog!
 - MS.3 accept water damage, ensure safe data storage – water landing is unlikely.
 - VE.2 is a higher severity – flight batteries is always a safety risk – but these are not your batteries?
 - Stick to the format in the SED guidelines (PxS = very low to very high)
 - Main risk is that it is not dark enough for the star tracker to work!
- Launch and operations (SED chapter 6)
 - It will be hard to calibrate magnetic sensors (esp. due to material of Launch Pad)
 - Is it possible to have a recalibration in flight?
 - Make sure equipment is not fragile; and fragile components are labelled, covered etc.
 - Large ore deposits might influence magnetic sensors
 - Make sure LED can be seen if on or off right before launch (recessed or shaded, consider visibility during night launch)
 - RBF/lens cover on the baffle to avoid dust/dirt/finger prints?
 - No late access activities that far
 - BX Payload Manager can give team warning before gondola cut-off
 - Team to consider turning experiment on while on ground
 - Have a look at the IRGF models and anomalies for around Northern Sweden – much information available on the web.
 - RBF?
 - Safety risk is detachment of the beam/upper box is a risk, mitigated by static load test, good clamp design and a safety cable
- Organisation, project planning & outreach (SED chapters 3.1, 3.2, 3.3 & 3.4)
 - Sometimes verbs missing (design, assemble, test...) in schedule
 - Finalise sensors before/after exams
 - Check about duration (60 weeks, 5 weeks) of activities
 - Schedule and test plan reflect the same timeline
 - You need a replacement for each WPs
 - How much budget you need and who sponsors it/what, and how much?
 - Budget seems optimistic, also include source of funding
 - Include all organizers and logos on website
 - Figures in appendix wrongly labelled
 - Provide a phone number for the student team as well.
 - Website link does not work.
 - Provide the link for the twitter, Facebook and google+ accounts in the main document.

5. Internal Panel Discussion

- Summary of main actions for the experiment team
 - Need performance requirements for software to see if raspberry pi can handle tasks
 - More details in SED

- PDR Result: conditional pass
- Next SED version due
v1.2 on March 24th



BEXUS

Experiment Critical Design Review

Flight: BX19

Payload Manager: Alexander Kinnaird

Experiment: GranaSAT

Location: ESTEC, Noordwijk, the Netherlands

Date: May 7th 2014

1. Review Board Members

Alex Kinnaird, SSC

Sylvain Vey, ESA

Gunnar Andersson, SSC

Piero Galeone, ESA

Simon Mawn, ZARM

Antonio de Luca, ESA

Dieter Bischoff, ZARM

Natacha Callens, ESA

Julia Grünhage, ZARM

Nora Newie, ESA

Document Review only:

Lucio Scolamiero, ESA

Koen Debeule, ESA

2. Experiment Team Members

Víctor Burgos González

Manuel Milla Peinado

Alejandro García Montoro

Eva Gamundi Alcaide

Teresa L. Aparicio Jiménez

3. General Comments

- Presentation
 - Perfect timing
 - Very clear presentation
 - Good that you showed us what happened between now and SED submission
 - We like that you tell us where you need tips
- SED
 - Use file naming convention (also for other documents)
 - Include bookmark
 - Include PDR report in appendix
 - Some formatting problems (font size, headers, etc)
 - Keep tables and figures with relevant sections, and keep table captions updated (table 4-17)

4. Panel Comments and Recommendations

- Requirements and constraints (SED chapter 2)
 - Still needs some improvements to make
 - Don't use word "gondola", when you refer to your experiment
 - Some performance requirements are design requirements
 - Missing link between functional to performance requirements (some key performance requirement, e.g. accuracy of the orientation measurement using each instrument, read out rate of the orientation measurement etc)
 - Requirements for autonomy needed (operational)
 - Mission modes need to be derived from requirements
 - P3 is standard, it cannot be a performance
 - P4 difficult to achieve – really needed as this?

- P5 is not performance, they do not control this ... is up to the gondola
 - P6 unless this experiment is all about power, this is a design requirement
 - P8 and P9 are operational
 - P.9 is also confusing, time frame for what?
 - D.7 “vacuum” shall be replaced by “low pressure environment”, while radiation and conduction become much more dominant in at float convection is still a factor, especially on ascent
 - “highest height” = “float altitude”
 - The entire experiment shall be designed to operate in the low pressure, temperature and vibration environment of the BEXUS flight (also transport, preparation and launch)
- Mechanics (SED chapter 4.2.1 & 4.4)
 - Gondola interface is good
 - Upper box 400mm distance from gondola – maybe add an additional Bosh junction element to make sure you have 400mm from gondola
 - Profiles for camera boom are good
 - Electrostatic behaviour of polystyrene should be considered, electronics must not touch it directly, but it's good otherwise (esp. for shock prevention)
 - Team uses 4 Bosh-elements because of recommendation by provider
 - Use open-end covers for Bosh profiles
 - Mechanical simulation looks good
 - Flawless CAD & manufacturing drawings
 - Rethink if accurate dimensions as 39.59, 36.69 or 57.71 are really necessary → production costs will very be high
 - Requirement that this rails where you attach is cleaned
 - Footprint doesn't match dimensions - footprint should include the mounting rails
 - Team bought camera glass – more detail needed. Be careful about the possibility of grazing angle light and internal reflection in thick glass
 - Shock might be a problem
 - Closure of box seems quite complicated, make sure you can lock the box properly (think of landing)
 - Clarify if upper box is on the outside or the inside side of the boom (on top gondola) – would be better for you to be at the outside – make this a requirement and be consistent in document
 - Your vibration requirements are too strict, the standard you use are too high and are not applicable for balloons - use spectrum for wheeled transportation (e.g. 8110g military standard – see “environmental testing” presentation) – re-do simulation
 - You state that the inner box mass is 4841.27kg...
 - The mechanical design of the upper box and mount seems particularly susceptible to vibration, and possible damage through vibration. A mechanical proto-flight test might be done soon to quality the design. An FEA might be too complicated and not correctly model the random vibration
 - Include modal characterisation of the camera on top of the boom as agreed at PDR – make sure you won't get of blurry images
- Electronics and data management (SED chapter 4.2.2, 4.2.3, 4.5, 4.7, 4.9)
 - Don't fly the 20x5 fuses (bad vibrations and low pressure performance)
 - Melting fuses have very high tolerances and you cannot reset them, use current limiting switches instead (e.g. Infineon ITS414x series)
 - Don't fuse your main line (fuse thermal control circuit etc.)
 - Distribution of 3.3V via a cable from the inner to the outer box is badly designed and highly undesirable because of low tolerances on the 3.3V and possibility to pick up interference from other systems- distribute a higher voltage and regulate it to 3.3V in the outer box. Use the 28V for instance
 - Use of DS1621 as a remote device connected by more than 1m cable is not recommended - SDA & SCL are low level signals, the should be distributed as differential pairs. This is not so easy for the SDA-signal since it is bi-directional - recommendation is to use a different solution (PT100/PT1000 sensor or AD592)
 - The PWM signal in the cable as power and sensor control signals will disturb the low level signal - recommended to use a separate twisted pair for the PWM if the function cannot be moved to the outer box altogether (The DS1621 has a thermostat mode)
 - It is also recommended to use twisted pair to distribute 28V power, since both your own

- experiment and TORMES will not like the magnetic field generated by the proposed solution
- o DA1620 is communication with 2 low level signal lines – this is not a good solution
- o consider putting all thermal protection in upper box so avoid additional cables (which are additional disturbances)
- o Re-design communication between upper box and main experiment
- o Timeline is quite generic - point out working modes of experiment (when, what, for how long...)
- o Compare energy you need with battery capacity (include power losses due to efficiency)
- o Power consumption timeline could be better explained with an annotated graph (power consumption vs. time).
- o Power budget: efficiency of converters unclear or missing
- o Buy expensive 32 GB SD cards for reliability reasons, and test extensively
- o How you want to distract and store data from SD card – have a clear concept
- o Grounding diagram needs to be provided (star-point grounds are recommended)
- o Maybe additional wire (could be safety line) for grounding of upper box is needed due to aluminium structure of boom
- o p127: regulator with cooling fin - in BX the fin does not do much
- Thermal (SED chapter 4.2.4 & 4.6)
 - o Patch heater: problem if not glued properly they tend to overheat and can burn
 - o Maybe RICARD or Minco heaters are alternative as they are well characterised
 - o Test your heater well, and well in advance
 - o Split into 3 heaters and have 1 flat on top, 1 left and 1 right and glue very thoroughly! (chance is won't work)
 - o What temperature sensors are you using? Put in correct SED chapter!
 - o Upper PBC with temperature sensor is close to camera
 - o Don't put temperature sensor too close to heater – you might get wrong reading and then heater turns off and on at wrong times
 - o Decouple sensor and heater (talk with your mentor!)
 - o Team is working on thermal simulation
 - o Temperature limitation of raspberry pi? – team clarified it is well enough insulated – give calculations (in appendix!)
 - o Condensation on glass possible problem – team will use silica bags and de-humidifier at launch campaign
 - o Behaviour of silica bags in vacuum and low temperatures unclear– test!
 - o External condensation is more critical, silica bags etc. won't help for this
 - o How will your performances be degraded by condensation
 - o Make sure you still have good quality of pictures at low temperatures (stripes on images of cold temperatures) – test if -5C are still good
- Software (SED chapter 4.8)
 - o Very good software overview – modularization very clear
 - o Team will not process magnetic data on board real-time
 - o Team will check if magnetometer works as ADS post-flight
 - o Team clarified they store raw images for post-processing
 - o Fully automatic experiment, only manual command is a possible shut-down
 - o Raspberry pi single board data handling tests been performed – data acquisition up to 3Hz
 - o REXUS16 team HORACE also performs similar horizon measurements, they use the same horizon tracking software – get in touch if you have problems with it
- Verification and testing (SED chapter 5)
 - o All requirements must be verified
 - o Don't do that much testing - better review and analysis before (some requirements maybe only R&A (e.g. D5, P2...), also for time and budget reasons)
 - o For flight requirements a review (of documentation) is better than analysis
 - o F1 and F2 are only partly verified by Test 1 (only software element)
 - o Functional test of the camera is required, probably with a mock or real night image
 - o T4 and T 11 are the same test
 - o Random vibration test is missing
 - o Use recommended military standard for wheeled vehicles (vibration test)
 - o How do you test shocks? Don't expose your experiment to unknown shocks (during testing). Calibrate your own test setup, so that you don't over-test

- At least one thermal-vacuum test should be used to verify the heater control
- Safety and risk analysis (SED chapter 3.5)
 - Delay of shipping is a risk
 - Risks in schedule are missing, e.g. delays, late for testing etc.
 - Be sure to include the 'little' things in your vacuum and thermal tests (such as the silica bags)
- Launch and operations (SED chapter 6)
 - Experiment summary table in chapter 4 and 6 must be same
 - Round your mass
 - Clear float altitude and duration to be stated in SED – team clarified above 11km and more than 1h
 - State how long you need float phase in darkness
 - Give us an example for 7th of October 2014 of what is night for you (timeframe)
 - Team clarified completely dark night not needed
 - Consider how aurora can influence your experiment
 - Requirement P8 needs clarification
 - Bring things kapton tape, insulating tape, thermal paste etc. yourself to launch campaign
 - Task T3 seems like it should come first. You will have a pre-allocated workspace.
 - Timeline – team plans to turn off by tele-command, clarify that recovery team turning off is only in case of E-Link loss
 - Experiment should be turned on either before pickup (i.e. at T-4hours) or after pickup at T2.5hours)
 - Add gondola pickup, sweet spot and line up to your timeline
 - Last access to experiment is during the sweet spot, before line up
 - State of you need notice before balloon cut-down and how much
 - Diagram 1 and 2 are superfluous, confusing and probably in the wrong place
 - A recovery sheet will be needed if the recovery team is to switch off your experiment
 - You should add a requirement in chapter 6 that the gondola upright on which the profile is fitted shall be cleaned of all materials (such as Velcro) before fitting
- Organisation, project planning & outreach (SED chapters 3.1, 3.2, 3.3 & 3.4)
 - Team members who finish studying this year will study until September (so stay part of the team)
 - WP6 is missing assembly and integration
 - 3 new team members – appreciated that you told ESA and included them on Joinspace.org
 - Make sure you have very good test plan and schedule as test period overlaps with exams
 - Caption table of travelling
 - Name event instead of saying place, also state date
 - You don't need to provide the travel cost as detailed – we mainly need to know who sponsors what and for what amount
 - Plans for future travel?
 - Describe logo in outreach part
 - Website: Sponsorship link to ZARM goes to SSC – to be changed

5. Internal Panel Discussion

- Summary of main actions for the experiment team
 - Electrical interface between the two boxes needs to be reconsidered
 - Thermal calculations to be provided
 - Test silica bags in (thermal-)vacuum
 - Further investigate condensation problem (contact SSC for further information about former BX flights)
 - Include modal characterisation of the camera on top of the boom
- CDR Result: conditional pass
- **SEDv2.1 version due May 28th**



BEXUS

Experiment Integration Progress Review



Page 1

1. REVIEW

Flight: BEXUS 19

Experiment: GranaSAT

Review location: Facultad de Ciencias, Granada

Date: 6th August 2014

Review Board Members

Alex Kinnaird (SSC)

Sylvain Vey (ESA)

Experiment Team Members

| | |
|----------------------------|-------------------------------|
| Emilio José Martínez Pérez | Teresa Lucía Aparicio Jiménez |
| Víctor Burgos González | Eva Gamundi Alcaide |
| Emilio García Blanco | Laura García Gámez |
| Alejandro García Montoro | Ramssel Lendínez Extremera |
| Manuel Milla Peinado | Carlos Manuel Morales Pérez |
| Pedro Manuel Vallejo Muñoz | |

2. GENERAL COMMENTS

2.1. Presentation

- The team gave a very good presentation outlining their current status and previous problems.
- Some text was too small and difficult to read.
- Better outlining of predicted problems/support areas would have been appreciated.

2.2. SED

- In general the SED is a reasonable standard for IPR.
- The document ID on the cover page shall match the filename (v3-0).
- The translation is generally very good.
- The team shall include copies of the review reports in the SED (not just link to other documents).
- Sensible vs. sensitive.
- In general the team should avoid referring to components only by their product code.



BEXUS

Experiment Integration Progress Review



Page 2

- Legends shall be included with graphs

2.3. Hardware

- The team presented near complete flight hardware.
 - The team lack the components for attaching the boom to the gondola.
 - The team did not present the finalised cabling between the top box and bottom box.
 - The team did not present the finalised L profiles for gondola attachment of the lower box.
- Nearly all hardware is 'homemade' which leads to an increased chance of manufacturing error, correct and thorough testing is therefore critical for this team more than most.

3. PHOTOGRAPHS



Figure 1: Upper Box



Figure 2: Upper box and boom



BEXUS

Experiment Integration Progress Review



Page 3

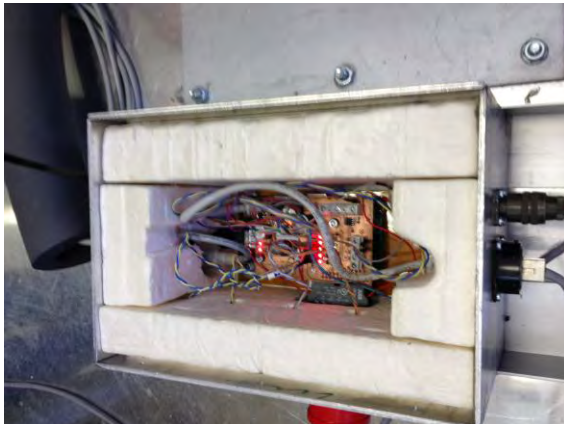


Figure 3: Lower Box

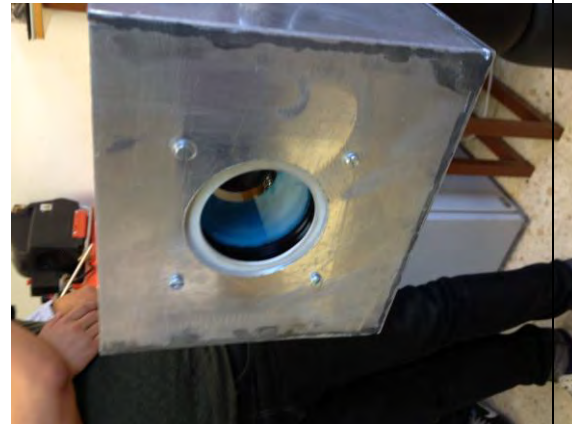


Figure 4: Camera face

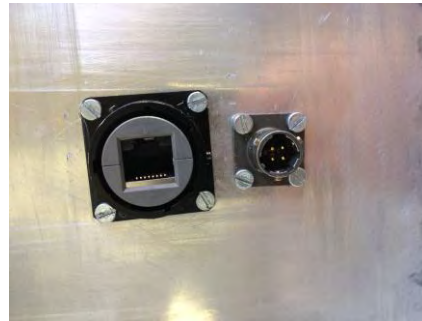


Figure 5: E-link (incorrect) and power connector

4. REVIEW BOARD COMMENTS AND RECOMMENDATIONS

4.1. Science

- Minor comment: In the SED the team state that a sun sensor can determine only 2 degrees of freedom, but techniques allow sun sensors to determine 3 degrees of freedom.
- Minor comment: The team may enhance their chapter 1 with a discussion relating to the preferred use of Infrared for the horizon sensor and why this is not an option for them.
- **The team are unsure about whether to include the second lens/filter at the end of their baffle. The team should look at the trade-off between the workload, and the pro-cons of the lens and make a decision ASAP. The lenses shall be in their finalised configuration before the system testing campaign.**
- The team confirmed they can deal with off-angle (skew) in their top box mounting.

4.2. Requirements and constraints (SED chapter 2)

- Requirements have been generally well improved since PDR.
- Requirements should be included for the interface between the top and bottom box.



BEXUS

Experiment Integration Progress Review



Page 4

- Some confusion between requirements P.1 and P.3.
- “Range of Orientation” should be replaced with “Accuracy”.
- Flight requirements may be included in your operational requirements, but shall definitely be included in chapter 6.

4.3. Mechanics (SED chapter 4.2.1 & 4.4)

- The team state their mechanical design and manufacture is a 100% complete
 - The team need to receive their gondola attachment components.
 - The team need to finalise the cable routing between the two boxes.
 - The team need to receive their L profiles for gondola attachment of the lower box.
- The team have simplified their box closure since CDR. They may further consider an analysis of this new lid, or carefully monitor its behaviour under vibration during the test.
- The team should perform a basic analysis to determine the number of turns or torque required for the gondola attachment components to avoid stressing the plates.
- The team should include rubber or high friction polymer plates into their gondola attachment components.
- In general rubber or high friction polymer plates should be used between the metal to metal mating on the top box to boom connection.
- A modal characterisation of the camera/boom system has not been performed. Completion of this analysis should now be a considered a ‘nice to have’.
- The dimensions of the upper box should be included in chapter 4.
- In general mechanical fixations are not optimised (little/poor consideration in number of bolts used/bolt size and position). If possible within the resource/time constraints these should be improved.
- The supporting bolts for both sets of PCBs need to be looked at. Especially the large M5 bolts used in the upper box PCB which are too close to the edge and present a significant point of stress concentration and probable fracture under vibrations and/or shock. The team may look into PCB mounts/standoffs (plastic).
- Nyloc nuts shall be used on the final assembly. Threadlocker and or Loctite should be used for smaller internal bolts.
- **The T-bolts presented by the team for gondola fixation are not sufficient. ESRANGE shall provide flight t-bolts for the team.**

4.4. Electronics and data management (SED chapter 4.2.2, 4.2.3, 4.5 & 4.7)

- The team state their electrical design and manufacture is 100% complete.
 - **The team need to ‘clean up’ the harnessing in both boxes, including cable routing, pairing/twisting, labelling and connectors.**



BEXUS

Experiment Integration Progress Review



Page 5

- The team need to finalise the cable between both boxes, including re-addressing the connector soldering/crimping of the amphenol connector (forum research).
- The team have improved the connection between the top box and bottom box using an I2C extender unit in both boxes. They have yet to finalise the cable and its routing. They may consider routing the cable through the Rexroth profile behind a plastic shield. Any shielding used on this cable shall be included in the thermal vacuum test.
- The team may further analyse their energy budget by including the expected State of Charge (SoC) or Depth of Discharge of Discharge (DoD) against experiment time ('nice to have').
- The team make all their PCBs in house – thorough visual inspection before and after vibration/shock testing is key.
- **Inspection and test during the review showed that the experiment was grounding to the chassis (both in the upper and lower box). This is not the intended grounding scheme of the team, and it may affect the sensitivity of their thermal sensor. It's suspected this ground loop is created through the poor fixation of the upper box PCB, but the team shall investigate and solve this problem ASAP.**
- **The E-link connector shall be switched to a code-A as per the BEXUS user manual.**

4.5. Thermal (SED chapter 4.2.4 & 4.6)

- The team state their thermal design and manufacture is 100% complete.
 - Much of the 'design' will not be complete until verified through test.
- The team have removed the silica bags from their design and as such are no longer required to test them. In any case they would have preferred silica patches to the bags.
- If the team decide to reintroduce their heater then a proper thermal control algorithm is required (with lower AND upper bounds).
- Further investigation may be required to deal with possible condensation issues. The team should contact other BEXUS teams and SSC to ask if this has been a problem in the past and how it has been resolved. The team provided an analysis of temperature vs. dew point which suggested that condensation should not be a problem.
- Initial thermal analysis shows that a hot spot may exist on the camera, and that the cold case is not an issue. However the team have not focused further analysis on the hot case.
- **Inspection of the running experiment showed potential hot spots in/around the processor and Ethernet connector – the team should have good confidence (through test and/or analysis) that these are not going to a problem.**
- The team shall work closely with their mentor over the coming weeks to properly complete their thermal analysis including a sensitivity analysis on their input



BEXUS

Experiment Integration Progress Review



Page 6

parameters, not least the ambient temperature. Inevitably the analysis is only proven following test.

- The team shall work with their mentor to determine a good thermal test procedure.
- The team shall contact the thermal-vacuum chamber owner/operator to determine the interfaces, specifically how many thermo-couples they can place on their experiment.

4.6. Software (SED chapter 4.8)

- The team state that their software is 80% complete.
 - The team need to further optimise both the star tracker and horizon sensor software.
- The team have significantly improved their line fit for the horizon sensor using a modified least squares approach.
- **A timeout to auto loop shall be included if the team step in to set star tracker or horizon sensor manually.**

4.7. Verification and testing (SED chapter 5)

- The team state their verification and testing is 40% complete.
 - The team lack their major system tests.
- Requirement O.3 (autonomous operation) should be verified through test.
- A ‘quick look’ method for determining test completion status would be appreciated (e.g. colour coding).
- The team plan to perform some kind of shock test, this shall be carefully planned and the shock environment properly characterised to ensure that this is not an intentionally destructive test.
- **A full functional test (flight simulation) shall be included (test 17).** Where possible this shall simulate partial failures (such as voltage drops and communication drop outs).
- The team shall speak to the vacuum chamber owner/operator about the insulation and whether it’s safe to test in their chamber – they may also speak to former teams (TORMES?).

4.8. Safety and risk analysis (SED chapter 3.4)

- **If the optical lens remains as a pressure vessel it shall be tested to 1.2x the maximum expected delta pressure it will undergo during flight. It shall be written as a safety risk in chapter 6.**
- TC.1 (camera not working), the severity should be raised to a 4 (experiment failure), but after testing you shall aim to reduce to probability to an A or B, and hence the risk to very low. The camera remains an unfortunate potential single point failure.
- The safety cable and fixation points demonstrated are sufficient.



BEXUS

Experiment Integration Progress Review



Page 7

4.9. Launch and operations (SED chapter 6)

- The team agreed that their boom, rear (gondola facing), and bottom face of the upper box may be coated in neoprene by the TORMES 2.0 team.
- The team confirmed they are OK with the current accommodation plan. They may consider sliding their experiment on their L beams in the direction of their E-Link and power connector (further into the gondola) to avoid accidental pressing of their 'power off' button.
- The team shall add the requirement that the vertical gondola strut on which they mount their boom is properly refurbished – they shall check this is requirement is also translated to the final version of the Campaign Requirements Plan.
- The team shall ensure the requirement for a modified light beacon is include in the final CRP.
- The team have a throttleable (by ground) data limit, they would ideally like to increase their data rate, this shall be handled at campaign in conjunction with the other experiments.
- The calibration of the magnetometer shall be done during the individual experiment preparation time at the start of the campaign – this should be performed on the balloon pad.
- The team shall not rely on the very course attitude information of the EBASS system. They shall cross-correlate their results between their own sensors. Further correlation may be available through careful interpretation of TORMES 2.0's limb looking antenna. The team may speak to TORMES with regards to this (they may need to log satellite data and/or carefully measure the location of the antenna more than is required for their own experiment).
- All LEDs, connectors and switches/buttons chare be clearly labelled.
- The team confirmed they only plan to send 4 people to the campaign – this shall include at least the ground station operator, the electronics engineer and the software engineer.
- The team confirmed they have read the ESRANGE User manual and ESRANGE Safety Manual and they have no questions, and believe they are fully compliant.
- In general the team shall use procedure checklists and verifiable procedures during their systems testing, launch campaign and data recovery.
- The team shall determine a safe data recovery process (bit-by-bit back up) for their SD card as data recovery is experiment critical.
- The team will use a Raspberry PI specific micro-SD card convertor, this shall be glued in place before flight.
- The team shall acquire an appropriate shipping container.

4.10. Organisation, project planning & outreach (SED chapters 3.1, 3.2 & 3.3)

- The team states that their main problems exist (and existed to a higher degree) within organisation and project management namely:



BEXUS

Experiment Integration Progress Review



Page 8

- Delayed delivery of components.
- Lack of support for the University departments during the holidays
- Man power due to illness, jobs and personal reasons.
- English!
- The team have sponsorship from Cocorocó which gives them a good working space in the city.
- The team are currently funding the experiment from their own funds, but expect reimbursement from the University at the end of the year.
- The team do not budget for additional attendees at the campaign or at the results symposium.
- Emilio Martínez is the new team leader with strong support from other team members in management areas. The team seem to have a good dynamic.
- A percentage completion column shall be shown in the Gantt chart.
- In general the Work Breakdown Structure and Gantt chart are very good.
- The team have recruited a marketing student who is working on a wider marketing campaign for the experiment, with a specific aim to provide outreach to the non-scientific/engineering community,
- The schedule was determined with the team during the review as follows:

| EXAMS | | | | | |
|-------------------------------------|--------------------------------|---|--|--|---------------------|
| Week 33 | Week 34 | Week 35 | Week 36 | Week 37 | Week 38 |
| Completion of Star Tracker Software | | | Delivery of gondola attachment components. | | EAR |
| Completion of magnetometer software | | | Tests 12 and 16 (shock and vibration) | | Experiment Shipping |
| | Test1 (star tracker software) | Test 14 (magnetic disturbances (may not be needed)) | | Tests 9 and 13 (temperature sensor and thermal-vacuum) | |
| | Test 3 (magnetometer software) | Test 17 (full functional test) | | | |

- Due to the late EAR and tight schedule the team have elected to carry their experiment with them on the flight.
- The schedule does not leave much margin, and the team face critical testing late in their project, it is critical that previous tests are not invalidated by modifications required due to test failures – test planning is critical!



BEXUS

Experiment Integration Progress Review



Page 9

4.11. End-to-end Test

- The experiment was demonstrated to nearly fully function through the ground station, with a mock star scene and inputted horizon. No dynamic behaviour was tested. The magnetometer/accelerometer GUI was not operational.

5. FINAL REMARKS

5.1. Summary of main actions for the experiment team

- Properly complete the thermal analysis and determine a good test produce, clarify tests 5 and 13. To be done in coordination with your mentor.
- Solve the grounding issue.
- Make a decision on the inclusion/removal of the second lens/filter.
- Clarify use of XPS in the vacuum chamber.
- Receive the gondola attachment components.
- Finalise the cabling between the two boxes.
- Clean up internal harnessing.
- Stick the schedule determined during the review – finalise software, and complete system testing.

5.2. Summary of main actions for the organisers

- The T-bolts presented by the team for gondola fixation are not sufficient. ESRANGE shall provide flight t-bolts for the team.

5.3. IPR Result: **conditional pass**

5.4. Next SED version due **17 August 2014**



BEXUS

Experiment Integration Progress Review



Page 10

6. INTEGRATION PROGRESS REVIEW – IPR

Experiment documentation must be submitted at least five working days (the exact date will be announced) before the review (SED version 3). The input for the Campaign / Flight Requirement Plans should be updated if applicable. The IPR will generally take place at the location of the students' university, normally with the visit of one expert.

The experiment should have reached a certain status before performing the IPR:

- The experiment design should be completely frozen
- The majority of the hardware should have been fabricated
- Flight models of any PCB should have been produced or should be in production
- The majority of the software should be functional
- The majority of the verification and testing phase should have been completed

The experiment should be ready for service system simulator testing (requiring experiment hardware, electronics, software and ground segment to be at development level as minimum)

Content of IPR:

- General assessment of experiment status
- Photographic documentation of experiment integration status, with comments were necessary
- Discussion of any open design decisions if applicable
- Discussion of review items still to be closed
- Discussion of potential or newly identified review item discrepancies
- Discussion of components or material still to be ordered or received by the team
- Clarification of any technical queries directed towards the visiting expert
- Communication and functional testing (Service system simulator testing and E-link testing for REXUS and BEXUS respectively)



BEXUS

Experiment Acceptance Review



Page 1

1. REVIEW

Flight: BEXUS 19

Experiment: Granasat

Review location: University of Granada, Granada

Date: 17th of September 2014

Review Board Members

Alex Kinnaird (SSC, Science Services Division, Launch and Operations)

Experiment Team Members

| | |
|----------------------------|---------------------------------------|
| Emilio José Martínez Pérez | Víctor Burgos González |
| Manuel Milla Peinado | Alejandro García Montoro |
| Emilio García Blanco | <i>Professor Andrés Roldán Aranda</i> |

2. GENERAL COMMENTS

2.1. Presentation

- The team gave a good overall presentation covering all the required points including expected outcomes of the review.

2.2. SED

- DOCID and file name should end DDMMYY
- The mass updates in the SED delivery email shall be included in chapter 4 (table 4-10, page 69) as well as chapter 6.
- The picture of Professor Roldan Adanda is misaligned.
- Test 9 (temperature) references the magnetometer test in the results – typo.
- Where possible photos of manufactured parts shall be included.
- SED 5 will be delivered around 3 months after the campaign, with the main updates (other than those required from this review) being in chapters 3 and 7.
- The results symposium will take place in Tromso in June 2015, more information can be found at <http://pac.spaceflight.esa.int/>

2.3. Hardware

- All flight hardware was presented except for the upper box PCB which is currently being manufactured with a new thermal sensor (see electronics).



BEXUS

Experiment Acceptance Review



Page 2

3. PHOTOGRAPHS



Figure 1: Boom fixation.



Figure 2: Complete experiment

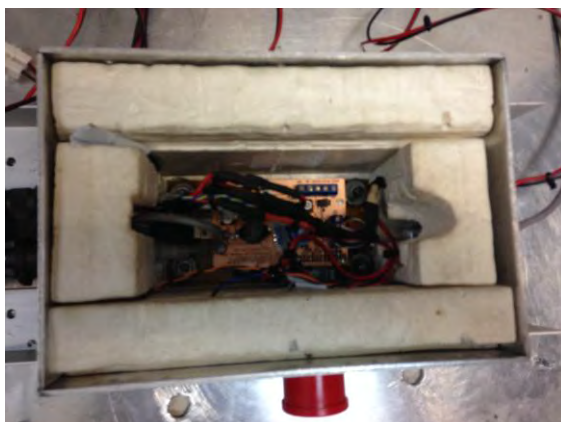


Figure 3: Lower box



Figure 4: Lower box with 'old' PCB

4. REVIEW BOARD COMMENTS AND RECOMMENDATIONS

4.1. Science

- The horizon sensor has now been verified and optimised within the scope of the experiment.
- The team shall state clearly all the attitude measurements they have and how they can be cross correlated.
- The team shall verify that the performance requirements of the star tracker are achievable and verifiable



BEXUS

Experiment Acceptance Review



Page 3

- The team shall also cross correlate their attitude measurements with those of the TORMES 2.0 ADS system.
 - The team must timestamp their data with real time (or at least know the RT equivalent for their Pi T0) in order to correlate with the TORMES 2.0 GPS time stamped data.
 - The team may also use the time, TORMES 2.0 GPS location, and sun location (from their image) to achieve coarse attitude determination.

4.2. Requirements and constraints (SED chapter 2)

- Requirements should not be renumbered, they may be re-worded with notes, retired or new requirements added.

4.3. Mechanics (SED chapter 4.2.1 & 4.4)

- The gondola attachment clamps are now present and seem very strong.
 - A rubber layer has been added between the clamps and the gondola and between the beam and the gondola.
 - The team shall check the data sheets for this rubber to check its durability under extreme cold and low pressure.
- A routed plastic pipe with thick thermal insulation has now been finalised for the cable routing between the top and the bottom box. The option of routing along the Bosch profile has been discarded.
 - Final fixation of the insulation shall be made at campaign (cable ties).
 - Final fixation of the inner box end of the insulation shall be made at campaign (cable tie?).
 - Further thermal insulation may be added into the top of the pipe (from inside the upper box) to aid in insulation and add stiffness to the cables.
- Good consideration and planning is still needed for final fixation (locking bolts, loctite, glue etc.), in particular the order, but the team has made a good start.
- The USB connectors are generally not fixed and it is not easy to fix them with glue, the best solution is to ensure the cable is pushing the connector rather than pulling it.
- A further 90 degree connector should be added on the beam to sit on top of the gondola.
- Cables shall be restrained in, or attached to, the XPS where possible.
- The plastic cap shall be modified and added to the bottom of the beam.

4.4. Electronics and data management (SED chapter 4.2.2, 4.2.3, 4.5 & 4.7)

- The incorrect crimping of the power Amphenol connector has been corrected.
- The incorrect coding of the E-link connector has been corrected.



BEXUS

Experiment Acceptance Review



Page 4

- The grounding issue has been corrected with the isolation of the PCB ground from the PCB supports with plastic washers.
- A time out of 15 minutes has been added to send the experiment back to automatic mode when in manual mode if no new manual mode request is sent.
- The team have produced a battery SoC (State of Charge) timeline which is very good and gives clear indication of the power margin.
- **The upper box PCB is been replaced with a new model with a new thermal sensor.**
 - The team should remember this PCB has not undergone the same qualification as the old PCB, and should, where possible, requalify with vibration testing and vacuum testing, at the very least thorough functional testing and a thorough visual inspection shall be carried out before the TVAC test.

4.5. Thermal (SED chapter 4.2.4 & 4.6)

- Due to the removal of the ‘second lens’ most issues of condensation are redundant, but a final test remains at TVAC. The team shall check their images as well as observing their lens through the observation window of the chamber during the test.
- The patch heater is now no longer an option and all reference shall be removed.
- **Prior to the TVAC testing, test 9 (thermal sensor calibration shall be complete), this can be done in the climatic chamber.**
- The ‘hot case’ problem still exists. The thermal analysis suggests a hot point on the camera of up to 80°C, the camera maximum operation temperature (manufacturer stated) is 45°C, it’s suspected that convective cooling has so far saved the team from a camera overheat. Vacuum testing here will be critical.
 - The team shall go the TVAC test with ideas in mind about what to do in case of camera overheating: thermal bridge, reduction in insulation, thermal gate etc.
 - The phrase in the SED ‘measures to avoid overheating will be taken’ shall be removed and replaced with something useful.

Thermal Vacuum test procedure

- The experiment shall be fully functional throughout the test.
- Pump down to 5 mbar with sufficient hold intervals, maintaining temperature at ambient. This is the worst case for your ‘hot spot’.
- Lower temperature with holds at chamber temperatures of critical interest: 0°C (electronics limits), -40°C (hot case float), -50°C (nominal float), -80°C (cold case float).
- Throughout the test the camera shall point out of the chamber observation window and the team shall visually monitor for condensation.
- Both the upper and inner box shall be tested simultaneously. Where possible:



BEXUS

Experiment Acceptance Review



Page 5

- the two boxes should not be in thermal contact;
- all 'free' (i.e. not covered surfaces on the gondola) shall be 'free' in the test.
- The two boxes shall not radiate heat towards one another.
- Extra calibrated thermal sensors shall be added to strategic points of interest.
- The team shall immediately contact their mentor to discuss to the TVAC test procedure.

4.6. Software (SED chapter 4.8)

- Small updates are being made in 'nice to have areas' such as image compression. The team have set a sensible internal deadline of the 24th of September for this work.
- The experiment shall store all raw data on board, only using compression for downlink.
- If possible the data rate available to the team may be increased during the campaign dependant on the other experiments and 'real' E-link limitations.

4.7. Verification and testing (SED chapter 5)

- In general the SED gives a good and clear overview of the tests.
- The team have completed one successful full flight simulation.
- Vibration testing was successfully completed, the test report shall be included in the SED and the following requirements marked as verified: D.14 and D.17. The video is a good example for other teams on how this test might be performed.
- The magnetometer test (test 3) is now complete, after the lab was opened following the summer. The report shall be included in the SED and the following requirements marked as verified: F.3, P.3.
- Test 9 (calibration of the thermal sensors) shall be completed ASAP, and requirements S.4 verified. This can be done at the University's climatic chamber.
- The TVAC test (see thermal) shall complete tests 5 and 12 and verify D.7, D.8, D.9 (shall be changed to T), D.12 (partially redundant as the patch heater has been removed), and D.12 (critical).
- Requirements D.2 (mechanical shock) and D.4 (mechanical harm to the gondola) have been verified by analysis and shall be marked as such.
- D.4 and D.5 are partially verified by the CRP, but will be fully verified by the gondola interference tests at the campaign (add T).
- O.6 (profile mounting) will be verified at campaign.

4.8. Safety and risk analysis (SED chapter 3.4)



BEXUS

Experiment Acceptance Review



Page 6

- Risk TC.9 (detachment of the upper box) should now be further mitigated as the vibration and static load test have been completed, and the safety cable was inspected at the EAR and deemed to be sufficient.
- Risk MS.4 (landing shocks); shall now have either the probability reduced (due to the vibration/shock testing) or the severity reduced (as the only required recovery is for the SD card).
- Risk MS.7 (SD card mechanical failure); shall now have the probability reduced due to the special Pi micro-SD card adapter, and the successful vibration/shock tests. Note, the final fixation of the SD card was not yet decided.
- As the CRP clearly states a night float for BEXUS 19, risk EN.1 (not dark enough to see the stars) shall have the probability reduced.

4.9. Launch and operations (SED chapter 6)

- Magnetometer calibration shall be done in conjunction with the TORMES 2.0 ADS calibration, **which shall be scheduled by SSC** to take place immediately after the gondola interface test (E-link). All experiments shall be operating, and the gondola rotated under the Dom crane. GranaSAT requires no access to complete this test.
- All LEDs and connectors are now labelled.
- The team must hand carry the inner and upper box to the campaign, they shall contact all airports before travelling to attempt to mitigate potential problems with security. It's suggested the team also carry relevant documentation (emails from ESA, SED, and acceptance letter). Transportation will be done in 'hard' travel cases.
- The team may ship their beam 'tomorrow'; **SSC will advise if the boom has not arrived before the 2nd** and, if not, the team can transport another with their hold luggage.
- Checklists are under production.
- **SSC shall modify the gondola curtains around the experiment fixations during the campaign.**
- The team know the torque required for their mechanical fixations, **SSC shall provide a torque tool for this.**
- The RBF still needs to be manufactured.
- The team shall move their day 2 tests to day 1 before the individual experiment test. The team shall view this test as more of a demonstration, and perform their own tests before.
- The team shall move their magnetometer calibration to after the E-link test.
- The RBF, LED checks, lens cleaning and test image shall all be performed at last access at T-1h30m, this means the experiment shall be turned on, and recording started at around this time (update flight plan).
- More team members shall be trained in the S/W and ground station operation.
- The log should be stored in more manageable chunks, either breaking up the applications or by time segments.



BEXUS

Experiment Acceptance Review



Page 7

- A full write test with the flight SD card should be completed.
- **SSC shall provide a ladder to remove the RBF and perform final checks.**
- A recovery sheet (A5 photo of mushroom button and directions) shall be provided at the campaign.
- The team now have a plan for data recovery from the SED card, but should also plan for the physical/mechanical recovery, such as how to safely remove the SED card, whether they want to dry it, or let it warm up before using it.
- Return shipment will be made with by the team with their hand luggage.

4.10. Organisation, project planning & outreach (SED chapters 3.1, 3.2 & 3.3)

Outreach

- The team shall make more effort to update their website as they move into the campaign. They shall include more photos of the flight hardware.
- The team admit their outreach campaign has been very static since IPR, and will work more with the wider GranaSAT (CubeSat) team.

Schedule

Now: Solve Software problem and long duration test.

Now – 24/09: Software optimisation (not tinkering!).

19/09: Delivery of new PCB, incoming inspection and installation and functional testing.

Calibration of thermal sensors.

21/09: Travel to Barcelona

22-23/09: TVAC test at UPC

24/09: Return from Barcelona.

25/09: Actions resulting from TVAC test.

26/09: Continued full functional testing ,flight simulations and campaign planning.

03/10: Travel to ESRANGE.

4.11. End-to-end Test

- The team performed an end to end test but experienced unexpected restarts.
- Quick investigation and testing suggested that this was due to a memory overload due to the test images installed.
 - **Further testing is required.**
- The experiment seems tolerant to voltage variation (25 to 32V) and E-link drop out.

5. FINAL REMARKS



BEXUS

Experiment Acceptance Review



Page 8

5.1. Summary of main actions for the experiment team

- **Solve software problem as seen in the end to end test and thoroughly re-test**
- **Thermal sensors calibration**
- **TVAC test and follow up actions**
- **Re-asses the system success criteria and performance requirement to make sure it is achievable**

5.2. Summary of main actions for the organisers

- **Schedule magnetometer calibration test.**
- **Inform the team of arrival of the beam on the 2nd of October.**
- **Modify gondola curtains at campaign.**
- **Provide torque tool and step ladder at campaign.**

5.3. EAR Result: **conditional pass**

5.4. Next SED version due: **25th September 2014**



BEXUS

Experiment Acceptance Review



Page 9

6. EXPERIMENT ACCEPTANCE REVIEW – EAR

Experiment documentation must be submitted at least five working days (the exact date will be announced) before the review (SED version 4). This will take place upon delivery of the completed experiment to EuroLaunch. The review may take place at either the location of the students' university, or a DLR, SSC or ESA institute.

Content of EAR:

- Team presentation of project status
- Follow-up of IPR action items
- Review of schedule status with respect to REXUS program timeline and upcoming activities
- Demonstration of the fully integrated experiment
- Experiment mass properties determination/discussion
- Mechanical and electrical interface checkout
- Electrical Interface Test (REXUS service system simulator test or BEXUS E-link functionality test)
- Flight Simulation Test (FST) – including a full end to end system demonstration
- Experiment acceptance decision: Passed/conditional pass/failed. If a conditional pass is elected, the immediate action items should be discussed, along with an appropriate deadline(s)

APPENDIX B – OUTREACH AND MEDIA COVERAGE

The activities named in 3.4 are now detailed:

- Social media accounts:
 - Twitter account: <http://www.twitter.com/GranaSAT>.

The Twitter account is used as a way of approaching people in a more informal way, using photographs, links to news and direct conversations with our followers to publicise the experiment.



Figure B 1 Twitter account

- Facebook page: <http://www.facebook.com/GranaSAT>

The Facebook page is used to keep the people informed of our activities, with more details than those given on Twitter, but maintaining direct contact with people.



Figure B 2 Facebook page

- Google+ account:

<https://plus.google.com/b/109416968570285086576/109416968570285086576/posts>. The Google+ account is used in the same way than the Facebook page. It is also offered to possible partners.



Figure B 3 Google+ account

- University mailing lists:

The university mailing lists are used to contact possible collaborators and to inform the whole university community about the experiment and the REXUS/BEXUS programme.



Student Experiment Documentation

- Institutional websites:

The experiment has appeared in the Faculty of Science website, the Higher Technical School of Computer Science and Telecommunications Engineering website and in the main communication channel of the University of Granada: CanalUGR (both in its Twitter account and on its website).

Figure B 4 CanalUGR, UGR website and website of the Higher Technical School of Information Technology and Telecommunications Engineering

- Institutional contact:

We have contacted the Rector of the University of Granada, as well as the Students Association in order to obtain institutional support.

- Press contact:

GranadaHoy and Ideal, two local newspapers, and 20minutos, a national newspaper, have published articles about our work.



Figure B 5 GranadaHoy cover and Ideal article, both published the 30th of October, 2014



DE GRANADA A LA ESTRATOSFERA

Sus padres son 15 alumnos y profesores de la Universidad de Granada. El 7 de octubre cambió la Alhambra por la es-

Figure B 6 20minutos article

Several digital newspapers have published articles about our work

- Granadaimedia, 24th of August, 2014:
<http://granadaimedia.com/granasat-satelite-universidad-granada/>
- Granadaimedia, 29th of October, 2014:
<http://granadaimedia.com/granasat-de-la-chana-las-estrellas/>



- El Confidencial, 29th of October, 2014:
http://www.elconfidencial.com/ultima-hora-en-vivo/2014-10-29/agencia-europea-envia-al-espacio-dispositivo-disenado-por-alumnos-de-granada_404107/
- Radio Intereconomía, 29th of October, 2014:
<http://www.radiointereconomia.com/2014/10/29/agencia-europea-envia-al-espacio-dispositivo-disenado-por-alumnos-de-granada/>
- Actualidad Universitaria, 28th of October, 2014:
<http://www.actualidaduniversitaria.com/2014/10/la-agencia-espacial-europea-envia-a-la-estratosfera-un-dispositivo-disenado-y-construido-por-estudiantes-de-la-universidad-de-granada/#more-45911>
- GranadaHoy, 29th of October, 2014:
<http://www.granadahoy.com/article/granada/1888083/la/agencia/espacial/envia/la/estratosfera/dispositivo/hecho/po/estudiantes/la/ugr.html>
- Ideal, 29th of October, 2014:
<http://www.ideal.es/miugr/201410/29/envian-estratosfera-dispositivo-creado-20141029145125.html>
- Actualidad Aeroespacial, 29th of October 2014:
<http://www.actualidadaaeroespacial.com/default.aspx?where=10&id=1&n=13959>
- Radio Granada, 29th of October, 2014:
<http://www.radiogranada.es/2014/10/29/un-dispositivo-granadino-en-el-espacio/>



Student Experiment Documentation

CENTRO

ACTUALIDAD

HISTORIAS DEL BARRIO

LOS PROBLEMAS DEL BARRIO

ACTUALIDAD

Granada en órbita

Archivado en: astronomía, Ciencia, Cocorocó, GranaSAT, I+D+i, Universidad de Granada



Es un 'sextante', aunque sus creadores se resisten a llamarlo así. Mira la posición de las estrellas y a partir de ella, calcula la propia. Como los antiguos marinos, pero en el espacio, con tecnología digital y cámaras fotográficas. Es el proyecto de un grupo de estudiantes de la Universidad de Granada que Europa va a poner en órbita, al que llaman GranaSAT porque esperan que sea el primer paso para tener un satélite universitario en la ciudad. El proyecto lo han ultimado desde el 'coworking' Cocorocó y lo presentan estos días en



Por Jose A. Cano

Periodista nacido en Sevilla y residente en Granada, que pasó por ello de estudiante a maestral. Atento a los debates, a la Historia y a contar lo que sucede. En Twitter: [@Jose_Cano00](#).

Más artículos de Jose A.

- » [Cesa la droga la del 'tagolla' millonaria](#)
- » [La carga policial del 20N, a los tribunales](#)
- » [Quisquero en Gran Vía](#)

Patrocinadores





Figure B 7 Granadamedia, the first newspaper that published our work

Dos equipos de universitarios españoles, en el programa Bexus de globos estratosféricos

Kirena.- Dos equipos de universitarios españoles, de los cuatro seleccionados por la Agencia Espacial Europea (ESA) y la Junta Nacional para la Investigación Científica y Técnica (JNICT), han participado en la ciudad avalesa de Vilaria en el programa germano-suizo para la realización de vuelos en globos estratosféricos llevando a cabo experimentos a más de 27.000 metros de altura.

VÍDEO Y GALERÍA: Un dispositivo granadino estratosférico

VIDEO PARA USO

Enviado a la estratosfera un dispositivo diseñado por estudiantes de la UGR

Llamado GranaSAT, fue lanzado con éxito el pasado 7 de octubre desde Kirtman (Suecia)

La Agencia Espacial envía a la estratosfera un dispositivo hecho por estudiantes de la UGR.

La Agencia Espacial Europea envía a la estratosfera un dispositivo diseñado y construido por estudiantes de la Universidad de Granada

AGENCIA EUROPEA ENVÍA AL ESPACIO DISEÑADO POR ALUMNOS DE GRANADA

Agencia Europea envía al espacio diseñado por alumnos de Granada

GranaSAT: De la Chan

Alumnos de la UGR han presentado los resultados del

Alumnos de la UGR han presentado los resultados del

La Agencia Espacial Europea ha enviado a la estratosfera a más de 27 kilómetros de altura, un dispositivo diseñado y construido por estudiantes de la Universidad de Granada, un seguimiento de estaciones meteorológicas y terrestres seleccionadas por la Agencia Espacial Europea para participar en el programa Bexus/Bexus del Centro Aeroespacial Alemán (DLR) y el

La Agencia Espacial Europea ha enviado a la estratosfera a más de 27 kilómetros de altura, un dispositivo diseñado y construido por estudiantes de la Universidad de Granada, un seguimiento de estaciones meteorológicas y terrestres seleccionadas por la Agencia Espacial Europea para participar en el programa Bexus/Bexus del Centro Aeroespacial Alemán (DLR) y el

Alumnos de la UGR han presentado los resultados del

Figure B 8 GranaSAT in digital press

- TV and videos

GranaSAT has appeared in the news programme of CanalsUR, the TV channel for Andalusia, and in El Salón, a culture programme of TG7, another local TV.



Figure B 9 GranaSAT in CanalSUR news programme



Figure B 10 GranaSAT members at TG7 programme

Information about GranaSAT has also been translated into Chinese, Russian, English, French and German by Andalusian Stories, an audiovisual news agency:



GranaSAT: 在平流层为欧洲航天局收集数据的技术

 andaluxiyaxinwen Historiasdeluz

[Subscribe](#) 5

48 visualizaciones

+ Añadir a Compartir More

Publicado el 28 de nov. de 2014
更多視頻: www.andaluxiyaxinwen.com

格拉纳达大学的学生和教师设计并建造出GranaSAT，已由欧洲航天局的设备发送到平流层。该器件能够发



GranaSAT BEXUS - Vibración Test

de GranaSAT Team

299 visualizaciones

5:39



GRANA-SAT 1

de UGR.CIENCIAS

165 visualizaciones

3:18



研究者们学习头胎行为，预测婴儿

多动症或自闭症的发展

de andaluxiyaxinwen Historiasdeluz

9 visualizaciones

1:50

Figure B 11 GranaSAT information in Chinese

- Congresses:
 - Desgranando Ciencia, 13th of December, 2014: Second edition of Desgranando Ciencia was held at Parque de las Ciencias of Granada by mid-December. It was an event of popular science where GranaSAT had the chance to participate and collaborate. Some of the members attended to explain what GranaSAT project is and what we did in BEXUS mission. GranaSAT had a poster and showed the flight experiment hardware.

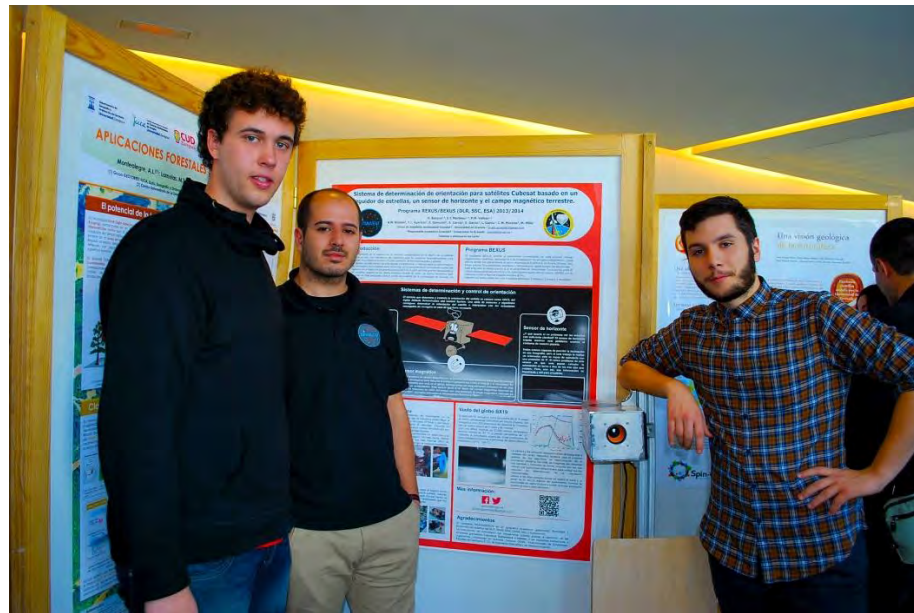


Figure B 12 GranaSAT members at Desgranando Ciencia congress

- Conferences:
 - Higher Technical School of Information Technology and Telecommunications Engineering conference, 29th of October, 2014: Presentation to the faculty students, during which we talked about our experience, the experiment results and the REXUS/BEXUS programme.

- Faculty of Science conference, 6th of November, 2014: During the Science Week, GranaSAT held a conference to tell students who were starting university soon about BEXUS experience.



Figure B 13 Faculty of Science conference

- Press conference:
GranaSAT held a press conference at the Higher Technical School of Information Technology and Telecommunications Engineering, organised by the University, on the 29th of October, 2014. University newspapers, local TVs, digital and local newspapers and other journalists were told about GranaSAT experience during half an hour. The impact during the following days was very important for the whole project, not only for BEXUS mission.
- Other:
<http://www.ea1uro.com/> chose GranaSAT website as “site of the month”:

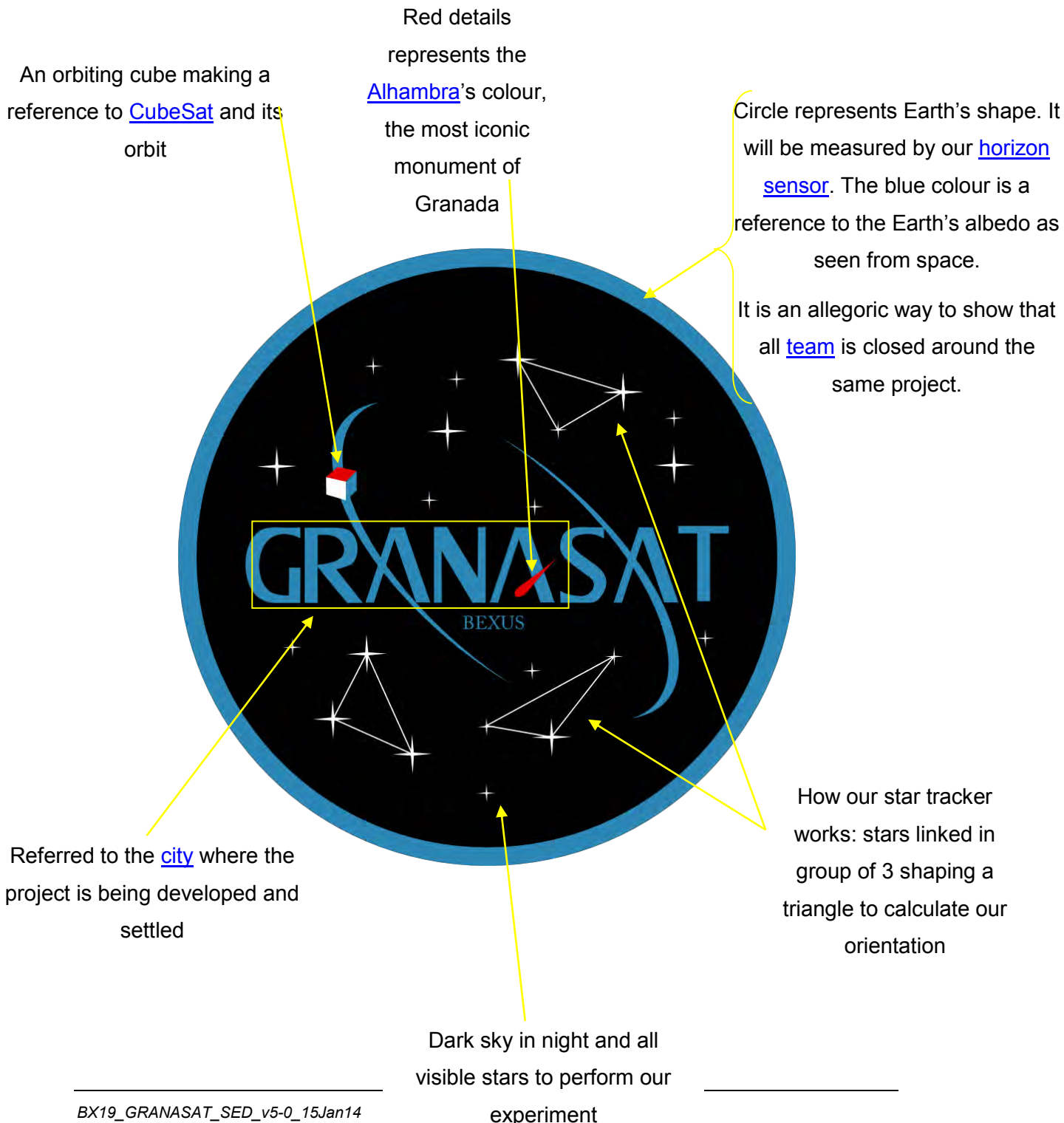
Student Experiment Documentation



Figure B 14 Ea1uro home page

B.1 Logo

Here is a brief description of our team logo, indicating the meaning of colours and shapes shown and other details that may not be seen at first glance:





APPENDIX C – ADDITIONAL TECHNICAL INFORMATION

C.1 Plans

The following plans can be found in the zip file named BX19_GranaSAT_SED-AppendixC_v4-2 attached with this document:

Table C.1 1 Drawings reference

| File name | Drawing |
|-------------------------------|---------------------|
| BX19_GranaSAT_CAD-01_v3-1.pdf | Complete model |
| BX19_GranaSAT_CAD-02_v3-1.pdf | Outer box |
| BX19_GranaSAT_CAD-03_v3-1.pdf | Outer metal |
| BX19_GranaSAT_CAD-04_v3-1.pdf | Baffle |
| BX19_GranaSAT_CAD-05_v3-1.pdf | Outer metal support |
| BX19_GranaSAT_CAD-06_v3-1.pdf | Inner box |
| BX19_GranaSAT_CAD-07_v3-1.pdf | Inner metal plate |
| BX19_GranaSAT_CAD-08_v3-1.pdf | Inner metal |

C.2 Outer Box Characteristics

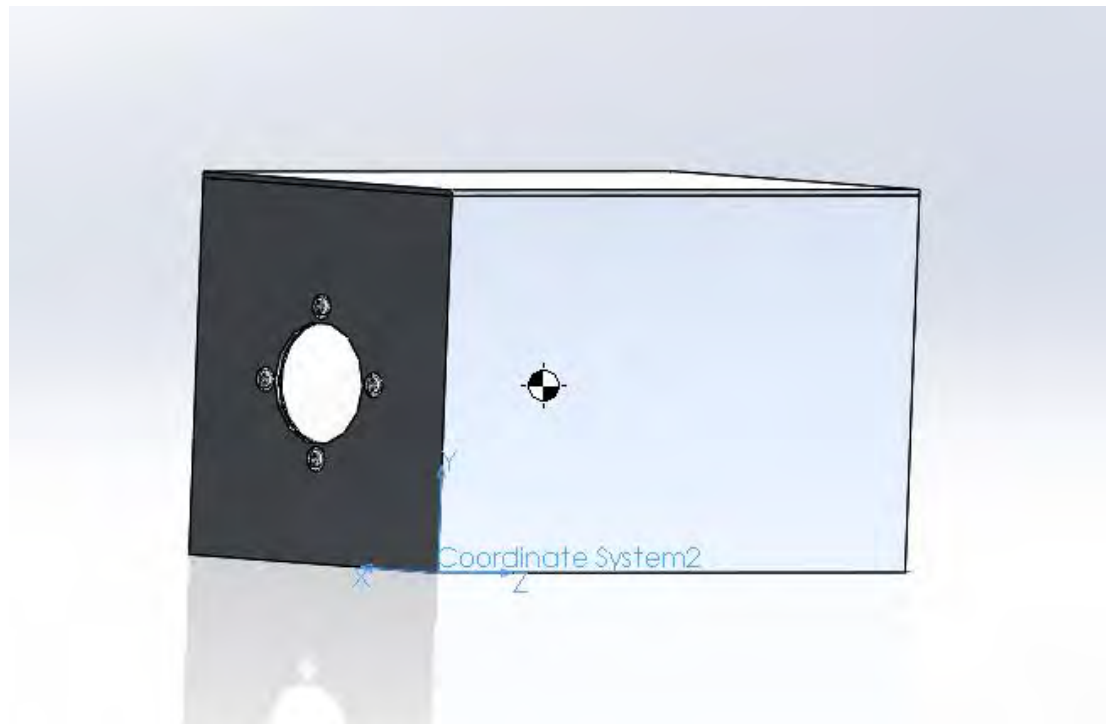


Figure C2-1 Outer box

Table C.2 1 Outer box characteristics

| | |
|---|---------------------------------------|
| Experiment mass (in kg): | 2.195 |
| Experiment dimensions (in m): | 0.142 x 0.128 x 0.248 |
| Experiment footprint area (in m ²): | 35.216 · 10 ⁻³ |
| Experiment volume (in m ³): | 4.508 · 10 ⁻³ |
| Experiment expected COG (centre of gravity) position (in m): | X = -0.005 Y = 0.018 Z = 0.0132 |

C.3 Profile

Table C.3 1 Profile characteristics

| | |
|-------------------------------|-----------------------|
| Experiment mass (in kg): | 1.643 |
| Experiment dimensions (in m): | 0.045 x 0.125 x 0.045 |



| | |
|--|-------------------------|
| Experiment footprint area (in m ²): | $2.025 \cdot 10^{-3}$ |
| Experiment volume (in m ³): | $2.531 \cdot 10^{-4}$ |
| Experiment expected COG (centre of gravity) position (in m): | X = 0 Y = 0 Z = 0 |

C.4 Inner Box Characteristics

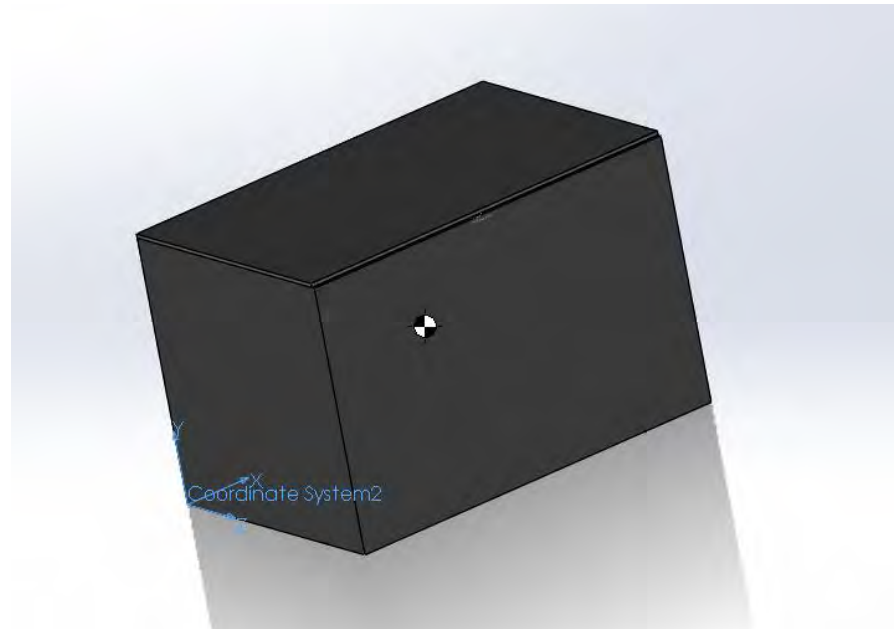


Figure C4- 1 Inner box

Table C.4 1 Inner box characteristics

| | |
|---|------------------------------------|
| Experiment mass (in kg): | 2.630 |
| Experiment dimensions (in m): | 0.157 x 0.144 x 0.228 |
| Experiment footprint area (in m ²): | $35.796 \cdot 10^{-3}$ |
| Experiment volume (in m ³): | $5.155 \cdot 10^{-3}$ |
| Experiment expected COG (centre of gravity) position (in m):: | X = -0.48 Y = -0.43 Z = 1.62 |



C.5 Electronics Schematics

The following schematics can be found in the zip file named BX19_GranSAT_SED-AppendixC_v4-2 attached with this document:

Table C.5 1 Electronic schematics reference

| File name | Schematic |
|---|------------------------|
| BX19_GranSAT_ElectronicSchematics-01_v4-2.pdf | General Electronic |
| BX19_GranSAT_ElectronicSchematics-02_v4-1.pdf | Inner box PCB |
| BX19_GranSAT_ElectronicSchematics-03_v4-2.pdf | Step down power supply |
| BX19_GranSAT_ElectronicSchematics-04_v4-2.pdf | Raspberry Pi |
| BX19_GranSAT_ElectronicSchematics-05_v4-2.pdf | Outer box PCB |
| BX19_GranSAT_ElectronicSchematics-06_v4-2.pdf | Outer box PCB Concept |
| BX19_GranSAT_ElectronicSchematics-07_v5.pdf | Grounding diagram |



C.6 Electronics Components

The following electronic components provide a general view of the electronic system. The table has information about the location, number and parameters of each electronic component. Furthermore, one can learn more about the components by clicking on the component names:

Table C.6 1 Electronic components

| Instrument | Model | Availability | Cost/p | Supplier | Number | Specifications | Reasons | Current Status |
|-----------------------------|------------------|--------------|--------|-------------------|--------|-------------------------------------|---|----------------|
| <u>Capacitor (in)</u> | 100 VFP | Standard | 0.524 | Panasonic | 5 | C = 100µF, Vmax = 35V | Good temperature range (-55 to 105 °C) | Available |
| <u>Capacitor (out)</u> | 102MHA0G | Standard | 0.336 | Alchip | 2 | C = 1000µF, Vmax = 6,3 V | Good temperature range (-55 to 105 °C) | Available |
| <u>Fast Diode</u> | SURS8320 T3G | Standard | 0.051 | ON semiconductor | 2 | 3.0 A | Very good frequency range | Available |
| <u>Inductor</u> | 2DO3316P-104MLB | Low | 0.91 | Coilcraft | 2 | L = 100uH | Good temperature, frequency and current range | Available |
| <u>Regulator</u> | LM2576 | Standard | 3.76 | Texas Instruments | 6 | 5V, 3A, Step-Down Voltage Regulator | High efficiency | Available |
| Diode LED | - | High | 0.15 | - | 6 | Status system information | Good luminosity | Available |
| <u>Mushroom push button</u> | IPK69 | Standard | 25.49 | Moeller | 1 | Round actuator | Good size and useful | Available |
| <u>Power connector</u> | PT02E8-4P | Standard | 8.65 | Amphenol | 1 | Military 4 pin | BEXUS recommendation | Available |
| <u>Link Outer-Inner Box</u> | MIL-DTL-26482 | Standard | 17.26 | Amphenol | 1 | Power connector | BEXUS recommendation | Available |
| <u>USB Connector</u> | Buccaneer PX0842 | Standard | 9.18 | BULGIN | 1 | USB A, female, box mount | Safe connector and good temperature range | Available |



| | | | | | | | | |
|---|-------------|----------|-------|--------------------|----|---|---|-----------|
| <u>Ethernet Connector</u> | RJF21B | Standard | 32.17 | Amphenol | 1 | 10BaseT,100Base TX and 1000 BaseT networks | BEXUS recommendation | Available |
| Cable Gland | - | Standard | - | - | 2 | Inner box / Outer box interface link | Diameter required | Available |
| <u>Temperature Sensor (1)</u> | DS1621 | High | 5 | Maxim integrated | 2 | -55°C to +125°C Vdd=5V, 9-bit value | Sample frequency required and good accuracy | Available |
| <u>Temperature sensor (2)</u> | TC74 | Standard | 1.18 | Microchip | 5 | Precision = ±2°C Input voltage between 2.7 V to 5.5 V | Good temperature range (-40 to 125 °C) | Available |
| <u>Magnetometer & Accelerometer</u> | LSM303DL HC | High | 3.67 | STMicroelectronics | 3 | Accelerometer & Magnetometer sensor | Sample frequency required, good accuracy and low cost | Available |
| <u>Resistor</u> | - | High | 0.46 | ARCOL | 10 | R = 4.7K | Good operational range | Available |
| LED holder | - | High | 0.27 | - | 8 | - | Diameter required and good temperature range | Available |
| <u>Current limitor</u> | ITS4141N | Standard | 1.70 | Infineon | 3 | Max. Input voltage = 48V | Current limitation at 1.1A | Available |
| <u>I²C extender</u> | P82B715 | Standard | 4.05 | NXP | 2 | Max. Frequency = 1 MHz | Improve the communication between the boxes | Available |



Student Experiment Documentation

| | | | | | | | | |
|--------|---|------|-----|--------|---|----|---|-----------|
| Buzzer | - | High | 0.5 | Murata | 1 | 5V | - | Available |
|--------|---|------|-----|--------|---|----|---|-----------|

C.7 Test Details

C.7.1 Star Tracker Test

Purpose

To determine the accuracy and robustness of the star tracker algorithm, calibrating the camera and analysing one hundred test images. The final objective is to test whether the requirements F.1, P1 and P.4 will be fulfilled.

Material and environmental factors needed

- A computer in which the star tracker will run and the calibration will be done
- The camera (DMK41BU02)
- A chessboard image to calibrate the camera
- The star tracker software

Test process

Before performing the test itself, the camera has to be calibrated and the test images have to be created. After the setup, the test is performed as described below.

Simulated scenario

The star tracker, which is in its final version, will receive one hundred test images, created artificially to be as similar as possible to the real images the camera will take in the flight.

Camera calibration

The Star Tracker precision depends highly on the camera calibration. Calibration consists on the determination of a set of parameters. Two kinds of camera parameters exists: The extrinsic and the intrinsic ones.

Intrinsic parameters are related to the camera geometrics and the optical characteristics. It includes the focal length, image centre misadjustment and lens distortion. The coordinates in the image frame obtained using the Thales' theorem:



$$\frac{u}{v} = \frac{f}{z} \begin{bmatrix} x \\ y \end{bmatrix} \quad (\text{Eq. C7 1})$$

Where x, y, z are the world coordinates of a point, f is the focal length and u, v are the image frame coordinates, are modified as follows:

$$x' = x/z \quad (\text{Eq. C7 2})$$

$$y' = y/z \quad (\text{Eq. C7 3})$$

$$x'' = x'(1 + K_1 r^2 + K_2 r^4) + 2p_1 x' y' + p_2 (r^2 + 2x'^2) \quad (\text{Eq. C7 4})$$

$$y'' = y'(1 + K_1 r^2 + K_2 r^4) + 2p_2 x' y' + p_1 (r^2 + 2y'^2) \quad (\text{Eq. C7 5})$$

$$r^2 = x'^2 + y'^2 \quad (\text{Eq. C7 6})$$

$$u = f_x x'' + c_x \quad (\text{Eq. C7 7})$$

$$v = f_y y'' + c_y \quad (\text{Eq. C7 8})$$

K_1 and K_2 correspond to the radial distortion parameters that cause a displacement of the point in the direction of r . The tangential distortion is modeled with p_1 and p_2 . The cause of this distortion is that the centres of the lens are not really collinear. As presented in [43], just two parameters for each kind of distortion are enough to characterize the camera in the majority of the cases.

Extrinsic parameters involve the 3D camera position and the orientation of the camera frame relative to a certain world coordinate system.

In this case, to find the calibration parameters we have worked with a camera calibration toolbox for MATLAB ® [44]. The procedure is described in the program documentation; here we will just show the results.

After running the program with a set of calibration images, the toolbox returns the camera parameters and their uncertainties, which can be consulted in Table C.7 1.

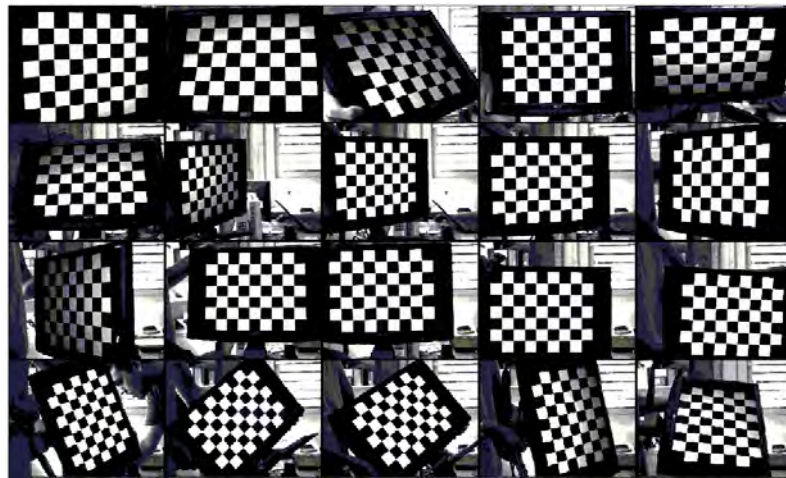
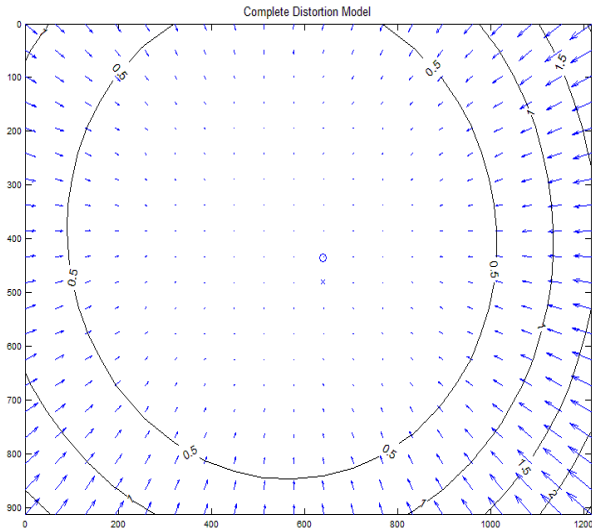


Figure C.7 4 Calibration images

Table C.7 1 Camera parameters

| Parameter | Value | Uncertainty |
|-----------|------------------|---------------|
| f_x | 2663.5187 pixels | 2.9305 pixels |
| f_y | 2664.8574 pixels | 2.8930 pixels |
| c_x | 637.9061 pixels | 5.0717 pixels |
| c_y | 434.1078 pixels | 4.1401 pixels |

The K_1 , K_2 , P_1 , P_2 parameters were not estimated properly. The error seems to be greater than the real value. For that reason, they were estimated iteratively. The complete distortion model of the camera obtained is showed below:



Pixel error = [0.1002, 0.1015]
 Focal Length = (2063.52, 2664.86)
 Principal Point = (637.906, 434.108)
 Skew = 0
 Radial coefficients = (-0.04655, 0.2029, 0)
 Tangential coefficients = (-0.0005047, -0.001118)

+/- [2.93, 2.893]
 +/- [5.072, 4.141]
 +/- 0
 +/- [0.01222, 0.2629, 0]
 +/- [0.0005278, 0.0006247]

Figure C.7 5 Complete camera distortion model

The final parameters used were estimated using the following process:

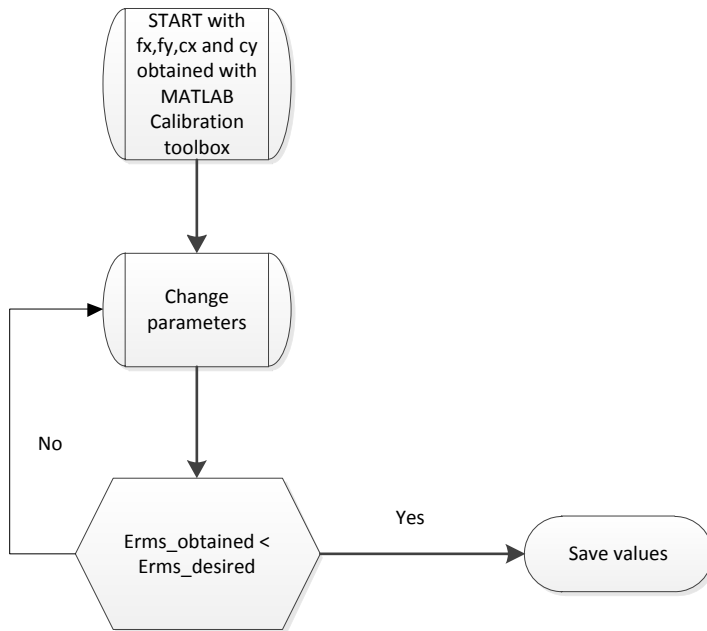


Figure C.7 6 Iterative process to obtain the camera distortion parameters

The final results are the following:

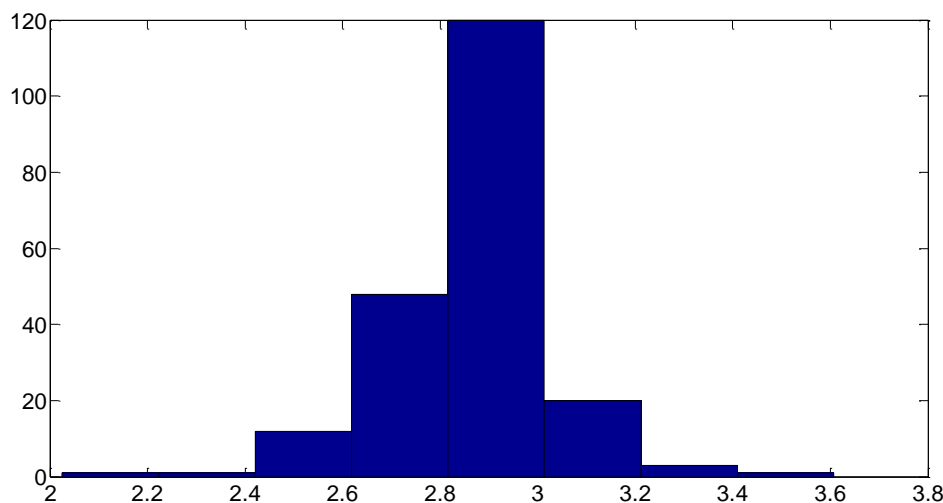
Table C.7 2 Final results

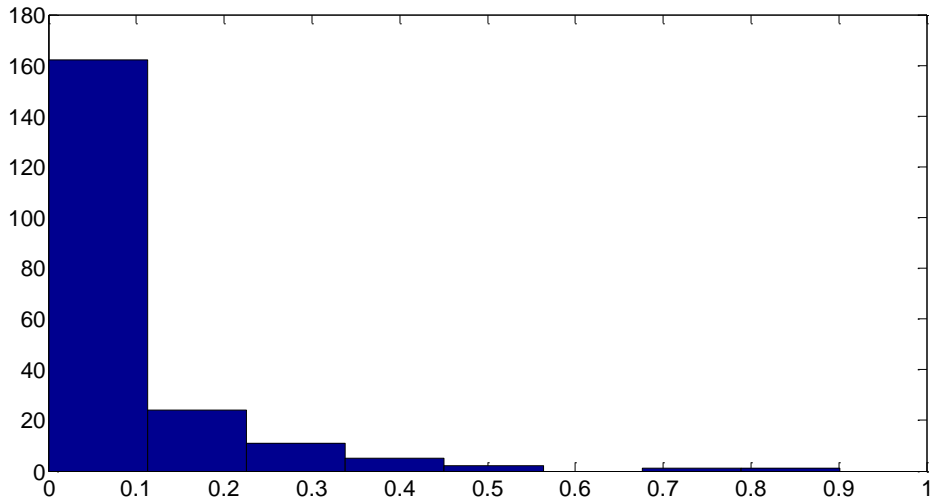
| Parameter | Value obtained |
|-----------|---------------------|
| f_x | 2657 px |
| F_y | 2657 px |
| C_x | 666 |
| C_y | 440 |
| K_1 | $1e-9 \text{ px}^2$ |
| K_2 | negligible |
| P_1 | negligible |
| P_2 | negligible |

The next two figures show respectively the relative error histogram of the angles measured between stars before and after calibration. All images used for this calibration were taken the 25th of August, 2014. The following table shows the relative error mean and standard deviation:

Table C.7 3 Relative error mean and standard deviation

| | Mean | σ |
|---------------------------|--------|----------|
| Before calibration | 2.8886 | 0.1664 |
| After calibration | 0.0862 | 0.1169 |

**Figure C.7 7 Relative error before calibration**

**Figure C.7 8 Relative error after calibration**

Training images

In order to be able to characterize the attitude error, a set of artificial test images was built following the next steps. This process is described in [1] and is explained here for completion.

1. Randomly attitude determination:

$$A = \begin{bmatrix} \cos\theta_1 & \sin\theta_1 & 0 \\ -\sin\theta_1 & \cos\theta_1 & 0 \\ 0 & 0 & 1 \end{bmatrix} \begin{bmatrix} \cos\theta_2 & 0 & -\sin\theta_2 \\ 0 & 1 & 0 \\ \sin\theta_2 & 0 & \cos\theta_2 \end{bmatrix} \begin{bmatrix} 1 & 0 & 0 \\ 0 & \cos\theta_3 & \sin\theta_3 \\ 0 & -\sin\theta_3 & \cos\theta_3 \end{bmatrix} \quad (\text{Eq. C7 9})$$

The yaw, pitch and roll angles ($\theta_1, \theta_2, \theta_3$) are generated using the MATLAB `rand()` function.

2. Once the attitude has been generated, the boresight direction is computed as follows:

$$\mathbf{u}_{bore} = A^T [\mathbf{0} \ \mathbf{0} \ 1]^T \quad (\text{Eq. C7 10})$$

3. Stars present in the image must satisfy the following equation:



$$\text{acos}(\nu_{star} \cdot u_{bore}) < FOV \quad (\text{Eq. C7 11})$$

Where ν_{star} is the unitary vector of the star in the Hipparcos catalog and FOV is the camera field of view.

4. Every star present in the image has a brightness that is computed using :

$$Star_{brightness} = t_{exp} \cdot \frac{\pi}{4} d^2 \cdot \tau \cdot \lambda \cdot 10^{-0.4m} \cdot G \quad (\text{Eq. C7 12})$$

Where t_{exp} is the exposition time in seconds, d is the aperture diameter in cm, τ is the transmittance of the camera, λ is the spectral range in μm and m is the magnitude of the star.

5. Using Eq. C7 3 the star centroid in the image frame is computed.
6. Blurry the centroids assigning a number of randomly points. Every pixel belonging to a star has a value that is computed as follows:

$$Pixel_{brightness} = \frac{1}{Star_{brightness}} \cdot p$$

Where p is the number of points chosen.



Figure C.7 9 Example of an artificially created image

Attitude determination

The attitude determination algorithm used was proposed by Markley in [37]. Once the stars have been identified, a matrix B is computed using the unitary vectors in the reference frame and the vectors in the camera frame.

$$B = \sum_{i=1}^n b_i r_i^T \quad (\text{Eq. C7 13})$$

Where the vector in the camera is b_i and r_i is the vector in the reference frame. After computation of B matrix, a single value decomposition is done:

$$B = USV^T \quad (\text{Eq. C7 14})$$

The actual attitude is finally found as follows:

$$A_C = U_+ V_+^T \quad (\text{Eq. C7 15})$$

Where

$$U_+ = U \begin{bmatrix} 1 & 0 & 0 \\ 0 & 1 & 0 \\ 0 & 0 & \det(U) \end{bmatrix}$$

$$V_+ = V \begin{bmatrix} 1 & 0 & 0 \\ 0 & 1 & 0 \\ 0 & 0 & \det(V) \end{bmatrix}$$

The error is computed as follows:

$$\text{Error}_{\text{matrix}} = A_c^{-1} A = \begin{bmatrix} \approx 1 & -\phi_z & -\phi_y \\ \phi_z & \approx 1 & -\phi_x \\ \phi_y & \phi_x & \approx 1 \end{bmatrix}$$

$$e_x = 90^\circ - \cos^{-1}(\phi_x) \quad (\text{Eq. C7 16})$$

$$e_y = 90^\circ - \cos^{-1}(\phi_y) \quad (\text{Eq. C7 17})$$

$$e_z = 90^\circ - \cos^{-1}(\phi_z) \quad (\text{Eq. C7 18})$$

Qualification test

The data obtained from both the calibration and the test itself should be analysed in order to determine the test success.

Table C.7 4 Qualification test

| Status | Definition |
|-----------|---|
| ✗ Failure | Any of the following cases: <ul style="list-style-type: none"> • The star tracker algorithm is not able to obtain the attitude. • The error in the attitude determination is greater than 1 arcmin. • The output frequency is less than 0.5 Hz |

| | |
|--|---|
| ✓ Test completion | The star tracker determines the attitude with an accuracy of, at least, 1 arcmin, and the output frequency is greater than 0.5 Hz |
|--|---|

Results

After the camera was calibrated and the artificial images were created, the Star Tracker software analysed one hundred of these images. The artificial images were created with a relative error close to 0.001 % in the angle measurement; for that reason, an additional error is introduced in the centroid algorithm. The next histogram shows the relative error in the angle measurement after the introduction of this error:

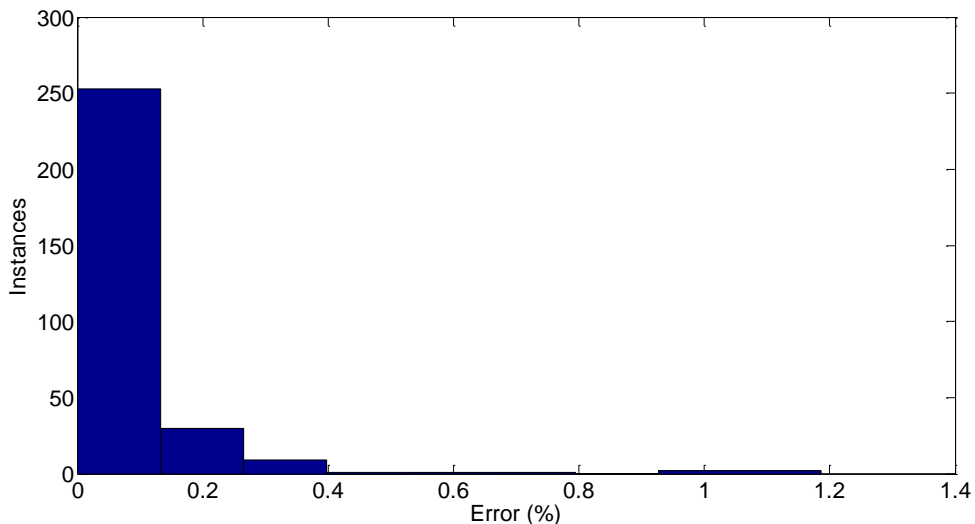


Figure C.7 10 Relative error histogram

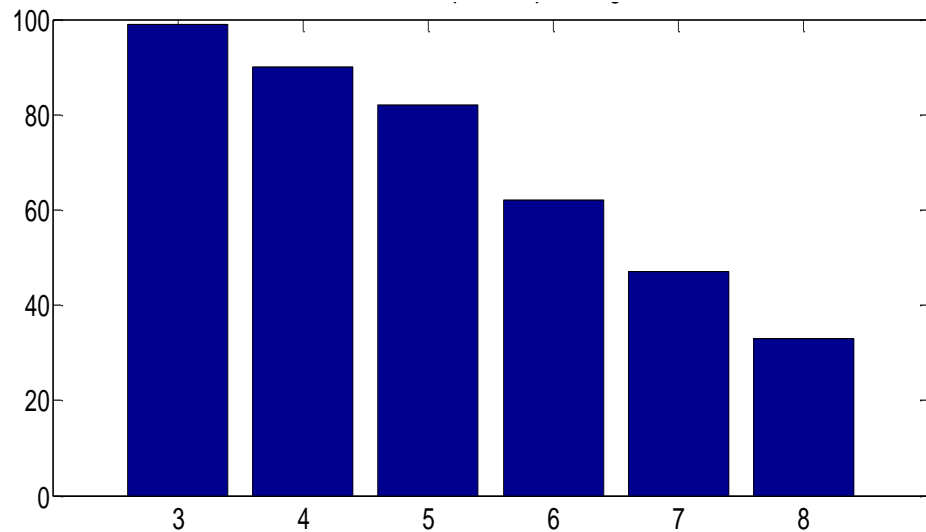
Table C.7 5 Errors in the images

| | Mean | σ |
|---|--------|----------|
| Real images relative error (%) | 0.0862 | 0.1169 |
| Artificial images relative error (%) | 0.0840 | 0.1184 |

The following table shows the mean and standard deviation of the absolute error in arcsecs considering a certain number of stars identified:

**Table C.7 6 Errors given a number of stars considered**

| Stars considered | Err x axis (arcsecs) | Err y axis (arcsecs) | Err z axis (arcsecs) |
|-----------------------------|---------------------------------|---------------------------------|---------------------------------|
| 3 | Mean=-22.94 $\sigma=70$ | Mean=-11.92 $\sigma=67.92$ | Mean=-6.41 $\sigma=70.83$ |
| 4 | Mean=-33.83 $\sigma=58.96$ | Mean=9.2481 $\sigma=59.05$ | Mean=-10.64 $\sigma=62.88$ |
| 5 | Mean=-26.51 $\sigma=53.81$ | Mean=15.84 $\sigma=62.70$ | Mean=-3.08 $\sigma=54.10$ |
| 6 | Mean=-25.90 $\sigma=54.05$ | Mean=20.22 $\sigma=50.87$ | Mean=-10.56 $\sigma=45.78$ |
| 7 | Mean=-21.94 $\sigma=42.02$ | Mean=21.67 $\sigma=49.33$ | Mean=5.25 $\sigma=51.21$ |
| 8 | Mean=-37.4120 $\sigma=48.72$ | Mean=20.56 $\sigma=39.06$ | Mean=-10.85 $\sigma=59.06$ |

**Figure C.7 11 Percentage of stars present in the catalogue per image**

Conclusions

In this section, the Star Tracker test was explained and the results were presented. Firstly, a camera calibration was done. After the calibration, a relative error in the angle measurement between stars was reduced to the 0.082 %.

After the calibration, the Star Tracker software analysed one hundred of test images, in the centroid algorithm an error was introduced to emulate the accuracy in the angle measurement achieved after the camera calibration.

In these artificial images, we found that at least three stars are present in the star catalogue used in 99 % of the cases. The Star Tracker software was able to identify all stars present in the catalogue with in the 100 % of the cases.

The absolute error per axis after the attitude determination was found -22.94 arcsecs, -11.92 arcsecs and -6.41 arcsecs in the x, y, z axes respectively.

These results confirm that the F.1, P.1 and P.4 requirements are fulfilled.

C.7.2 Horizon Sensor Test

Purpose

To decide which circle fitting method, between MLS and Kåsa, is the best one to implement in the horizon sensor.

Material needed

A computer.

Test process

To simulate the real Earth's horizon with the real measurement errors, the following conditions have been taken into account:

Test facility

Laboratory in the Faculty of Sciences with a computer in which the algorithm can run.

Simulated scenario

The algorithm to detect the Earth circumference produces some errors due to the albedo and the atmosphere. To simulate those errors in the measurements,



given a circle and a level of measurement goodness, a set of 50 points from the outer semi-circumference has been generated.

These points are the input for the test, which has been repeated with 100 circles and 10 levels of goodness, giving us 1,000 measures of the accuracy of both methods.

The circles radius varies from 100 to 10,000 units. The level of goodness varies from 0 % to 10 % of the circle radius.

Since the error in the points is generated randomly, the measurements for each pair radius-goodness have been repeated 1,000 times, in order to obtain the mean of all these measurements.

The stored data from each pair radius-goodness, in each iteration, consists of:

- 50 generated points.
- The centre obtained from Kåsa.
- The centre obtained from MLS.
- The distance between Kåsa centre and the real centre.
- The distance between MLS centre and the real centre.
- The distance between Kåsa centre and MLS centre.

General procedure

In the following scheme the general behaviour of the test can be seen.

1. For RADIUS from 100 to 10,000
 - a. Generate a circle C_{RADIUS} .
 - b. For GOODNESS from 0.0 to 0.1
 - i. For each ITER from 0 to 1,000
 1. Generate 50 random points $P_{ITER,GOODNESS,RADIUS}$.
 2. Obtain KÅSA centre and its distance to real centre.
 3. Obtain MLS centre and its distance to real centre.
 4. Obtain difference between MLS and KÅSA centre distances to the real one.
 - ii. ITER loop end



- c. GOODNESS loop end
- 2. RADIUS loop end

The pseudo-code is the following:

```

Const int NUM_CIRCLES = 100;
Const int NUM_GOODNESS = 10;
Const int NUM_ITER = 1000
Const int NUM_POINTS = 50;

for (i = 0; i < NUM_CIRCLES; ++i) {

    radius[i] = 100 + 1000*i;

    for (j = 0; j < NUM_GOODNESS; ++j) {

        goodness_perc[j] = 0.1 * j / NUM_GOODNESS;

        distance_MLS = distance_KÅSA = 0;

        for (k = 0; k<NUM_ITER; ++k) {

            for (m=0; m<NUM_POINTS; ++m) {

                random_angle = rng(0, M_PI);
                points[m] = generate_point(radius,
random_angle);

                write_to_file(points[m]);
            }

            MLS_centre = MLS_method(points)
            KÅSA_centre = KÅSA_method(points);

            Write_to_file(MLS_centre, KÅSA_centre);

            distance_MLS += distance(MLS_centre,
ZERO);
            distance_KÅSA += distance(KÅSA_centre,
ZERO);

        } //END OF ITER LOOP

        distance_MLS /= NUM_ITER;
        distance_KÅSA /= NUM_ITER;

        write_to_file(distance_MLS);
        write_to_file(distance_KÅSA);
    }
}

```



```

        write_to_file(distance_KÅSA - distance MLS); i

    } //END OF GOODNESS LOOP
} //END OF CIRCLES LOPP

```

Measured times

The difference between MLS and KÅSA distances to the real centre can be seen on the following table, where the columns represent the measurement error and the rows, the circle radius. Only the values for ten different circles, and five levels of goodness, are provided:

Table C.7 7 Differences between MLS and Kåsa

| | 0.00 % | 0.02 % | 0.04 % | 0.06 % | 0.08 % |
|--------------|---------------------|----------------------|----------------------|----------------------|----------------------|
| 1000 | $2.1 \cdot 10^{-5}$ | $-3.8 \cdot 10^{-6}$ | $-1.1 \cdot 10^{-5}$ | $-3.8 \cdot 10^{-6}$ | $-3.1 \cdot 10^{-5}$ |
| 2000 | $9.2 \cdot 10^{-5}$ | $5.7 \cdot 10^{-5}$ | $-1.5 \cdot 10^{-5}$ | $-2.3 \cdot 10^{-5}$ | $6.1 \cdot 10^{-5}$ |
| 3000 | $1.4 \cdot 10^{-4}$ | $-1.5 \cdot 10^{-5}$ | $3.8 \cdot 10^{-5}$ | $-3.1 \cdot 10^{-5}$ | $-6.1 \cdot 10^{-5}$ |
| 4000 | $1.9 \cdot 10^{-4}$ | $-1.5 \cdot 10^{-5}$ | 0.0 | $1.1 \cdot 10^{-4}$ | $-2.1 \cdot 10^{-4}$ |
| 5000 | $4.0 \cdot 10^{-4}$ | $3.1 \cdot 10^{-5}$ | $-1.2 \cdot 10^{-4}$ | $2.1 \cdot 10^{-4}$ | $2.1 \cdot 10^{-4}$ |
| 6000 | $2.5 \cdot 10^{-4}$ | $-2.3 \cdot 10^{-5}$ | $-7.6 \cdot 10^{-5}$ | $1.2 \cdot 10^{-4}$ | $9.2 \cdot 10^{-5}$ |
| 7000 | $3.0 \cdot 10^{-4}$ | $-7.6 \cdot 10^{-6}$ | $9.2 \cdot 10^{-5}$ | $1.5 \cdot 10^{-4}$ | $-1.2 \cdot 10^{-4}$ |
| 8000 | $3.5 \cdot 10^{-4}$ | $1.5 \cdot 10^{-5}$ | $9.2 \cdot 10^{-5}$ | $1.2 \cdot 10^{-4}$ | $-1.8 \cdot 10^{-4}$ |
| 9000 | $3.5 \cdot 10^{-4}$ | $4.6 \cdot 10^{-5}$ | $-3.1 \cdot 10^{-5}$ | $2.4 \cdot 10^{-4}$ | 0.0 |
| 10000 | $5.7 \cdot 10^{-4}$ | $-1.5 \cdot 10^{-5}$ | $-3.1 \cdot 10^{-4}$ | $6.1 \cdot 10^{-5}$ | $-1.2 \cdot 10^{-4}$ |

Results

Since the greatest difference (in absolute value) between the distances of both calculated centres to the real one is $6.72 \cdot 10^{-4}$, which is a completely despicable value, we can conclude that both methods provide an accuracy similar.

As the implementations and the computational complexity of the KÅSA method is greater—it includes complex matrix operations, we conclude that the best method to implement in the horizon sensor is the MLS method.

C.7.3 Magnetic Field Test

Purpose

To take magnetic measurements with the magnetic sensor to see if it behaves the way we want. Using conventional magnetometers, it is interesting to see the behaviour of

sensors that are built into handheld devices, but we must make the appropriate test to see if the sensor is able to measure the field that will meet on board.

Material needed

- 3D Helmholtz coils
- LSM303DLHC sensor
- Raspberry Pi
- Wind Rose
- Compass
- Gaussmeter, model: GM08-0822
- Bipolar operational power supply/amplifier, KEPCO, model: BOP 50-8M 0 to ± 50 V, 0 to ± 8 A.

Test Process

1. Put the X axis oriented to magnetic north with the analog compass.
2. Once the X axis is oriented to magnetic north, we must introduce a current that causes a deviation in the compass of 45 degrees. This current has to be written down, which is the one that causes the field produced in 3D Helmholtz coils to be equal to the Earth's magnetic field. This is because the two magnetic field vectors (both applied by us as the Earth's magnetic) are perpendicular and have the same module, as we can see in figure 1.

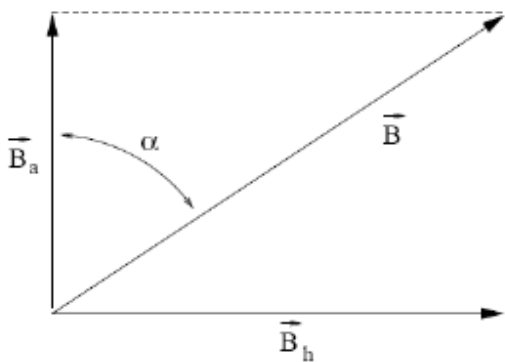


Figure C.7 12 Magnetic field vectors

B_h = Earth's magnetic field vector

B_a = Generated magnetic field vector

α = Angle.

As we can see in the equation $\alpha = \arctg \frac{B_h}{B_a}$, when $\alpha=1$, B_h is equal to B_a . This

way, we know the Earth's magnetic field to cancel it and to take it into account for the measurements.

3. This field has to be measured with both the Gaussmeter and the magnetic sensor.
4. Now, the magnetic field measured during the flight has to be simulated with the IGRF model. All measurements have to be taken both with the magnetic sensor (which is connected to the Raspberry Pi) and the Gaussmeter.

Qualification Test

To pass or fail the test the following must occur:

Table C.7 8 Qualification test

| Status | Definition |
|-------------------|--|
| ✗ Failure | Gaussmeter measurements are different from the ones taken by the magnetic sensor after calibration |
| ✓ Test completion | In any angle, after calibration, gaussmeter and magnetic sensor measurements are equal. |

The LSM303DLHC sensor must operate properly, taking measurements similar to the ones taken with Gaussmeter (there might be a slight variation).

Manufacturing of the magnetic fields in three dimensions

As we did not have a 3D magnetic field generator, we had to make it ourselves. To do so, we created 3D Helmholtz coils as shown in the figure below.



Figure C.7 13 3D Helmholtz coils

This field generator has three pairs of coils with different sizes $L_1 = 70 \text{ cm}$, $L_2 = 73 \text{ cm}$ and $L_3 = 76 \text{ cm}$. All together form a cube. Each pair produces a magnetic field on X, Y and Z axis respectively.

To estimate the number of turns of copper wire that must be given to each coil, we use the law of Biot-Savart for a square loop:

$$B = \frac{N\mu_0 a^2}{\left[\left(\frac{d}{2}\right)^2 + a^2\right]^{\frac{3}{2}}} \cdot I \quad (\text{Eq. C7 19})$$

And we obtain:

- For the coil of side 70 cm $\rightarrow N = 149$ turns
- For the coil of side 73 cm $\rightarrow N = 146$ turns
- For the coil of side 76 cm $\rightarrow N = 144$ turns

To generate a uniform field separation between pairs of coils must be $0.54 \cdot L$.

The zone that has a uniform magnetic field is delimited by $0.54 \cdot L \cdot 37 \text{ cm}$. We manufactured the coils with these data. The main features of these coils are shown in the following table.

Table C.7 9 Coils features

| Field | Coil | L (cm) | R (Ω) | Difference | I (A) | B* |
|-------|------|--------|----------------|------------|-------|----|
|-------|------|--------|----------------|------------|-------|----|



| | | | | (Ω) | (%) | | (Gauss) |
|-------|-------|------|-------|------|------|------|---------|
| B_x | X_1 | 73.2 | 37.72 | 0.2 | 0.53 | 1.03 | 2.05 |
| | X_2 | 73.2 | 37.52 | | | 1.03 | 2.13 |
| B_y | Y_1 | 76.2 | 38.18 | 0.1 | 0.26 | 1.03 | 2.56 |
| | Y_2 | 75.9 | 38.28 | | | 1.03 | 2.54 |
| B_z | Z_1 | 70.9 | 36.95 | 0.23 | 0.62 | 1.03 | 2.37 |
| | Z_2 | 70.6 | 37.18 | | | 1.03 | 2.25 |

***B:** Magnetic field measured in the middle of each coil.

Sensor Calibration in the Laboratory

In order to run different tests with the sensor LSM303DLHC, firstly, we need to calibrate this sensor.

This calibration is done via software. The steps to follow are:

- Select the range of measures in which will the sensor work.
- Calculate quantum of ADC.

$$\Delta = \frac{\text{Range}}{\text{Values}} \quad (\text{Eq. C7 20})$$

Where:

- **Δ:** Quantum.
- **Values:** Number of digital values that the sensor can take. [2,047; -2,048]. Then Values is always equal to 4,095.
- **Range:** Values of the range in which is configured the sensor. For example, if we configure the sensor to work in a range ± 1.3 gauss the value that we use in this equation is $1.3+1.3 = 2.6$
- Multiply the value measured by the quantum.

Test

With the above, we can now perform tests to see how the magnetic sensor behaves, introducing it into the magnetic field generator as it can be seen in the following figure.

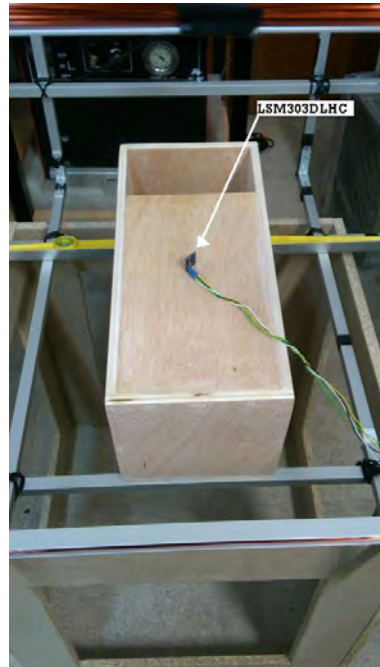


Figure C.7 14 Position sensor

To generate the field, we use the bipolar operational power supply/amplifier, KEPCO, model: BOP 50-8M 0 to $\pm 50V$, 0 to $\pm 8A$, controlled via MATLAB and GPIB. We check the measurements with the gaussmeter model: GM08-0822, shown in the figure below.

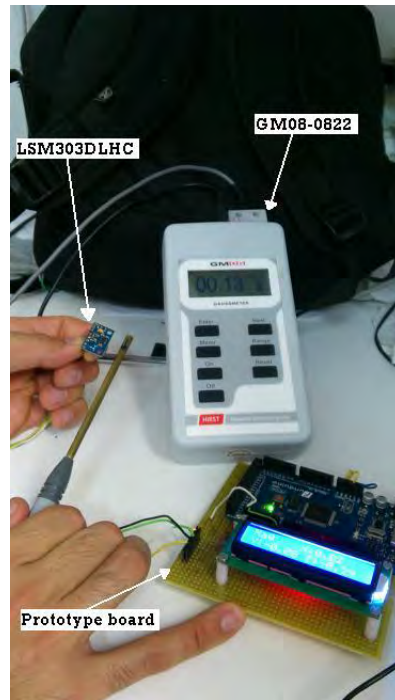


Figure C.7 15 Instruments

The results can be seen in the prototyping board, shown in the LCD. For testing purposes, we are using an Arduino board.

To take the measurements we followed the configuration shown in the following image:

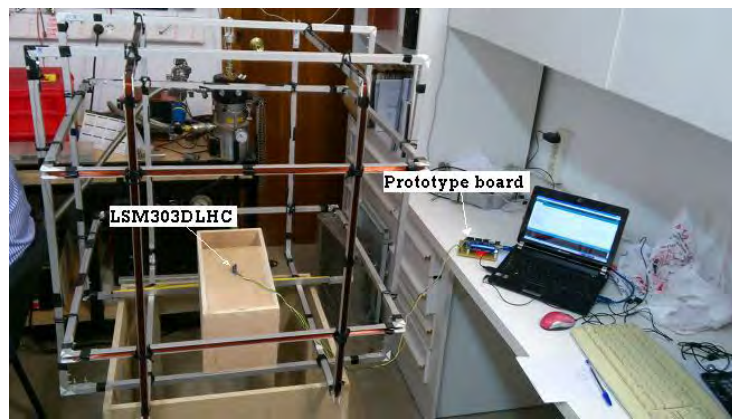


Figure C.7 16 Measurements

Results

As described in test process, a compass is placed in the middle of the two coils. The axis that joins the centre of the two coils has to be perpendicular to the needle of the compass when it can freely point to north.

The source generator is switched on until the compass needle points 45° with respect to the initial position. The values applied to the coils are described in the following table:

Table C.7 10 Voltage and intensity applied to the coils

| Measure n° | 1 | 2 | 3 | 4 | 5 |
|---------------------------|--------|--------|--------|--------|--------|
| voltage ± 0.01 V | 9.18 | 9.15 | 9.23 | 9.19 | 9.18 |
| Intensity ± 0.0001 A | 0.1214 | 0.1220 | 0.1216 | 0.1211 | 0.1215 |
| angle value $\pm 1^\circ$ | 45 | 44 | 45 | 45 | 46 |

Once those values are known, the Earth's magnetic field is calculated and the values shown in Table C.7 11 are obtained.

Table C.7 11 Earth's Magnetic Field estimated

| Measure n° | 1 | 2 | 3 | 4 | 5 |
|--|-----|-----|-----|-----|-----|
| Earth's m. f. $\pm 0.3 \cdot 10^{-6}$ T | 8.2 | 8.9 | 8.7 | 7.5 | 8.3 |

Earth's magnetic field measured by our sensor is shown in Table C.7 12.

Table C.7 12 Earth's Magnetic Field measured

| Measure n° | 1 | 2 | 3 | 4 | 5 |
|--|-----|-----|-----|-----|-----|
| Earth's m. f. $\pm 0.8 \cdot 10^{-6}$ T | 8.8 | 8.9 | 8.7 | 8.8 | 8.7 |



Because of the similitude of both tables, we can finally conclude that our magnetic sensor measures as expected.

C.7.4 Power Electronics Test

Purpose

Test the Step-Down voltage regulator in order to check the efficiency of the LM2576.

Material and environmental factors needed

- 2 x Multimeters (voltage and current).
- Banana wires.
- Laptop (to collect the data).
- Power supply generator.
- Bakelite perforated breadboard
- Electronic components: Step-Down voltage regulator (LM2576), capacitors, inductor, diode, power resistor ($10\ \Omega$).
- Wires to test.
- Solder and tin.

Test process

In the laboratory, calculate the efficiency of the LM2576 to know if this component is adequate for our experiment.

Test facility

Build the step down voltage regulator circuit in a breadboard.

Simulated scenario

- The scenario simulates the situation and conditions that the PCBs will withstand. To have this, we supply 28 V with the power supply generator.

General procedure:

1. Sold the components to the breadboard.
2. Connect the banana wires between the power supply generator and the breadboard.
3. Measure the current changing the input voltage (15 V - 30 V) to know the efficiency in different situations.
4. Measure the current at relevant points and take the data.

Qualification tests

When a test is intended to show formal compliance with contract requirements, the following definitions are recommended:

Table C.7 13 Qualification test

| Status | Definition |
|-------------------|---|
| ✗ Failure | To have a low efficiency and need to change the step down voltage regulator. |
| ✓ Test completion | To have a high efficiency and not need to change the step down voltage regulator. |

Final verification

The LM2576 has a high efficiency (80 % more or less). This component is correct for our experiment. More details in Power Electronics Test.

C.7.5 Thermal Test

Purpose

To use low temperature tests to obtain data to help evaluate effects of low temperature conditions on material safety, integrity and performance during storage, operation and manipulation. This method is used to evaluate material likely to be deployed in a low temperature environment during its life cycle and the effects of low temperature have not been assessed during other test (e.g. low pressure tests).

Low temperatures have adverse effects on almost all basic material. As a result, exposure of material to low temperatures may either temporarily or permanently impair the operation of the material by changing its physical properties.

Material and environmental factors needed.

A low temperature chamber or powerful freezing refrigerator is needed to achieve this test.

The exposure duration will be of 4 hours to simulate the same environment the experiment is going to experience during flight.

Data acquisition is needed in order to register chamber temperature vs time conditions and tested item temperatures.

Test process



In the laboratory, make sure that the rate of temperature changing do not exceed 1 °C per minute to prevent thermal shock at the beginning of the test.

Test facility

The tested item must have all its parts plugged and connected, and electronics must be in operating conditions in order to ensure that we test the real experiment conditions. Temperature sensors are needed in critical components to register the minimum temperature during experiment and its relationship with the possible malfunction of the electronics parts.

Simulated scenario

The tested item will be exposed to -80 °C. Electronics may be sensitive to low temperatures causing its malfunction. The exposure time will be as near as possible to 4 hours to ensure that hard cold situations do not affect at all to the tested item.

The air humidity is not a problem because we want to test the resistance of the item to humidity/condensation conditions too. So no dry air is needed.

General procedure

1. With the tested item in its operational configuration and installed in the test chamber, adjust the chamber air temperature to -80 °C, at a rate of approximately 0.8 °C/min (from 25 °C to -80 °C in \approx 2 hours). If the freezing rate is superior, then freeze the tested item as fast as possible.
2. Make a visual examination of the tested item as chamber access limitations will allow, and document the results. Make sure that electronics keep working. In case of electronics failure, register the minimum temperature of operation and stop the test. Go to step 2.i.
 - i. Document which element has failed (thermal patch, insulation... document it so the team can make the necessary changes), repair/change it and retake the experiment in step 1.
3. Once the minimum temperature arrives, keep it for at least 2 hours more, and document any incidence occurred (ice formation, electronics malfunction, etc.).

4. Warm the freezing chamber to a rate of 11 °C/min, or as fast as possible. With this step we want to test if the experiment withstands thermal shock.
5. Once finalized, complete a visual examination of the tested item and document the results. Is there any bending or permanent deformation? Do the electronics work properly (important: not only work, but work properly, e.g., there's no malfunction)? Is there any other anomaly caused by the intense cold (frozen parts that becomes fragile due to cold)? Document it. If any anomaly is observed, go to step 2.i.

Qualification test

Table C.7 14 Qualification test

| Status | Definition |
|-------------------|---|
| ✗ Failure | Any of the following cases: <ul style="list-style-type: none"> • Plastic is broken due to cold. • Insulation does not protect the test item as intended. • Humidity problems (condensation, electronics failure due to ice, ...) |
| ✓ Test completion | Electronics work as intended, insulations have protected the item as simulated numerically, no part of the tested item is weaker due to cold, and humidity does not affect the experiment. |

References

The methods shown here can be found in Method 502.5-1 to 500.5-9 in [45].

Set up

The test was performed on September 22nd. The facilities, located in the Universitat Politècnica de Catalunya, were provided by TORMES 2.0 team. The chamber has the following features:

Table C.7 15 Chamber features

| | |
|-----------------------------|---------|
| Minimum temperature reached | -196 °C |
|-----------------------------|---------|

| | |
|--------------------------|----------------------------|
| Minimum pressure reached | $1 \cdot 10^{-6}$ mbar |
| Leakage level | $1 \cdot 10^{-8}$ mbar l/s |

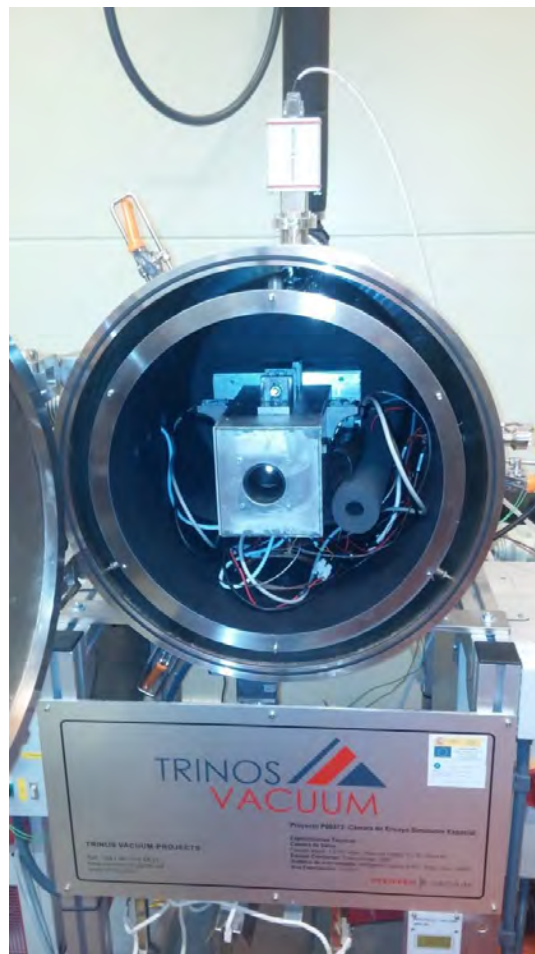


Figure C.7 17 Thermal-vacuum chamber used

During the entire test, the experiment was fully operational. The temperature was monitored with the following devices:

Table C.7 16 Temperature sensors and monitored items

| Sensor | Monitored item |
|--------|----------------|
| DS1621 | Outer PCB |
| TC74 | Camera |

| | |
|------------------------------|--------|
| Raspberry CPU sensor | CPU |
| Chamber temperature sensor 1 | Camera |

Test results

This test shows the evolution of the monitored temperatures. The pressure evolution can be seen in Table C.7 15.

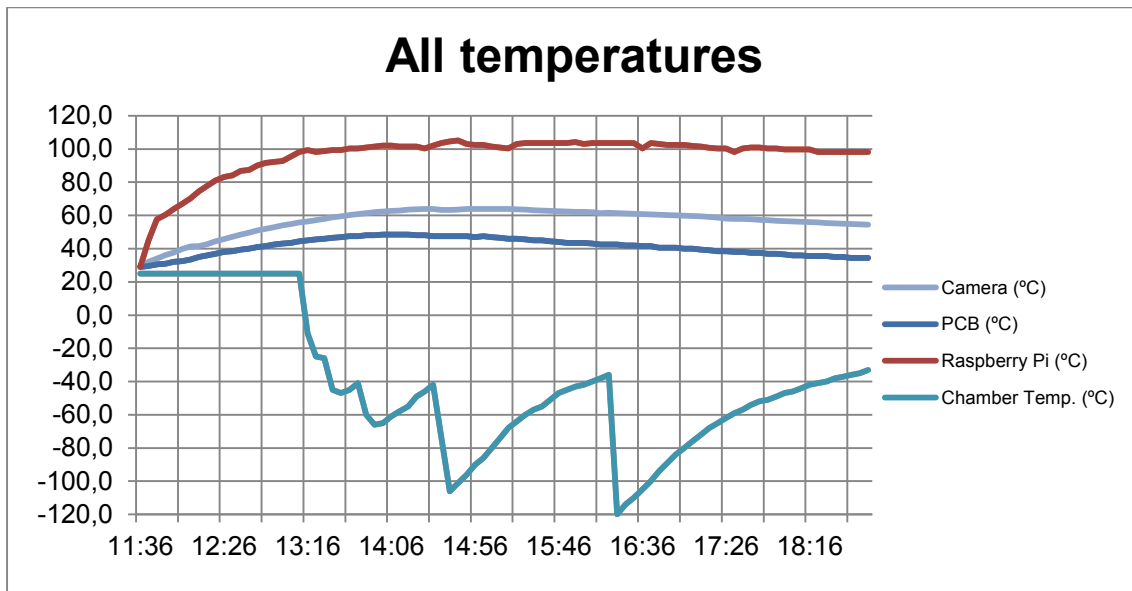


Figure C.7 18 Temperature evolution

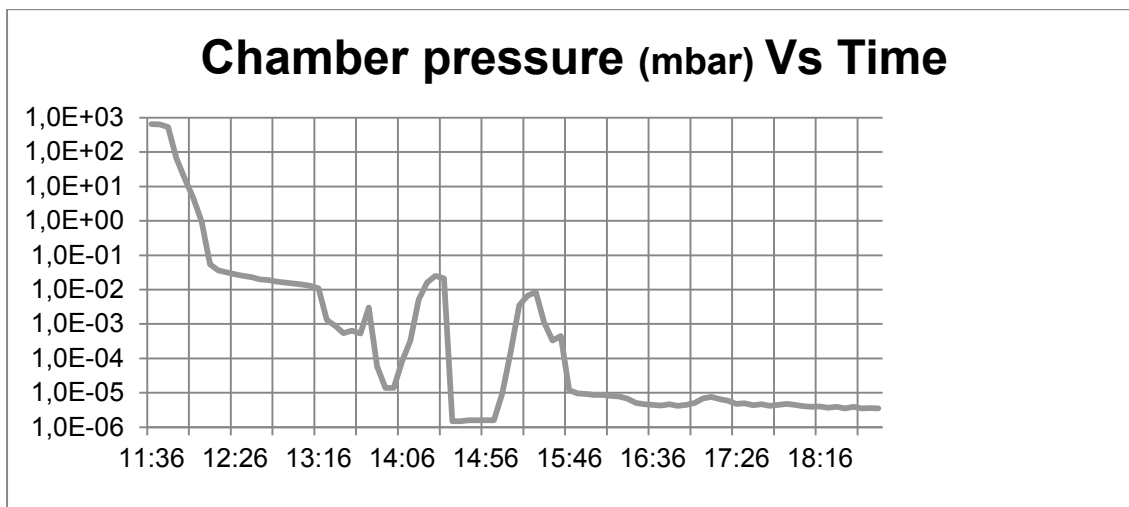


Figure C.7 19 Pressure evolution

The Raspberry Pi reached a steady state near to 100 °C and, according to the RPI datasheet, the maximum admissible temperature is 85 °C. However, despite of a higher temperature in the CPU, its performance did not decrease at any time. As observed in the previous graph, the steady state was maintained during 6 hours.

The outer PCB sensor measured maximum temperatures of 50 °C. Once the liquid nitrogen was injected, the minimum temperature measured—at the end of the test—was 34 °C.

The camera plot is similar to the PCB plot, but temperatures were higher. The images taken did not present any error, even at the maximum temperature reached (64 °C).

Thermal simulations comparison

Outer box simulations with SolidWorks gave higher temperatures than the ones measured during the TVAC test (80 °C simulated, 65 °C measured). This incongruence can be explained because of the differences between the simulated XPS insulation and the real one. There is about 25 % less XPS in the real outer box than the simulated one. Considering this, camera temperature after a 5 hours flight is predicted to be 60 °C in a hot case (-60 °C outside).

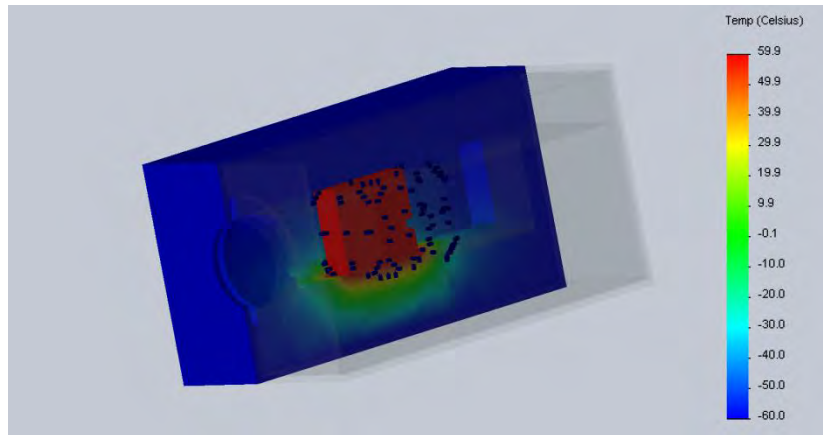


Figure C.7 20 Outer box thermal simulations redone

About the inner box simulation, the rising temperature of the RPI CPU (up to 100 °C) was not predicted. We think that the complex assembly makes hard to perform a reliable simulation.

Problems detected and solutions

Raspberry Pi CPU temperature was very high during almost the entire time of the TVAC test, exceeding datasheet temperature range. Despite of the experiment being working properly, we have decided to attach a heat sink to it, like the one depicted in 4.6.1.4. Reducing the XPS insulation is not a safe solution because we cannot perform another TVAC test and thermal simulations may be not helpful enough. Furthermore, to create new thermal bridges will increase the inner box assembly complexity.

During the test, a substance appeared on the internal side of the lens, as shown in the image below:



Figure C.7 21 Blurry lens after the TVAC test

When we opened the TVAC chamber the following day, we proceeded to disassemble the outer box. It was found only on the inner side of the lens. There was no deposit detected on the PCB, camera, XPS isolant, etc. It had a strange smell, a dark colour and a greasy touch. We have enough reasons to think that the substance came from the baffle paint.

A whole new baffle with no paint is ready to be outgassed in a vacuum chamber. This new baffle can substitute the old one. Thus, we do not expect to have blurry images during the flight.

C.7.6 Power Consumption Test

Purpose

To prove if one pack of the gondola batteries (13 Ah) is enough for the total power consumption of our experiment.

Material and environmental factors needed

- 2 x Multimeters (voltage and current).
- Banana wires.
- Laptop (to control the sensors, camera, etc.).
- Ethernet cable.
- Power Supply Generator.

- Full experiment.

Test process

In the laboratory, calculate the total power (and current) consumption of our experiment.

Test facility

Turn on and turn off the different parts and components of our experiment, and measure the voltage and current in some points.

Simulated scenario

The simulated scenario is the future situation that we will have in the launch.

To do this, we turn on and turn off the devices of our experiment.

General procedure:

1. Connect the banana wires between the power supply generator and our experiment and turn on the full experiment.
2. Turn on and turn off the different devices of the experiment by software control.
3. Measure the current in the relevant points and take the data.

Qualification tests

When a test is intended to show formal compliance with contract requirements, the following definitions are recommended:

Table C.7 17 Qualification test

| Status | Definition |
|-------------------|---|
| ✗ Failure | One pack of batteries cannot withstand the total current consumption and more packs are needed. |
| ✓ Test completion | One pack of batteries is needed in our experiment. |

Final verification

The experiment has a correct consumption to endure the entire flight. More details in Power Electronics Test.



C.7.7 Raspberry Pi Test

The times measured in test 7 (Test Plan), were obtained with the system call `gettimeofday()`, which has an accuracy of a microsecond. The value measured in each subtest has followed the following procedure:

1. Isolation of the code that has to be measured
2. Initialisation of two variables that stores the initial and the final instant: `struct timeval initial, final`
3. Measure of the initial instant at the beginning of the isolated code with `gettimeofday(&initial, NULL)`
4. Measure of the final instant at the end of the isolated code with `gettimeofday(&final, NULL)`

The test has been made in favourable conditions. The workload of the Raspberry Pi was minimal: no other user processes were running and only the Ethernet connection, the screen to view the results and the camera were connected to the computer. The test has been repeated 20 times, each of them measuring the time spent in 1,000 images. All the results are shown in the following table.

Table C.7 18 Test 7 results

| | Reading and memory allocation (s) | Storing in the SD (s) | Reading, memory allocation and storing in the SD (s) |
|-------------------|--|------------------------------|---|
| 01 – 1,000 Images | 200.243 | 31.018 | 267.786 |
| 02 – 1,000 Images | 200.049 | 29.282 | 269.753 |
| 03 – 1,000 Images | 199.967 | 29.382 | 267.952 |
| 04 – 1,000 Images | 199.964 | 29.056 | 267.694 |
| 05 – 1,000 Images | 199.915 | 30.859 | 267.226 |
| 06 – 1,000 Images | 200.373 | 30.294 | 268.623 |
| 07 – 1,000 Images | 200.037 | 29.779 | 267.290 |
| 08 – 1,000 Images | 200.234 | 29.486 | 268.560 |
| 09 – 1,000 Images | 200.228 | 29.886 | 268.956 |
| 10 – 1,000 Images | 199.974 | 31.351 | 268.166 |
| 11 – 1,000 Images | 200.178 | 30.140 | 267.687 |
| 12 – 1,000 Images | 200.035 | 30.768 | 266.815 |
| 13 – 1,000 Images | 200.036 | 29.219 | 267.331 |
| 14 – 1,000 Images | 200.037 | 29.344 | 268.483 |
| 15 – 1,000 Images | 200.045 | 29.003 | 268.368 |
| 16 – 1,000 Images | 199.975 | 28.885 | 268.688 |
| 17 – 1,000 Images | 200.368 | 29.623 | 269.758 |



| | Reading and memory allocation (s) | Storing in the SD (s) | Reading, memory allocation and storing in the SD (s) |
|---------------------------|--|------------------------------|---|
| 18 – 1,000 Images | 199.912 | 29.846 | 268.687 |
| 19 – 1,000 Images | 199.975 | 30.669 | 267.619 |
| 20 – 1,000 Images | 200.044 | 28.722 | 266.957 |
| Mean- 1 image (ms) | 200.079 | 29.831 | 268.120 |
| Max frequency (Hz) | 4 (4.998) | 33 (33.523) | 3 (3.730) |

C.7.8 Magnetometer calibration Test

Purpose

Because of hard and soft iron disturbances in magnetometer measurements, it is necessary to build a software that reads from the magnetic sensor, removes hard and soft iron contributions and returns real magnetic field information. This software needs to be tested in order to ensure that the corrections are performed properly and test if some parameters used for calibration are well calculated.

Material and environmental factors needed

The magnetic chip LSM303DLHC and a computer in reading data mode is needed.

Test process

Test facility

Place the sensor inside the outer box. This will give us the soft and hair iron disturbances because of the aluminium and metals of boxes and PCBs and magnetic fields created for the operation of the electronics.

Simulated scenario

We want to simulate the real operating scenario, in which we have magnetic field disturbances because of metallic parts of boxes, magnetic field created by electronics (especially coils) and a continuous spinning movement, as the gondola ascension is not smooth. We need a software that measures the spinning angle and determinates the gondola position.

We have to clarify that in Kiruna the magnetic conditions are going to be different and we will have to perform a characterisation of this conditions there.

The objective of this test is make the same characterisation and measurement procedure that the one we are going to perform in Kiruna in order to see if corrections done via software and parameters used for that are correct.

General procedure

1. Place the magnetic sensor inside the outer box with all electrical components switched on. Avoid being close to high metallic constructions or any other object that might alter the magnetic field.
2. Rotate or spin the outer box only in the horizontal plane. Record the measurements taken with the magnetic sensor. Do this spinning movement changing the speed: first, faster; and then, slower. Perform this during, at least, 10 spins. If we represent this measurements, we should obtain something like Table C.7

19

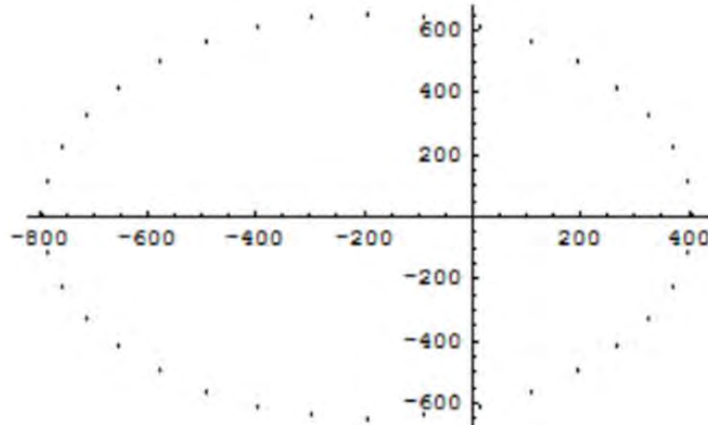


Figure C.7 22 Uncalibrated magnetometer measurements

3. Use the next algorithm to calibrate the measurements (where *raw()* are the raw or direct measurements given by the magnetic sensor and *max()* and *min()* are the maximum and minimum of those values respectively) :

- a. $\text{Offset}(x) = [\min(x) + \max(x)] / 2$
 $\text{Offset}(y) = [\min(y) + \max(y)] / 2$
- b. $\text{VM}(x) = \max(x) - \text{offset}(x)$
 $\text{VM}(y) = \max(y) - \text{offset}(y)$
- c. $\text{Vm}(x) = \min(x) - \text{offset}(x)$
 $\text{Vm}(y) = \min(y) - \text{offset}(y)$
- d. $\text{Avg}(x) = [\text{VM}(x) - \text{Vm}(x)] / 2$
 $\text{Avg}(y) = [\text{VM}(y) - \text{Vm}(y)] / 2$
 $\text{TotalAvg} = [\text{Avg}(x) + \text{Avg}(y)] / 2$
- e. $\text{Scale}(x) = \text{TotalAvg} / \text{Avg}(x)$
 $\text{Scale}(y) = \text{TotalAvg} / \text{Avg}(y)$
- f. $\text{Pre_trim}(x) = \text{raw}(x) - \text{offset}(x)$
 $\text{Pre_trim}(y) = \text{raw}(y) - \text{offset}(y)$
- g. $\text{Trim}(x) = \text{Pre_trim}(x) \cdot \text{scale}(x)$
 $\text{Trim}(y) = \text{Pre_trim}(y) \cdot \text{scale}(y)$

4. The *trim()* measurements are the calibrated ones. If we represent this we will obtain the following figure:

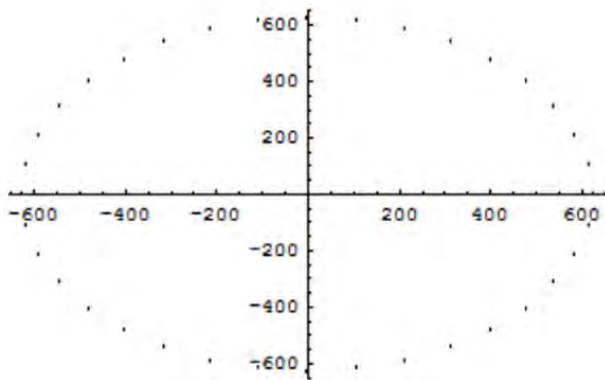


Figure C.7 23 Calibrated magnetometer measurements

Qualification test

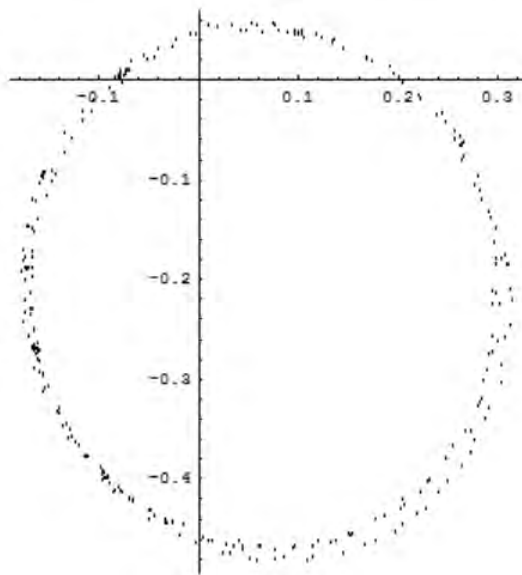
The verification matrix for this test is very simple:

Table C.7 19 Qualification test

| Status | Definition |
|-------------------|--|
| ✗ Failure | The calibrated data is not circle-shaped when represented. |
| ✓ Test completion | The calibrated data is circle-shaped when represented |

Results

First, we take raw data by spinning the experiment as depicted before. If we represent it, we get Figure C.7 24

**Figure C.7 24 Raw data represented**

As we can see in the figure above, data is ellipse-shaped and it is not centred in $(0, 0)$, which means they have an offset.

Then, we apply the calibration explained in *General Procedure* and represent the data, shown in Figure C.7 25

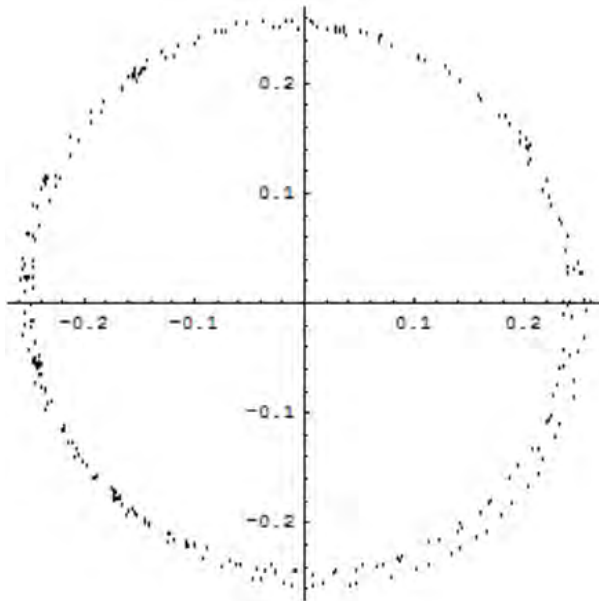


Figure C.7 25 Data after calibration

The data now has the shape of a circle, centred in (0, 0), that means no offset. For this reason, we conclude that the test is completed and successfully performed.

C.7.9 Temperature Sensor Test

Purpose

To ensure the right data acquisition by the temperature sensors in order to discard malfunctioning. This sensor is important because it is going to register temperatures in the camera body during flight, and it is the sensor we are going to use in the facilities during thermal test. For that reason, we need to ensure that this sensor registers properly the temperatures and discard a possible overheating in camera body.

Material needed

It is necessary to put the sensor into a cold and hot scenario to prove its good performance in any situation, even rapid changes. For this reason, we will perform this test before the thermal test.

The facilities used for this test should have a way to provide the real temperature inside them, so that we can compare this value with the one provided by our sensor.



Test process

Test facility

Place the sensor already configured to take measurements inside the provided facility, near the sensor that is going to provide us the real temperature. The objective of placing them close is to minimize the possible different readings. These data is going to be collected by a computer. There is no a special requirement in temperature change rate.

Simulated scenario

We want to simulate the final flight of our experiment, and prove that the temperatures given by the sensor are correct and that we can trust them to make further calculations.

General procedure

1. Switch on the temperature sensor, the thermal chamber and the elements which are going to give us the real temperature inside the chamber.
2. Wait a little until the first temperature changes are effective inside.
3. Read the real temperature inside the chamber (thermometer provided with the facility) and the reading given by our temperature sensor.
4. Do these readings when temperature is descending, in the lowest point and ascending (the temperature sensor might be sensitive to one-direction temperature changes, we need to test it when the chamber is freezing and warming).
5. Collect all data and make a comparison.

Qualification tests

Table C.7 20 Qualification test

| Status | Definition |
|-------------------|--|
| ✗ Failure | If error is higher than 5 %. That means that sensors have a high error while measuring and they are not reliable enough. |
| ✓ Test completion | The chamber temperature sensor data and the one taken by the sensors do not differ more than a 5 %. |

Results

As described before, temperature sensors are placed inside the thermal and vacuum chamber. They record data temperature and are compared with data provided by chamber operator (assuming those data can be taken as a reference).

In table C.7 21, left column, are found the values registered by TC74 sensor. In the same table, centre column, are found the values registered by the thermometers inside the chamber. In the right column is found the relative error (that can't overcome the 5 % to get this test achieved).

All data registered is not shown, because this test was performed during several hours, taking one measure each minute. Only representative data is shown in table Table C.7 21.

Table C.7 21 Data measured during the test

| TC74 Sensor temperature | Chamber temperature | Relative Difference (%) |
|-------------------------------|------------------------|-------------------------------|
| 25,6 | 27,1 | 6,64 |
| 30,9 | 32,8 | 5,02 |
| 35,1 | 36,9 | 3,76 |

| TC74 Sensor temperature | Chamber temperature | Relative Difference (%) |
|-------------------------------|------------------------|-------------------------------|
| 40,8 | 41,9 | 4,03 |
| 45,2 | 45,5 | 1,95 |
| 50,8 | 52,7 | 3,05 |
| 55,4 | 56,9 | 0,18 |
| 60,6 | 61,8 | 3,04 |
| 65,4 | 66,4 | 0,45 |
| 70,1 | 71,1 | 0,42 |
| 75,3 | 76,9 | 0,66 |
| 80,7 | 80,7 | 0,62 |
| 85,2 | 85,6 | 1,85 |

Not many values overcome 5 %. Especially when temperatures are high. When temperatures are low, the relative error is stable around 3-4 %. Except those values, the rest are proper to pass this test.

Therefore, we can give a conditional pass to this test, assuming that some values (not many) can have an error superior to 5 %. That is the threshold specified to make a good measure in the qualification test.

C.7.10 Computational Capability Test

Purpose

To test the processing frequency in order to test whether the S.5 requirement is fulfilled.

Material needed

Raspberry Pi and processing software.

Test process

In order to test the processing time with the real computational workload, the following conditions have been taken into account:

Test facility

Laboratory in the Faculty of Sciences with a Raspberry Pi in which the algorithm run.

Simulated scenario

The processing algorithm run along with the final software prototype, having into account the capturing, processing and storage of the images, with the capturing and storage of the accelerometer and the magnetometer measurements, as well as the sending of all the data collected.

To do so, a laptop has been used to run the client software.

General procedure

To obtain the most precise and reliable time measurements, the function `clock_gettime()`, along with the monotonic clock, `CLOCK_MONOTONIC`, have been used.

The time has been measured 5 times each time, for reliability reasons. The timestamp has been stored before the processing code and after it:

```
const int ITER = 5;
clock_gettime(CLOCK_MONOTONIC, &before);
for (count = 0; count < ITER; ++count) {
    obtainAttitude(image);
}
clock_gettime(CLOCK_MONOTONIC, &after);
```

Measured times

Some of the times measured are shown in the following table, along with the final mean and the maximum frequency allowed.

Table C.7 22 Times measured

| Iteration – Number of images | Mean time per image (s) |
|------------------------------|-------------------------|
| 0001 – 5 | 0.320448994 |
| 0500 – 5 | 0.302668449 |



| | |
|----------|-------------|
| 1000 – 5 | 0.337983548 |
| 1500 – 5 | 0.257142526 |
| 2000 – 5 | 0.370227360 |
| 2500 – 5 | 0.210931629 |

| | |
|--------------------------------|--------------|
| MEAN TIME PER IMAGE (s) | 0.3232118138 |
| Max Frequency (Hz) | 3 (3.0934) |

Qualification test

The results have to be compared with S.5 requirement to see whether it is fulfilled.

Table C.7 23 Qualification test

| Status | Definition |
|-------------------|--|
| ✗ Failure | The maximum frequency is lower or equal than 0.5 Hz. |
| ✓ Test completion | The maximum frequency is greater than 0.5 Hz. |

Results

The maximum frequency allowed by the processing algorithm is 3 Hz. Since S.5 requires that the system shall process the images with a frequency of 0.5 Hz, we can conclude that the requirement S.5 is fulfilled.

C.7.11 Connection Bandwidth Test

Purpose.

To measure the times spent in the sending of the collected data through a TCP connection restricted to 500 KiB/s at download and 0.1 KiB/s at upload. The final objective is to test whether the performance requirement S.6 will be fulfilled.

Material and environmental factors needed

A laboratory with a local network with both the Raspberry Pi and the Ground Segment laptop connected to it.

Test process

To simulate the real workload with the real connection restrictions, the following conditions have been taken into account:

Test facility

Laboratory in the Faculty of Sciences with a set up local network, including a router and a switch.

Simulated scenario

The local network of the test facility is much faster than the E-Link, so the bandwidth has to be restricted in order to simulate the real scenario. To test S.6 requirement, the restriction of the bandwidth has been the following:

- Download: 500 KiB/s
- Upload: 0.1 KiB/s

To do so, the application Trickle, which provides an easy interface to restrict connectivity speeds, has been used.

The simulated workload represents only the size of an image—1,228,800 B. Since this size is five orders of magnitude larger than the heavier of the other data—the magnetometer and accelerometer measurements size is 14 bytes with the timestamp overhead, the test results can be extrapolated to the real scenario.

To make the test even more realistic, the final software prototype has been used, taking into account the capturing, processing and storage of the images, along with the capturing and storage of the accelerometer and the magnetometer measurements.

As in the real experiment, the server-side software ran in the Raspberry Pi and the client-side software in the Ground Segment laptop.

General procedure

To obtain the most precise and reliable time measurements, the function `clock_gettime()`, along with the monotonic clock, `CLOCK_MONOTONIC`, have been used.

The time has been measured in the client side software, storing the timestamp before the downloading code and after it:



```

clock_gettime(CLOCK_MONOTONIC, &before);

for(k=0; k<num_images; ++k) {
    getImage(image_data);
}

clock_gettime(CLOCK_MONOTONIC, &after);

```

To ensure the test is correct, the time has been measured with different values of num_images, from $2^0 = 1$ to $2^9 = 512$. Furthermore, each set of images have been repeated three times. The pseudo-code of the test is the following:

```

const int ITER_TEST = 10;
const int REDUNDANCY = 3;
int num_images = 1;

for(i=0; i<ITER_TEST; ++i) {
    elapsed_sum = 0;

    for(j=0; j<REDUNDANCY; ++j) {

        clock_gettime(CLOCK_MONOTONIC, &before);
        for(k=0; k<num_images; ++k) {
            getImage(image_data);
        }
        clock_gettime(CLOCK_MONOTONIC, &after);

        elapsed = diff_times(&before, &after);
        elapsed_sum += elapsed;

        write_to_file(elapsed);
    }

    elapsed_mean = elapsed_sum/REDUNDANCY;

    write_to_file(elapsed_mean);

    num_images *= 2;
}

```

Measured times

The results of the time measurements can be seen on the following table:

Table C.7 24 Raw time measurements

| Time spent in receiving (s) | |
|------------------------------------|-------------|
| 1 image | 2.401633827 |



| | |
|-------------------------|--------------------|
| | 2.391886355 |
| | 2.391886355 |
| MEAN 1 image | 2.398404272 |

| | |
|--------------------------|--------------------|
| 2 images | 4.803189357 |
| | 4.802953295 |
| | 4.803244394 |
| MEAN 2 images | 4.803129015 |

| | |
|--------------------------|--------------------|
| 4 images | 9.605646219 |
| | 9.605729480 |
| | 9.606135585 |
| MEAN 4 images | 9.605837094 |

| | |
|--------------------------|--------------------|
| 8 images | 19.21159940 |
| | 19.21157621 |
| | 19.21235654 |
| MEAN 8 images | 19.21184405 |

| | |
|---------------------------|--------------------|
| 16 images | 38.42340545 |
| | 38.42380857 |
| | 38.42470289 |
| MEAN 16 images | 38.42397230 |

| | |
|---------------------------|--------------------|
| 32 images | 76.84931527 |
| | 76.84867917 |
| | 76.84822685 |
| MEAN 32 images | 76.84874043 |

| | |
|---------------------------|--------------------|
| 64 images | 153.694629 |
| | 153.6943466 |
| | 153.6930958 |
| MEAN 64 images | 153.6940238 |

| | |
|----------------------------|--------------------|
| 128 images | 308.4145578 |
| | 307.3930926 |
| | 307.3895356 |
| MEAN 128 images | 307.7323954 |



| | |
|----------------------------|--------------------|
| 256 images | 614.7921378 |
| | 614.7839957 |
| | 614.7819652 |
| MEAN 256 images | 614.7860329 |

| | |
|----------------------------|---------------------|
| 512 images | 1,229.563639 |
| | 1,229.562114 |
| | 1,229.565023 |
| MEAN 512 images | 1,229.563592 |

Qualification test

The results have to be compared with S.6 requirement to see whether it is fulfilled.

Table C.7 25 Qualification test

| Status | Definition |
|-------------------|--|
| ✗ Failure | The maximum frequency is lower or equal than 0.1 Hz. |
| ✓ Test completion | The maximum frequency is greater than 0.1 Hz. |

Results

After some mathematics with the raw measurements, the results, including each set of images and the final result with the time spent in receiving one image, are the following:

Table C.7 26 Test 11 results

| | Time spent in receiving (s) | Mean – 1 image (s) |
|------------|-----------------------------|--------------------|
| 1 Image | 2.398404272 | 2.398404272 |
| 2 Images | 4.803129015 | 2.401564508 |
| 4 Images | 9.605837094 | 2.401459274 |
| 8 Images | 19.21184405 | 2.401480506 |
| 16 Images | 38.42397230 | 2.401498269 |
| 32 Images | 76.84874043 | 2.401523138 |
| 64 Images | 153.6940238 | 2.401469122 |
| 128 Images | 307.7323954 | 2.404159339 |
| 256 Images | 614.7860329 | 2.401507941 |
| 512 Images | 1,229.563592 | 2.401491390 |

| | |
|---------------------------|--------------------|
| Mean - 1 image (s) | 2.401455776 |
| Max frequency (Hz) | 0.4 |

As the maximum frequency allowed by the connection restrictions is 0.4 Hz, we conclude that S.6 requirement is fulfilled.

C.7.12 Vacuum Test

Purpose

Use low pressure (altitude) tests to determine if material can withstand and/or operate in a low pressure environment and/or withstand rapid pressure changes. Low pressure tests are needed to know the response of the physical and chemical characteristics of the experiment materials under rare pressure conditions, i.e.:

- Leakage of gasses or fluids.
- Deformation, rupture or explosion of sealed containers.

Material and environmental factors needed

A low pressure chamber is needed for this test. The real conditions need to be characterised mathematically to ensure the development of the test is as real as possible.

Test process

We need to ensure that the experiment withstands low pressure conditions as well as rapid decompression scenarios. For that reason, we propose two tests.

Test facility

Configure the tested item for operating, including electrical or mechanical parts. The tested item must be in the same conditions of operation that the ones that we will find in the real experiment in order to know the possible electronics heat dissipation problems due to low conductivity with air. No pressure metres are needed, just ensure that sealed parts and electronics work well.

Simulated scenario

In the real experiment, the tested item will be exposed to low/rare pressure conditions. That can be a problem, especially for those parts that involve air contained, such as foams, air inside protective chambers, or even fluids or lubricants that can expand due to low pressure conditions. In addition, the rapid

decompression can be a problem, because the pressure shocks involve more problems than a simple pressure change.

The pressure changes in real atmosphere are a lineal correlation with altitude.

General procedure

Due to the conditions mentioned before, we will perform 2 tests: one for low pressure conditions, and another one for rapid decompression.

Low pressure conditions

- With the tested item in its operational configuration, install it in the chamber and adjust the chamber air pressure to the corresponding pressure found at 26 km of altitude, i.e., 2.1 kPa. The change from normal to low pressure has to be made in 1h 30m (the estimated ascent time is 1h 43m), and done gradually, as shown in Figure C.7 26. In this picture, the blue line represents real atmosphere pressure profile, whereas the red line shows the laboratory pressure profile.

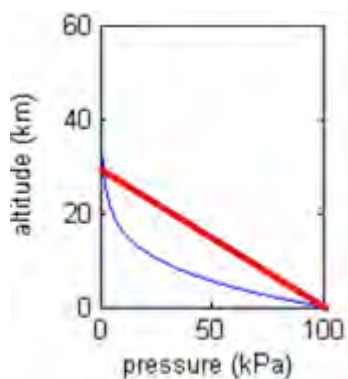


Figure C.7 26 Real atmosphere and laboratory pressure profiles

- Maintain the conditions for a minimum of one hour.
- Decompress the chamber at low rate, for example, from low to normal pressure in 30 min.

Rapid decompression



1. Follow the step 1 of the low pressure conditions test.
2. Maintain this stabilized low pressure for at least 10 minutes.
3. Decompress the chamber at high rate, which means from low to normal pressure in 10 minutes.

Qualification test

A visual inspection has to be made after 2 tests achieved.

Table C.7 27 Qualification test

| Status | Definition |
|-------------------|---|
| ✗ Failure | Any of the following cases: <ul style="list-style-type: none"> • Electronics failure. • Foams and/or insulators have increased their volume. • There is leakage or spill of liquids or insulating silicones. • Permanent deformations or bending due to pressure. • Glass broken or damaged. • Inflated or exploded components. |
| ✓ Test completion | There is no permanent deformations, the components with air inside them are not inflated or separated of where they are supposed to be, no glass breaking and no electronics failure. |

Electronics have to work perfectly, foams and insulators have to maintain their normal volume, and the regions that contain air inside them have to have their walls with no permanent deformations or bending.

If there's a conflictive component, it is necessary to substitute it and make sure that it can withstand low pressure conditions after reading its datasheet.

References.

The methods shown here can be found in Method 514.6, and Annexes A, B, C and D in [45].

Results



This test was realized simultaneously with Test 5, Thermal Test, and the results are shown in section Power Electronics Test.

C.7.5 Thermal Test.

C.7.13 Vibration Test

Purpose

To develop material to function in and withstand the vibration exposures of a life cycle including synergistic effects of other environmental factors, material duty cycle and maintenance, and to ensure that the structure and electronics are able to endure a short journey in a car trailer or cargo.

In general, the mechanical factors found in this environment are road shocks caused by large bumps and potholes.

Material and environmental factors needed

For all tested items, the material is placed inside a cargo in random positions to ensure we test all possibilities, such as shock with walls, falls or bounces. A duration of 20 minutes represents 240 km of transportation (two wheeled trailer and tracked vehicle), over the various road profiles found in the transport scenario, which are represented by:

- Coarse washboard (150 mm waves 2 m apart), at 8 km/h.
- Belgian block road, at 32 km/h.
- Radial washboard (50 mm to 100 mm waves), at 24 km/h.
- 50 mm washboard, at 16 km/h.
- 75 mm spaced bump, at 32 km/h.

Test process

Test facility

Configure the tested item for shipment including protective cases and/or packing. Place accelerometers inside the package to ensure the data acquisition is as realistic as possible.

Simulated scenario

The cargo has freedom to bounce, scuff and collide with other cargo and with the sides of the vehicle. The loose cargo environment includes conditions experienced by cargo transported in a vehicle traversing irregular surfaces. This test replicates the repetitive random shock environment incurred by cargo transported under these conditions.

The tested item must be placed in random places inside the cargo, and perform at least 3 tests.

The same conditions that we will find during item life cycle must be replicated, what means to have active and plugged all mechanical and electrical connections, and ensure that they are functional.

Accelerometers and sensors must be placed in properly places to ensure data acquisition is not influenced by position or external factors.

General procedure:

1. Mount the tested item on/in the vehicle as required in the test plan to simulate the same environmental conditions.
2. Apply low level vibration to the test item/fixture interface (low velocities in the roads specified in section *Material and environmental factors needed*). Verify that the instrumentation system functions as required.
3. Apply the required vibration levels (up to the maximum speed) to the test/fixture interface. Apply additional environmental stresses as required (as solar radiation or dust). Monitor vibration levels and, if applicable, tested item performance, continuously through the exposure.
4. When the required duration has been achieved, stop the vibration. Repeat steps 2 to 3 if new tests are needed.
5. Inspect the tested item, fixture and instrumentation. If there is a failure, wear, looseness or other anomalies are found, repeat test from step 1.
6. Ensure that instrumentation works properly after the test stops. If the instrumentation fails, repeat test from step 2.
7. Make a visual inspection including packing and hardware. Ensure that no mechanical degradation is found.



Qualification tests

When a test is intended to show formal compliance with contract requirements, the following definitions are recommended:

Table C.7 28 Qualification test

| Status | Definition |
|-------------------|--|
| ✗ Failure | "Materiel is deemed to have failed if it suffers permanent deformation or fracture; if any operation or assembly loosens; if any moving or movable part of an assembly becomes free or sluggish in operation". Ensure this statement is accompanied by references to appropriate specifications, drawings and inspection models. |
| ✓ Test completion | "A vibration qualification test is complete when all elements of the test item have successfully passed a complete test. When failure occurs, stop the test, analyse the failure, and repair the test item. Continue the test until all fixes have been passed a complete test. Qualified elements that fail during extended tests are not considered failures, and can be repaired to allow test completion". |

Final verification

The experiment is supposed to endure up to 10 g, so this vibration test should be accomplished without no problem.

References

The methods shown here can be found in Method 500.5-1 to 500.5-7 in [45].

Results

We used the recorded accelerations measurements to estimate how hard the vibration test was and to establish a comparison between this test and the mechanical simulations. By using MATLAB, the register is plotted as follows:

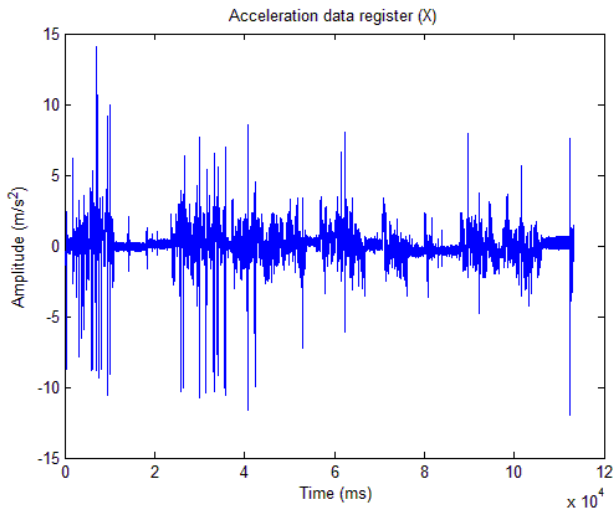


Figure C.7 27 Acceleration measurements in X axis

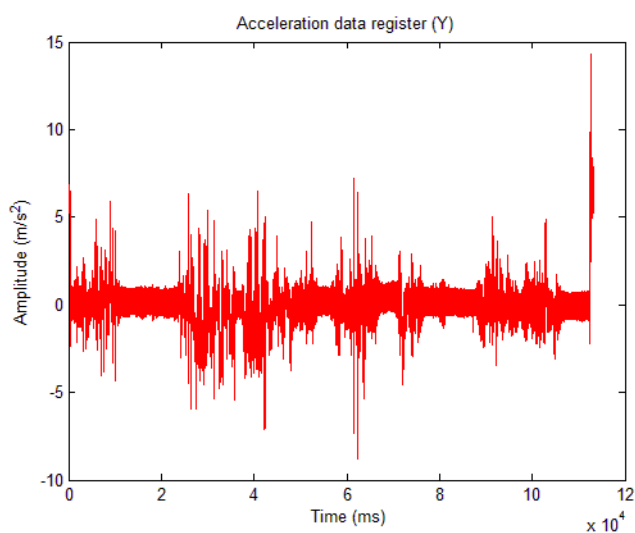


Figure C.7 28 Acceleration measurements in Y axis

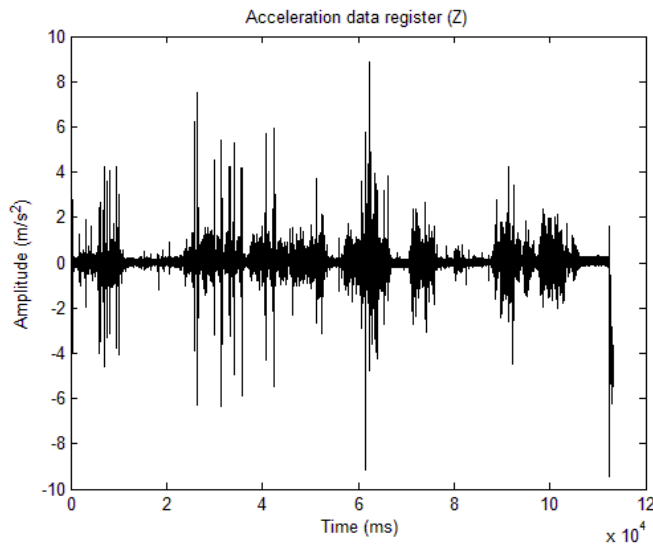


Figure C.7 29 Acceleration measurements in Z axis

Maximum accelerations were registered during the first part of the trip: the tough ride in the parking lot. A Fast Fourier Transformation provides a plot like this:

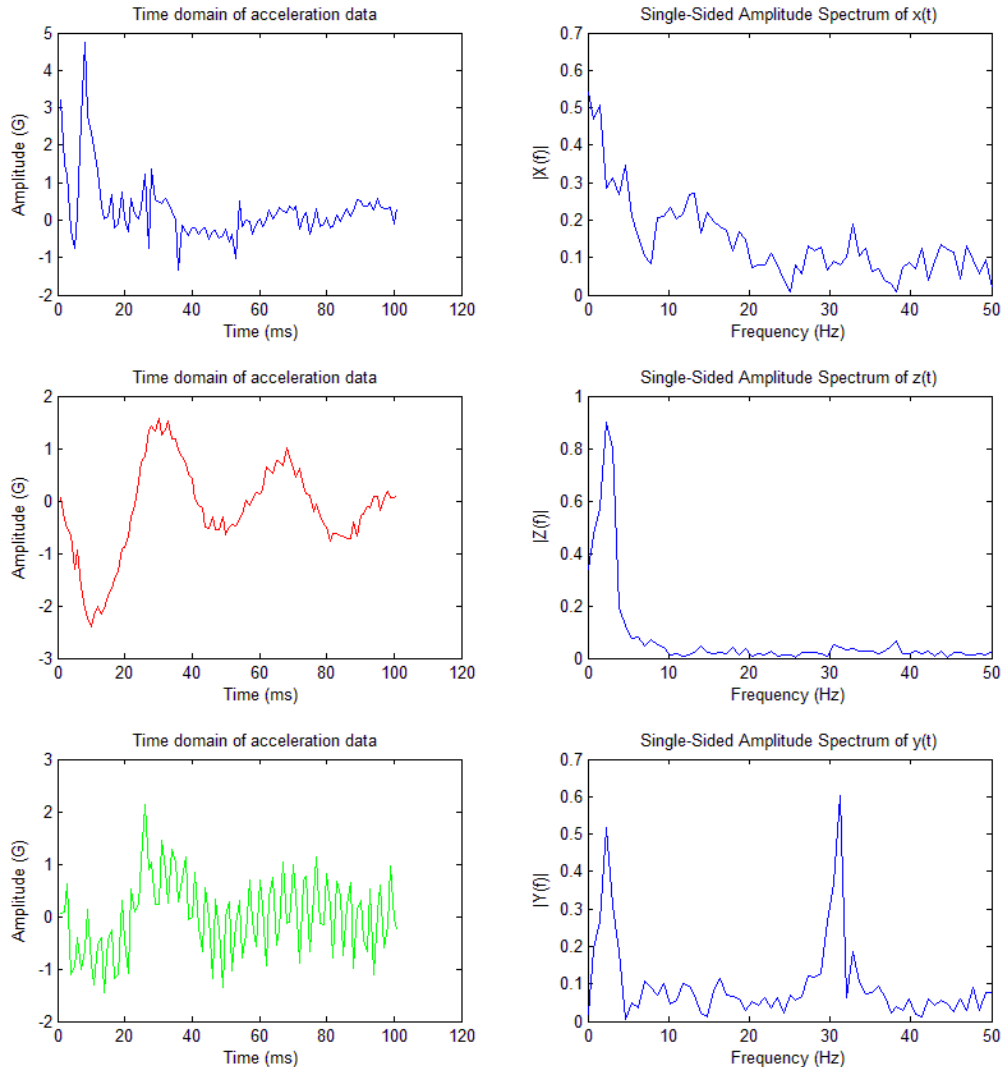


Figure C.7 1 Fast Fourier Transformation from the accelerometer measurements

These plots correspond with a possible bump during the second part of the ride. There is a main frequency noticeable: 30 Hz. It could be the frequency of the first vibration mode of the installed outer box and boom. Logically, this frequency is higher than the obtained in the mechanical simulation and the modal characterisation because the boom was longer than the one used in the simulations and combines stronger materials.

With a basic algorithm in MATLAB, we plotted the power spectral density (PSD) in the three axes. Results are as follows:

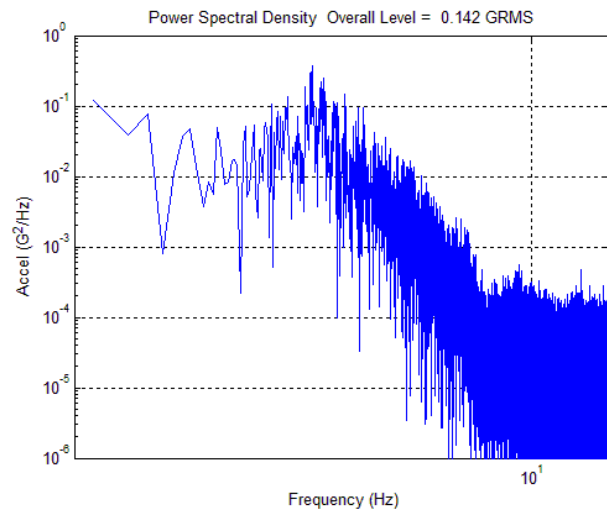


Figure C.7 30 PSD for X axis

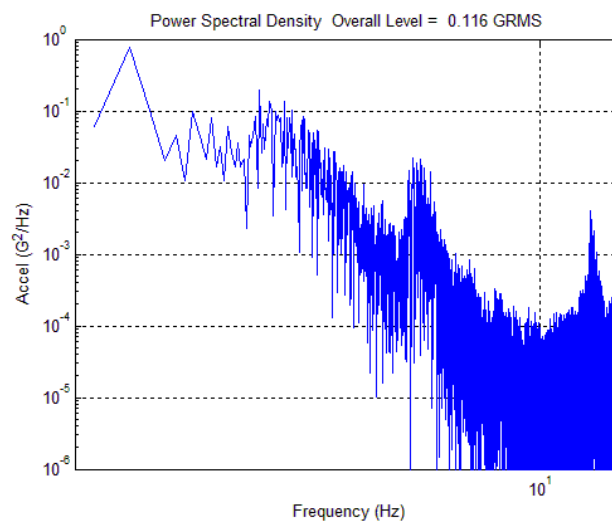


Figure C.7 31 PSD for Y axis

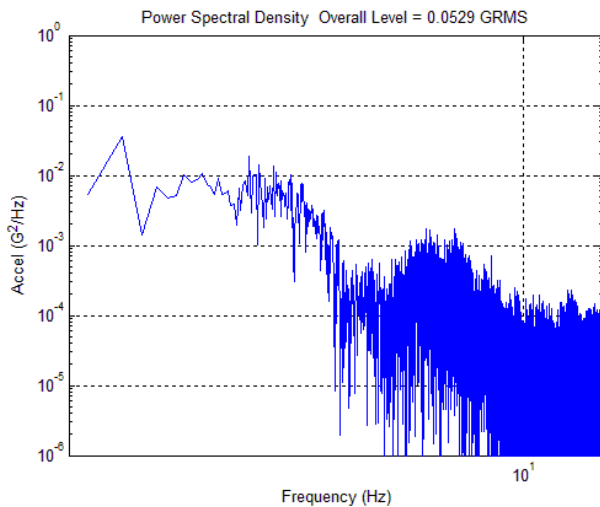


Figure C.7 32 PSD for Z axis

Compared with the standard PSD used in the random vibration simulation, the results of the test performed are similar to the simulated ones.

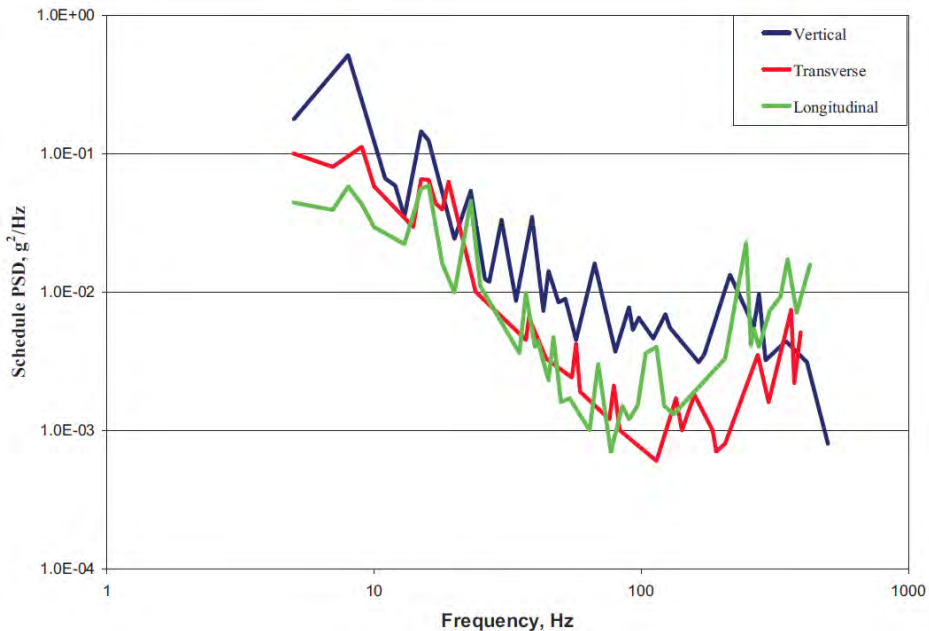


Figure C.7 33 Random vibrations from a composite wheeled vehicle

In conclusion, as there were no damage or malfunction detected, the experiment passed the vibration test successfully.



C.7.14 Fusible Test

Purpose

To know if the component chosen like current limiter was good for the experiment. Also, ensure that the voltages in some points of this component.

Material and environmental factors needed

- Multimeter.
- Breadboard.
- Wires.
- Solder and tin.
- Power Supply Generator.

Test process

In the laboratory, make sure that the circuit choose to the current limitator is correct.

Test facility

Place the components in the breadboard, with their wires in each pin of the ITS4141N.

Simulated scenario

The simulated scenario is the circuit that we will place in the inner and outer box PCBs later. To do this, we probe this circuit with the R_{GND} of 150Ω . When we knew the correct operation of this circuit in the breadboard, we sold it in the PCB.

General procedure:

8. Sold the wires to the component because this component is SMD and was impossible use it in the breadboard.
9. Connect the wires to the bread board and the V_{input} (from the Power Supply Generator) too.
10. Measure the voltage in the relevant points.

Qualification tests

When a test is intended to show formal compliance with contract requirements, the following definitions are recommended:

Table C.7 29 Qualification test

| Status | Definition |
|-------------------|--|
| ✗ Failure | Not to have the needed voltage in the output of this component with the resistor chosen. |
| ✓ Test completion | The voltage of the output of ITS4141N is adequate for the experiment. |

Final verification

The experiment is supposed to have an input of 28 volts.

References

The datasheet of this component can be found at [46].

C.7.15 I²C Bus Extender Test**Purpose**

The use I²C with long distances and low temperatures can damage the signal sent through the wires. In order to avoid this problem we use an I²C-bus extender.

The objective of this test is to ensure that we obtain a good signal quality in the inner box by using a 3 metre wire and to analyse how much the use of the I²C extender can improve the I²C signal.

Material and environmental factors needed

The materials used in this test are:

- Three metres of twister pair shielded wire.
- Oscilloscope
- I²C-bus extender (NXP P82B715)
- I²C Component (DS1621)
- Raspberry Pi

Test process**Test facility**

The test has to simulate a real communication between the boxes. Thus, we use the inner box PCB and the outer box PCB and we add two I²C-bus extender just in the output of the I²C port of the PCBs.

Simulated scenario

The scenario that we want to obtain is long distances between boxes in order to confirm if a good signal arrives to the other box by using a 3 metre wire.

General procedure:

11. Plug I²C-bus extender to I²C bus.
12. Link the boxes with a 3 metre wire.
13. Start to read the DS1621 sensor I²C data.
14. Measuring of peak-to peak voltage and time rise of the signal received at the end of the wire.
15. Unplug I²C-bus extender and remove the 3 metre wire.
16. Direct connection between I²C bus and the DS1621 sensor.
17. Measuring of peak-to-peak voltage and time rise of the signal received in the end of the wire

Qualification tests

To ensure a good I²C communication through a long wire and to confirm that I²C-bus extender P82B715 improves the quality of the signal. We can say the I²C-bus extender improves the quality of the signal when the peak-to-peak voltage is increased and the rise time stays with similar values.

Table C.7 30 Qualification test

| Status | Definition |
|-------------------|--|
| ✗ Failure | Any of the following cases: <ul style="list-style-type: none"> • The I²C communication with 3 metre wire is not possible • I²C-bus extender does not improve the signal quality. |
| ✓ Test completion | The I ² C communication is possible with 3 metre wire and the I ² C-bus extender improves the signal quality. |

C.7.16 Full Functional Test

Purpose.

- To test the function of every subsystem while working together, in a flight-like scenario.
- To test the experiment as a whole unit, to see whether the F.1, F.2, F.3, O.1, O.2 and O.6 requirements are fulfilled.

Material and environmental factors needed

- The whole experiment mounted as in flight, with the finished software in both the server and the client side.
- A laboratory with a local network with both the experiment and the Ground Segment laptop connected to it.
- A power supply.

Test process

To simulate the real flight with the real connection failures, as well as temporal failures in the power connector, the Ethernet connector, the USB connector and the I²C connector. In order to reach this scenario, the following conditions have been taken into account:

Test facility

Laboratory in the Faculty of Sciences with a set up local network—including a router and a switch—and a power supply

Simulated scenario

To simulate the flight conditions, the whole experiment is mounted as if in Esrange. The camera is facing a screen, which is connected to an external computer and from where we are able to put some star or horizon scenes.

As the local network of the test facility is much faster than the E-Link, the bandwidth has to be restricted to 2 Mb/s in both the download and the upload, in order to simulate the real scenario. To do so, the application Trickle, which provides an easy interface to restrict connectivity speeds, is used.

To simulate the possible hardware failures, the connectors that link the inner box with the outer box and that connect the inner box with the gondola will be temporarily and manually disconnected.



To see whether the requirements are fulfilled, the following issues will be monitored:

Table C.7 31 Requirements to be tested by full functional test

| Requirement | Description | Check |
|-------------|--|---|
| F.1 | The experiment shall obtain its orientation using the star sensor | |
| F.2 | The experiment shall obtain its orientation using the horizon sensor | Checked while the test is being performed with the measurements received by the Ground Station. |
| F.3 | The experiment shall obtain its orientation using magnetic field measurements | |
| O.1 | The orientation shall be obtained autonomously by the CPU | |
| O.2 | The whole experiment shall work autonomously after it has been turned on | Checked after the test, inspecting the log stored in the SD by the Raspberry Pi. |
| O.6 | The measurements obtained shall be send to the ground segment to verify the good operation of the system | Checked while the test is being performed, with the output of the client both in the terminal and in the GUI. |

General procedure

To make the test similar to the real flight scenario, the following steps will be taken:

1. Mount the experiment in its final set up:
 - a. Mount the inner box.
 - b. Mount the outer box.
 - c. Mount the outer box in the boom.
 - d. Connect the inner box with the outer box using the link, the USB, the Ethernet and the power connector.
2. Connect the inner box to the local network.

3. Connect the inner box to the power with the gondola power conditions, 28V.²
4. Connect the Ground Station to the local network.³
5. Send commands from the Ground Station to let the server start measuring and storing data (capturing images, measuring temperature and measuring magnetic field and accelerations).
6. Start receiving measurements.⁴
7. Check the flight modes⁵ :
 - a. Check the AUTO mode works and the decision algorithm chooses the correct attitude determination subsystem.
 - b. Check the STAR TRACKER mode works and the star tracker obtains the correct attitude.⁶
 - c. Check the HORIZON SENSOR mode works and the horizon sensor obtains the correct attitude.⁷
8. Check the Ethernet connection robustness⁸:
 - a. Disconnect Ethernet connector from the inner box. Reconnect it.
 - b. Disconnect Ethernet connector from the switch. Reconnect it.
 - c. Disconnect Ethernet connector from the Ground Station. Reconnect it.

² After step 3, the experiment shall work autonomously. O.2 will be checked after the completion of the test inspecting the log stored in the SD by the Raspberry.

³ After step 4, the server and client side should be connected and should be able to send/receive commands.

⁴ O.6 and F.3 will be checked from this step inspecting the client log and its GUI. F.1 and F.2 will be also partially checked from here.

⁵ These parameters are changed from the Ground Station. O.1 requirement will be checked after the test inspecting the log while in AUTO mode.

⁶ F.1 will be checked in this step.

⁷ F.2 will be checked in this step

⁸ The success of the connection loss handling will be checked after the completion of the test, inspecting the log stored in the SD by the Raspberry.



9. Check failures in data connectors⁹:
 - a. Disconnect I2C connector. Reconnect it.
 - b. Disconnect USB connector. Reconnect it.
10. Check failures in the power connector:
 - a. Disconnect power connector between the inner box and the power supply. Reconnect it.
 - b. Check that the Raspberry reboots, the program starts again and the connection is restored.

Qualification test

The results have to be compared with F.1, F.2, F.3, O.1, O.2, and O.6 requirements to see whether they are fulfilled.

Table C.7 32 Qualification test

| Status | Definition |
|-------------------|--|
| ✗ Failure | F.1, F.2, F.3, O.1, O.2 or O.6 are not fulfilled. The connection is not robust against failures. The data handling is not robust against failures. The experiment is not robust against power failures. |
| ✓ Test completion | F.1, F.2, F.3, O.1, O.2 and O.6 are fulfilled. The connection and the data handling are robust against failures. The whole experiment is robust against power failures. |

Results

The test was performed twice, leading to a failure the first time. After having isolated the error and having corrected it, the second time the test was performed it was completely successful. In the following table, the steps taken and their success are depicted:

Table C.7 33 Full Functional Test attempts

| Step | 1 st attempt | 2 nd attempt |
|------|-------------------------|-------------------------|
| 1 | ✓ | ✓ |
| 2 | ✓ | ✓ |
| 3 | ✓ | ✓ |
| 4 | ✓ | ✓ |

⁹ The robustness against those failures will be checked with the client log and GUI while the test is running. Furthermore, it will be checked after the test with the Raspberry log .

| Step | 1 st attempt | 2 nd attempt |
|--------|-------------------------|-------------------------|
| 5 | ✓ | ✓ |
| 6 | ✓ | ✓ |
| 7 – a | ✓ | ✓ |
| 7 – b | ✓ | ✓ |
| 7 – c | ✓ | ✓ |
| 8 – a | ✓ | ✓ |
| 8 – b | ✓ | ✓ |
| 8 – c | ✓ | ✓ |
| 9 – a | ✗ | ✓ |
| 9 – b | ✗ | ✓ |
| 10 – a | ✗ | ✓ |
| 10 – b | ✗ | ✓ |

In the first attempt, the steps 1-6 were successful. Step 7 was controlled from the Ground Station, changing the mode from AUTO, to STAR TACKER and to HORIZON SENSOR. All modes worked properly. The Ethernet connection failures, tested in step 8, were also completely successful. After reconnecting the Ethernet, the communication was restarted in 16 seconds.

The problem in the first attempt arose at step 9 – a, when the I²C connector was disconnected. The connection fell and all the inner box LEDs stopped blinking. The test was aborted and the log in the SD was inspected.

It was confirmed that the fatal error was caused by a bug in one of the temperature sensors, the TC74. Instead of throwing an error and let the rest of the program continue, the process was stopped with a return statement. The error was corrected and the test begun again.

In the second attempt, all steps were successful. From step 1 to step 7 the test behaved like in the first attempt. In step 8, the communication was restarted 18 seconds after reconnecting the Ethernet.

Step 9 was completely successful, with the I²C sensors and the camera recovered after disconnecting and reconnecting their connectors. The errors were successfully stored in the log, and the process was able to recover its full functionality, autonomously, after the sensors and the camera were reconnected.



Step 10 worked properly. The Raspberry Pi shut down and, when it rebooted, the connection was restored. The LEDs started blinking and, in the following inspection of the log and of the data stored, it was confirmed that the recovery was successful.

C.8 Simulation Details

C.8.1 Thermal Simulation

This section describes the parameters used in the thermal simulations done in SolidWorks. This intends to be a guide to perform the thermal simulations as realistic as possible and similar to ours.

The following parameters will be described for each part:

- Thermal conductivity and thermal transmittance (where available).
- Contacts with other parts.
- Emissivity and vista factor.

There is no thermal resistance between connections. We suppose heat transfer is perfect between two surfaces. This means that the surfaces of two materials in contact touches perfectly each other (this contact idealization saves computation time). The temperature increasing will be given by two parameters:

- Specific heat of material C_s , i.e., the physical quantity of heat energy required to change the temperature, measured in $J/kg \cdot K$.
- Thermal transmittance between surfaces K , i.e., the rate of transfer of heat through a surface or volume when there is a difference in temperature across the structure, measured in $W/m^3 \cdot K$.

The camera emits 2.5 W. See Thermal Design for more details.

Table C.8 1 Date simulation

| Part n° | C_s | K | Contacts with part n°... | Emissivity & Vista factor ⁽¹⁾ | Notes and comments |
|---------|-------|-----|--------------------------|--|--------------------|
| 0 | - | - | - | - | 2 |
| 1 | 900 | 200 | 0; 8 | - | 3 |
| 2 | 900 | 200 | 0; 7 | - | 3 |

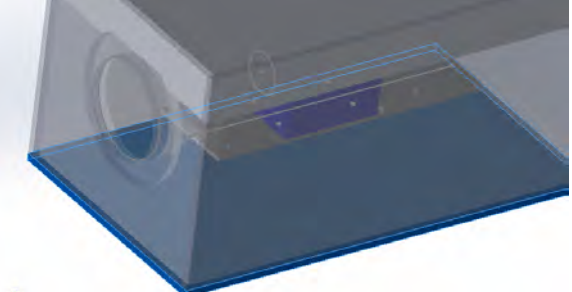
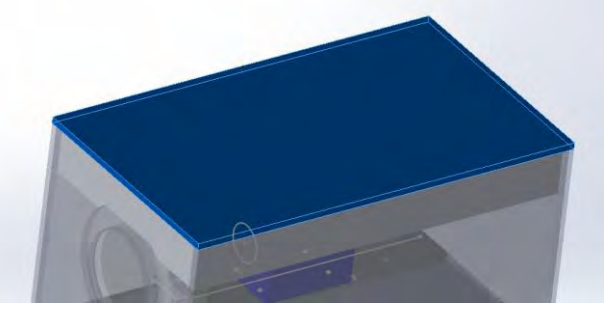
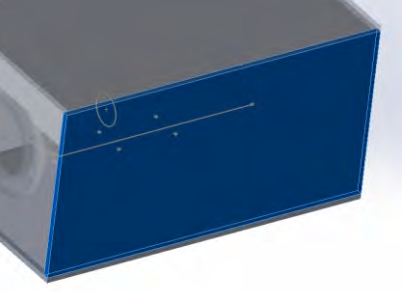
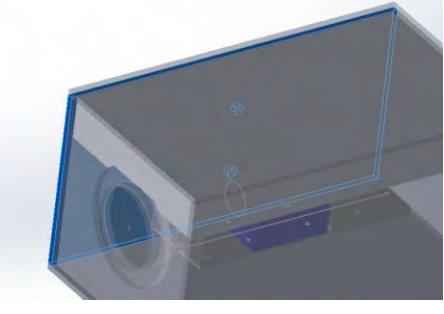
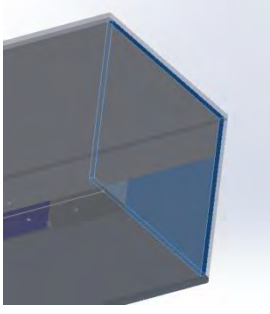
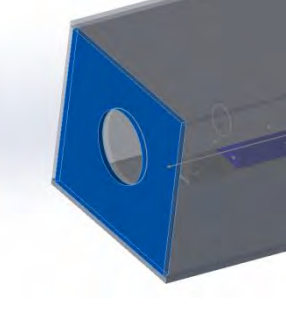
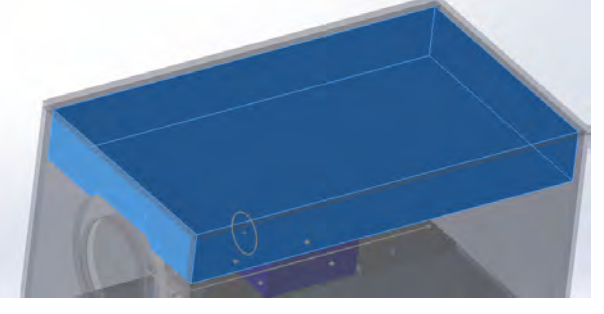


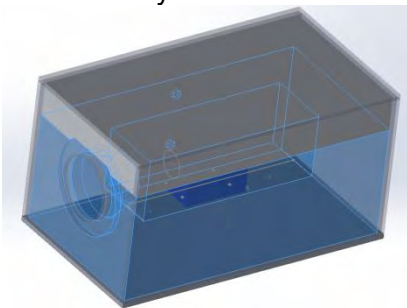
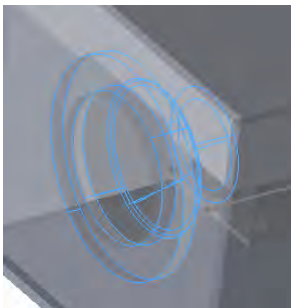
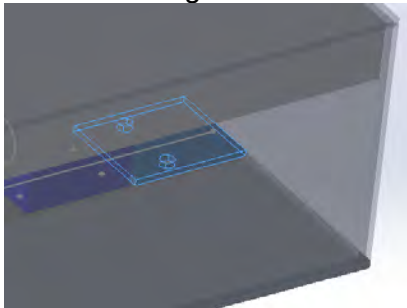
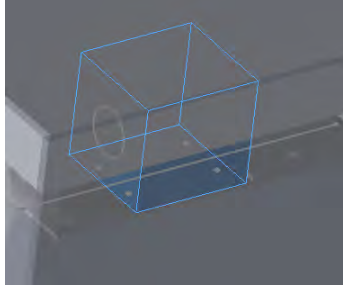
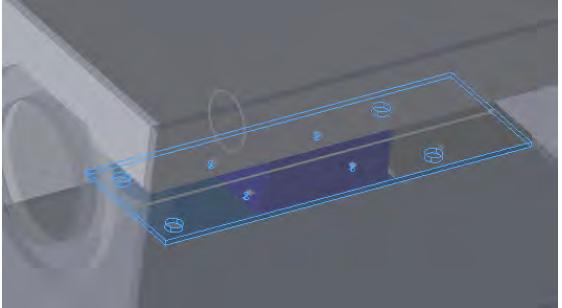
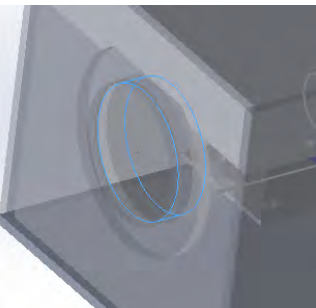
| Part n° | C _s | K | Contacts with part n°... | Emissivity & Vista factor ⁽¹⁾ | Notes and comments |
|---------|----------------|--------|------------------------------|--|--------------------|
| 3 | 900 | 200 | 0; 7; 8 | - | 3 |
| 4 | 900 | 200 | 0; 7; 8 | - | 3 |
| 5 | 900 | 200 | 0; 7; 8 | - | 3 |
| 6 | 900 | 200 | 0; 7; 8 | - | - |
| 7 | 1,500 | 0.033 | 2; 8; 12 | - | 4 |
| 8 | 1,500 | 0.0033 | 1; 3; 4; 5; 6; 7; 12; 13; | - | 4 |
| 9 | - | - | None | - | - |
| 10 | - | 124 | None | 0.05 & 0.5 | - |
| 11 | 900 | 200 | None | - | 4 |
| 12 | 900 | 200 | 7; 8; 13 | 0.05 & 0.5 | 3 |
| 13 | - | 124 | 12; 8 | - | - |
| 14 | 834.61 | 0.7498 | None | - | - |

Notes and comments:

1. Only applicable when radiation is considered.
2. Environment at -80 °C.
3. Part made of aluminium. Very good thermal conductor. Mechanical parameters considered in table 1.
4. Insulation of extruded polystyrene. Mechanical parameters in Table C8- 2
5. Empty cell means “not necessary to consider” or “not applicable”.

Table C8- 1 Images part and numeration

| | |
|---|---|
| 0 External environment |  1 – Bottom face |
|  2 – Top face |  3 – Left lateral |
|  4 – Right lateral |  5 – Rear face |
|  6 – Front face |  7 – Top insulation |

| | |
|--------------------------------------|--|
| 8 – Body box insulation |  |
| 9 – Baffle |  |
| 10 – Magnetometer |  |
| 11 – Camera lens |  |
| 12 – Camera body |  |
| 13 – Camera and magnetometer support |  |
| 14 – Filters |  |

**Table C8- 2 Material parameters in SolidWorks simulation**

| Parameters/ Material | Young Module (E_x) [N/m²] | Cutting Module (G_{xy}) [N/m²] | Tensile strength (σ_{x,t}) [N/m²] | Compressive strength in the 1st material direction (σ_{x,c}) [N/m²] | Thermal expansion Coefficient (α_x) [K⁻¹] | Density (γ) [kg/m³] |
|---------------------------------|---|--|---|--|---|---|
| Aluminium | $6.9 \cdot 10^{10}$ | $2.7 \cdot 10^{10}$ | $6.8936 \cdot 10^7$ | $2 \cdot 10^7$ | $2.4 \cdot 10^{-5}$ | 2,700 |
| Extruded polystyrene | 2.5 | 0.2 | 0.43 | 0.362 | $6 \cdot 10^{-5}$ | 28 |

APPENDIX D – LAUNCH CAMPAIGN ADDITIONAL INFORMATION

D.1 Launch Campaign Checklists

CHECKLIST Day 1 – Unpacking, mounting and basic test

- Choose workspace and setup equipment**
- Unpack all components**
- Check off components list**
 - Inner box
 - Outer box
 - Boom
 - Boom grip
 - Inner box grip
- Check all structures**
- Check electrical connections**
 - Check components
 - Check ground connection
 - Check 28 V connection
 - Check I²C connection
- Magnetometer calibration**
- Mounted into gondola**
- Power connection checked and connected to gondola power**



- E-link connector checked**
- Ground station connected directly to experiments**
- Communication and functional test**
- Dismount if required**

CHECKLIST Day 2 – Individual test

- Unplug Ethernet connection & Check data saved**



- Unplug USB camera connection & Check data saved**



- Unplug power gondola connection & Check data saved**



Unplug link between & Check data saved



*In this photography we can see a hole without component. At the time this picture was taken, we were testing the connector (Ethernet). However, the correct position is shown in the first photography of this page.

CHECKLIST Day 3 – Gondola Interference Test

- Experiment connected to the E-Net and gondola power supply**
- G/S set up in ground station area**
- Communication and functional test (One by one)**
- Communication and functional test (Whole gondola)**
- Experiment connected to the E-Link**
- RF Interference check with E-Link**
- Communication and functional test (One by one)**
- Communication and functional test (Whole gondola)**



D.2 Data Recovery Procedure

Actions to be taken before the flight:

1. Prepare Ground Station laptop to have a safe mode:
 - a. Without GUI, without external programs, with Ethernet and wireless connectivity disabled.
 - b. With the access to the external devices disallowed to any program unless they provide a password. With the write permission in any SD turned off for every user.
 - c. With any connected HDD automatically mounted in the folder /media/HDD/ .
 - d. With the folder ~/SDBackUP/ created.

Actions to be taken after the recovery –this process can be easily automated with a bash script, coded and tested before the flight-:

1. Turn on Ground Station laptop, with the battery completely charged and connected to the electrical grid.
2. Enter safe mode.
3. Run `lsblk` command and write down all the devices connected.
4. Plug the SD in the laptop slot.
5. Check the pathname of the SD:
 - a. Run `lsblk` command and write down the new device connected, probably something like `mmcblk0`, with a value of approximately 32 g in the `SIZE` column.
 - b. Check that `/dev/mmcblk0` exists.
 - c. Run `dmesg` to double check that the SD pathname is `/dev/mmcblk0`: this name should appear in the last lines of the command output.
6. Enter the following command:


```
dd bs=4M if=/dev/mmcblk0 of=~/SDBackUP/backup.iso
```
7. Wait until the backup is completed and enter `sync` command.
8. Wait until the command ends and unplug the SD.
9. Connect an empty external hard drive in the laptop.
10. Copy the SD backup into the hard drive with the following command:



```
cp ~/SDBBackup/backup.iso /media/HDD/backup.iso
```

11. Wait until the backup is completed and enter sync command.
12. Wait until the command ends and unplug the external hard drive.

D.3 Assembly Procedure

D.3.1 General Procedure

- To ensure the mechanical fixation, all the nuts shall be nyloc nuts. If this is not possible, they shall be fixed with glue.
- To reduce the risk of break in the wires due to vibrations, all the wires shall be fixed with glue or cable ties.

D.3.2 Inner Box Assembly Procedure

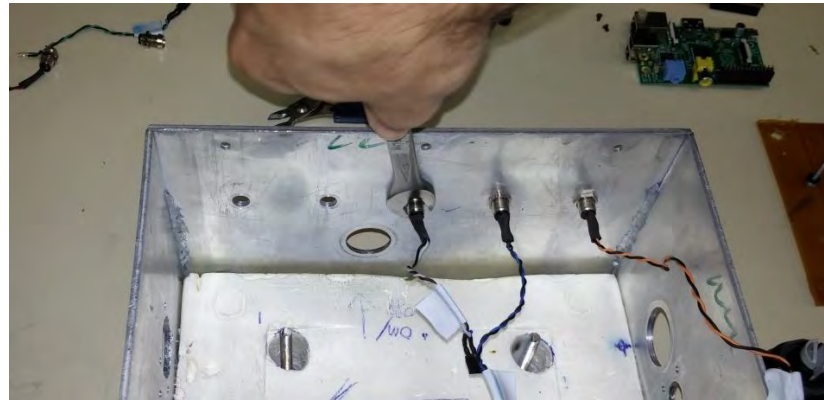
1. Screw four long 6 mm bolts to the bottom side of the inner box.
 - 6 mm bolts x4
 - 6 mm metal washers x 4
 - 6 mm nuts x4
 - 11 mm wrench from the inside
 - 11 socket wrench from the outside
2. Screw eight 8 mm to the inner box in order to fix the two aluminium rails.
 - 8 mm bolts x8
 - 8 mm metal washers x8
 - 8 mm nuts x8
 - Aluminium rails x2
 - 13 mm wrench from the inside
 - 13 socket wrench from the outside



3. Place the XPS insulation on the bottom of the inner box. Be sure to place it in the correct orientation.



4. Screw the five LEDs.
 - LED x5
 - 11 mm wrench x1
 - Be careful to place them in the correct order. As seen from the outside and from left to right: orange, blue, white, green and red cables.



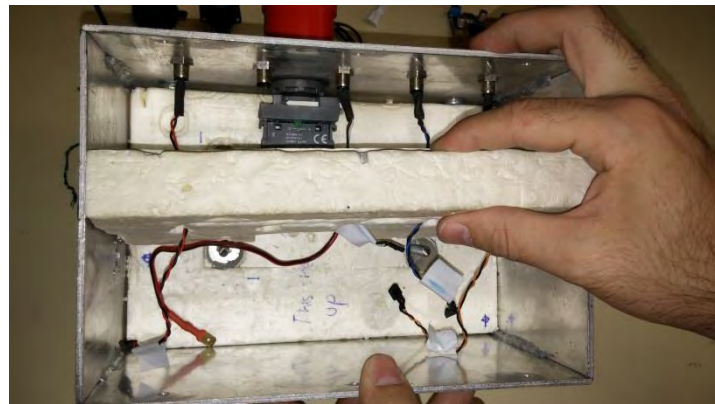
5. Mount the mushroom switch.
 - Mushroom switch x1



6. Fasten the nut with the hand. Then, attach the ABB connector.



7. Attach the XPS insulation next to the mushroom switch.

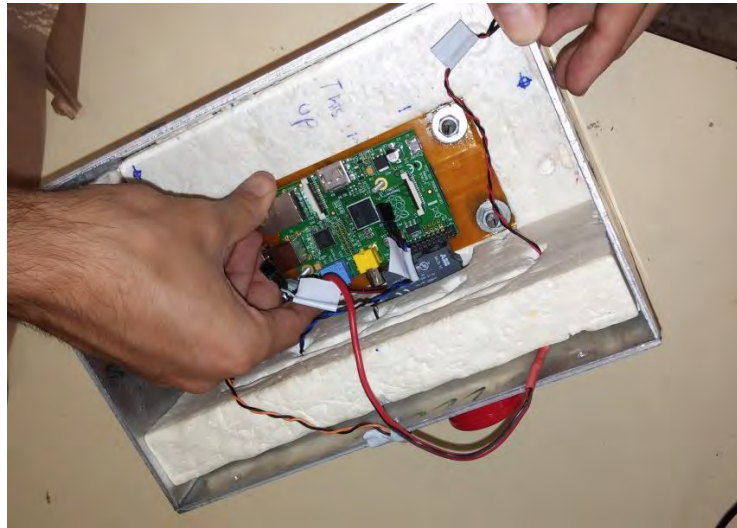


8. Place the orange plastic plate and screw it to the bottom XPS isolant.

- 6 mm metal washer x4
- 6 mm nuts x4
- 11 mm socket wrench from the outside



9. Place the Raspberry Pi on the two bolts.



10. Attach the USB connector fastening the nut from the inside of the box with the hand. Place the plastic washer on the outside.

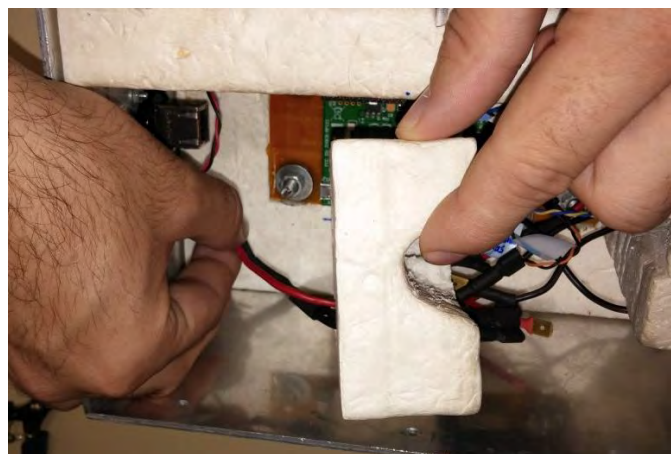


11. Attach the Ethernet, Power and Link connectors.

- 4 mm bolts x12
 - 4 mm nuts x12
 - 4 mm metal washer x11
 - Screwdriver x1
 - 5.5 mm socket wrench x1
- Use the screwdriver and the socket wrench at the same time to attach the connectors easily. Instead of a metal washer, place the short black cable –the one with a metal hole on it-, on the up-right bolt of the power connector.



12. Place the XPS insulation on the right and the left side of the inner box. Be careful with the cables that have to pass through the insulation.



13. Place washers on the two bolts that pass through the Raspberry Pi.

- Big plastic washers x4
 - Small plastic washers x2
 - Brown plastic washers x2
- Place, on each bolt, the following –the order is important-:
- A small white washer

- A big white washer
- A small white washer



14. Place the PCB on the two bolts and attach it, using the brown washers between the PCB and the nuts.

- 4 mm nuts x2
- Brown washer x2
- 5.5 mm socket wrench x1

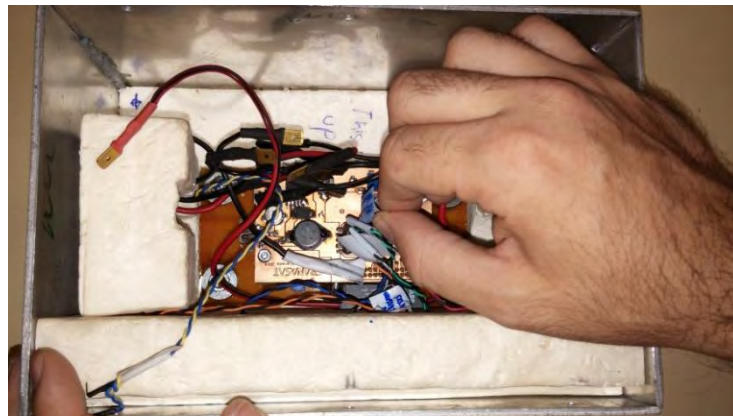




15. Orient the box in such a way that the red mushroom button points to the operator. Connect the LED connectors in the following order -from up to down-

:

- Camera (Red)
 - Experiment connection status (Green).
 - Magnetometer and Accelerometer (White).
 - Ethernet (Blue)
 - Image processor status (Orange).
- The black cables shall be on the right side.



16. Plug the Ethernet cable. It requires some precision.



17. Plug the USB type B cable. It requires some precision.



18. Tighten both the screws that fasten the yellow and blue cables to the blue connectors. The yellow one shall be placed on the SDA+ connector, while the blue one shall be connected on the SCL+ connector.

- Screwdriver x1



19. Connect the two red pairs of cables with no specific order. Connect the four black pairs of cables with no specific order. Be careful not to connect any red cable with a black one.

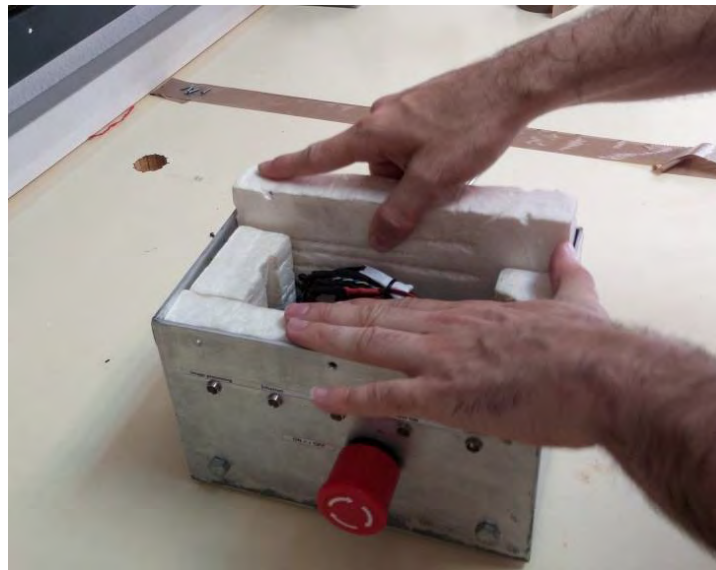


20. Fix the cables with flanges.

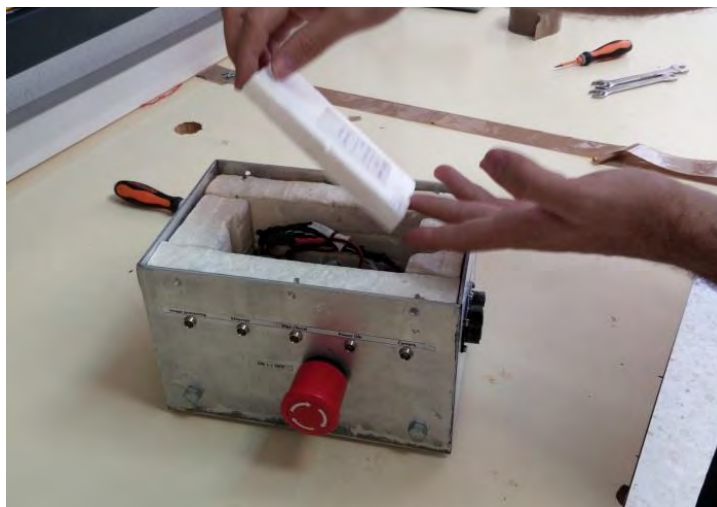
- Flanges x9



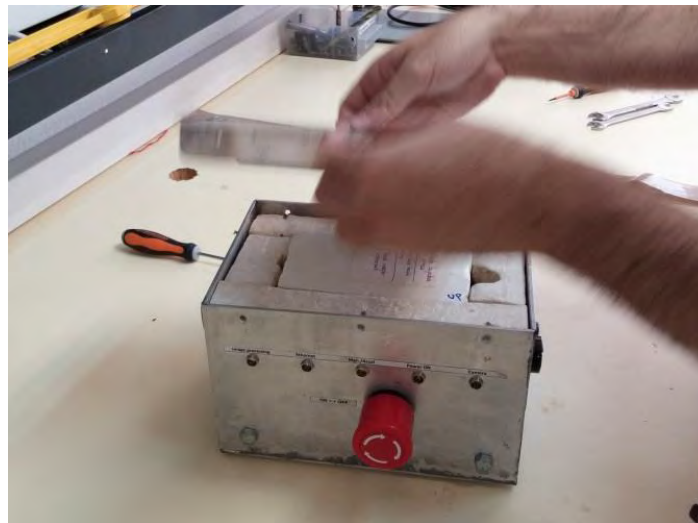
21. Place the XPS insulation on the opposite side of the red mushroom button. It may require some strength.



22. Place the XPS insulation located underneath the lid.

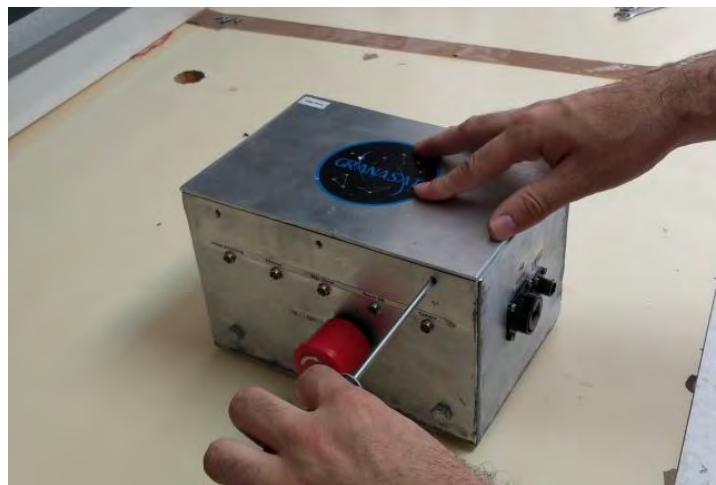


23. Place the inner box lid.



24. Tighten the six bolts that attach the inner box lid to the box.

- 4 mm bolts x6
- Screwdriver x1



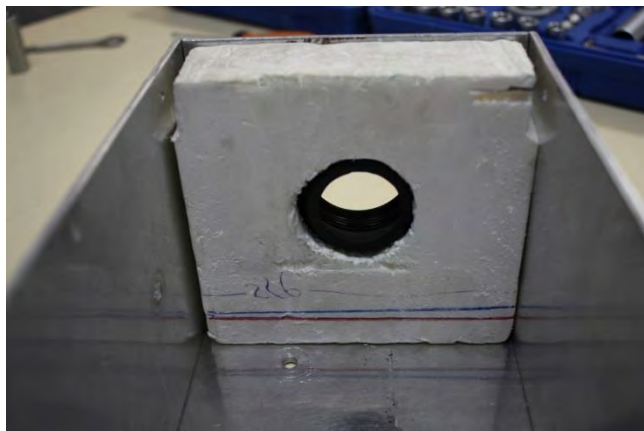
D.3.3 Outer Box Assembly Procedure

1. Attach the baffle with four 4 mm bolts. Do not forget the rubber piece placed between the aluminium and the baffle.
 - 4 mm bolts x4
 - 4 mm screws x4
 - 4 mm washers x4
 - Screwdriver x1

- 6 mm wrenchx1
- Time: 4 – 5 minutes.



2. Place the XPS insulation onto the baffle. Orient the XPS insulation in such a way that it leaves the notch on the top.
 - Time: 5 seconds.



3. Attach three long 6 mm 8.8 bolts on the bottom of the outer box.

- 6 mm 8.8 bolts x3
- 6 mm screws x3
- 6 mm washers x3
- 10 mm wrench x2
- Make sure to tighten the bolts properly. Time: 2 – 3 minutes.



4. Attach the structure through which the cables pass.

- 3 components of the fixation.
- Time: 20 seconds.



5. Place the XPS insulation on the bottom of the outer box.

- Time 5 seconds.



6. Attach a 90 degrees connector on the bottom of the outer box.

- 90 degrees connector x1

- Nyloc nut x1
- 8 mm 8.8 T bolt x1
- Use the connector with two protrusions on one side. The bolts must be loose. Time: 2 – 3 minutes.



7. Attach another 90 degrees connector on the left face of the outer box.
 - 90 degrees connector x1
 - Nyloc nuts x1
 - 8 mm 8.8 T bolts x1
 - The bolts must be loose. Time: 2 – 3 minutes.



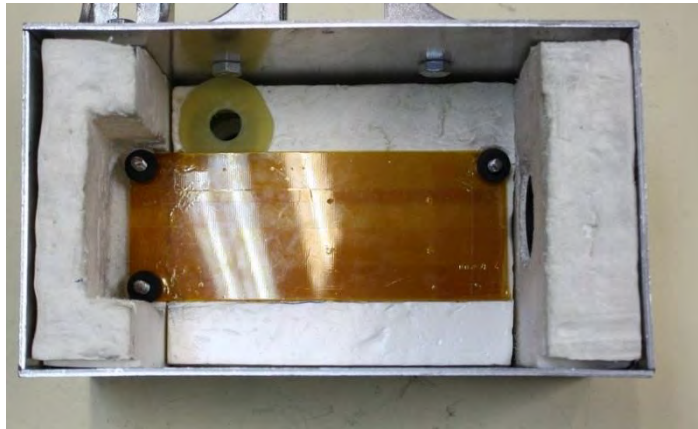
8. Place the XPS insulation on the back face of the outer box.
 - Time: 5 seconds



9. Place and attach the fibre glass plate on the bottom XPS insulation.
 - Fibre glass plate x1
 - Rubber plates x3
 - Time: 20 seconds



10. Place and attach the round plate under the fibre glass plate.
 - Time: 20 seconds



11. Attach two connectors on the right side of the outer box.

- 90 degrees connectors x2
 - 8 mm 8.8 bolts x2
 - Nuts x2
 - Washers x2
- Use the connector with no protrusions. Fixations should be a bit loose.
- Time: 2 minutes.



12. Take a “test” boom and put it between the connectors. Orient the connectors to the boom. Tighten the bolts that attach the connectors with the outer box starting from the connector of the bottom side of the box.

- Time: 6 – 7 min



13. Place the transparent thermo-resistant plastic washer on the 3 bolts inside the box.
 - Plastic washers x6
 - Time: 30 seconds



14. Place the camera + PCB on the plastic washer and attach it.
 - Camera + PCB x1
 - Plastic washers x3
 - 6 mm nutsx3
 - 6 mm wrench x1
 - Be aware to adjust accurately the camera orientation with the nut placed the nearest to the baffle. Time: 3 minutes.



15. Place two XPS insulations on the right and the left side of the outer box.

- Time: 1 minute.



16. Attach a 90 degrees connector to the outer box lid.

- 90 degrees connector x1
- 8 mm 8.8 bolts x1
- Nyloc nuts x1
- The bolt must be loose. Time: 1 minute.

17. Place the last XPS insulation on the top of the outer box.

- Time: 30 seconds.



18. Close the outer box.

- 4 mm bolts x5
- Screwdriver x1

- Do not attach the bolts tightly yet. Time: 2 minutes.

19. Take a “test” boom again and place it between the 90 degrees connectors.

Now, attach the lid and the connector bolts tightly. The outer box assembly is now completed. Time: 2 minutes.

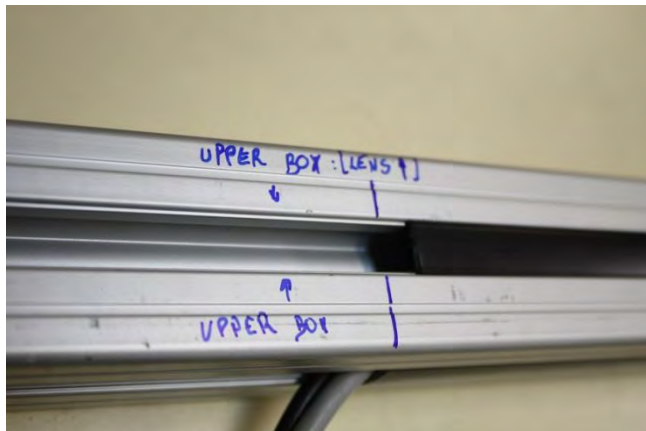
- Steel plates x2
- T bolts 6 mm x2
- Nuts x2
- Wrench x1

- Time: 3 minutes.



20. Place plastic covers in the rest of boom gaps.

- Time: 2 minutes.



21. Attach the outer box to the boom.

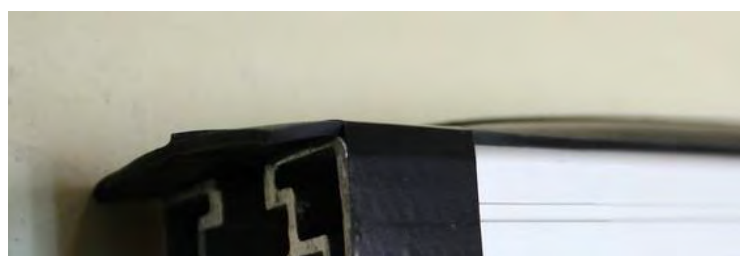
- 8 mm nuts x4
- 8 mm 8.8 T bolts x4
- 13 mm wrench x1
- Start tightening the T bolt of the bottom side of the outer box. Next, orient the T bolts on the left, right and outer side. Finally, tighten the three bolts to fix the outer box to the boom properly. Time: 10 minutes.

22. Finish placing plastic covers above the outer box attachments.



D.3.4 Boom Assembly Procedure

1. Place the rubber on the boom and fix it with insulating tape. The insulating tape must be placed on the gondola marks.
 - o Time: 3 minutes.

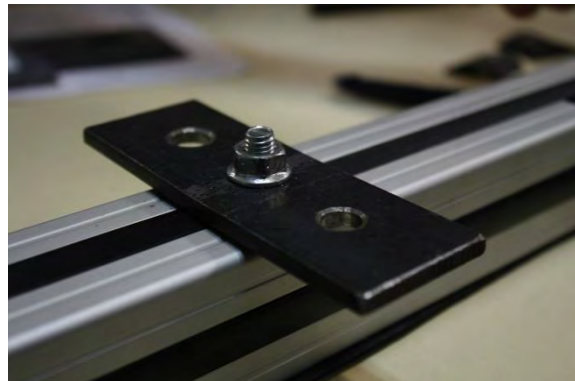


2. Place the plastic tube insulation and insert into the tube the USB wire and Link cable.

- Time: 5 minutes.
- 3. Cover the plastic tube with the foam insulation, starting from the top.
 - Time: 1 minute.
- 4. Fix the top side of the plastic tube to the outer box fixation.
 - Time: 3 minutes.
- 5. Place plastic cover trims in all the rails of the boom.
 - Time: 1 minute.



- 6. Place the steel plates on the boom marks -14 cm from the gondola sides- and attach them with the central bolt. Between the boom and every plate, a rubber square must be placed.
 - Rubber squares x2
 - Time: 8 minutes.





7. Place the security steel cable between the boom rails and the plastic cover trim.
 - Time: 3 minutes.



8. Finish the security steel cable with two U-grabbers and ensure it to the gondola with one steel carabiner.
 - Time: 15 minutes.



9. Fasten both the foam and the plastic tube insulation to the gondola attachments with several cable ties.
 - Time: 5 minutes.

D.4 Recovery Sheet



GranaSAT Recovery Sheet.

How to **switch off** the experiment:

